Spinal Cord Cellular Response To Wear Debris From Metal-on-Metal Total Disc Replacements

Helen Lee

Submitted in accordance with the requirements for the degree of

Doctor of Philosophy

The University of Leeds
School of Mechanical Engineering

September 2016

The candidate confirms that the work submitted is her own and that appropriate credit has been given where reference has been made to the work of others.

Acknowledgements

First and foremost I would like to take this opportunity to express my gratitude to my primary supervisor; Professor Joanne Tipper. From start to finish you have offered constant guidance, kind words of encouragement and unrelenting support, without your wealth of knowledge and expert supervision this PhD would not have been possible. To you I will be eternally grateful for my accomplishments over the past five years.

I would also like to thank my co-supervisors; Professor Richard Hall and Dr James Phillips, your expertise in the fields of Mechanical Engineering and Biomaterials and Tissue Engineering have been invaluable to my work. I would like to thank James for all the Skype chats, visits to Leeds and for the opportunity to work in his lab at the Open University. Your enthusiasm for science is truly inspirational and I feel very privileged to have had the opportunity to work with you. I would like to thank Richard for his help with the Mechanical Engineering aspect of my project, your excellent advice has been incredibly important in the past few years. I would like to thank you all for providing me with the opportunity to work at a first class institution, I have had an amazing team supporting me.

I would like to thank all members of the iMBE at the University of Leeds who have made this an amazing five years, I have thoroughly enjoyed being a part of such a fantastic team of researchers, you are an incredibly inspiring group of scientists. I would like to give specific mention to Iraklis Papageorgiou and Ruth Craven for your supervision in the lab and for always being there to help whenever I needed it.

The mechanical engineering aspect of my project was completely new to me and I would like to thank Stuart Micklethwaite, Imran Asif, Sha Zhang and all the technical staff in Mechanical Engineering for their invaluable help with the particle generation and characterisation aspect of my project.

I would like to give a huge thanks to Jeni Smith, you are an incredible friend. You have seen me through the highs and lows of this project and have kept me motivated right to the very end. Your unfaltering enthusiasm and drive to succeed is incredible and I wish you the best of luck in the future.

I would like to express my appreciation to Jess Kirk, your passion for science and enthusiastic nature is truly amazing. Thank you for all the coffee trips and words of encouragement in the final stages of my PhD, you made me so determined to succeed.

On a personal note I would like to give my deepest thanks to my amazing boyfriend Richard!! Your love and support has been unfaltering and I appreciate everything you have done to help me through this PhD, I am so lucky to have you in my life. You have taught me to believe in myself and to never give up. Sorry for all the nights where I'd wake up at 4am and need to write something else in my thesis. Thank you for your amazing pep talks and for always telling me to…. "just keep swimming".

I would like to give special thanks to my incredible family, especially to my Mum and Dad who have always supported me and taught me to go my own way in life. Everyday you inspire me, seeing how successful you have both been has always driven me to succeed in my own life. I cannot thank you enough for your support throughout this PhD, I couldn't have done it without you.

Finally I would like to express my deepest gratitude to my Grandad Joe, who unfortunately was not able to see me complete my PhD. You always believed in me. Even when I took the road less travelled you never questioned me. When times were tough your faith in me pulled me through. I will never forget the endless hours you spent with me as a child nurturing my talents and encouraging me to follow my dream of becoming a Doctor. Your kind heart will never be forgotten. To you I dedicate this thesis.

Abstract

Total disc replacements, are valuable interventions for the spinal surgeon for the treatment of back pain associated with degeneration of the intervertebral disc. The longevity of these devices is compromised by wear and there are growing concerns within the neurosurgical community regarding the exposure of periprosthetic tissues to metal particles and/or ions. Considering the potential for metallic wear debris and ions to trigger inflammation, genotoxicity, cytotoxicity, hypersensitivity and pseudotumour formation, coupled with evidence that nanoscale metal particles can compromise the barrier function of the outer meningeal layer, it is imperative to determine the effects of metallic wear particles on cells of the spinal cord. It was hypothesised that, utilising a 3D type-I collagen gel, enabling glial cells to behave in a more physiologically relevant manner than when cultured in monolayer, the effects of increasing concentrations of metallic wear particles on glial cell viability, cellular reactivity, and cytokine release could be more accurately determined.

Clinically relevant cobalt chrome and stainless steel wear particles were generated using a six-station pin-on-plate wear simulator. Initially in 2D culture C6 glial, PC12 neuronal cells and primary astrocytes with microglia were cultured with increasing concentrations of metallic particles ($0.05\mu m^3$-$50\mu m^3$ debris per cell) and their effect on cell viability and DNA integrity assessed. Using a more physiologically relevant 3D culture environment the effects of increasing metallic particles ($0.5\mu m^3$-$50\mu m^3$ debris per cell) on cell viability, cellular activity and cytokine expression were investigated using live/dead staining, immunocytochemistry and an enzyme linked immunosorbent assay, respectively.

This study highlighted the necessity for appropriate cell culture environments in biomaterial biocompatibility testing. In 2D culture all cobalt chrome particle doses triggered significant reductions in primary astrocyte and microglia viability, however, in 3D culture, cobalt chrome particles (30-39nm in length) only adversely affected the viability of primary astrocytes and microglia in co-culture when cultured with the highest cobalt chrome particle dose ($50\mu m^3$ debris per cell) after two and five days in culture (41.8% and 54.2% viable cells, respectively) and with $5\mu m^3$ debris per cell after five days in culture (70.5% viable cells). In 2D culture, after 24 hours in culture $0.5\mu m^3$, $5\mu m^3$ and $50\mu m^3$ stainless steel particles per cell caused significant reductions in cell viability (38.8%, 38.9% and 24.9% reductions respectively) however, no adverse effect on viability was observed in 3D culture. Ions released from cobalt chrome caused significant

reductions in astrocyte viability (in isolation) at all doses after two days in culture, this effect was not as pronounced after five days. Ions from cobalt chrome particles only caused adverse effects on the viability of astrocytes and microglia after five days at the 5μm^3 per cell ion concentration in 3D culture. Ions released from stainless steel caused significant reductions in astrocyte viability (in isolation) at all doses after five days in culture. Stainless steel ions caused adverse effects on the viability of astrocytes and microglia after five days with the 50μm^3 per cell ion concentration. DNA damage was observed with both astrocytes and microglia and astrocytes in isolation with both biomaterials tested. Intriguingly, when glial cells were cultured with stainless steel wear particles, the DNA damage observed did not correlate with cell death. Increasing particle volumes of cobalt chrome did not trigger the release of TNF-α, however 50μm^3 stainless steel debris per cell caused the release of significantly elevated levels of TNF-α after 48 hours in culture (29.9 $pg.ml^{-1}$). Stainless steel wear particles did not stimulate astrocyte reactivity unlike cobalt chrome wear products, which had a dose dependent affect on astrocyte activation. The effect was more pronounced in the presence of microglia. Thus the use of 3D culture, whereby glial cells behaved in a more physiologically relevant manner, with a low baseline of reactivity and more representative of the *in vivo* cellular spatial arrangement was a more appropriate cell culture environment for determining the biological response of cells of the central nervous system to metal wear particles. The results from this study would suggest that stainless steel is more biocompatible than cobalt chrome.

Table of Contents

List of Tables

List of Figures

List of Abbreviations

2D ……Two Dimensional

3D ……Three Dimensional

µg ……Micrograms

µl ……Microlitres

µM ……Micromolar

µm ……Micrometres

μm^3……Micrometres Cubed

Al…… Aluminium

ALVAL ……Aseptic Lymphocyte-dominated Vasculitis Associated lesions

AMP……Ampere

ANOVA …… Analysis of Variance

APC ……Antigen Presenting Cell

API ……Active Pharmaceutical Ingredient

ARMD ……Adverse Reactions to Metal Debris

ASTM ……American Society for Testing and Materials

ATP…… Adenosine Triphosphate

B…… Boron

Bal…… Balance

BSA…… Bovine Serum Albumin

C…… Carbon

Cm^3 ……Centimetres cubed

CNS…… Central Nervous System

CNTF ……Ciliary Neurotrophic Factor

Co…… Cobalt

CO_2 ……Carbon Dioxide

CoCr…… Cobalt Chromium

CoCrMo ……Cobalt Chrome Molybdenum

CPS…… Counts Per Second

Cr…… Chromium

cTDR…… Cervical Total Disc Replacement

DDD ……Degenerative Disc Disease

DMEM…… Dulbecco's Modified Eagle's Medium

DMSO…… Dimethyl Sulfoxide

DNA ……Deoxyribonucleic acid

DNase ……Deoxyribonuclease

DOF ……Degrees of Freedom

DPBS ……Dulbecco's Phosphate Buffered Saline

DTH ……Delayed Type Hypersensitivity

EBSS ……Earle's Balanced Salt Solution

ECM ……Extracellular Matrix

EDTA ……Ethylenediaminetetraacetic Acid

EDX ……Energy Dispersive X-Ray Spectroscopy

ELISA…… Enzyme-Linked Immunosorbent Assay

FBS ……Foetal Bovine Serum

FDA ……Food and Drug Administration

Fe ……Iron

FEGSEM ……Field Emission Gun Scanning Electron Microscope

FGF-23 ……Fibroblast Growth Factor-23

g …… Grams

GAG ……Glycosaminoglycan

GFAP ……Glial Fibrillary Acidic Protein

GFS ……General Function Score

GM-CSF ……Granulocyte- Macrophage Colony Stimulating Factor

GPa ……Gigapascal

H_2O_2 ……Hydrogen Peroxide

HCl ……Hydrochloric Acid

HRP ……Horseradish Peroxidase

IFN-γ …… Interferon-gamma

ISO ……International Organisation for Standardisation

IVD ……Intervertebral Disc

KPa ……Kilopascal

KV ……Kilovolt

LDH ……Lactate Dehydrogenase

LPS ……Lipopolysaccharide

mAMP ……Milliamp

Mc ……Million cycles

MEM ……Minimum Essential Medium

mg ……Milligrams

$MgSO_4$ ……Magnesium Sulphate

MIF ……Migration Inhibitory Factor

ml ……Millilitres

mM ……Millimolar

mm ……Millimetres

mm^3 ……Millimetres Cubed

Mn ……Manganese

Mo ……Molybdenum

MOM…… Metal-On-Metal

MSD……Minimum Significant Difference

MtROS ……Mitochondrial Reactive Oxygen Species

MTT……(4,5-dimethylthiazol-2-yl)-2,5-diphenyltetrazolium bromide

N ……Newton

N_2 ……Nitrogen

NaOH…… Sodium Hydroxide

Ni ……Nickel

Nm ……Nanometre

NP……Nucleus Pulposus

OD ……Optical Density

P ……Phosphorous

PBS ……Phosphate Buffered Saline

PDL ……Poly-D-Lysine

PE ……Polyethylene

PFA ……Paraformaldehyde

pg ……Picograms

PLGA ……Poly (lacto-co-glicolic acid)

PMMA ……Polymethylmethacrylate

ROS ……Reactive Oxygen Species

RPM ……Revolutions Per Minute

RPMI ……Roswell Park Memorial Institute Medium

S ……Sulphur

SBTI ……Soy-Bean Trypsin Inhibitor

SEM ……Scanning Electron Microscopy

Si ……Silicon

TDR…… Total Disc Replacement

TEM ……Transmission Electron Microscopy

TGFα ……Transforming Growth Factor-alpha

TGF-β1 ……Transforming Growth Factor- Beta-1

Ti ……Titanium

TNF-α ……Tumor Necrosis Factor-alpha

UHMWPE ……Ultra High Molecular Weight Polyethylene

$U.ml^{-1}$ ……Units per millilitre

v/v ……Volume/ Volume

VAS ……Visual Analogue Scale

V……Volt

W ……Tungsten

w/v ……Weight/ Volume

w/w……Weight/Weight

Chapter 1
Introduction

1.1 Spinal anatomy and biomechanics

The spine is a complex columnar structure, encompassing hard and soft tissue components. The vertebral column supports the head, enables movement of the upper limbs and protects the spinal cord from damage. The spine serves as a rigid support but must also be flexible to allow movement of the neck and back. The segmental nature of the spinal column and presence of intervertebral discs is ideally suited to this multipurpose nature. The spine is comprised of 33 vertebrae. The first 24 vertebrae have intervertebral discs between them, whilst the remaining nine vertebrae are fused and have no discs. The spine is categorised into five morphologically distinct regions; cervical, thoracic, lumbar, sacral and coccygeal. In an adult spine there are seven cervical vertebrae (C1-C7), twelve thoracic vertebrae (T1-T12) and five lumbar vertebrae (L1-L5) (Figure 1.1). The next five bones are fused together and are named the sacrum, with the remaining four bones making up the coccyx. The morphology and function of the vertebrae differ along the length of the spine. The cervical vertebrae allow maximum flexibility and range of motion for the head (Kurtz & Edidin, 2006). The thoracic vertebrae support the ribs and enable flexibility of the spine. The lumbar vertebrae are the largest and strongest of the vertebral bodies and are optimised for structural support.

Each vertebra is predominantly comprised of cancellous bone with a thin outer vertebral shell. Each vertebra consists of an anterior portion, the vertebral body, which resists compression under load. The vertebral body is the largest part of a vertebra, cranially and caudally it is flat. The posterior regions of the vertebrae form a vertebral arch (Figure 1.2). The vertebral arch comprises two pedicles (short processes that extend out from the side of the vertebral body), two laminae (broad, flat plates which extend out from the pedicles joining in a triangular conformation, yielding a hollow vertebral foramen) and seven processes; spinous process, transverse process, superior articular process, inferior articular process, mammillary process, accessory process and uncinate process. The function of the vertebral arch is to protect the spinal cord and facilitate motion by offering anchorage for muscle attachment (Martini & Nath, 2008).

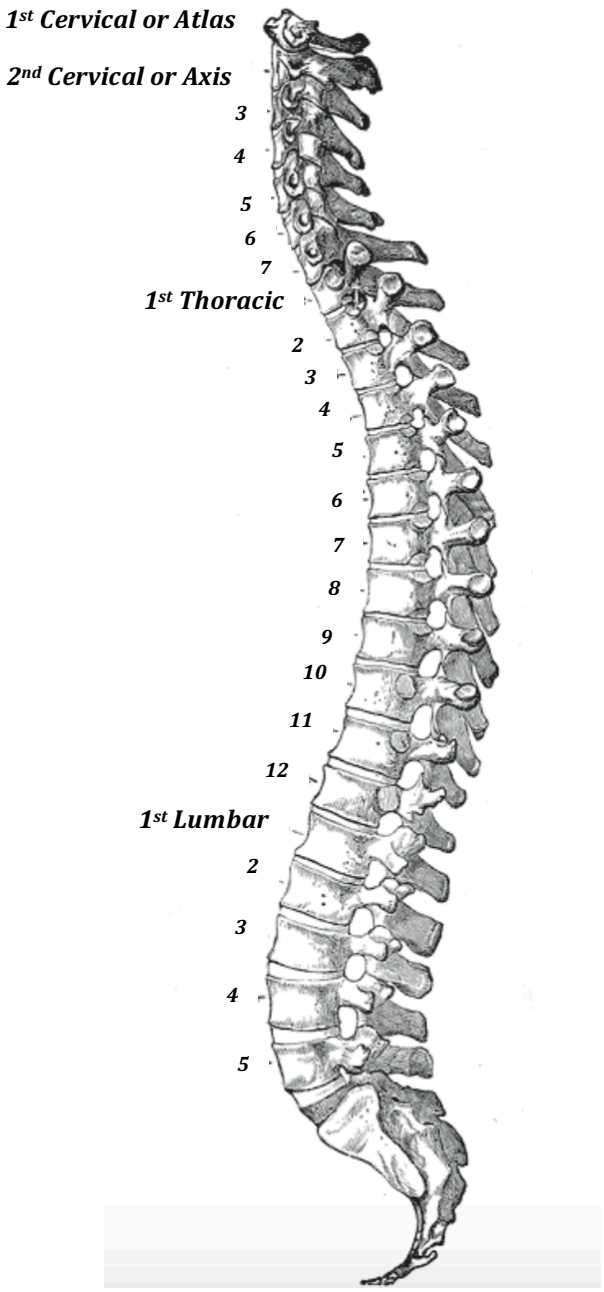

Figure 1.1 The cervical, thoracic, lumbar, sacral and coccygeal regions of the adult spine. The vertebrae are designated C1-C7, T1-T12, L1-L5 in the cranial to caudal direction (Gray, 1918).

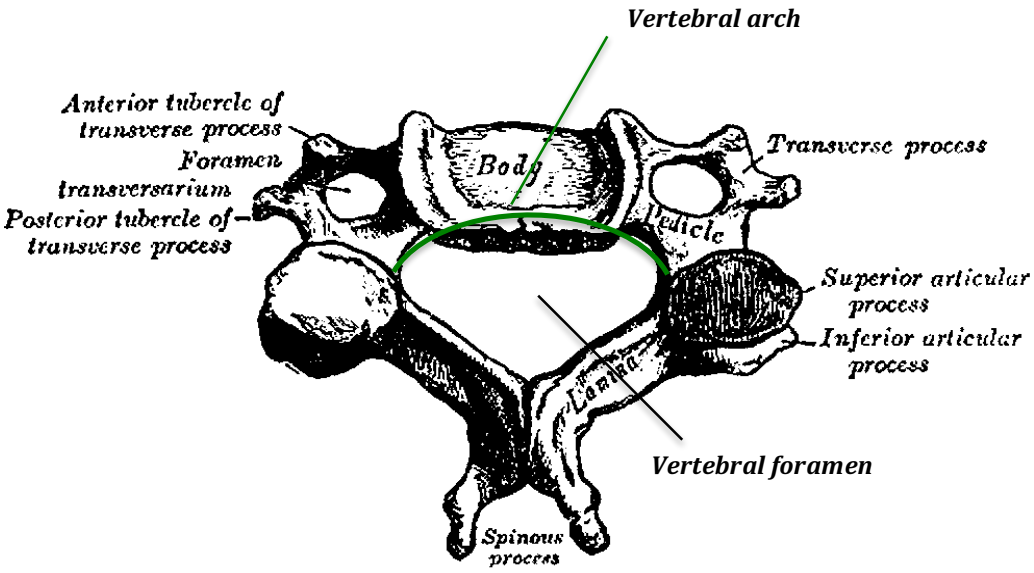

Figure 1.2. Anatomy of a human cervical vertebra. The processes, pedicles, lamina and vertebral body (Gray, 1918).

Cervical vertebrae are the smallest vertebrae in the vertebral column. The body of a cervical vertebra is small and is broader from side to side than from front to back. The first cervical vertebra, the atlas, has no body or spinous process and is considerably different in shape to the majority of the remaining vertebra. The atlas is a ring-like bone comprising an anterior and posterior arch and two lateral masses (Figure 1.3). The atlas, along with C2, the axis, forms a joint connecting the skull with the spine.

The thoracic vertebrae support the ribs and enable flexibility of the spine. The vertebral bodies in this region are roughly cylindrical in shape. The upper thoracic vertebrae are similar in shape to those of the cervical vertebrae. The mid thoracic vertebrae are heart shaped and the lower thoracic vertebrae are kidney shaped, similar to the lumbar vertebrae (Watson et al., 2008). The lumbar vertebrae are the largest in the spine and enable larger loads to be sustained.

It is crucial to understand the anatomy and biomechanics of the spine in a healthy system, in order to treat spinal pathologies appropriately. The biomechanics of the spine has been widely researched and information regarding spinal stability, torque resistance, intervertebral pressure and load bearing are readily available (Benzel, 2001; Adams & Dolan, 2005; Winkelstein, 2012; Poitout, 2016).

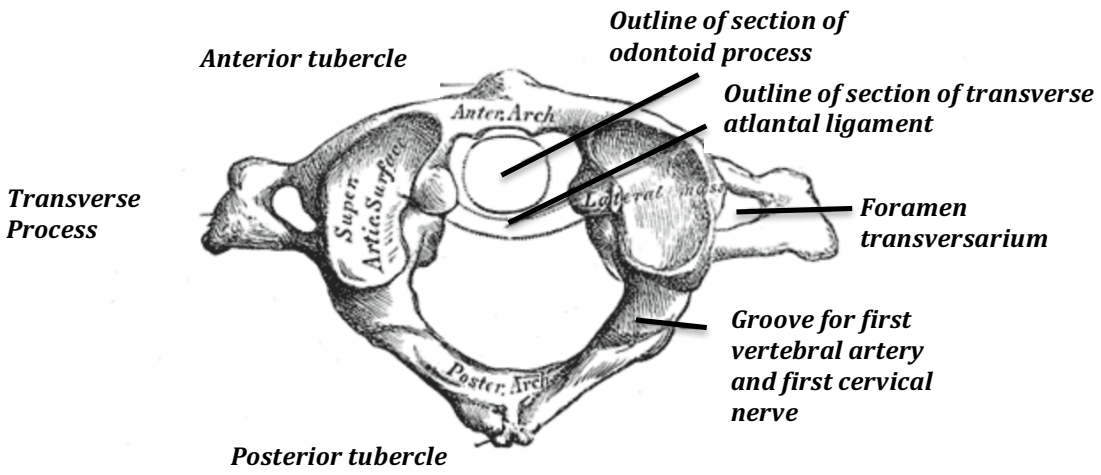

Figure 1.3 The atlas is the first cervical vertebra of the cervical spine. This vertebra has no body or spinous process (Gray, 1918).

The curved nature of the spine is designed to bear load as it evenly distributes the load along the vertebral column. The weight of the body is transmitted through the vertebral column to the hips and lower limbs. However, as most of the body weight lies anteriorly, the spinal curvature brings the weight in line with the body's axis.

When describing movement within the spine, a tri-axis coordinate system, utilising x, y and z-axes, is employed to explain displacements. The spine moves with six degrees of freedom: flexion extension (angular movement in the sagittal plane around the Y-axis), lateral bending (angular movement in the frontal plane around the X-axis), axial torsion and traction (angular movement in the transverse plane around the Z-axis) (ISO 18192-1). Together with the intervertebral discs, facet joints also enable motion, have load-bearing capability and move with six degrees of freedom; (Smith & Fernie, 1991). These facet joints are typical diarthrodial joints possessing cartilage surfaces, which provide a low-friction interface to allow motion in a healthy spine (Jaumard et al., 2011). During full extension of the spinal column, the lower facet joints have been reported to support 16 % of the applied load and resist torsion due to their bony interactions.

Upon axial loading of the vertebral column, axial compression of the intervertebral discs occurs. If the load is not applied to the body's centre of rotation, the vertebral column will bend to take the load.

1.2 The healthy intervertebral disc

A functional spinal unit is comprised of two vertebrae and an intervertebral disc and is the smallest physiological motion unit of the spine. The intervertebral disc (IVD) lies between adjacent vertebrae and links them together. The role of the IVD is mechanical in

nature, allowing the persistent transmission of load, arising from body weight and muscle activity within the spinal column, enabling 3D motion (Raj, 2008). The intervertebral discs enable; bending, flexion and torsion by providing flexibility. The intervertebral disc is a complex structure comprised of three regions; the gelatinous nucleus pulposus (NP) at the centre of the disc, which is contained inferiorly and superiorly by cartilage end plates and is contained circumferentially by the annulus fibrosus (AF).

1.2.1 The nucleus pulposus

The nucleus pulposus (NP) comprises randomly orientated fibres of collagen, water, proteoglycans and radially aligned elastin fibres embedded in an aggrecan-containing hydrated gel. The random alignment of the collagen fibres plays a crucial role in the tissues isotropic mechanical properties, meaning the mechanical properties of the tissue are identical, regardless of direction of application. The collagen fibres account for approximately 20% of the dry weight of the NP. Type II collagen makes up 80% of the collagen content of the NP, the remaining collagen content comprises types; V, VI, IX and XII. Dispersed within this hydrated gel in low numbers (5000/mm^3) are chondrocyte-like cells, these cells are sometimes located in a capsule within the matrix (Colombier et al., 2014) and are predominantly involved in the production of type II collagen and aggrecan. Approximately 30-50% of the dry weight of the NP is proteoglycan and approximately 70-80% of the total weight of the NP is water.

After water, proteoglycans are the most abundant substance in the NP and play a crucial role in the function of the IVD. The main proteoglycan present in the IVD is aggrecan. Aggrecan possesses a brush-like assembly. This proteoglycan macromolecule is made when many aggrecan molecules attach to a long hyaluronan molecule via link proteins. These proteoglycans possess a net negative charge, which attract positively charged ions into the NP to achieve electroneutrality, here the ion concentration within the tissue is greater than the concentration outside the tissue surrounding the NP, yielding an osmotic pressure within the IVD, causing the entry of water into the tissue. The entry of water into the tissue, the in-balance in ion concentrations and the negative charge of the glycosaminoglycan contribute to intradiscal pressure within the NP. It is this pressure, which enables the disc to transmit compressive loads within the spine.

1.2.2 The annulus fibrosus

The nucleus pulposus is surrounded by the annulus fibrosus (AF), which is comprised of concentric rings (15-25) of collagen fibres (lamellae) embedded within a proteoglycan matrix (Figure 1.4). The collagen fibres within each lamella are parallel to one another but

are arranged at approximately 60° to the vertical axis (Yu et al., 2007), switching from 60° left of the longitudinal axis to 60° right of the axis between lamellae (Figure 1.4). It is this layered structure, which allows the IVD to withstand large loads, applied in multiple directions. Elastin fibres play a key role in maintaining the structure of the IVD. When the IVD deforms under load, the elastin fibres enable the disc to return to its original height and shape (Yu et al., 2002). The fluid present in the NP deforms under load, however, the volume cannot be compressed, and as a result compression forces are transmitted in all directions to allow deformation of the NP. When load is applied, the height of the NP decreases, whilst the radial distance increases towards the AF (Guerin & Elliot, 2006). The inner region of the AF is occupied by cells that have a similar nature to cells of the NP (Setton & Chen, 2004). Within the outer region of the annulus are fibroblast-like cells. These are long, thin cells that lie in parallel with the collagen fibres.

1.2.3 Cartilage end plates

End plates, the interface between the hard bony vertebra and the pliant intervertebral disc, are comprised of a bilayer of cartilage, <1mm thick, and bone. The deep calcified region of the end plate is adjacent to the vertebrae. This layer is covered with hyaline cartilage, comprising proteoglycans, water and collagen (predominantly type II and some type I collagen). Here the collagen fibres are aligned vertically, in parallel with the ends of the vertebrae (Lotz et al., 2013). This uniform structure assists the even distribution of load across the IVD.

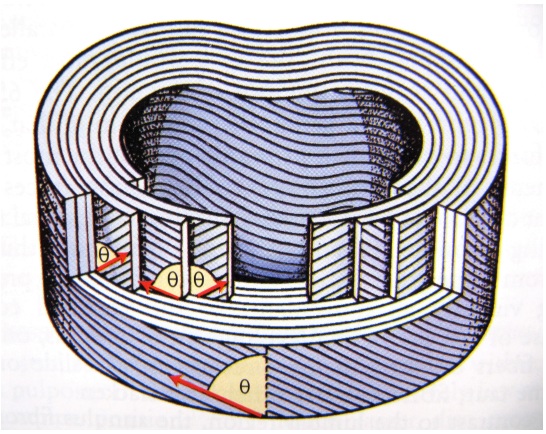

Figure 1.4 The organisation of the annulus fibrosus. The collagen fibres are organised in multiple concentric rings with alternate layers running in interchanging directions at a 60° angle to the vertical axis (Neumann, 2010).

1.3 Degenerative disc disease

Degenerative disc disease (DDD) is a common condition of the ageing process and for most people is asymptomatic. For certain individuals the morphological alterations associated with disc degeneration can cause back pain. The characteristic signs of DDD

include; pain and stiffness in the back, which may spread to the neck and to the extremities; shoulders, arms, hands, legs and feet.

There is a strong association between back pain and degeneration of the intervertebral disc (Urban & Roberts, 2003). Over 75% of low back pain is associated with DDD (Schaff, 1998). In a healthy disc the nucleus is well hydrated and applies a hydrostatic pressure (or intradiscal pressure) on the annulus, enabling transfer of loads between adjacent vertebral bodies (discussed previously in section 1.2.1). In the case of a degenerated disc both the NP and the AF alter with age (Kurtz & Edidin, 2006). As the body ages the proteoglycan concentration in the NP decreases and the nucleus becomes less hydrophilic, resulting in a loss of fluid from the disc. The dehydration that follows is caused by alterations in the keratin sulphate to chondroitin sulphate ratio, changes in the collagen fibres and an increase in collagen-proteoglycan binding (Kurtz & Edidin, 2006). Such alterations cause the nucleus to become less resilient and more fibrous in nature. Dehydration causes the level of deformation under load to be considerably greater, resulting in reduced disc height and pain. The fibres of the annulus are no longer loaded under tension, as they are in the healthy disc. Instead the inner layers of the annulus may bulge inwards under compression. Changes to the mechanical loading of the AF may increase inter-laminae sheer stresses, which have the potential to result in cracks, fissures or tears in the tissue. Tears in the AF may lead to the expulsion of NP material, disc herniation or may even cause delamination of the annulus layers (Iatridis & Gwynn, 2004).

Degeneration significantly alters the cartilaginous end plates of the IVD. The end plates become thinner and calcify, diminishing the blood supply to the end plates. The blockage of the marrow contact channels, which in a healthy disc enables the passage of fluid to and from the end plate, restricts the removal of waste materials from the nucleus (such as lactic acid) and prevents the entry of nutrients such as glucose and oxygen (Maroudas et al., 1975, Ayotte et al., 2001). This lack of material transport prevents the maintenance of IVD chondrocytes, depleting the ability of the cells to function normally and maintain the ECM.

Decreased disc height as a result of degeneration impacts other localised structures such as the facet joints, again causing pain. Treatment for back pain associated with DDD begins with conservative treatment, the reduction of physical activity and the prescription of anti-inflammatory medication. This level of treatment has been found to be effective in patients suffering from back pain, within the first three months of

treatment. The remaining patients whose pain levels do not improve are considered for surgical intervention, which has a much greater economic burden than conservative treatment. Spinal fusion and total disc replacements are regarded as the most commonly utilised treatment modalities for reducing back pain associated with disc degeneration.

1.4 Spinal Fusion

Spinal fusion is the current gold standard for the treatment of degenerative disc disease (Serhan et al., 2011; Shichang et al., 2016). Approximately 450,000 spinal fusion procedures are performed annually in the U.S. (HCUP, Nationwide Inpatient Sample (NIS) Healthcare cost and utilisation project, 2011). In addition to this, approximately 16,000 revision fusion surgeries are performed each year (Kirkpatrick et al., 2005). There are numerous fusion devices available to the spinal surgeon including; segmental and non-segmental constructs or rigid and non-rigid connectors involving several types of instrumentation; rods, plates, hooks, wires and screws all of which are composed of different biomaterial combinations, approximately 35% of which are medical grade 316L stainless steel and 65% titanium alloy (Figure 1.5).

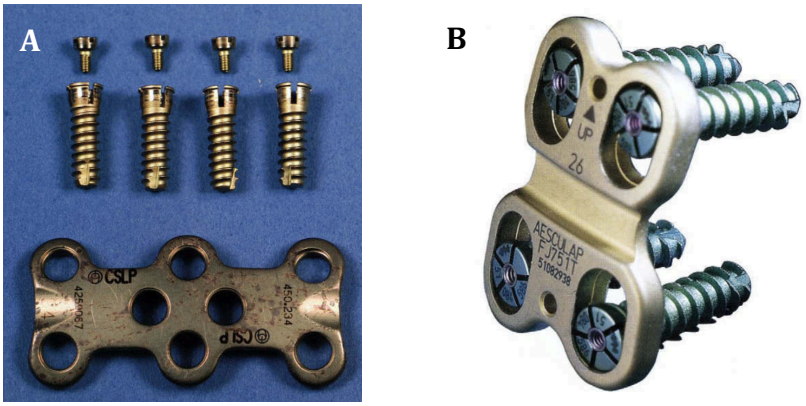

Figure 1.5 Spinal fusion devices A) Cervical spine three-level locking plate with four unicortical screws and anchoring expanding screws removed less than one year after surgery (Kurtz & Edidin, 2006). B) ABC dynamic cervical fusion plate and screw system, with variable angle screws to reduce stress shielding in the cervical spine (Kurtz & Edidin, 2006).

Spinal fusion surgery aims to restore disc height, reduce pain and re-establish stability in a specific spinal segment, relieving neurologic symptoms with minimal complications (Bohlman et al., 1993; Neuman, 2014). Spinal fusion promotes growth of bone over a joint or space in the spine, limiting the ability of the fused bones to move. The prevention of motion reduces the pain associated with instability.

1.4.1 History of spinal fusion

Early spinal fusion procedures involved the removal of the pain causing disc and utilised bone harvested from the Iliac crest to fill the joint space and promote bone growth and union between adjacent vertebrae (Kurtz & Edidin, 2006). There are difficulties with this procedure, including problems with donor site morbidity and instances of non-fusion. The need to minimise problems with harvest site complications has led to the development of various commercial bone graft substitutes (Kurtz & Edidin, 2006). Allografts, the use of demineralised bone matrix and hydroxyapatite to ensure the formation of a lasting union following spinal fusion surgery, have been used with varying rates of success (Heary & Madhavan, 2008). Kim et al. (2016) reported a 52% fusion rate using hydroxyapatite and demineralised bone for lumbar interbody fusion, which was not statistically different from a 62.2% success of fusion in a matched autograft group. An 80.8% fusion rate was reported when demineralised bone was used to fuse multiple vertebrae compared to an 85.7% fusion rate when using autologous laminectomy bone for long multi-segment posterolateral spinal fusion (Fu et al., 2016). The results of both studies highlight the similarity in the rate of fusion between autologous bone and the use of demineralised bone matrix.

In 1953 Paul Harrington developed posterior hooks and rods for spinal fusion. The Harrington Rod is a stainless steel distraction rod, with hooks at both ends for attachment to the vertebral laminae and possesses a ratchet mechanism for adjustment (Figure 1.6).

Figure 1.6 The Harrington rod system. Secured with hooks at both ends. Removed after being *in vivo* for 13.5 years (Kurtz & Edidin, 2006).

This instrumentation was restricted as it could only attach to the spine in two locations, at either end of the rod. Also the rod was rigid and straight, which did not recreate the natural curvature of the spine (Good, 2010). A 12.5% incidence of failed instrumentation was reported (Erwin et al., 1980) following the analysis of over 2000 medical records from 1961-1974. To account for the problems faced by the Harrington rod system including hardware fracture, loosening, corrosion and non-union (Prikryl et al., 1989; Lark et al., 2013), segmental instrumentation was developed in 1973 by Edwardo Luque. This two-rod system was contoured, restoring the normal spinal curvature. These rods were attached to the vertebrae by wires passed through the lamina of each vertebra. In

the 1980's the Cotrel-Dubousset instrumentation was developed, here two flexible rods were used, this instrumentation enabled multiple fixation points along the spine using hook and rod combinations (Figure 1.7) (Good, 2010). Survivorship rates between 71% and 91.5%, after two years have been reported with the Cotrel-Dubousset instrumentation (Boos et al., 1992; Bago et al., 2003). The predominant failure modes for this instrumentation were; screw breakage, bending or loosening. Further advances have been made and pedicle screw systems have enhanced spinal fusion surgery by providing a more rigid fixation system, yielding an improved fusion rate and permitting fewer segments to be fused.

Figure 1.7 The Cotrel-Duboussett fusion instrumentation; rods, hooks and transverse rod connectors, retrieved after 8.3 years *in vivo* (Kurtz & Edidin, 2006).

1.4.2 The success of spinal fusion

Previously there has been much debate within the literature regarding the success of spinal fusion in comparison to non-operative alternatives. The success of a spinal fusion procedure can be measured in numerous ways; pain relief, promotion of union, improved stability, minimal complications and ability to return to normal function.

It has been suggested that pain relief achieved from spinal fusion is greater than that from conservative treatments alone. Utilising numerous pain, disability and depression measurement systems; the Visual Analogue Scale (VAS), the Oswestry Low Back Pain Questionnaire, the Million Score, the General Function Score (GFS) and the Zung Depression Scale, Fritzell et al. (2001) reported a 33% reduction in back pain in patients who were treated with a spinal fusion procedure, compared with a 7% reduction in pain in the nonsurgical treatment group. However, due to a significantly greater number of patients in the surgical treatment group (222) compared to the conservative treatment group (72) in this study, there may be the introduction of unintended bias.

In contrast, Fairbank et al. (2005) compared the effects of lumbar fusion with an intensive non-surgical rehabilitation programme for the treatment of chronic low back pain. Two years post-surgery, or post rehabilitation, each patient was scored using the Oswestry disability index. No significant difference in the level of improvement was observed between the two groups. Fritzell et al. (2001) utilised a wider range of pain and disability scores compared to the single measurement used in this study, which may have led to a more thorough analysis of the patient's condition.

In addition to the ability of spinal fusion to treat pain associated with DDD, there are numerous complications and long term-implications to consider. Spinal fusion does not restore the normal biomechanics of the spine. As a result it is common for patients to experience adjacent level effects (ALE) post spinal fusion surgery, due to a lack of mobility in the fused segment (Yoshihara, 2013). Here segments either side of the fused vertebral body experience hastened degeneration, as these vertebral bodies try to compensate for the immobile region. The global motion of the spine is unaffected but the spine recruits alternative regions to carry out the same tasks. This could result in further surgery being necessary. Following a cervical fusion procedure, ALE have been reported at a rate of 2.9-8% per year of follow up (Hilibrand et al., 1999; Goffin et al., 2004; Ishihara et al., 2004; Horsting et al., 2012). Considering that there is much debate within the literature regarding the effectiveness of spinal fusion to treat back pain as a result of DDD compared to non-surgical alternatives and with increasing incidences of adjacent level effects, alternative motion preservation devices were sought (De Kleuver et al., 2003).

1.5 Total disc replacement

The aim of total disc replacements (TDR) is to preserve motion (where fusion limits motion), reduce pain associated with DDD and to maintain the normal kinematics of the functional spinal unit, thus potentially avoiding ALE (Hochschuler et al., 2002; Phillips & Garfin, 2005). The most common design observed in TDR's are the fixation of metal end plates (stainless steel, titanium or the most commonly used cobalt chrome) into the vertebral bodies above and below the disc space with either a metal or a polyethylene articulation (predominantly metal-on-polyethylene articulations) (Veruva et al., 2014). The FDA have strict regulations when considering patients for cervical total disc replacements (cTDR). Auerbach et al. (2008) identified that only 43% of patients considered for cervical total disc replacement actually met the necessary requirements. The FDA contraindications for cTDR are detailed in Table 1.1.

Table 1.1 Contraindications for total disc replacement surgery set out by the FDA

FDA Contraindications	
Mechanical	Cervical instability, previous surgery at the level to be treated, rheumatoid arthritis, reduced spinal motion, excessive loss in disc height.
Biological	Hepatitis, HIV, diabetes, pregnancy, infection, obesity, osteoporosis, autoimmune disease, metallurgy.

Upon designing a TDR there are a number of criteria which need to be considered for a successful implant (Hallab & Singh, 2014). The total disc replacement should; preserve motion, restore disc height, restore stability to the spinal segment, accurately transmit loads, perform for the life span of the patient, resist wear and corrosion to the greatest degree possible, be stable, failsafe, revisable and monitorable. Currently seven cTDR's have been approved by the FDA, on the basis that preclinical testing has provided sufficient evidence that they meet the above criteria of a successful device. These devices are outlined in Table 1.2 and shown in Figure 1.8.

Table 1.2 The seven cervical total disc replacements approved by the FDA

FDA Approved cervical total disc replacements				
Prosthesis	Manufacturer	Material	Articulation	Year approved
PRESTIGE® ST	Medtronic	Stainless steel	Metal-on-Metal	2007
ProDisc C®	Depuy Synthes	Cobalt Chrome And Polyethylene	Metal-on-Polyethylene	2007
Bryan c	Medtronic	Titanium	Metal-on-polyurethane	2009
PCM cervical disc®	Nu Vasive	Cobalt Chrome And Polyethylene	Metal-on-Polyethylene	2012
Secure®-C	Globus Medical	Cobalt Chrome And Polyethylene	Metal-on-Polyethylene	2012
Kineflex-C ®	Spinal Motion	Cobalt Chrome	Metal-on-Metal	2013
Mobi-C®	LDS Spine	Cobalt Chrome And Polyethylene	Metal-on-Polyethylene	2013

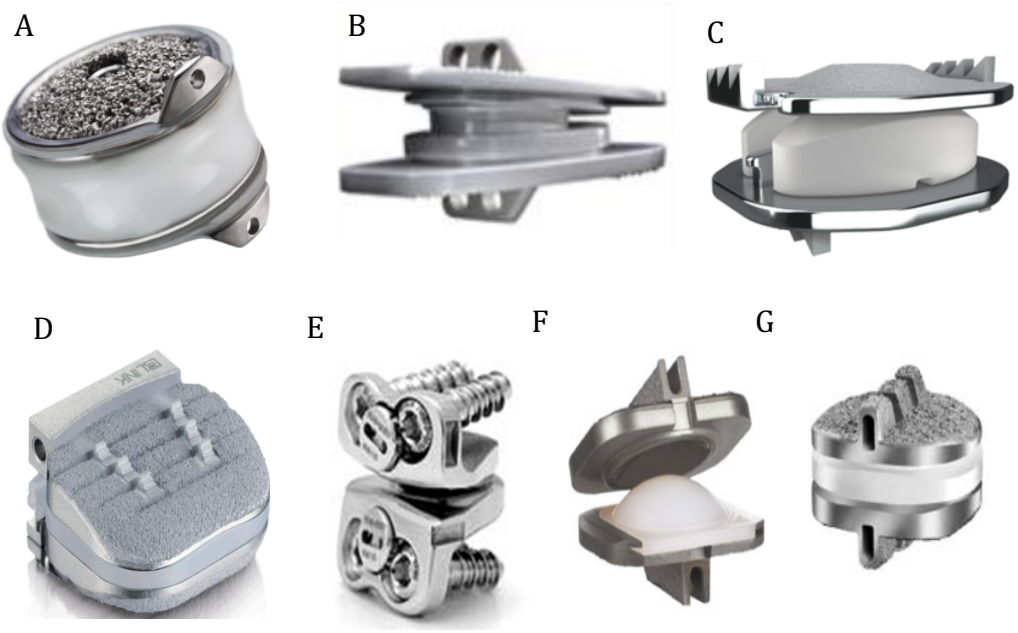

Figure 1.8 Current FDA approved cervical total disc replacements A) Bryan Cervical disc (O'Boynick & Darden, 2016) B) Kineflex-C ® (Palepu et al., 2012) C) Mobi-C® (O'Boynick & Darden, 2016) D) PCM cervical disc® (O'Boynick & Darden, 2016) E) PRESTIGE® ST cervical disc (O'Boynick & Darden, 2016) F) ProDisc C® (O'Boynick & Darden, 2016) G) Secure®-C (Vaccaro et al., 2013).

Although total disc replacements aim to alleviate some of the problems associated with spinal fusion, these implants present different problems and failure mechanisms. Such issues include hyper-mobility, hypo-mobility, material wear and adverse reactions to wear particles such as; osteolysis, metallosis and pseudotumour formation (Reeks & Liang, 2015). There has been much debate in the literature regarding the effectiveness of TDR compared to spinal fusion surgery, in terms of relieving pain associated with DDD.

Sasso et al. (2011) conducted a four-year follow up clinical investigation comparing the ability of the Bryan cTDR and the Atlantis cervical plating fusion system to reduce pain associated with DDD. A 15-point improvement in the neck disability index score, neurological improvement, absence of serious adverse incidents in association with the implant or implant procedure and lack of additional surgical intervention was regarded as a surgical success. Patients who received a cTDR demonstrated an 85.1% success rate in the treatment of DDD compared to 72.5% in the spinal fusion group (Sasso et al., 2011). Zigler et al. (2007), reported that the ProDisc-L total disc replacement provided pain relief and improved function in patients that were equal to the benefits provided by fusion surgery. Here, the VAS and Oswestry disability index scores significantly improved

in both treatment groups as early as 6-weeks post-surgery and remained so throughout the 24-month follow-up period with no significant difference between the two conditions. In a similar investigation Guyer et al. (2009), found no significant differences in the improvement in pain intensity scores when patients were treated with the Charité III lumbar TDR and the BAK fusion cage to reduce pain, after two and five years post-surgery. However, with large differences between the numbers of patients allocated to each surgical treatment group (205 in the TDR group and 99 in the fusion group) implications of bias cannot be discounted.

The comparison between the effectiveness of spinal fusion instrumentation and total disc replacements to relieve pain associated with degenerative disc disease is still lacking a high quality, long-term prospective study. Controlled, long-term (longer than ten years) follow-up studies with equal group sizes, relevant control groups and more uniform methods of analysing success are required to establish the efficiency and the longevity of the devices. The results presented by Sasso et al., (2011), Zigler et al., (2007) and Guyer et al. (2009) predominantly focus on short-term success. The existing evidence, specifically regarding long-term effectiveness and/or safety is considered insufficient to justify or refute the widespread use of TDR preferentially to spinal fusion for a single level degenerative disc.

A key motivator in the use of TDR to treat back pain associated with DDD lies in its ability to preserve motion and thus reduce the risk of ALE and the need for additional surgery. However, there are conflicting findings presented in the literature regarding the ability of TDR to minimise this complication. A series of published meta-analyses regarding the incidence of ALE following spinal fusion and TDR have demonstrated minimal clinically relevant differences between the two surgical procedures (Heller et al., 2009; Murrey et al., 2009; Bartels et al., 2010; McAfee et al., 2012). However, within the literature there have been numerous reports of elevated rates of ALE in patients undergoing a spinal fusion procedure to treat DDD compared to patients receiving a TDR (Robertson et al., 2005; Coric et al., 2011), with incidences of severe ALE radiographic changes in as many as 24.8% of patients with fusion instrumentation and 9% in those treated with TDR (Coric et al., 2011). Garrido et al. (2011) observed a greater incidence of ALE in patients after anterior cervical discectomy and fusion compared to patients who received a Bryan cervical disc, with 36% of patients presenting no ossification (indicative of a hastened degeneration of the neighboring functional spinal unit) in the fusion group after two years and 16% had no ossification at four years compared to 75% of patients had no ALE at two years and 48% had no ossification after four years in the TDR group. However, due to

disproportionate group sizes, short follow up periods (four years) and the use of radiographs in isolation to evaluate the incidence of ALE, there is likely to be unintended bias in these findings. Such investigations highlight the necessity for clinical analysis in addition to the use of radiographic findings to report the onset of ALE.

Numerous criteria are required to determine the incidence of ALE, including; a patient history, a physical examination prior to surgery (for post-surgery comparison), neurological evaluation of the patients strength, sensation, and reflexes in addition, to evaluate using; plain radiography, myelography, computerised tomography and MRI imaging pre and post-operatively (Hilibrand et al., 1999). Though the work of Garrido et al. (2011), Robertson et al. (2005) and Coric et al. (2011) quote Hillibrand's findings as a standard for detecting ALE, none of these studies used the same level of analysis to assess ALE occurrence (Nunley et al., 2013).

1.6 Biomaterials used in total disc replacements and spinal fusion

Two major biomaterials are utilised when designing total disc replacements and spinal fusion instrumentation; metals (cobalt chrome, stainless steel and titanium), and polymers (UHMWPE, polycarbonate urethane, polyether urethane). Each material possesses different characteristics, which makes it suitable for use in spinal implants.

1.6.1 Metals used in total disc replacements and spinal fusion instrumentation

Metals deliver an unparalleled combination of high strength, ductility, hardness, fracture toughness, corrosion resistance and biocompatibility for use in the design of orthopaedic implants and are cost-effective (Hallab & Singh, 2014). Metal alloys, a mix of two or more metals, enable desirable characteristics of several materials to be combined into one biomaterial for use in the production of orthopaedic implants. Pure metals are not often used in these applications, as they tend to be soft, brittle and reactive. Stainless steel, cobalt chrome and titanium have been used in metal-on-metal articulations or in conjunction with polyethylene and ceramic components for total disc replacements for the past 50 years.

1.6.1.1 Stainless steel

Stainless steel, an alloy of; iron, nickel and carbon, with a minimum of 10.5% chromium by mass, does not easily rust or corrode. Stainless steel has been used in the design of total disc replacements since the 1980's. It was first used in the Bristol/Cummins device, this device introduced an articulating metal-on-metal coupling based on a ball and socket design, secured to the vertebral body with a plate and screw fixation system (Chapman &

Riew, 2012). Over the years this device was modified to encompass a more anatomically relevant end plate design and a porous coating to promote bony ingrowth (the PRESTIGE® ST), which received FDA approval in 2007. Stainless steel has also been used in spinal fusion instrumentation. In more recent years cobalt chrome and titanium metals have been seen as more favourable and they have more desirable yield strength and are less susceptible to corrosion and fatigue (Bankston et al., 1993).

1.6.1.2 Cobalt chrome

Cobalt chrome, an alloy of cobalt and chromium, exhibits superior mechanical and wear properties when compared to stainless steel and titanium. Due to the presence of 5-7% molybdenum in this alloy it is sometimes referred to as cobalt chrome molybdenum. High carbon wrought cobalt chrome used for orthopaedic applications (in accordance with ASTM F75) has a high yield strength and is approximately twice as stiff as titanium. Cobalt chrome is commonly used in total disc replacements as a result of its theoretical corrosion resistance for implantation. Within the spine, cobalt chrome is commonly used in both metal-on-metal and metal-on-polyethylene total disc replacements (Kineflex-C®, Mobi-C®, PCM cervical disc®, ProDisc C® and the Secure®-C).

1.6.1.3 Titanium

Titanium has a lower Young's modulus compared to cobalt chrome and stainless steel, which matches more closely to the Young's modulus of bone, resulting in greater mechanical compatibility, osseointegration and fixation. This observation has resulted in titanium being used on the outer surface of cervical total disc replacement end plates for long-term fixation (Pham et al., 2015). The Bryan, ProDisc C® and Mobi-C total disc replacements utilise this technology. The Bryan cTDR encompasses titanium end plates and a polyurethane core. The ProDisc C® is comprised of titanium plates, coated with plasma sprayed rough pure titanium. The Mobi-C® possesses cobalt chrome end plates, with a roughened titanium surface coated with hydroxyapatite. Titanium is not regarded as a viable material for articulating bearing surfaces due to inferior wear characteristics and poor abrasion resistance (Head et al., 1995). Interestingly, titanium produces fewer artefacts when imaged using MRI, compared to stainless steel and cobalt chrome alloys (Taksali et al., 2004). The stainless steel PRESTIGE® total disc replacement generated significant artefacts, limiting post-operative imaging of the implant and adjacent spinal segments (Boden et al., 2004).

1.6.2 Polymers in total disc replacements

Polymers are typically regarded as bio-inert materials. The most common polymer used in total disc replacements is ultra-high molecular weight polyethylene (UHMWPE). However, as observed in total hip and disc replacements this material wears at an elevated rate compared to metal-on-metal articulations and so in more recent years efforts have been made to reduce the wear by crosslinking the polymer (Kurtz et al., 1999; McKellop et al., 1999; Muratoglu et al., 2001). This was effective in reducing wear in hips but altered the mechanical properties of the material. Doping with anti-oxidants such as vitamin E has also been used to reduce wear in the hip (Oral et al., 2004; Reno & Cannas, 2006; Oral et al., 2007; Oral & Muratoglu, 2011).

1.7 Wear of orthopaedic biomaterials

The longevity of any orthopaedic device is compromised by wear, regardless of the biomaterial combinations selected. However, some material combinations wear more than others (Chen & Thouas, 2015). Metal biomaterials are capable of forming two types of wear products; metal wear particles (from frictional articulation) and metal ions (from corrosion) (Doorn et al., 1996; Tipper et al., 2005).

1.7.1 Mechanisms of wear in total joint arthroplasty

The most commonly observed mechanisms of wear in total joint arthroplasty are; adhesive wear, abrasive wear and third body wear. By understanding the mechanisms of wear of an orthopaedic implant, surgeons, clinicians and material scientists alike can better understand the performance of the device *in vivo,* this information can be used in future implant development.

Adhesive wear occurs when two materials are in contact, and adhesion bonding takes place. Here the pressure between the two contacting surfaces is great enough to cause plastic deformation and adhesion (Eyre, 1976). This bonding results in the shearing of material upon articulation. Burnishing, associated with adhesive wear has been observed with metal-on-polyethylene and metal-on-metal total disc replacements (Kurtz et al., 2009). Burnishing is characterised by a polished glossy appearance and is the result of plastic deformation of a surface due to articulation, this occurs if the contact stress between the articulations is larger than the yield strength of the material.

When one surface is much harder than the other abrasive wear may occur, this is evidenced by scratching and is commonly seen with metallic and polyethylene implants for TDR. Abrasive wear is due to hard protuberances forced to move against a softer

surface. At a microscopic level, surfaces are not entirely smooth, they possess irregularities, upon articulation these asperities meet; the protrusions must either deform or fracture. When two surfaces are brittle, the asperities fracture and break off. However, if one material is softer than the other the harder surface will damage the softer surface causing progressive loss of the softer material. This mechanism of wear can occur either at the primary articulation or at other secondary surfaces (Bozic & Ries, 2005).

Third-body wear occurs when third-body particles become embedded in the articulating bearing. This in turn can scratch the metal bearing surface. The formation of a scratch in the metal results in the formation of a trough, with metal elevated on either side of the depression. These ridges cause further abrasive wear of the polyethylene component.

Metallic implants and their wear products are subject to corrosion when exposed to the *in vivo* environment. It is essential to understand the mechanisms of corrosion in order to understand the host response to corrosion by-products.

1.8 Corrosion

There are two key features that govern how and why a metal corrodes, the first attribute is the thermodynamic driving force; oxidation and reduction reactions and the second phenomenon involves kinetic barriers, which limit the rate of corrosion.

The corrosion of wear particles *in situ* causes alterations to the size and shape of the wear debris generated by metal-on-metal implants, which may affect the host response. Cobalt and titanium ions are more soluble than aluminium and chromium ions, as a consequence of this, cobalt and titanium are readily removed from the region of the implant, whereas aluminium and chromium persist in periprosthetic tissues (Shahgaldi et al., 1995). This corroborated the findings of Case et al. (1994), where five times more cobalt and twice as much chromium was found in the lymph nodes than in the synovium of individuals with failed metal-on-metal total hip replacements. During corrosion, metal atoms lose electrons forming free metal ions in solution; these can either disseminate away from the metal surface or can lead to the formation of metal oxides or organometallic compounds. These products can exist as solids or can be soluble. The second factor, which governs the process of corrosion of metallic biomaterials are kinetic barriers, which are physically capable of limiting the oxidation and reduction reactions. The most common example of a kinetic barrier is the formation of a passive oxide layer on the surface of the metal. These kinetic barriers prevent the migration of metal ions from the metal into solution, inhibit the movement of metal anions from solution to the metal and reduce the migration of

metal ions across the metal-solution barrier. These passive oxide films must encapsulate the surface of the metal and must remain undisturbed upon application of mechanical stresses and abrasion, which is anticipated in the articulation of orthopaedic implants (Jacobs et al., 1998). Generally speaking the more the oxide layer is compromised the less able the oxide layer is able to prevent corrosion.

All metals corrode when exposed to biological systems, the products of corrosion are typically oxides (Cr_2O_3 and CoO), metal phosphates, metal salts, metal ions bound to proteins or organometallic compounds (Hallab et al., 2009). Metal ions can combine with serum proteins and trigger an immune response (Goodman, 2007). Metal-protein complexes can be regarded as candidate antigens in the onset of a hypersensitivity response (Martin, 2004). The most common forms of corrosion observed in total disc replacements are fretting corrosion, crevice corrosion and galvanic corrosion leading to a "battery effect".

1.8.1. Fretting corrosion

Fretting corrosion, most commonly associated with modular taper junctions in total hip arthroplasty and with modular fusion instrumentation in the spine, is correlated with micro-motion between metal-on-metal components. Fretting corrosion typically occurs between two bodies, which have a small oscillatory motion of small amplitude, in particular where the motion is no greater than 100μm (Waterhouse, 1972). Fretting corrosion occurs as a result of contact between a few "high spots" or asperities between the materials. Micromotion between the two surfaces causes the production of wear products and material transfer. Cyclic loading causes disruption of the passive oxide film of the metal, leaving the exposed biomaterial and wear products subject to oxidation and corrosion.

1.8.2 Crevice corrosion

Crevice corrosion occurs as a result of part of the metal surface being shielded or in a restricted environment (the crevice) compared to the rest of the metal, which is exposed to an electrolyte. Initially anodic (oxidation) and cathodic (reduction) processes occur at the surface of the metal causing the formation of metal ions. As oxygen is used up in these reactions, more oxygen diffuses in from the surrounding electrolyte. The crevice now acts as an anode and the overall charge within the crevice is positive, there is now a potential difference between the crevice (positively charged) and the outside solution. Negatively charged ions from the electrolyte (normally chloride ions) diffuse into the crevice to balance the charge. The chloride ions enhance the corrosive effect and form complexes

with metallic ions, which upon interaction with water, form acid. This continues the metallic attack, referred to as an autocatalytic process (Bryant, 2013).

1.8.3 Galvanic corrosion

Galvanic corrosion is an electrochemical process, which occurs when two dissimilar metals are in contact in the presence of an electrolyte. Here one metal behaves as an anode and the other as a cathode. The less noble metal is more likely to behave as an anode in the presence of an electrolyte, the more noble metal is more likely to behave as a cathode. The electro-potential difference between the two materials provides a driving force for the anode to dissolve into the electrolyte, resulting in the collection of deposits on the cathodic metal (Hesketh, 2012). The electrolyte allows the migration of ions between the anode and the cathode, which leads to the metal at the anode corroding more quickly than it otherwise would, causing an inhibition of corrosion at the cathode (the battery effect). Galvanic corrosion is a particular problem for modular hip replacement systems, and due to the modular nature and use of mixed metals in total disc replacements there is a growing concern that galvanic corrosion may also be a problem with these devices (McTighe et al., 2015).

1.9 Wear and corrosion in modular implants

Though the wear rates of metal-on-metal total hip replacements are significantly lower than metal-on-polyethylene total hip replacements the wear particles produced upon articulation are smaller at approximately 30nm in length (Firkins et al., 2001). These small particles provide a large surface area and energy for ion release. Metal wear products from metal-on-metal and metal-on-polyethylene devices have the potential to disseminate widely throughout the body with particles found in the lymph nodes, spleen, bone marrow and liver (Langkamer et al., 1992; Case et al., 1994; Shea et al., 1997; Urban et al., 2000; Campbell et al., 2003; Urban et al., 2004). These metal particles can enter numerous cell types and be phagocytosed by macrophages. Total disc replacements are being increasingly implanted into younger patients (Karnoub et al., 2015), this may mean that metal particles may be present within the body for extended periods of time, potentially for 30-40 years. There have been concerns regarding the release of cobalt and chromium ions, which may elevate the risk of cancers such as leukaemia and lymphoma and the development of masses of necrotic tissue, pseudotumors (Guyer et al., 2011). Elevated concentrations of chromium ions have been found in the urine and blood of patients with metal hip devices (Jacobs et al., 1996). This phenomenon combined with an unacceptable number of total hip replacement revision procedures associated with an adverse tissue reaction has lead to the withdrawal of certain implants from the market

(Langton et al., 2011; Hug et al., 2013). Most noted in the literature was the withdrawal of the ASR™ hip resurfacing system and the ASR™ acetabular system in 2010, due to revision rates of 12% and 13%, respectively after five years (reported in the Seventh annual report from the National Joint Registry (NJR) for England and Wales). In addition to this, there have been growing concerns within the orthopaedic community regarding corrosion in modular hip devices, referred to as "trunnionosis". A modular head-neck junction can correct leg length inequality and permits alterations to femoral head diameter even after the stem has been implanted (McTighe et al., 2015). Depending on loading and the relative activity of a patient this taper junction can be susceptible to varying stresses, which may trigger fretting and/or corrosion.

Jacobs et al. (2014) in a recent report of 20 patients who had received metal-on-polyethylene total hip replacements found mechanically assisted crevice corrosion occurring at the taper junction at a mean follow-up of 3.9 years (0.7–17.3 years). Under normal mechanical loading the interface between the two mating surfaces of the taper junction is designed to be mechanically stable to prevent adverse effects such as loosening, fracture, wear or fretting damage. Although there is an intimate fit between the trunnion and the bore, which prevents disassembly of the device, small gaps may occur between the mating surfaces as a result of manufacturing tolerances between the components. Fluid entry and micro-motion (fretting) within these gaps and cyclic loading of the device may result in damage to the passive oxide layer leading to crevice corrosion. There is evidence in the literature that both the mechanical and corrosive processes occurring at the taper junction and cause the production of particulate debris and metal ion release (Pansard et al., 2012). There have been extensive reports within the literature regarding the adverse effects of the wear particles and ions associated with trunnion wear from metal-on-metal, metal-on-polyethylene and ceramic-on-ceramic total hip replacements (Hohman et al., 2011; Cooper et al., 2012; Vundelinckx et al., 2013; Jacobs et al., 2014), however, gross failure of tapers has been less widely reported in primary total hip replacements, with only a few case studies reported (Botti et al., 2005; Banerjee et al., 2015).

As spinal devices are often modular in nature this important lesson learned from total hip arthroplasty could be crucial to the design of better performing total disc replacements.

1.10 Wear simulation

One of the key factors affecting the longevity of total disc replacements is the wear resistance of the implant. The rapid evolution and improvement of wear simulation to

determine the wear performance of metals, polymers and ceramics used in total joint replacement has culminated in a more accurate prediction of the wear performance of biomaterials *in vivo*. By more closely simulating the *in vivo* conditions in terms of loading, lubrication and kinematics, the results of simulator studies can feedback and improve the design of total joint replacements.

Numerous methodologies for simulating wear have been used; pin-on-disc, pin-on-plate, sphere-on-disc wear simulators and whole joint simulators.

A crucial requirement for an appropriate method for wear simulation must be the ability to enable direct comparison between devices (Grupp et al., 2009). The development of multi-directional wear simulators was a crucial development for determining the *in-vitro* performance of biomaterials (Tipper et al., 1999; Baykal et al., 2014). In more recent years, advanced methods of wear simulation have been seen with the development of hip, knee and spine simulators which can be modified to closely mimic anatomical loading and kinematics.

In recent years, simulator testing of orthopaedic implants has vastly improved and there are now international testing standards; ISO and ASTM guidelines, for simulator input parameters for hip, knee and spine implants (ISO 14242, ISO 14243, ISO 18192 and ASTM F2423-05, respectively). International standards aim to establish uniform procedures for implant testing and to produce data that can be reproducible and comparable within and between different research laboratories for testing and reporting of the wear performance of total joint replacements. It must, however, be recognised that there are numerous variations in the *in vivo* conditions and numerous interpretations of the ISO and ASTM standards. An isolated simulation with definitive parameters may not be representative of the *in vivo* conditions.

Previously simplistic linear motion was used to determine the wear performance of orthopaedic biomaterials. Baykal et al. (2014) utilised a pin-on-disc wear simulator and test parameters in accordance with ASTM F732 (Standard Test Method for Wear Testing of Polymeric Materials Used in Total Joint Prostheses) to determine whether pin-on-disc testing was capable of correctly ranking the wear performance of non-irradiated, conventional (25-50kGy) and highly cross-linked (≥90kGy) UHMWPE. The mean wear rates of non-irradiated, conventional and highly cross-linked UHMWPEs were 7.03 mm^3/million cycles, 5.39 mm^3/MC and 0.67 mm^3/MC, respectively. Upon comparison of these wear rates with others reported in the literature that complied with the ASTM F732

guidelines, the mean wear rate of the highly cross linked UHMWPE was lower than the conventional and non-irradiated UHMWPE materials. Thus, pin-on-disc simulators can be used to compare highly cross-linked and conventional UHMWPEs despite different test parameters. However, narrowing the allowable range for standardised test parameters could improve the sensitivity of multi-axial testers in correctly ranking materials.

ISO 18192 (2011) stipulates guidelines for a test procedure to investigate the relative angular movement between articulating components in intervertebral spinal disc prostheses. It specifies the pattern, size of the applied force, speed and duration of testing, the orientation of the sample and provides a detailed specification for the test environment in order to simulate physiological conditions. In accordance with ISO 18192 calf serum, should be utilised as the test lubricant at a concentration of 20g ± 2g of protein/L. Six components should be used for wear testing. The details of the motion and loading parameters outlined by ISO 18192 are shown in Tables 1.3 and 1.4, respectively.

In accordance with ISO 18192 the superior component of the total disc replacement should be orientated in the superior position, enabling the axis of rotation in its neutral position to be situated at the centre of the axes of rotation of the test machine, this should be the same for the inferior component so as to avoid preloading in the initial test position.

Table 1.3. Angular displacements for both cervical and lumbar total disc replacements outlined by ISO 18192

Implant type	Angle	Flexion/Extension	Axial Rotation	Lateral bending
Cervical	Minimum	-7.5°	-4°	-6°
	Maximum	7.5°	4°	6°
Lumbar	Minimum	-3°	2°	2°
	Maximum	6°	-2°	-2°

Table 1.4. Loading parameters for both cervical and lumbar total disc replacements outlined by ISO 18192

Implant	Load (N)	
Cervical	Minimum	50
	Maximum	150
Lumbar	Minimum	600
	Maximum	2000

The intended sequence of the motion of the device outlined by the ISO standard is initially lateral bending followed by flexion/extension and finally axial rotation. The motions test the components in four degrees of freedom; flexion/extension, lateral bending, axial rotation and axial force and should be operated at a frequency of 1 Hz. Though the guidelines outlined in ISO18192 do not fully reproduce the complex *in vivo* loads and motions, they provide a structured testing system so wear data obtained within the parameters of this test method can be compared between differing total disc replacement implants, but may differ from wear rates observed clinically.

ASTM F2423-05 (2011), the Standard Guide for Functional, Kinematic, and Wear Assessment of Total Disc Prostheses provides similar guidelines on the wear simulation of a total disc replacement in terms of concentration of calf serum used in the test lubricant (20g of protein/L of medium) to ISO 18192. However ASTM F2423-05 suggests a minimum sample size of five for each kinematic/load profile. The key difference between these two standards is between the guidelines for test profiles, angular displacements and loading parameters. The test parameters for loads and motions of cervical total disc replacements outlined by ASTM F2423-05 are shown in Table 1.5 and should be operated at a frequency no greater than 2Hz. Between the two international standards, for the cervical spine, the parameters for flexion extension, lateral bending and axial load are comparable, however the level of axial rotation is greater in the ASTM F2423-05 guidelines. For the lumbar spine, the parameters for flexion extension, lateral bending, axial rotation and axial load are comparable.

Table 1.5 Loading parameters for both cervical and lumbar total disc replacements outlined by ASTM F2423-05

	Cervical		Lumbar	
Test Profile	Axial load (N)	Range of Motion	Axial load (N)	Range of Motion
Flexion extension	100	±7.5°	1200	±7.5°
Lateral bend	100	±6°	1200	±3°
Rotation		±6°	1200	±6°

In vitro spinal simulations performed on cobalt chrome lumbar metal-on-metal total disc arthroplasties in accordance with these international standards have revealed steady-state wear rates of 0.33 ± 0.12 mm^3 per million cycles in flexion extension and 0.43± 0.06 mm^3 per million cycles in combined motion, flexion extension, lateral bending and axial

rotation in accordance with ASTM F2423-05 (Paré et al., 2007). Such wear rates are significantly lower than conventional metal-on-polyethylene lumbar total disc replacements, which were reported to be 13.4-16.1mm^3 /million cycles in spine simulation studies (Hyde, 2012). Kurtz et al. (2012) compared simulator and *in vivo* retrieved metal-on-metal PRESTIGE®. Cervical total disc replacements. The parameters used for the spine simulation included; five million cycles with coupled motion; lateral bending (± 4.7°) and axial rotation (± 3.8°) with a 49N axial load followed by ten million cycles with flexion extension (± 9.7°) with 148N axial load. It is important to note that in the first five million cycles the parameters for lateral bending and axial rotation did not meet the guidelines of the international standards. Also the serum utilised in this study had a protein concentration of 11.5g/L, which is not comparable to parameters detailed in ISO-1819-2 and ASTM F2423-05. Kurtz et al. (2012) reported a wear rate of 0.74mm^3/million cycles in the first five million cycles and 0.03mm^3/ million cycles in the latter 10 million cycles of the test. Thus highlighting how coupled motion increases the wear rate in spine simulations. Despite the similarities in wear mechanisms between the *in vitro* and *in vivo* devices, the degree of wear was found to be much greater during the *in vitro* test when compared with the retrievals, regardless of their implantation time.

Using four individual wear testing regimes; in accordance with the parameters outlined by ISO 18192, lowered axial loading, altered centre of rotation and low cross shear, Hyde et al. (2015) assessed the wear performance of the metal-on-polyethylene Charité lumbar total disc replacement. The simulator parameters employed were as follows; for the ISO standard wear test; 600-2000N load, -3° flexion, 6° extension, ± 2° axial rotation and lateral bending, for the reduced load test; a load of 300-1000N was employed, however all other parameters matched the ISO standard. To achieve low cross shear the same parameters as the ISO test were used, however the flexion and extension and lateral bending parameters were changed from 90° out of phase to 0° in phase. Finally for the altered centre of rotation test the centre of rotation was inferior to the lower end plate as it would be *in vivo*. The wear rate was highest when the centre of rotation was altered with a wear rate of 17.8mm^3/million cycles reported. Thus demonstrating that by inducing changes to the kinematics and loading inputs of the standard testing regime (in accordance with ISO 18192) wear phenomena not found in standard ISO cycle results can be observed.

The International standard ISO 18192 only specifies parameters for four degrees of freedom in spine simulations. Two additional degrees of freedom exist in the spine *in*

vivo; anterior and posterior shear and lateral shear. Vicars et al. (2010) used a five-degree of freedom spine simulation to determine the effect of the addition of anterior-posterior shear on the wear of the ProDisc-L metal-on-polyethylene total disc replacement. The four-degree of freedom test met the parameters stipulated by ISO 18192 and the five degree of freedom test added an AP load of +175N anterior -140N posterior load. Vicars et al. (2010) reported a wear rate of 12.7 mg/million cycles with the four degree of freedom test and a lower 11.6mg/million cycle with the five degree of freedom test. These wear rates were larger than those reported by Nechtow et al. (2007) using the same implant and same parameters as the four-degree of freedom test by Vicars et al. (2010). Though the parameters were identical different wear rates of 4.64mg/million cycles and 5.30mg/ million cycles were reported. This study highlighted the problem upon comparing wear performance using the same parameters with differing simulator set ups. Thus caution should be employed when comparing results across TDR simulation, different simulator parameters as well as different test specimens and test environments. All conditions should be reported to enable informed conclusions.

1.11 Metal particle isolation and characterisation

To fully understand the mechanisms behind the wear of total disc replacements and the subsequent response of localised tissues to particulate debris, metal wear debris from *ex vivo* tissues from around failed implants must be analysed in terms of shape, size and chemical composition. It is crucial to optimise the particle isolation procedure and minimize changes to the debris as a consequence of the reagents used. *Ex vivo* particles from around fusion devices are not well characterised at this time and there has been limited characterisation of particulate debris from around metal-on-metal total disc replacements (Kurtz et al., 2005; Anderson et al., 2006) and spinal fusion instrumentation (Senaran et al., 2004; Kim et al., 2007). Efficient isolation and characterisation of metal wear particles generated *in vivo* provides essential information for the generation of clinically relevant CoCr and stainless steel particles and allows determination of the validity of *in vitro* spine simulators and pin-on-plate wear simulators. There are numerous challenges to overcome to develop an efficient protocol for the isolation of metal wear particles, for instance the small sizes and volumes of the particles make it difficult to isolate all the particles and minimize the effects of particle loss. The tendency of small (nano) particles to agglomerate means that it can be difficult to size these particles accurately. Previous methodologies to isolate metal debris from hip simulator serum have utilised alkaline treatments, but it is known that these reagents alter the size, shape and composition of the metal particles (Catelas et al., 2001). Thus there has been more interest in the use of enzymatic protocols for particle isolation (Doorn et al., 1998).

Catelas et al. (2001) performed a systematic study of the effects of different protocols, both enzymatic and alkaline, on metal particles isolated from hip simulator lubricants. The results highlighted that alkaline treatments performed on both large and small particles (generated in water) caused a decrease in the particle size. These effects increased with longer incubation periods and with greater concentrations of potassium hydroxide. The effects of the reagents used in each protocol were less pronounced on the particles generated in 95% (v/v) serum than on those generated in water, suggesting that the serum (and the proteins and lipids within it) had an initial protective effect on the particles, perhaps limiting the oxidizing action of the reagents. In terms of minimising alterations to particle size, shape and chemical composition and reducing particle agglomeration, enzymatic protocols yielded more promising results compared to other protocols. However this methodology is not without its drawbacks, particle loss is one of the main problems with this process. The enzymatic digestion process developed by Brown et al., (2007) involved numerous centrifugation (2), wash (12), dilution (12), heating (5) and digestion (12) processes to ensure the removal of serum proteins and any contaminants. Throughout this protocol the samples were often transferred between centrifugation tubes, here particles may be lost through inefficient transfer. Particles may also be lost during the centrifugation steps upon removal of supernatants. As a result of these factors it was difficult to isolate low wear volumes. Attempts have been made to minimise particle loss by utilising a single pass of ultracentrifugation following enzymatic digestion, which removed proteins and contaminants and deposited particles onto silicon wafers for imaging. During centrifugation, particles were passed through numerous layers of denaturants and a metal-selective high-density layer that reduced protein and nucleic acid contamination. This methodology reduced aggregation, and provided well-dispersed particles on a platform for size analysis (Billi et al., 2012). Within the literature, a novel particle isolation method has been developed to enable the recovery of 80% of ceramic particles from simulator serum used in wear testing of ultra-low wearing materials using enzymatic digestion in conjunction with a sodium polytungstate density gradient (Lal et al., 2016). This protocol is yet to be adapted for the use with metallic wear particles.

1.12 Retrieval analysis

The use of motion preservation devices as a treatment modality for back pain associated with DDD still remains in its early stages. This technology will progress with pace by facing its failures and learning from its successes (2000 NIH consensus statement). By observing the failures of metal-on-metal total hip and knee replacements and drawing parallels between these concerns and the adverse effects observed with metal-on-metal

total disc replacements, clinicians and researchers alike can learn from these failures and feed these into future developments of total disc replacements.

The retrieval of an implant normally arises following a revision procedure; this may be due to failure of the device, subsidence of the device or late onset pain. Following retrieval, the explanted device and periprosthetic tissue samples are analysed to gain a better understanding of how the implant has performed *in vivo* and to elucidate why the prosthesis and its biomaterials failed (Kurtz et al., 2009). Potential material responses include; wear, fracture, plastic deformation and creep. Adverse reactions to the implant by the host include, inflammation in response to wear of the device, infection and accumulation of metallic ions and particles in remote organs of the body (or periprosthetic tissues).

1.12.1 Retrieval analysis of total disc replacements

There is limited information within the literature regarding retrieval analysis from failed metal-on-metal total disc replacements (Kurtz et al., 2005; Anderson et al., 2006), however there is a growing number of clinical retrieval investigations revealing the modes of failure, wear mechanisms and size of wear particles produced by metal-on-polyethylene total disc replacements (Choma et al., 2009; Kurtz et al., 2009; Kurtz et al., 2012) and metal fusion instrumentation.

Retrieval analysis of a single Maverick™ cobalt chrome-on-cobalt chrome lumbar total disc replacement (removed as a result of nerve root impingement after one year *in situ*), presented micro-abrasion, evidenced by microscopic scratches at the articulating surfaces, as the predominant mechanism of wear in this metal-on-metal device. This mechanism of wear was consistent with wear mechanisms observed in metal-on-metal (cobalt chrome) total hip replacements (Kurtz et al., 2005). Although this is an important preliminary investigation into the *in vivo* performance of MOM TDR's, isolation and characterisation of debris from periprosthetic tissues was not performed. To date characterisation of metallic wear particles from around failed metal-on-metal total disc replacements has not been conducted.

In a similar clinical investigation, Anderson et al. (2006) performed a retrieval analysis on the Bryan and the PRESTIGE® cervical discs. Reasons for implant retrieval included; infection, adjacent level effects and persistent pain post operatively. There were no obvious signs of wear on the polymeric component of the Bryan implants and no evidence of titanium found in the periprosthetic tissues. However, with only a small sample size

analysed, there was not sufficient evidence to confirm that titanium particles were not produced in this device. Varying amounts of polymer debris was observed; in some instances this had not elicited an inflammatory response, evidenced by the presence of macrophages and foreign body giant cells, whereas in others macrophages had been recruited. Fretting corrosion was observed on the screw heads of the explanted stainless steel PRESTIGE® devices. Metallic wear debris, identified in all periprosthetic tissue samples, triggered the recruitment of macrophages. However this study was conducted on a minimal number of explants (n=2). It is therefore difficult to extrapolate these findings to normally functioning prostheses *in vivo.*

The few retrieval analysis studies of metal-on-metal total disc replacements indicate that the main mechanisms of wear include micro-abrasion and fretting corrosion between the plate and screw interface. Though the wear products were not characterised in terms of size, shape or chemical composition, Anderson et al. (2006) reported the presence of metallic particles in periprosthetic tissue, which triggered the recruitment of macrophages and foreign body giant cells, in a chronic inflammatory response. A similar biological response was reported by Austen et al. (2012). Here macrophages and a limited number of foreign body giant cells were associated with UHMWPE particles generated by Mobidisc® total disc replacements. Analysis of periprosthetic tissue samples from around the Activ-L® device revealed the mean number of UHMWPE particles found in the periprosthetic tissue was three particles/mm^2 periprosthetic tissue. These particles ranged from 2.05-9.59μm in size and were round to oval in shape. The particles generated by the Mobidisc® were 2.05-73.56μm in size. Though the results of this study demonstrate similar sizes of particles from around metal-on-polyethylene devices compared to particles observed in periprosthetic tissue surrounding failed metal-on-polyethylene total hip replacements (10nm-1mm (Tipper et al., 2000)) the number of particles produced was much lower.

Choma et al. (2009) reported an individual retrieval of a ProDisc-L (cobalt chrome on UHMWPE lumbar total disc replacement) as a result of unremitting low back pain after 16 months *in situ.* Analysis of the device revealed there was evidence of burnishing on the dome, anterior rim and back-side of the polyethylene core, which is also consistent with the adhesive, abrasive wear mechanisms observed in metal-on-polyethylene total hip replacements. The burnishing observed at the anterior rim was accompanied by plastic deformation, consistent with impingement by the superior end plates. Chronic impingement, invariably between the polyethylene core and the end plate was also

observed by Kurtz et al. (2008) in 70% of polyethylene mobile bearing retrievals. Pitting, delamination or fracture of the polyethylene core was not observed in this Pro-Disc-L retrieval. Polarised light microscopy was used to evaluate the presence of polyethylene wear debris in periprosthetic tissue samples taken from around the failed Pro-Disc-L. Particles of approximately 1μm in size were observed in the periprosthetic tissue. There was no report of infection or adverse tissue response. Particles in the sub-micron range could not be detected due to the diffraction limit of the imaging techniques employed (0.2μm) and thus their presence could not be eliminated.

In one of the few long-term follow-up investigations of the performance of metal-on-polyethylene total disc replacements, periprosthetic tissue from around failed Charité devices was analysed (*in situ* 3-16 years) (Kurtz et al., 2012). A chronic inflammatory reaction involving macrophages, giant cells and lymphocytes, in association with both phagocytosed and non-phagocytosed polyethylene particles (>2μm in size) was observed in 15 of the 16 patients analysed. Further in depth analysis from five periprosthetic tissue samples revealed >1 billion particles.gram^{-1} of tissue. The cellular response and presence of micron sized polyethylene particles in the periprosthetic tissue presented in this study were comparable to the findings presented by Austen et al. (2012), who found UHMPWE particles contained in macrophages surrounding failed metal-on-polyethylene lumbar Activ-L total disc replacement.

Ultra-high molecular weight polyethylene particles as small at 30nm have also been isolated from periprosthetic tissue (Richards et al., 2008) from around total hip replacments though in this study the majority of the particles were found to be 0.1μm-0.99μm in size. The number of nanoscale particles only represented a small proportion of the total volume of wear. Tipper et al. (2000) reported UHMWPE particles isolated from around failed total hip replacements had a wide range of sizes and morphologies, particles ranging from the nanoscale to 100μm have been identified *in vivo*. Particles between 50nm and 2μm in size were isolated from periprosthetic tissue from around the failed metal-on-polyethylene (SB Charité) total disc replacements using a tissue digestion protocol and using scanning electron microscopy (Punt et al., 2011). The size of UHMWPE particles reported by Punt et al. (2011) were within the size range of particles identified *in vivo* around failed metal-on-polyethylene total hip replacements (Doorn et al., 1998). Thus it may be extrapolated that if there are parallels between the size of polyethylene particles from failed metal-on-polyethylene total hip and disc replacements the metallic

wear particles produced by metal-on-metal total disc replacements may be of similar size to those observed in metal-on-metal THR i.e. in the nanoscale size range.

1.12.2 Retrieval analysis of spinal fusion instrumentation

Retrieval analysis has revealed substantial levels of corrosion of the stainless steel Harrington rod spinal fusion system (Aulisa et al., 1982). Corrosion was most prominent at the rod-hook junction. Fretting was also found in this region of the fusion instrumentation, evidenced by the production of metal shavings. Histological analysis of periprosthetic tissue revealed the presence of metallic particles associated with a granulomatous tissue containing monocytes, fibroblasts and macrophages. Similarly Senaran et al. (2004) analysed metallic debris surrounding stainless steel spinal fusion implants associated with late operative site pain. Substantial metallic debris was found localised around the rod-transverse connector junction and lesser amounts around pedicle screws, similar to the findings presented by Anderson et al. (2006), where debris was found localised around the screw heads of the Prestige metal-on-metal TDR. Histology of these periprosthetic tissues revealed the presence of macrophages at the bone-metal interface with particles of 1-10μm reported using polarised light microscopy, the resolution of which would not be sufficient to detect submicron wear particles. In a retrieval study conducted by Kirkpatrick et al. (2005) numerous forms of corrosion were observed in modular fusion instrumentation made from stainless steel or titanium alloys. Crevice corrosion, fretting corrosion and mechanically assisted crevice corrosion were detected. Fretting damage and crevice corrosion were the two alterations most commonly observed in the stainless steel instrumentation. Though the examination of metal fusion instrumentation and metal-on-metal and metal-on-polyethylene total disc replacement wear performance using retrieval analysis is no longer in its infancy it still remains far from complete. With small numbers of retrievals and limited long-term findings, the relationships between TDR bearing design, wear debris release, and impingement damage remain poorly understood. Because of the more detailed clinical and retrieval history describing their performance, metal-on-polyethylene TDRs provide the starting point for validating realistic wear and fatigue test protocols to characterise TDRs during the research and development phase of implant design.

1.13 The host response to metallic wear particles: lessons learned from total hip replacements

The host biological response to wear debris differs depending on the biomaterial selected, debris size, volume, number, shape and chemical composition. The differences in wear characteristics and biological responses to metal-on-polyethylene and metal-on-metal

bearing surfaces are shown in Table 1.6 below. (Adapted from Golish & Anderson, 2012). The biological responses to metal wear debris will be discussed in more detail.

Table 1.6 Comparison of the wear characteristics and subsequent biological response to metal-on-polyethylene and metal-on-metal bearing surfaces in total hip arthroplasty.

Property	Metal-on-Polyethylene	Metal-on-Metal
Bearing material	Cobalt chrome (CoCr)-UHMWPE	CoCcr-on-CoCr
Wear debris	Polyethylene (PE)	CoCrMo and CrO
Size of particles	Variable (10nm->1000μm)	~50nm (variable)
Particle morphology	Round/needle/flake/ribbon	Round/needle
Corrosion potential	Minimal	Chromium Phosphates and Cr-protein compounds
Cellular response	Macrophage and giant cells	Lymphocytic and macrophage
Host biochemical reaction	RANKL (receptor activator of nuclear factor kappa-B ligand), cytokines	Cytokines
Systemic effect	Polyethylene in liver and spleen	Ion levels elevated in blood and urine
Hypersensitivity	Occasional with metal allergy	Type IV hypersensitivity
Pathobiology	Osteolysis and aseptic loosening	Osteolysis, aseptic loosening and pseudotumor

Due to a limited number of studies within the literature regarding the wear mechanisms (Kurtz et al., 2012), size and morphology (Pasko et al., 2016) of particles produced by metal-on-metal total disc replacements, and due to similarities being reported in terms of wear mechanisms and size of particles between metal-on-polyethylene total hip and disc replacements (Doorn et al., 1998, Tipper et al., 2001, Tipper et al., 2006; Choma et al., 2009; Punt et al., 2011; Tipper et al., 2012; Tipper et al., 2013; Hyde et al., 2015) parallels may be made between the biological response to metal-on-metal total hip and disc replacements.

Osteolysis induced by wear particles from metal-on-metal total hips, though not as prominent in the literature, compared to osteolysis caused by metal-on-polyethylene

devices, may be linked with a hypersensitivity reaction (Park et al., 2005; Korovessis et al., 2006; Holloway et al., 2009) and should be considered in metal-on-metal TDR.

1.13.1 Osteolysis in association with total disc replacements

The UHMWPE particles generated in metal-on-polyethylene TDR articulations range from 0.01-100μm in length (Punt et al., 2011; Tipper et al., 2012; Tipper et al., 2013). Considering UHMWPE particles from metal-on-metal total hip replacements it has been reported that these particles are actively phagocytosed by macrophages at the interface between the implant and the bone (Green et al., 1998). Phagocytosis of polyethylene wear particles triggers the release of inflammatory cytokines, IL-6, IL-1 and TNF-α by macrophages, resulting in an inflammatory response and bone resorption (Green et al., 1998).

In 2007, Van Ooij et al. described four cases of osteolysis in patients who had received Charité metal-on-polyethylene TDR's. Previously this phenomenon was not thought to occur in the spine due to the lack of a synovium and a low range of motion (Büttner-Janz et al., 2003). The process by which the polyethylene wear particles are contained at the location of implantation for sufficient periods of time to induce osteolysis is not clear due to the fact there is no real joint space. However it is possible that the host develops a pseudocapsule after surgery around the implant, forming a contained region conducive to the initiation of osteolysis (Devin et al., 2008). Histology of periprosthetic fibrous tissue samples from around failed metal-on-polyethylene total disc replacements has revealed an inflammatory tissue with polyethylene particles localised within the tissue and within multi-nucleated giant cells. The observation of polyethylene particles was limited to the use of polarised light microscopy. This meant that the particles could only be imaged to 0.1-1μm in size, submicron particles could not be identified. Ideally a size distribution obtained by tissue digestion and subsequent electron microscopy analysis would have provided a more detailed account of particle sizes *in vivo* (Van Ooij et al., 2007). In a similar clinical case study Devin et al. (2008) reported an individual case of osteolysis in a 50-year old man who received the ActoFlex trial TDR (titanium end plates and an poly-olefin core). As this implant had been *in situ* for 19 years, this case highlights the fact that although early short-term reports may have positive clinical outcomes the clinical course can be devastating with long-term follow-up (Devin et al., 2008). Patients who are candidates for disc arthroplasty are generally much younger and more active than patients recommended for lower extremity total joint replacement, which places increased mechanical demands on the implant.

1.13.2 Mechanism of osteolysis

Several mechanisms of osteolysis have been identified *in vivo*. The prevailing cause of osteolysis around joint replacement is due to the increased bone resorption triggered by cytokine signalling from macrophages, which have been stimulated by particles in the surrounding periprosthetic membrane. This activation process is dependent on the size and number of UHMWPE particles in the periprosthetic tissue. Particles in the size range 0.2-0.8μm at a concentration of 10-100μm^3 per cell are thought to trigger macrophage activation (Green et al., 1998; Green et al., 2000; Matthews et al., 2001).

Macrophages respond to the presence of wear particles by taking up the particles by phagocytosis, however, this process is not capable of eliminating bio-inert polyethylene wear debris and causes the release of biochemical mediators associated with inflammation, cellular recruitment and bone resorption in an innate immune response (Ingham & Fisher, 2000). Cytokines and cell signalling molecules found localised in the periprosthetic tissue include; TGF-β, TNF-α, IL-1α, IL-1β, IL-3, IL-6, IL-8, IL-11, macrophage colony stimulating factor (M-CSF), Platelet-derived growth factor (PDGF), receptor activator of nuclear factor κ-B (RANK) and its corresponding ligand RANKL, prostagliandin-E_2 (PGE_2) and adhesion molecules (Abu-Amer et al., 2007). The interaction of these cytokines with monocytes, macrophages, epithelial cells, giant cells, pre-osteoclasts, T-cells, hematopoietic stem cells, osteoblasts and osteoclasts, in the process of bone resorption is detailed in Figure 1.9. The communication between RANK and RANKL stimulates the differentiation of pre-osteoclasts to osteoclasts, responsible for the breakdown of bone, leading to osteolysis and subsequent loosening of the implant (Kandahari et al., 2016). The role of key cytokines in osteolysis is summarised in Table 1.7.

Table 1.7 The role of key cytokines involved in the mechanism of osteolysis

Molecular effector	Role
TNF-α	• Increases RANKL expression • Strongly augments RANKL-induced osteoclastogenesis • Inhibits osteoclast apoptosis • Enhances the production of macrophage activation and attraction of chemokines.
IL-1	• Increases RANKL expression • Inhibits osteoclast apoptosis
IL-3	• Stimulates hematopoietic stem cells to differentiate into bone resorbing osteoclasts
IL-6	• Secreted by osteoblasts in response to to IL-1β, and TNF-α stimulation • Released by stimulated macrophages and associated with increased osteolysis
PGE-2	• Stimulates the expression of the RANK ligand on osteoblasts.
M-CSF	• Stimulates hematopoietic stem cells to differentiate into bone resorbing osteoclasts

If the polyethylene particles are too large or the macrophages can no longer phagocytose the debris, frustrated phagocytosis occurs. Here, the activated macrophages continually try to take up the material and continue to produce pro-inflammatory cytokines and chemokines, resulting in the further recruitment of macrophages. The macrophages become frustrated and fuse together forming multi-nucleated giant cells, indicative of the cells attempting to "wall-off" the particles and protect the surrounding tissue from damage (Ingham & Fisher, 2000). The continued release of chemokines and pro-inflammatory cytokines subsequently activate osteoclasts, which begin to resorb bone surrounding the device (Figure 1.9).

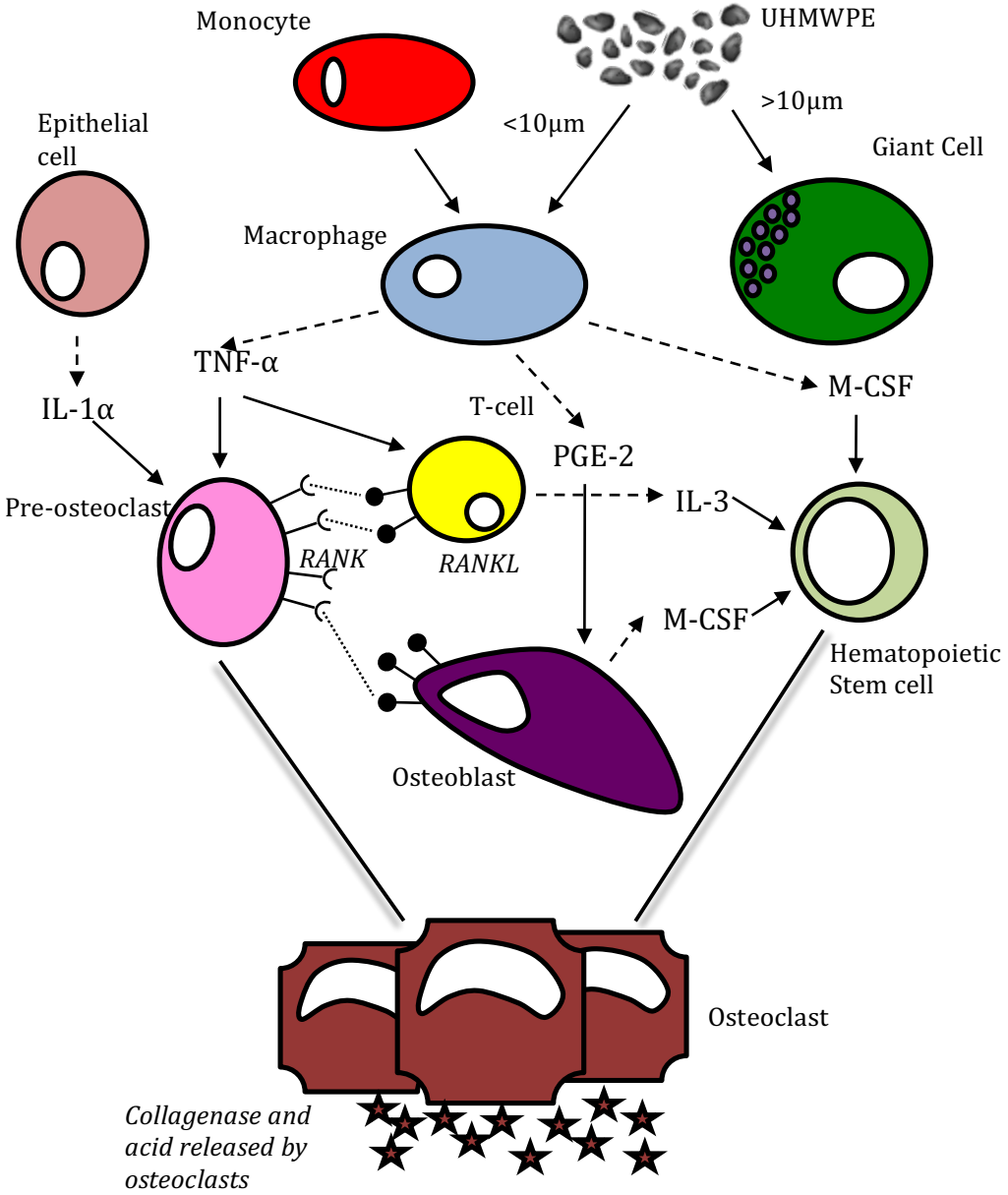

Figure 1.9 The mechanism of osteolysis. PE debris >10μm are taken up by giant cells. Particles <10μm are phagocytosed by macrophages inducing the release of cytokines causing the proliferation of osteoclasts. The balance between osteoblasts and osteoclasts is altered and triggers bone resorption (Adapted from Gowland, 2014).

1.14. Hypersensitivity and pseudotumors in association with metal total disc replacements

Although metals are essential elements within the human body, when metal ion concentrations surpass normal levels there is an increased risk of a toxic response in the human body in the form of cytotoxicity, genotoxicity, potential carcinogenicity and metal hypersensitivity (Sargeant & Goswami, 2007). Metal ions, produced from nano-scale wear debris or as a result of corrosion are capable of triggering a hypersensitivity reaction (Hallab et al., 2001). When metals are in contact with biological environments they corrode, the ions released from this process, while not sensitizers on their own, can trigger an immune response by forming complexes with native proteins. These metal-protein complexes are regarded as candidate antigens (allergens) for eliciting hypersensitivity responses. Numerous implant metals are capable of triggering a delayed-type hypersensitivity reaction, the most common is nickel, followed by cobalt and chromium. This phenomenon linked with the well-documented increase of cobalt and chromium ions in the blood and urine of patients with metallic total hip replacements, supports the idea of a risk of hypersensitivity response with other metal-on-metal arthroplasties including metal-on-metal total disc replacements (Teo & Schalock, 2016). In addition, pseudotumour-like reactions can be triggered by high wearing implants but can also be caused by low wear due to metal hypersensitivity (Campbell et al., 2010).

There is however, controversy within the literature; do metal-on metal implants fail as a result of a pre-existing metal hypersensitivity or does the metal hypersensitivity occur because of the release of large numbers of nanoscale metallic wear particles and subsequent release of ions? (Thyssen et al., 2010).

Soft tissue inflammatory reactions to metal wear particles are a well-documented complication of metal-on-metal total hip replacements and there is growing evidence in the literature that such adverse reactions are associated with metal-on-metal total disc replacements. These reactions commonly referred to as adverse reactions to metal debris (ARMD), have been termed; inflammatory pseudotumour, aseptic lymphocytic vasculitis associated lesion (ALVAL) and metallosis (Daniel et al., 2012; Drummond et al., 2015). A pseudotumour is a clinical term given to a non-infectious, aseptic, mass of necrotic tissue, that is either solid or cystic, formed from a fibrous exudate developed as a result of an inflammatory response (Davis & Morrison, 2016). An aseptic lymphocyte-dominated vasculitis-associated lesion (ALVAL), identified histologically, defines the individual cellular response that is stimulated periprosthetically in response to metal particles and cobalt and chromium ions. The mechanism behind an ALVAL is thought to be a T

lymphocyte mediated type IV hypersensitivity reaction. Here cytotoxic T cells and activated monocytes/macrophages cause tissue damage (Watters et al., 2010). An ALVAL reaction was previously thought to be proportional to the amount of wear debris released, but more recently has been reported in patients with smaller amounts of wear debris also (Langton et al., 2011). A metallosis response can be defined as aseptic fibrosis, local necrosis or loosening of an implant due to metallic corrosion and wear. It has been suggested within the literature that pseudotumors and metallosis are continuous with the same pathological spectrum of disease (Teo & Schalock, 2016).

1.14.1. Type IV hypersensitivity mechanism

Type IV hypersensitivity, or delayed type hypersensitivity (DTH), is characterised by the process of antigen presentation in local tissues by antigen presenting cells and involves presentation of antigen in association with MHC class II molecules. The occurrence of such a reaction is evidenced by elevated levels of numerous immune cells and markers located in the periprosthetic tissue including; CD3+ and CD4+ T lymphocytes, $CD11c^{+}$ macrophages/dendritic cells and cells with abundant expression of MHC class II (Perry et al., 1995; Torgersen et al., 1995)

A type IV hypersensitivity response to metals requires both a sensitisation (afferent) phase and an elicitation (efferent) phase, which is responsible for the recruitment and activation of specific T cells to a hapten challenge. In the afferent (sensitisation) phase metal ions (haptens) produced by mechanical wear or physiochemical corrosion sensitise T-cells in the secondary lymphoid tissue (lymph nodes or spleen).

The next phase of the reaction is referred to as the effector phase, here metal ions produced by mechanical wear or physiochemical corrosion bind to endogenous proteins, to form metal-protein complexes (antigen). The T-cells which were stimulated (in the afferent stage), upon interaction with antigen presenting cells (APC's) presenting the metal-protein complexes at the site of the pathological reaction, secrete cytokines such as IFN-γ, IL-1 and IL-2, which attract macrophages and other lymphoid cells (Murphy et al., 2008; Athanasou, 2016). These cytokines play a crucial role in the chemotaxis of monocytes to the site of DTH reaction. Interferon gamma and TNF-α also prevent the migration of macrophages away from the site of DTH. It is this mechanism, which can cause significant tissue damage; as activated macrophages trigger the activation of more $CD4^{+}$ T cells, which in turn activate more macrophages and the cycle continues.

1.14.2 Adverse tissue reactions to total disc replacements

In an isolated clinical case study reported by Cavanaugh et al. (2009) where a 39 year old woman received a CoCrMo cervical total disc replacement, six months post-surgery she began to experience radicular pain associated with a large yellow mass of tissue extending into the epidural space, presumed to be a pseudotumor.

Similarly to the isolated case presented by Cavanaugh et al. (2009) Guyer et al. (2011) reported four case studies of pseudotumour development in the cervical and lumbar spine following total disc replacement with cobalt chrome molybdenum metal implants. Each of the four patients had successful primary surgeries with good initial clinical outcomes, however over time they each developed increasing pain levels and neurological problems. Upon investigation large soft-tissue masses were observed which protruded into the epidural space causing neural compression, (Guyer et al., 2011). Histological analysis of these tissues showed them to contain; macrophages, lymphocytes and eosinophilic granulocytes indicative of type IV hypersensitivity (Guyer et al., 2011). In particular with the one cervical device a mass of black tissue was observed. This was not found to contain metal particles using backscattered electron imaging, however, the detection limit of this technique was 0.1μm and as mentioned previously, the size of metal debris from metal-on-metal articulations have been found to be in the nanoscale size range, therefore the resolution of the technique may not have been sufficient to detect nanoscale metal particles. However, with the three lumbar cases, analysis of the periprosthetic tissue identified a delayed type hypersensitivity reaction. In these cases metallic particles were identified within macrophages, which were similar to particles generated in metal-on-metal total hip replacements (Jacobs et al., 2009). Inspection of the retrieved devices showed micrometre and sub-micrometre scale scratches associated with third body abrasive wear.

1.14.3 Metal wear from total disc replacement and associated genotoxicity

A growing concern within the neurosurgical community is that, due to the nanoscale nature of the particulate debris, the wear particles are able to disseminate widely throughout the body, meaning there is a potential for tumours to develop in regions distant from the metal prosthesis (Tsaousi et al., 2010).

Both cobalt and chromium are recognised by the International Agency for Research on Cancer, commissioned by the European Union, as human carcinogens. Commonly, chromium occurs in two distinct forms; Cr III and Cr VI (though it is also found less commonly as Cr IV and Cr V). Chromium VI ions are capable of entering cells and upon

entry are reduced to Cr III and free radicals (Figure 1.10); such as thyl and hydroxyl radicals which are particularly harmful to cells, causing damage to the DNA and organelles. Cr III is known to trigger numerous different types of DNA damage including oxidative DNA damage, Cr-DNA adducts, single strand breaks and DNA-protein cross links. This damage to DNA can alter its ability to replicate via interference with DNA polymerase, inhibition of transcription and finally via genetic mutations. Such negative consequences can result in apoptosis, yielding necrotic tissue (Singh et al., 1998).

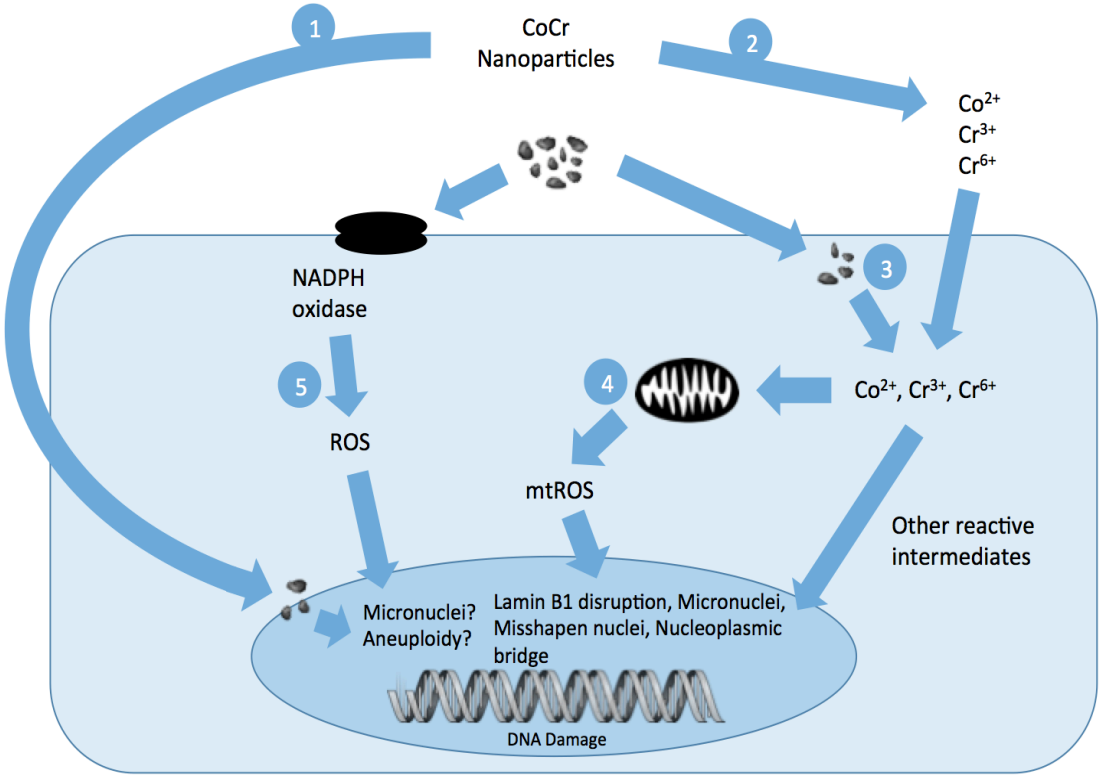

Figure 1.10 Proposed mechanisms of genotoxicity triggered by cobalt chrome nanoparticles. Adapted from Raghunathan et al. (2013). NADPH oxidase triggers production of reactive oxygen species within two hours of exposure. Prolonged exposure to CoCr particles results in sustained release of intracellular ROS associated with disruption to lamin B1, misshapen nuclei and micronuclei, CoCr nanoparticles can damage cytoskeletal elements and cause chromosomal clumping and numerical aberrations either directly or via ROS. Corrosion of CoCr particles can generate metal ions that can lead to genotoxicity. CoCr particles are taken up by cells and release further metal ions, triggering the release of ROS to result in genotoxic effects.

1.15 *In vivo* investigation into the biological response to wear debris.

Although retrieval studies have been used to determine the effects of cobalt chrome and stainless steel wear particles on the tissues surrounding total joint replacements and to determine the size and morphology of wear products produced by orthopaedic implants,

a more thorough understanding regarding the molecular mechanisms of adverse effects such as cytotoxicity, genotoxicity, hypersensitivity, inflammation and osteolysis is required for the advancement of orthopaedic implants. Animal models allow a controlled study into individual aspects of the biological response and compatibility of biomaterials for total joint arthroplasty.

One of the earliest investigations into the toxicity of CoCr particles *in vivo* was conducted in 1983 by Meachim and Brooke. Here, cobalt chrome particles (500nm-50μm), with approximately 80% between 1μm and 2μm were used. Cobalt chrome particles (30mg) were injected into the medial pouch of the synovial cavity in the patella-femoral articulation in guinea pigs. The short-term response to CoCr was investigated at intervals between one day and one-month post operatively. Histological analysis of the periprosthetic tissue showed progressive incorporation of the particles into the synovial fluid and found the smaller particles had been taken up by macrophages and fibroblasts. Larger particles triggered the recruitment of multi-nucleated giant cells and subsequently triggered fibrosis. This research highlighted the ability of CoCr particles to disseminate throughout the body as particles were found in the lymph nodes. There are limitations in the experimental design in that a large volume of particles was injected into the synovial cavity, which would not accurately mimic the mechanism of wear release into the synovial cavity and may cause damage. Additionally, the injection procedure could trigger inflammation making it difficult to ascertain whether the effect was the result of the CoCr particles or simply a response to the method of particle application. The milled particles used in this study were larger than would be found *in vivo,* thus the validity of their findings is somewhat questionable. Milled particles do not produce the correct morphology that would be seen *in vivo.*

In an effort to overcome the limitations of previous work regarding the crude mechanism of particle administration and non-clinically relevant particle sizes, Brown et al. (2013) investigated the biological consequences of clinically relevant micro (average particle size 2.9μm) and nano-scale (average particle size of 32nm) cobalt chrome particles using a murine model, with the aim of understanding the *in vivo* biological response to metallic particles generated from metal-on-metal total hip replacements. Here the mice were repeatedly exposed to micro and nanoparticles at 0, 6, 12 and 18 weeks and analysis of immunological and genotoxic effects performed at 1, 4 and 40 weeks. The use of repeat injections aimed to reduce the concentration of a single dose and simulated progressive release of particles. The mice were exposed to three test conditions; 4×10^9 nanoscale CoCr particles per injection, 1.2×10^{10} nanoscale CoCr particles per injection and 4.5×10^4

micron sized CoCr particles per injection. Brown et al. (2013) detected elevated levels of chromium ions in the knees with all test conditions, when compared to the sham control after one and four weeks. No significant inflammatory response was observed and no evidence of pseudotumour formation. However DNA damage was reported in the bone marrow at one and 40 weeks post injection. The findings of this study revealed that the response to the larger micron sized particles was Th1 driven and indicative of a hypersensitivity reaction. There are however some limitations to this investigation, firstly the purpose of the study was to investigate the response of metal-on-metal particles generated in total hip replacements but the mice were injected in the knee. The site of injection was so small it was difficult to discern whether the particles had been administered to the intended site, this could have been improved with a larger animal model such as a rat. Secondly the particles were injected (which may trigger inflammation) at four time points, which although better than a single injection to mimic the release of wear debris over time, perhaps continuous perfusion of low doses would have been a more appropriate model.

More recently, Cunningham et al. (2013) assessed the effect of epidural application of 11 biomaterials on the spinal cord and systemic tissues in New Zealand White rabbits with the aim of further understanding the host biological response to unintended metallic wear debris produced by metal-on-metal bearing surfaces. The metallic particles tested in this study were stainless steel (0.2-37μm), titanium (0.2-18.5μm) and cobalt chrome (0.2-9.3μm). A mass of 4mg of each particle type was added to the surface of the dura mater in a dry, endotoxin free, sterile format. No evidence of particles in systemic tissues was reported, however, there was evidence of the formation of epidural fibrous tissue in all test groups and none in the control groups (epidural exposure alone). Upon histological examination of this tissue evidence of phagocytosed particles and a local inflammatory response was reported. There were, however, flaws in the experimental design of this study; the metallic particles were commercially sourced and not generated by articulation in a simulator, meaning the elemental composition of the particles may be dissimilar to those generated *in vivo* from medical grade metal components. The particles utilised were large (micron sized) compared to those that would be generated *in vivo* from metal-on-metal total disc replacements. A key limitation of this study lies in the fact that the particles were administered based on weight, this did not account for the difference in particle size of the different biomaterials. Thus for the smaller metallic particles, a greater number of particles per gram of tissue would be delivered than the larger particle sized materials. Moreover, the particles were applied directly onto the dura which is a some-

what crude simulation of wear debris generation and is not representative of the build-up of wear debris seen *in vivo* over time.

In an attempt to understand the response of the spinal cord to titanium wear particles generated in a spine simulator Chang et al. (2004). Administered titanium particles to the epidural space of New Zealand white rabbits following a laminotomy at L2 or via a lateral flank approach at L2-L3. Interestingly, the host tolerated these particles well (<5μm and 5-15μm), adverse effects such as necrosis, fibrosis or granulomatous tissue were not observed in any of the specimens at any time point. A low number of titanium particles were observed in the local tissue, smaller particles were phagocytosed by macrophages and at the time points tested this had not elicited an inflammatory response. There were numerous shortcomings to this investigation, primarily this study was not quantitative in that no obvious signs of inflammation or adverse effects were seen, however histology and cytokine expression were not explored. No control groups were used in this study and finally minimal particle characterisation was performed.

Though the use of animal models has provided an invaluable holistic view of the biological response of metallic wear particles, to ascertain the fine details of the cellular mechanisms involved, a more controlled, specific, simplistic model is required. There are reoccurring limitations with these models. The current research using animal models to assess the biological response to metallic wear particles have predominantly used particles that are at least 10 times larger than is anticipated to be produced *in vivo* from metal-on-metal total disc replacements, with predominantly micron sized particles used. Further work needs to be conducted to determine an appropriate method of particle administration with continuous perfusion being regarded as a potential technique to more closely model continuous particle release and reduce the risk of inflammation. *In vitro* cellular models involving individual and co-cultured cell populations exposed to wear particles of varying doses would allow the effects of cell viability, cellular reactivity, cytokine release and DNA damage to be investigated in a more controlled manner. This has lead to the use of *in vitro* investigations to determine the cellular response to metallic wear particles.

1.16 *In vitro* investigation of the biological response to metal wear debris

In vitro cellular models offer several advantages over whole animal studies when used to determine the behaviour of specific cell populations to external stimuli. The use of simplified *in vitro* models enable the assessment of various cellular outcomes in response to well defined parameters while providing greater control over cellular components,

manipulation and monitoring (LaPlaca et al., 2007). In recent years numerous studies have been performed to determine the effect of metallic wear particles on cell viability, DNA integrity, cytokine release, proliferation, reactivity and differentiation. A wide array of cell types (cell lines and primary cells) have been used to ascertain the cellular response to medical grade cobalt chrome and stainless steel wear particles used in orthopaedic implants including; histiocytes, osteoblast precursors, macrophages, fibroblasts, glial cells, dural epithelial and dural fibroblast cells.

To determine the effect of CoCr wear particles on cell viability Germain et al. (2003) cultured U937 human histiocytes and L929 fibroblast cells with commercially available CoCr and pin-on-plate wear simulator generated CoCr particles. The CoCr particles (29.5nm from pin-on-plate simulator and 9.87μm commercially available particles) were cultured with U937 cells at increasing particle to cell ratios; 0.005, 0.05, 0.5, 5 and 50μm^3 debris per cell. The CoCr particles generated using a pin-on-plate wear simulator significantly reduced the viability of U937 and L929 cells after five days in culture, when cultured with 50μm^3 and 5μm^3 CoCr debris per cell. The commercially available CoCr particles, which were not clinically representative in terms of size and chemical composition, did not adversely affect cell viability at any dose and time point tested. (Germain et al., 2003). In a similar *in vitro* study U937 cells were cultured with cobalt chrome particles (150nm-6.5μm in length) generated from an ASR hip implant using a hip simulator. After five days in culture with 5mg of cobalt chrome wear debris a significant (77%) decrease in cell viability was observed (Posada et al., 2014).

Clinically relevant nano and micron sized cobalt chrome particles were cultured with human fibroblasts to determine the effects of different size ranges of particles on fibroblast viability, cytokine release and DNA damage (Papageorgiou et al., 2007). After 24 hours in culture the nano-sized CoCr particles triggered four times more DNA damage than the micron-sized CoCr particles. In terms of viability, the nano CoCr particles triggered a time and dose dependent reduction in viability, whereas micron-sized CoCr particles did not adversely affect viability until after four days in culture. No effect on the release of IL-6, IL-10, TNF-α and FGF-23 was observed. These studies on the effect of cobalt chrome particles on the viability of U937, L929 and human fibroblast cells highlight the importance of particle size and elemental composition on the biological response to metallic wear particles. The commercially available particles utilised by Germain et al. (2003) and the particles generated by Posada et al. (2014) were larger than clinically relevant particles observed from around failed metal-on-metal total hip

replacements (~50nm). Additionally, the elemental composition of the commercially available particles will have varied from the debris generated from medical grade cobalt chrome, thus direct associations between the biological responses observed and potential *in vivo* responses cannot be made. Furthermore, the particle dosing regimen selected by Posada et al. (2014) was not physiologically relevant. The use of clinically relevant particles by Papageorgiou et al. (2007) was crucial in obtaining a more precise understanding of the biological response of human fibroblasts to CoCr wear particles. Metallic nanoparticles are capable of generating significantly more superoxide and hydroxyl free radicals than micron size particles, which are involved in DNA damage and thus there may be differences in the DNA damage, viability and inflammatory responses of fibroblasts as a result.

In one of the limited *in vitro* investigations assessing the cytotoxic effect of stainless steel, Li et al. (2014) investigated the effect of 316L stainless steel and high-nitrogen, nickel free austenitic stainless steel on the viability of MC3T3-E1 mouse osteoblast precursor cells. The MC3T3-E1 cells were cultured with bulk materials for five days and an MTT assay used to determine their effects on cell viability. Neither material adversely affected cell viability at any time point tested. Though this study investigated the biocompatibility of bulk 316L stainless steel it provides a preliminary insight into the cellular response to currently available medical grade stainless steels and potential alternative biomaterials. In another study the response of bulk and particulate 316L stainless steel on the viability of the RAW murine macrophage cell line was investigated by Bailey et al. (2005). The stainless steel particles produced by N_2 gas atomization were spherical and 1-100μm in diameter. The 316L stainless steel particles significantly reduced the viability of RAW cells when compared to the cell only negative control. This response was not observed with the nitrogenated stainless steel particles. The particles used in this study were generated using N_2 gas atomization which did not yield clinically relevant sized particles, nor was this method representative of the mechanism of wear observed *in vivo*. Generation of particles using a pin-on-plate wear simulator or hip/spine simulator would have been a more appropriate method for particle generation. Furthermore, a quantitative measure of viability was not utilised, which would have been preferable. Upon comparison with the work conducted by Li et al. (2014) it can be concluded that although bulk stainless steel did not adversely affect cell viability but the stainless steel particles did.

To date much of the work conducted to determine the cellular response to CoCr and stainless steel wear particles has been conducted in macrophage, fibroblast, osteoblast,

histiocytic and epithelial cells. More recently there have been a limited number of studies investigating the CNS cellular response to metallic wear particles from total disc replacements (DeGuzman and VandeVord, 2007; Papageorgiou et al., 2014).

De Guzman and VandeVord. (2007) used the C6 rat glioma and the Rat2 fibroblast cell line to determine the response of cells of the CNS to; CoCr and titanium used in total disc replacements. The CoCr particles were on average 5.7μm in diameter (1-20μm) whereas the titanium particles were 2.3μm in diameter (0.1-68μm). An increase in the viability of C6 glial cells was observed when cultured with low doses of CoCr and titanium (0.625 $mg.ml^{-1}$ and 1.25$mg.ml^{-1}$). However, a significant reduction in viability was observed with the higher doses (2.5 $mg.ml^{-1}$ and 5 $mg.ml^{-1}$) of CoCr and titanium. A significant decrease in viability was observed when Rat2 cells were cultured with high doses of CoCr (1.25 $mg.ml^{-1}$ 2.5 $mg.ml^{-1}$ and 5 $mg.ml^{-1}$) and titanium (2.5$mg.ml^{-1}$). There are numerous limitations with the experimental design of this study, firstly the particles, of unknown origin were large when compared to the clinically-relevant size ranges for these materials seen in the literature (Doorn et al., 1998). The viability of both cell types was only assessed after 48 hours in culture, further time points would have revealed the longer term response of C6 and Rat2 cells to materials used in total joint arthroplasty.

More recently the use of an advanced organ culture model of the dura mater has been applied to simulate the effect of clinically relevant CoCr nanoparticles generated in total disc replacements on the dura mater, the outermost membrane of the meninges, a protective tri-layer structure surrounding the spinal cord (Papageorgiou et al., 2014). After the dura mater was exposed to CoCr nanoparticles (20-60nm, generated using a pin-on-plate wear simulator) a loosening of the epithelial layer and alterations to the underlying collagen matrix were observed. These structural changes were linked to an increase in production of MMP-1, -3, -9 and-13. The CoCr nanoparticles also triggered an increase in production of IL-6, IL-8 and TNF-α. Such observations may lead to particle infiltrate across the dura mater membrane. Though cellular cytotoxicity was not observed the significant alterations to the epithelial layer compromised the integrity of this protective barrier and could have a serious impact on periprosthetic tissues due to nanoparticle penetration (Papageorgiou et al., 2014). The CoCr nanoparticles used in this study were within the predicted size range of particles from metal-on-metal total disc replacements.

With mounting evidence in the literature regarding the wear of metal-on-metal total disc replacements and with lessons learned from total hip replacements, in terms of

inflammation, osteolysis and pseudotumour formation, there is growing concern regarding the impact of metal nanoparticles produced by total disc replacements on the periprosthetic tissues surrounding these devices and with evidence presented by Papageorgiou et al. (2014) that nanoscale cobalt chrome particles are capable of altering the structural integrity of the meninges it is imperative to study the effect of metallic wear products on cells of the CNS. Much of the work conducted to determine the cytotoxic effects of wear particles from orthopaedic implants has utilised 2D culture, which in itself has limitations, advanced 3D constructs may provide a more appropriate cell culture environment for biocompatibility testing.

1.17 The use of advanced 3D culture systems.

Much of the current understanding of the *in vitro* biological response to wear particles is based on cell culture studies, which have utilised homogenous populations of cells cultured in two-dimensional (2D), flat, plastic tissue culture wells. However *in vivo,* cells are arranged in a more complex matrix, an information-rich, stimulating environment containing numerous extracellular matrix (ECM) components and cell-secreted factors. Within this three dimensional (3D) environment, multiple cell types interact heterotypically. The main advantage of utilising 2D culture is that its simplistic nature allows the application of reductionist approaches to understand individual cellular responses, however the 2D model may not accurately capture the natural behaviour of cells *in vivo* (Baker & Chen, 2012; Adcock et al., 2015).

A 3D culture environment encapsulates the cells within an ECM, providing structural support and nutrition from all directions, unlike the 2D system. The main objective of 3D cell culture is to bridge the gap between the somewhat primitive monolayer cell culture studies and complex whole animal models. The use of the intermediate 3D culture enables the control and precise manipulation of a cell culture system, while providing a growth environment that mimics the host tissue as closely as possible, enabling the cells to behave as they would *in vivo* (Haycock, 2011).

It is now a well-established phenomenon that when cells are isolated from tissue and cultured in 2D their phenotype becomes flatter, the rate of cellular division changes and the differentiated phenotype is lost (Von der Mark et al., 1977). Such observations have led to the opinion that the dimension in which cells are cultured determines the fate of their phenotype. As such, monolayer culture drives abnormal cell function and dedifferentiation, whereas a 3D culture environment provides a more physiologically representative setting (Weaver et al., 1997).

Previously, various naturally derived polymers have been used for 3D cell culture including collagen, chitosan (Li et al., 2012), glycosaminoglycans (Chwalek et al., 2014), agarose (Chun & Mun, 2015), alginate (Andersen et al., 2015) and starch (Salgado et al., 2004). There are numerous advantages for the use of naturally occurring polymers as they generally exhibit low cellular toxicity, good biocompatibility and a minimal inflammatory response. Though recently there has been a growing interest in synthetic polymers such as; poly (glycolic acid), poly (lactic acid), polyester and polyurethanes (Carletti et al., 2010).

Type I collagen, has been used extensively for the culture of cells in a 3D environment especially in the fields of; tissue engineering, drug delivery (Obarzanek-Fojt et al., 2016), toxicology and spinal cord injury repair (Han et al., 2010; Macaya et al., 2013; Altinova et al., 2014), as this material is capable of supporting numerous cell types and is highly adaptable to mimic *in vivo* conditions. In recent years, collagen gels have been used to enable cells of the CNS; neurons and glial cells; astrocytes, microglia and oligodendrocytes to interact and behave as they would *in vivo* by creating an environment similar to that of the CNS (East et al., 2009).

East & Phillips. (2008) utilised type I collagen gels for the 3D culture of cells of the CNS as it is readily available and easy to control and manipulate, for cell monitoring and visualization. Type I collagen provides a scaffold structure on which additional extracellular matrix (ECM) components can be deposited, as the 3D environment undergoes modification.

Haw et al. (2014) demonstrated the importance of a cells physiological environment in governing cell-to-cell interactions, response to stimuli and contact with the ECM which governs cellular proliferation, phenotype, migration and differentiation. By culturing BV2 microglia in a 3D matrix with the aim of providing a physiologically relevant environment. BV2 cells were cultured in three separate environments, 2D monolayer, and collagen-coated monolayer and in a 3D collagen gel. The microglia morphology differed between the 2D and 3D systems. In the collagen gel the BV2 cells exhibited a ramified phenotype, which was not observed in 2D culture. Similar levels of viability were reported in all culture systems. *In vitro* BV2 microglia become activated when exposed to lipopolysaccharide. One of the key markers of activation for this cell type is the expression of CD40. CD40 expression was elevated by 70% when moving from 2D to 3D culture. Thus by culturing the BV2 cells in a simple, more physiologically relevant matrix a more appropriate model of cell activation was developed.

In one of the limited number of studies utilising 3D culture to determine the effects of metals on cell viability Tasneem et al. (2016) utilised a collagen hydrogel to determine the effect of increasing concentrations, 10pM-10μM, of three heavy metals; cadmium, mercury and lead on the viability of embryonic murine neural stem cells after 14 days in culture using a live dead assay. After 14 days in culture lead and mercury appeared to adversely affect cell viability at particle doses as low as 100pM, this was not the case for cadmium with 1nM being the lowest dose to adversely affect viability.

In addition to selecting an appropriate physiologically relevant cell culture environment for *in vitro* investigations into the host response to metallic wear particles, appropriate cell types are also required.

1.18 Cell types used to model cells of the CNS

Cell lines of immortalised glial cells such as PC12 neuronal and C6 glial cells have been shown to be extremely useful to model cells of the CNS when large numbers of cells are necessary and they circumvent the issue of culture impurity (De-Guzman & VandeVord, 2007). However these cells differ to primary glial cells and neurons in many ways. Primary astrocytes have a limited potential to proliferate, this effect is often observed in the culture of primary astrocytes, where the cellular phenotype changes after more than two passages (Calvo et al., 1991). Conversely, cell lines rapidly proliferate. The molecular expression profiles of cell lines can also differ from primary cells. For instance upon activation astrocytes up-regulate GFAP, this cellular response is not seen with C6 cells as they express very little GFAP if any at all (Eddleston & Mucke, 1993).

Previous work using the astrocyte-like C6 cell line (De Guzman & VandeVord, 2007) and primary astrocytes (East et al., 2009) in 2D culture has revealed a highly reactive cell profile under controlled conditions (without being exposed to reactive triggers). When considering a complex biological response such as the kind triggered when cells of the spinal cord are exposed to CoCr wear particles, the simplicity of 2D monolayer culture is not advanced enough to accurately mimic the *in vivo* CNS environment. Advanced 3D culture systems are advantageous in that they enable the reproduction of the *in vivo* spatial arrangement of cells, allow polarized cell attachment and perfusion to opposite faces of the cell (in 2D monolayer one side would be adhered to the base of the culture flask) and enable more advanced cell signalling with co-cultures (East et al., 2012).

Having taken what has been determined from metal-on-metal total hip replacements and from a limited number of cases of total disc replacements regarding the potential for

metal wear particles and subsequent ions to induce inflammation, genotoxicity, cytotoxicity, hypersensitivity and pseudotumour formation, coupled with the results of the Papageorgiou et al. (2014) organ culture study, it is imperative to determine the effects of cobalt chrome and stainless steel wear particles on the cells of the CNS such as astrocytes and microglia. Cobalt chrome is the predominant biomaterial used in metal-on-metal total disc replacements, stainless steel has been used in total disc replacements (PRESTIGE® cervical disc replacement) and in spinal fusion instrumentation (the Harrington rod and Cotrel Duboussett fusion system). Astrocytes and microglia, the resident macrophages of the central nervous system play crucial roles in responses to CNS damage. By culturing these cells in co-culture and isolation using a 3D collagen gel construct the biological response to metallic wear particles, in terms of cell viability, DNA damage, cellular reactivity and cytokine release may be elucidated.

1.19 Aims and objectives

Hypothesis- The use of a 3D type-I collagen gel, allowing glial cells to behave in a more physiologically relevant manner, would more precisely determine the biological response of CNS cells in co-culture and in isolation, to metallic wear particles, compared to the use of simplistic 2D culture.

This project aims to investigate the biological responses of specific CNS cell populations, primary astrocytes and microglia in co-culture and astrocytes in isolation to clinically relevant metallic wear debris using a physiologically relevant 3D cell culture system. This can be broken down into the following objectives;

1) To generate clinically relevant metallic (cobalt chrome and stainless steel) wear particles using a six-station pin-on-plate wear simulator.

2) To characterise the morphology and size of the wear particles using field emission gun scanning electron microscopy (FEGSEM).

3) To investigate the biological responses of primary astrocytes and microglia in co-culture and primary astrocytes in isolation to cobalt chrome and stainless steel wear debris.

   a) To compare the response of primary rat astrocytes and microglia in co-culture, and neuronal (PC12) and astrocytic (C6) cell lines to cobalt chrome and stainless steel wear particles in 2D culture in terms of cell viability and DNA integrity.

b) To determine the biological response of primary astrocytes and microglia (in isolation and co-culture) to wear particles in 3D culture. To determine the effects of cobalt chrome and stainless steel wear particles and ions on cell viability. To investigate the effects of cobalt chrome and stainless steel wear particles on the expression of glial fibrillary acidic protein (GFAP, indicative of reactive astrocytes) and TNF-α.

Chapter 2
Materials and Methods

2.1 Materials

The general materials used in this study are shown in the Appendices.

2.1.1 General materials

The general materials including; chemicals, reagents, equipment, consumables, antibodies and stains used in this study are shown in the Appendices in Appendix I, Appendix II, Appendix III and Appendix IV, respectively.

2.1.2 Measurement of pH

A Jenway 3020 pH meter was used to measure the pH of solutions. The pH meter was calibrated prior to use, with three solutions of varying pH (4, 7 and 10), these were made from buffer tablets dissolved in deionised water. To alter the pH of solutions, 6M sodium hydroxide (NaOH) or 6M hydrochloric acid (HCl) was used. Sodium hydroxide or hydrochloric acid was added drop-wise (solutions were prepared in glass duran bottles of varying sizes and thoroughly mixed using a magnetic stirrer and stirrer bar) until the required pH was reached.

2.1.3 Sterilisation

Three different methods of sterilisation were employed to sterilise equipment and solutions.

- 2.1.3.1 Filter sterilisation- Solutions containing proteins, growth factors and supplements, which were not suitable for heat sterilisation, were filter sterilised. In a class II safety cabinet, solutions were placed in a sterile disposable syringe and passed through a filter with a pore size of 0.22μm. Solutions sterilised in this way included MTT solution, solutions for primary cell isolation, poly-d-lysine (used to coat tissue culture flasks) and 10x minimum essential medium used in the production of collagen hydrogels.
- 2.1.3.2 Dry heat sterilisation- Items were placed in a hot air oven at a temperature of 190°C for four hours. Items suitable for this type of sterilisation included; the dissection kit and pre-weighed cobalt chrome and stainless steel wear particles.

- 2.1.3.3 Moist heat sterilisation- items not suitable for dry heat sterilisation or filter sterilisation were sterilised using an autoclave at a temperature of 121°C for 20 minutes under 103 KPa pressure. PBS solution was sterilised using this method.

2.1.4 Sterilisation of the dissection kit

The dissection kit, used for primary astrocyte and microglia cell isolation, comprised; fine tweezers, standard tweezers, scalpel blade holder, two small spatulas, curved scissors and standard dissection scissors. Any sharp utensils were wrapped in foil at the tip to prevent blunting. The dissection kit was heat sterilised in an oven at 190°C for 4 hours (section 2.1.3.2) the day before dissection.

2.2 Cells

2.2.1 Primary astrocytes and microglia. Primary astrocytes and microglia were isolated from P2 Wistar rat cortices in accordance with the protocol first stated by East et al. (2009) and outlined in Chapter 2, section 2.4.1.6.2. The cells were cultured at the University of Leeds, UK. The cortices were obtained in accordance with UK Animals (Scientific Procedures) Act 1986 under the Home Office Schedule One procedure (Home Office Project license: PPL70/8085).

2.2.2 The PC12 neuronal cell line (rat) pheochromocytoma was donated by Dr. James Phillips, University College London, London, UK.

2.2.3 The C6 glial cell line (rat) was donated by Dr. James Phillips, University College London, London, UK.

2.3 Stock solutions

2.3.1 Alkaline electrophoresis buffer

The buffer was prepared by the addition of 18g of sodium hydroxide (NaOH) pellets, 3ml 0.5M EDTA to1.5L of distilled water in a glass duran bottle. The solution was mixed using a magnetic stirrer bar and stirrer.

2.3.2 Astrocyte cell line (C6) culture medium

Ham's F12 nutrient mixture (without phenol red) was supplemented with 10% (v/v) foetal bovine serum (FBS), 2mM L-glutamine, 100 $U.ml^{-1}$ penicillin and 100 $U.ml^{-1}$ streptomycin. This solution was stored at 4°C for up to one month and used for the culture of C6 astrocyte-like cells.

2.3.3 ATP-Lite™ substrate solution for use in the ATP-lite™ assay

The lyophilised substrate solution provided as part of the ATP-Lite™ kit was reconstituted with 25ml of substrate buffer solution (also provided in the kit). The contents of the vial were mixed thoroughly by inversion (avoiding the production of bubbles) and left to stand for five minutes resulting in a clear homogenous solution. Five, 5ml aliquots were produced. The aliquots were wrapped in foil to limit contact with light (as the solution is light sensitive) and stored at -20°C for up to three months.

2.3.4 Biotinylated anti-rat TNF-α solution

In a clean glass vial the biotinylated anti-rat TNF-α was diluted with the biotinylated antibody diluent provided in the enzyme linked immunosorbent assay (ELISA) kit. For a 96 well plate, 240µl of biotinylated antibody was diluted in 6360µl biotinylated antibody diluent.

2.3.5 Bovine serum albumin solution

Bovine serum albumin (BSA) solution was prepared by floating 400mg of BSA on top of 10ml of disaggregation medium (section 2.3.8). This was allowed to dissolve at room temperature and then mixed well by inverting the universal slowly several times. This solution was filter sterilised prior to use. The solution was discarded after use and not stored.

2.3.6 Camptothecin

Camptothecin, was used as a positive control in 2D cell culture studies. A working concentration of 2 $\mu g.ml^{-1}$ was used in the *in vitro* studies. A 1$mg.ml^{-1}$ stock solution of camptothecin was generated by dissolving camptothecin in DMSO. By diluting the stock 1:250, adding 4µl of camptothecin stock to 996µl supplemented medium. The solution was further diluted 1:2 when the cells were seeded in a volume of 100µl supplemented medium and the camptothecin in supplemented medium (100µl) added on top.

2.3.7 Concentrated and dilute inhibitor solutions.

Concentrated inhibitor was prepared by adding 13ml disaggregation medium, 1ml of pre-prepared soy-bean tryspin inhibitor (SBTI) 2$mg.ml^{-1}$ (working concentration of 133$\mu g.ml^{-1}$), 1ml of pre-prepared DNase (2000$U.ml^{-1}$), working concentration of 133$U.ml^{-1}$ and 150µl, 150mM $MgSO_4$ (final concentration 1.5mM) to a labelled universal. This solution was mixed slowly by inversion to avoid creating bubbles.

The dilute inhibitor (SBTI working concentration of 21.28µg.ml^{-1}) was prepared by adding 16.8ml of disaggregation medium (section 2.3.8) to 3.2ml of concentrated inhibitor. These solutions were filter sterilised prior to use. These solutions were discarded after use and not stored.

2.3.8 Disaggregation medium

A volume of 99ml Earle's balanced salt solution (EBSS) was transferred to a glass beaker. Glucose powder (252mg) and 2ml 150mM magnesium sulphate ($MgSO_4$) was added to the EBSS. Finally, 300mg of bovine serum albumin (BSA) was floated on top of the solution, this was allowed to dissolve without agitation at room temperature (for approximately 10 minutes). Once the BSA had fully dissolved, the solution was mixed thoroughly using a magnetic stirrer and stirrer bar for 10 minutes at room temperature. This solution was filter sterilised prior to use, any excess was discarded once the cell isolation procedure was complete.

2.3.9 DNase stock solution

Deoxyribonuclease I type II from bovine pancreas (Sigma, UK lyophilised powder) 20,000U (2,000U.mg^{-1} of protein) was re-suspended in 10ml of distilled water, dispensed into 1ml aliquots (2000U.ml^{-1}) and stored at -20°C until required.

2.3.10 DNA unwinding solution

Sodium hydroxide (NaOH) pellets (1.2g) were added to 300µl of 0.5M EDTA in 150ml distilled water, the solution was mixed thoroughly using a magnetic bar and heated stirrer platform and allowed to cool to room temperature before use.

2.3.11 Ethylenediaminetetraacetic acid (EDTA) Solution (0.5M)

A volume of 250ml of 0.5M EDTA was prepared by re-suspending 36.53g of EDTA (Sigma, UK) in 250ml of distilled water. The powder was dissolved using a magnetic stirrer and stirrer bar. This solution was stored at room temperature until required for up to one month.

2.3.12 Goat serum blocking solution

Goat serum blocking solution 5% (v/v) was made up on the day of use. A slight excess of what was required was made up in sterile PBS. The excess solution was discarded.

2.3.13 6M Hydrochloric acid

A volume of 246ml of stock hydrochloric acid (Sigma, UK) was slowly added to 125ml of deionised water. The final volume was adjusted to 500ml of deionised water. This solution was stored at room temperature.

2.3.14 Live Dead stain

A volume of 1µl of calcein and 2µl ethidium-homodimer was added to every 4mls of pre-warmed (37°C) supplemented medium. This solution was prepared fresh at the start of each experiment.

2.3.15 Magnesium Sulphate solution (150mM)

A mass of 0.361g magnesium sulphate powder (Sigma, UK) was re-suspended in 20ml of distilled water and mixed using a magnetic stirrer and stirrer bar until the powder was completely dissolved. The solution was stored at 4°C for up to one month until required.

2.3.16 Neuronal cell line (PC12) culture medium

RPMI 1640 culture medium (without phenol red) was supplemented with 10% (v/v) Horse serum, 5% (v/v) foetal bovine serum (FBS), 2mM L-glutamine, 100 $U.ml^{-1}$ penicillin and 100 $U.ml^{-1}$ streptomycin. This solution was stored at 4°C for up to one month.

2.3.17 Paraformaldehyde 4% (w/v) as a fixative for collagen hydrogels

A 1L stock of 4% (w/v) paraformaldehyde (PFA) solution was prepared by adding 800ml to a glass beaker. The glass beaker was placed on a hot plate and the solution heated to 60°C. A mass of 40g PFA powder was added to the heated PBS (ensuring the PBS did not reach boiling point) and the solution stirred. The pH of the solution was raised by adding 1M sodium hydroxide (NaOH), drop-wise, until the powder dissolved (the powder would not dissolve at the existing pH). The solution was allowed to cool and the final volume made up to 1L using PBS. The pH was adjusted to approximately pH 6.9 by the drop-wise addition of 0.1M hydrochloric acid (HCl). The solution was filter sterilised and 20ml aliquots stored at -20°C until required.

2.3.18 Phosphate buffered saline (PBS)

Phosphate buffered saline (PBS) was prepared by adding ten PBS tablets to 1L of distilled water. A magnetic stirrer and stirrer bar was used to dissolve the PBS tablets. The pH was adjusted to pH 7, using 12M hydrochloric acid (HCl) and 6M sodium hydroxide (NaOH).

The solution was sterilised using an autoclave and stored at room temperature for up to one month.

2.3.19 Poly-D-Lysine solution

Poly-d-lysine was used to coat 25cm^3 and 75cm^3 tissue culture flasks to enable adhesion of primary astrocytes and microglia to tissue culture plastic for cell culture. Approximately 50ml stock solution was prepared by dissolving 50mg.ml^{-1} of poly-d-lysine (PDL) powder in distilled water. The solution was filter sterilised using a 0.22µm filter and sterile 50ml syringe. Aliquots of 10ml were transferred into universals and the solution was stored at -20°C until required (for up to two years).

2.3.20 Primary astrocyte and microglia cell culture medium

Dulbecco's modified Eagle's medium (DMEM) 500ml was supplemented with 20% (v/v) FBS, 2mM L-glutamine, 100 U.ml^{-1} penicillin and 100 U.ml^{-1} streptomycin. This solution was stored at 4°C for up to one month.

2.3.21 6M Sodium hydroxide (Na0H)

A volume of 158ml of stock sodium hydroxide (Sigma, UK) was slowly added to 125ml of deionised water. The final volume was adjusted to 500ml of deionised water. This solution was stored at room temperature.

2.3.22 Soy-bean trypsin inhibitor stock solution

A mass of 100mg trypsin inhibitor from glysine max (soybean) was re-suspended in 50ml of distilled water and dispensed into 1ml aliquots (2mg.ml^{-1}) and stored at -20°C until required.

2.3.23 Standard diluent buffer

The contents of the 10x concentrate vial provided in the enzyme linked immunosorbent assay (ELISA) kit was added to a graduated cylinder containing 225ml of distilled water before use and agitated to mix thoroughly.

2.3.24 Streptavidin-HRP solution

The contents of the streptavidin vial provided in the enzyme linked immunosorbent assay (ELISA) kit were diluted with 0.5ml of HRP diluent (also provided in the kit).

2.3.25 SYBR gold solution

A volume of 1µl of 10,000x SYBR gold was diluted in 30ml of 10mM tris-HCl pH 7.5, 1mM EDTA buffer. This solution was stored at 4°C for up to eight weeks.

2.3.26 Tris-HCl (1M)

A mass of 121g of tris base was dissolved in 800ml of distilled water and mixed thoroughly using a magnetic stirrer and stirrer bar. The pH of the solution was adjusted to pH 7.5 using 6M hydrochloric acid the solution was once again mixed thoroughly and made up to one litre with distilled water. This solution was stored at room temperature until required for up to three months.

2.3.27 10mM Tris-HCl 1mM EDTA buffer

Tris-HCl EDTA buffer was prepared by mixing 5ml of 1M tris-HCl (section 2.3.26) with 1ml of 0.5M EDTA (2.3.11) in 500ml of distilled water. This solution was stored at room temperature until required for up to three months.

2.3.28 Triton X-100

A stock 0.1% (v/v) Triton X-100 solution was prepared by adding 1ml of Triton X-100 to 1L of distilled water. This solution was stored at room temperature for up to three months.

2.3.29 Trypsin for primary cell isolation

Trypsin solution (working concentration 250µg.ml^{-1}) was prepared by adding 19ml of disaggregation media to 1ml of pre-prepared 5mg.ml^{-1} trypsin. This solution was filter sterilised prior to use. The solution was discarded after use and not stored.

2.3.30 Trypsin stock solution

A weight of 50mg of trypsin from bovine pancreas (Sigma, UK) was re-suspended in 10ml of distilled water. The solution was dispensed into 10x 1ml aliquots (5mg.ml^{-1} trypsin) and stored at -20°C until required.

2.3.31 Wash buffer for use in Enzyme Linked Immunosorbent Assay

The 200x wash buffer concentrate (provided in the enzyme linked immunosorbent assay kit) was diluted 200 fold with distilled water to produce a 1x working solution. The contents (10ml) of the provided washing buffer concentrate were poured directly into a clean 2L graduated cylinder. The solutions were mixed gently by inverting the cylinder

taking care to avoid the production of bubbles. The remaining solution was stored at 4°C for up to one week.

2.4 Methods

2.4.1 Tissue culture

All cell types; C6 (rat brain, glial astrocytic cell line), PC12 (rat adrenal gland, pheochromocytoma neuronal cell line) and primary rat astrocytes and microglia were cultured in cell culture medium (sections 2.3.2, 2.3.16 and 2.3.20, respectively). The resurrection, isolation, maintenance and passaging of C6, PC12 and primary astrocytes and microglia were performed in class II safety cabinets using aseptic technique. All cells were cultured at 37°C in 5% (v/v) CO_2 in air. Prior to use all media and supplements were warmed to 37°C in an incubator.

2.4.1.1 Resurrection and maintenance of C6 and PC12 cell lines.

Both cell lines were removed from liquid nitrogen storage and thawed in a 37°C water-bath. Once the cell stock had thawed, the contents (1ml) were transferred to a universal, the cryovial was washed with 1ml of pre-warmed supplemented cell culture medium to ensure all the cells were removed from the vial. An additional 8ml of pre-warmed supplemented culture medium was added to the cells in the universal. The cell suspensions were then centrifuged at 150g for 10 minutes at room temperature to remove the cryoprotectant.

The supernatant was carefully aspirated from the cell pellet, which was re-suspended in 3ml of the appropriate supplemented medium. The cell suspensions were transferred to 25cm^3 cell culture flasks and an additional 7ml of culture medium was added. The cells were incubated at 37°C in 5% (v/v) CO_2 in air. When the cells were 80% confluent they were passaged and transferred into larger 75cm^3 cell culture flasks.

2.4.1.2 Cell passaging of C6 astrocytic cell line

Prior to passaging, the appropriate cell culture medium was warmed to 37°C in an incubator. The cells were viewed using an inverted light microscope to ensure they were approximately 80% confluent prior to splitting. The cell culture medium was removed from the 75cm^3 flask. The monolayer of cells was washed twice with 10 ml DPBS (without calcium or magnesium) to remove any residual culture medium. Trypsin/EDTA (5ml) was added to each flask and incubated for five minutes at 37°C in 5% (v/v) CO_2 in air. The flasks were gently tapped to detach the adherent cells from the tissue culture plastic and transferred to a universal. A further 10ml of pre-warmed supplemented medium was added to the suspended cells to inhibit the trypsin. The cells were centrifuged at 150g for

10 minutes at room temperature. The supernatant was aspirated from the cell pellet and re-suspended in 3ml of the appropriate cell culture medium. The cells were counted using the trypan blue exclusion assay (section 2.4.1.4) and a seeding density between 5 x 10^5 and 1 x 10^6 was used to seed the cells into fresh 75cm^3 tissue culture flasks. The culture medium was changed or topped up every 3-4 days until the cells were confluent and ready to be passaged again.

2.4.1.3 Cell passaging of PC12 neuronal cell line.

Prior to passaging the appropriate cell culture medium was warmed to 37°C in an incubator. The cells were viewed using an inverted light microscope to ensure they were approximately 80% confluent prior to splitting. The cell culture medium containing suspended non-adherent cells was removed from the 75cm^3 flask and placed in a universal. The cells were centrifuged at 150g for 10 minutes at room temperature. The supernatant was aspirated from the cell pellet and re-suspended in 3ml of the appropriate cell culture medium. The cells were counted using the trypan blue exclusion assay (section 2.4.1.4) and a seeding density between 5 x 10^5 and 1 x 10^6 was used to seed the cells into fresh 75cm^3 tissue culture flasks. The culture medium was topped up every 3-4 days until the cells were confluent and ready to be passaged again.

2.4.1.4 Cell counting using the trypan blue exclusion assay.

The number of viable cells was determined using the trypan blue exclusion assay. When a cell dies the integrity of the membrane becomes compromised allowing the trypan blue dye to permeate the cell, thus dead cells appear blue when viewed using light microscopy (and thus were excluded from the count) and the living cells (cell membrane integrity intact) appear colourless.

Cells were passaged and the cells and supplemented medium transferred into a universal. Cellular aggregates were removed by gentle agitation and pipetting. Trypan blue 0.2% (v/v) was mixed with each cell suspension at a ratio of 1:10, a volume of 90µl of the cell suspension was placed into an eppendorf and 10µl of trypan blue was added. Using 70% (v/v) ethanol, a haemocytometer was cleaned prior to performing the cell count and a glass coverslip was gently adhered onto the chamber of the haemocytometer.

A volume of 10µl of the cell suspension: trypan blue mixture was loaded into the haemocytometer chamber, which was then placed under an inverted light microscope to perform the cell count. A minimum of 100 cells were counted within the 25 square counting grid (Figure 2.1). Generally, the number of viable cells in 6 squares exceeded 100

cells, thus the number of viable cells in 6 squares was counted and the number of cells present in 1ml of medium was calculated using the equation outlined below.

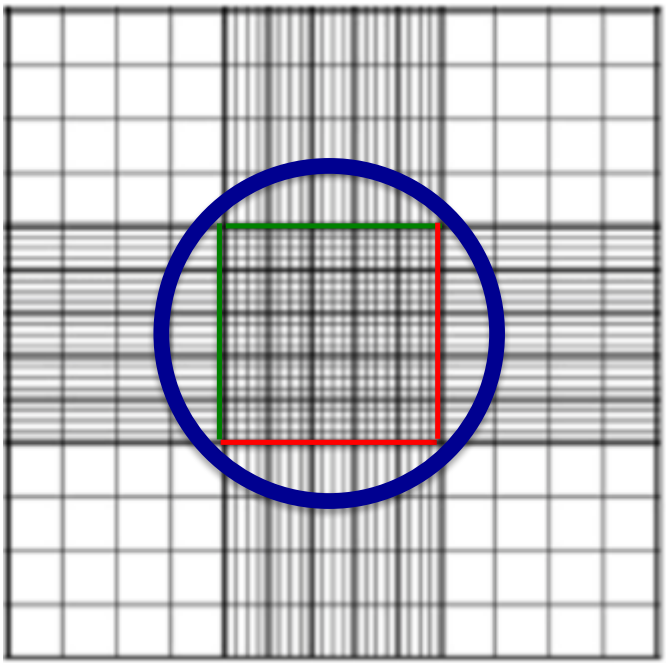

Figure 2.1. Neubauer haemocytometer 25 square counting grid. Cells located on the top and left extremity lines were included in the count (green lines). Cells positioned on the bottom and right extremity lines were not included in the cell count (red lines).

Number of viable cells=

$$\frac{\text{(Total number of cells- number of blue stained cells)}}{\text{Number of squares counted}} \times (25/6) \times 1\text{x}10^{4} \times (10/9)$$

Here 25/6 was the correction factor for the total number of cells in a known area (the central 25 squares), 10/9 was the correction for the dilution factor when adding trypan blue to the cell suspension and 1 x 10^{4} was the dilution factor per ml.

2.4.1.5 Cell Cryopreservation

So as to maintain a stock of each cell type, after passaging, a proportion of the cells were cryopreserved for later use when needed. Cells were passaged and detached from the tissue culture flasks using trypsin. The cell pellet was re-suspended at a seeding density of 1x10^{6} cells per ml in cryopreservation medium; 70% (v/v) supplemented medium, 20% (v/v) FBS and 10%(v/v) filter sterilised dimethyl sulphoxide (DMSO). Cryovials containing cellular aliquots (1ml) were transferred to a cryofreezing pot containing isopropanol. The vials were frozen at -80°C overnight and then transferred to liquid nitrogen for storage in the long term.

2.4.1.6 Primary Astrocyte and microglia cell isolation and culture

Primary astrocytes and microglia were isolated from P2 Wistar rat pups so as to investigate the effect of metallic wear particles on cells of the CNS.

2.4.1.6.1 Coating tissue culture flasks with Poly-D-Lysine for culture of primary astrocytes and microglia.

Prior to the collection of P2 Wistar rat pups, 75cm^3 tissue culture flasks were coated with 4mls of poly-d-lysine (PDL) 50$mg.ml^{-1}$ (section 2.3.19) and incubated at 37°C in 5% (v/v) CO_2 in air (the number of flasks to be coated was dependent on the size of the litter of pups- 2 cortices per flask). The PDL enabled the primary cells to adhere to the tissue culture plastic. After the one-hour incubation, PDL was aspirated from each flask and discarded. To eliminate residual PDL the flasks were washed twice with 4mls of PBS and once with 4mls of supplemented medium and left to dry (with caps on) in the 37°C incubator in 5% (v/v) CO_2 in air for 30 minutes.

The day prior to the rat cortex dissection and cell isolation, the required dissection kit was dry heat sterilised (section 2.1.4 and section 2.1.3.2). The solutions required for the isolation protocol including; disaggregation medium, trypsin, concentrated inhibitor, dilute inhibitor and BSA were prepared fresh on the day of the dissection (section 2.3.8, 2.3.29, 2.3.7 and 2.3.5 respectively).

2.4.1.6.2 Isolation of primary astrocytes and microglia.

Primary astrocytes were isolated from the cortices of P2 (2 day old) Wistar rat pups. The animals were collected from The University of Leeds, Central Biomedical Services (between six and eight pups per litter). The tissue was obtained in accordance with the Home Office Schedule 1 procedure in a home office licenced laboratory at The University of Leeds.

Prior to the dissection of the rat cortices, 10ml of sterile disaggregation medium (section 2.3.8) was added to two tissue culture dishes (60 x 10mm), in order to prevent the tissue from drying out. Prior to and during dissection, the heads were stored on ice in a 50ml falcon tube. Each head was removed from the tube on ice and sprayed liberally with 70% (v/v) ethanol before being brought into the class II cabinet. The snout was held between the thumb, index finger and middle finger, pinching very slightly to maintain a firm grip. Care was taken to ensure the ears were still visible and the snout pointed down towards the palm of the hand. This positioning ensured accurate, repeatable alignment when the initial incisions were made.

The cavity at the back of the skull, where the brain stem joined the brain, was located and sterile, curved scissors were inserted into this hollow region. An incision was made around the edge of the skull to the front of the head aligning the scissors above the ear and through the eye. Care was taken to keep the inner blade still and make the cut with the outer blade only, so as to protect the brain tissue from damage.

Using tweezers the skull was carefully peeled back making sure the brain tissue remained in position. The cortex was carefully loosened from the rest of the brain using a spatula. The cortex was removed from the skull and placed on the lid of a sterile tissue culture dish. Excess brain tissue was removed using the spatula. Using fine tweezers the meninges were peeled away from the cortex tissue. The cortex was then inverted and the vascular tissue underneath removed using fine tweezers. The meninges were then discarded along with other waste tissue. The cortices were then placed in the tissue culture dishes containing 10ml of disaggregation medium. This procedure was repeated for each head and three cortices placed in each tissue culture dish containing disaggregation medium. The dissection equipment was thoroughly washed in 70% (v/v) ethanol between dissections.

Once all the cortices were dissected, the disaggregation medium was removed from the tissue culture dishes, the cortices transferred to fresh sterile tissue culture dish lids and chopped into $1mm^3$ cubes using the flat edge of the scalpel blade. The chopped tissue was placed into fresh tissue culture dishes containing 7ml of filter sterilised trypsin solution (section 2.3.29) and incubated for 15 minutes at 37°C in 5% (v/v) CO_2 in air.

After the incubation period the cortices were removed from the incubator and 7ml of sterile dilute trypsin inhibitor added (section 2.3.7). The contents of each dish were then transferred to sterile 50ml falcon tubes (one falcon tube per tissue culture dish). The cortices were centrifuged at 400g for approximately five seconds. The supernatant was aspirated and discarded and the remaining pellet re-suspended in 10 drops of sterile concentrated inhibitor (section 2.3.7). The tissue was mechanically dissociated by aspiration using a wide bore pipette tip and a P1000 Gilson pipette. The tissue was allowed to settle for approximately five minutes at room temperature, the cell suspension was collected and transferred to a sterile 15 ml falcon tube. A further 10 drops of concentrated inhibitor were added to the tissue debris, the tissue mechanically dissociated, (as described previously) and allowed to settle, the supernatant was removed and pooled with the first supernatant. This step was repeated a total of five times pooling together all the supernatants. In the 15ml falcon tube, the cell suspension (pooled

supernatants) was underlaid with an equal volume of BSA solution (section 2.3.5). The solution was centrifuged at 400g for five minutes at room temperature. The supernatant was removed and discarded and the cell pellet re-suspended in 12ml of supplemented DMEM medium, pre-warmed to 37°C. The PDL coated flasks were filled with 8mls of fresh supplemented medium and 3ml of cell suspension (the flasks were seeded with 1.5-2 cortices per flask depending on the number of pups in the litter, the pooled cells from one litter were split evenly between four flasks and one flask of cells used per investigation). The cells were incubated at 37°C in 5% (v/v) CO_2 in air. The cells were cultured for 2 weeks prior to use. After one week in culture, half of the medium was removed and replaced with 6mls of fresh supplemented DMEM medium. The cells were only passaged once (section 2.4.1.6.3). Once again the tissue culture flasks were pre-coated with PDL prior to passaging.

2.4.1.6.3 Passaging of primary rat astrocytes and microglia.

After two weeks in culture, the primary rat astrocytes and microglia were passaged (this was performed only once to prevent differentiation into a more fibroblast-like cell type). Due to the use of PDL to enable the primary astrocytes and microglia to adhere to tissue culture plastic, a process not employed with the cell lines utilised in this study, the method of passaging the primary cells was slightly modified when compared to the method utilised with the C6 glial and PC12 neuronal cell lines.

The appropriate supplemented cell culture medium was warmed to 37°C in an incubator for one hour prior to passaging the primary astrocytes and microglia. The cell culture medium was removed from each 75cm^3 flask. The primary rat astrocytes and microglia were washed twice with 10ml DPBS (without calcium or magnesium) and 5ml Trypsin/EDTA added to each flask and agitated at 150rpm for 10 minutes at 37°C in 5% (v/v) CO_2 in air in an incubator. The 5ml cell, trypsin/EDTA suspension was transferred to a universal. A volume of 5ml of pre-warmed supplemented medium was added to the suspended cells in the universal to inhibit the trypsin. An additional 10ml of supplemented medium was added to each flask and the remaining cells, which had not detached, were removed using a cell scraper. The cells were centrifuged at 150g for 10 minutes at room temperature. The supernatant was aspirated from the cell pellet and re-suspended in 3ml of the appropriate cell culture medium. The cells were counted using the trypan blue exclusion assay (section 2.4.1.4) and a seeding density of 1 x 10^6 used to seed the cells into fresh 75cm^3 tissue culture flasks. A volume of 3ml of pre-warmed supplemented medium was added every 3 days until the cells were confluent.

2.4.1.6.4 Separation of primary astrocytes and microglia into individual cell populations

To further understand the cellular mechanisms behind the biological response of primary astrocytes and microglia to cobalt chrome and stainless steel nanoparticles additional experiments were performed with primary rat astrocytes in isolation. This was achieved by shaking off the non-adherent microglia from the adherent astrocytes.

To eliminate microglia from the astrocyte culture, once the cells were 80% confluent the filter caps of each flask were removed and replaced with closed caps in a class II safety cabinet. The flasks were placed onto a shaker in a 37°C incubator, the closed caps carefully loosened (enabling CO_2 to enter the flasks) and the level of CO_2 in the incubator allowed to reach 5% (v/v). The caps were then tightened and the flasks were shaken for 4 hours at 150rpm. During the four-hour incubation period new 75cm^3 flasks were coated with PDL (section 2.4.1.6.1) in preparation for passaging.

After the 4 hour incubation period the medium (containing predominantly microglia) was added to the fresh PDL coated flasks and allowed to grow overnight. A volume of 12ml of supplemented DMEM medium was added to the confluent flasks containing astrocytes only. The flasks were then returned to the incubator at 37°C in 5% (v/v) CO_2 in air.

2.4.1.6.5 Preparation of cellular 3D collagen gels.

Primary astrocytes and microglia in co-culture and primary astrocytes in isolation were cultured in a 3D collagen hydrogel to determine the biological effects of cobalt chrome and stainless steel on cells in a more physiologically relevant environment than a 2D monolayer cell culture system.

Primary astrocytes and microglia or primary astrocytes in isolation were seeded in collagen gels at a seeding density of 1 x 10^5 cells per 100µl gel. The cells from a single 75cm^3 flask were utilised per investigation (for instance in the culture of primary astrocytes and microglia with increasing concentrations of cobalt chrome wear particles, for two days in culture, to investigate the effect of these particles on cell viability). For cell only gels, the volume of gel required per experiment was calculated. The gel composition was as follows, 80% (v/v) type I acidified rat tail collagen, 10% (v/v) 10x minimum essential medium (MEM), 5.8% (v/v) neutralising solution (predominantly sodium hydroxide, remaining contents remain confidential to TAP biosystems) and 4.2% (v/v) cells re-suspended in supplemented medium.

To produce the 3D collagen hydrogels, firstly the 10x MEM was added to a universal. Using a wide bore pipette (so as to reduce cross shear in the collagen gel) the type I rat tail collagen was added to the 10x MEM and mixed well with a smooth swirling action so as to avoid the production of bubbles. The neutralising solution was added and a colour change from luminous yellow to peach was observed. The addition of the neutralising solution provided an optimum pH for the growth of the primary astrocytes and microglia and began the setting process of the gel. The cell (or cell and particles or particles only) solution was finally added and the solution mixed thoroughly to ensure an even distribution of cells and particles throughout the viscous gel, once again bubbles were avoided at this stage. A volume of 100µl gel was pipetted into flat bottom 96 well plates using a wide bore pipette and the gels allowed to set for 10 minutes at 37°C in 5% (v/v) CO_2 in air. Six replicates were produced per test condition. Supplemented medium (200µl) was added to the surface of each gel (once set). For the DMSO control a volume of 100µl of supplemented medium and 100µl 99.9% (v/v) DMSO was added to the surface of each gel and allowed to penetrate through the porous hydrogel.

When the cells were exposed to cobalt chrome and stainless steel wear particles, the appropriate volume of cobalt chrome or stainless steel debris was calculated and the solution ultra-centrifuged and the water supernatant discarded. The cell solution was then added to the particles and the gels made according to the same protocol as stated previously.

For the culture of primary cells with cobalt chromium and stainless steel ions, the equivalent particle volumes for each particle dose (0.5µm^3, 5µm^3 and 50µm^3 debris per cell) were incubated for 24 hours at 37°C in 5% (v/v) CO_2 in air in supplemented medium (the volume of medium required was 200µl per 100µl gel and scaled up to make a 20% excess to account for any evaporation). After the 24-hour incubation period the sample was ultra-centrifuged and the supernatant (containing the metal ions) removed and transferred to a fresh universal, leaving the particles behind. A volume of 200µl of the supernatant was added to the surface of each cellular gel and allowed to penetrate the gel. The gels were then incubated for two and five days at 37°C in 5% (v/v) CO_2 in air.

2.4.2 Cell viability assays

To determine the effects of cobalt chrome and stainless steel wear particles on the viability of C6 astrocytic cells (cell line), PC12 neuronal cells (cell line) and primary astrocytes and microglia in a simple 2D culture system, each cell type was seeded with

increasing concentrations of metallic particles (0.05μm^3 debris per cell- 50μm^3 debris per cell). In 2D culture the effect on viability was determined using an ATP Lite™ assay (PerkinElmer, USA). The ATP Lite™ assay utilises the principal that living, metabolically active cells produce ATP (adenosine triphosphate). The level of ATP is significantly reduced when a cell undergoes apoptosis or necrosis. When ATP from lysed cells interacts with the added D-Luciferin and Luciferase (in the provided ATP substrate) light is produced. The level of light generated is proportional to the concentration of ATP and thus is an indicator of cell viability.

2.4.2.1 ATP-lite™assay (2D culture system)

The ATP-Lite™ assay was used to determine the effect of cobalt chrome and stainless steel wear particles on the viability of C6 glial cells, PC12 neuronal cells and primary astrocytes and microglia in a 2D culture system. Here, all the supplemented medium (200μl) was removed from each well. The PC12 neuronal suspension cells clustered together in a pellet-like formation at the bottom of the U bottomed wells and great care was taken not to disturb this pellet and hence remove cells in the process when removing the supernatant. The adherent cell types remained adhered to the tissue culture plastic of the flat-bottomed 96-well plates. A volume of 100μl of fresh supplemented medium was added to each well. A volume of 50μl of mammalian lysis solution was added to each well. The plate was shaken at 700rpm for 5 minutes. Following this 50μl of ATP substrate solution was added to each well and the plate sealed with a micro-plate sealing film, wrapped in foil and agitated on the plate shaker at 700rpm for a further 5 minutes. A volume of 100μl from each well was transferred to a white 96 well optiplate. The plate was dark adapted for 10 minutes and the average luminescence count for each well (average over 10 seconds per well) recorded. The output for this assay was presented as average luminescence counts per second (CPS).

2.4.2.2 Effect of cobalt chrome and stainless steel wear particles on cell viability (3D) using the live dead assay.

Primary astrocytes and microglia and primary astrocytes in isolation (seeding density 1x10^5 cells per 100μl gel) were cultured in a 3D system with all doses of stainless steel or cobalt chromium particles (0.5μm^3 -50μm^3 debris per cell) for 48 hours and five days at 37°C in 5% (v/v) CO_2 in air. DMSO was used as a positive control to trigger cell death.

After the appropriate incubation period with the cobalt chrome and stainless steel wear debris, 48 hours or five days, the supplemented medium was removed from the top of

each gel and the supernatant was transferred to a non-coated 96 well plate and stored at -80°C for later use in the ELISA assay. The gels were washed twice for five minutes with sterile DPBS (without calcium and magnesium). During the wash steps the live dead stain solution was prepared (see section 2.3.14). After the necessary wash steps, 100µl of the supplemented medium, with the addition of calcein and ethidium homodimer, was added to each gel, the 96 well plate was wrapped in foil and incubated for one hour at 37°C in 5% CO_2 in air.

After the one-hour incubation period the residual live dead stain was removed and discarded and once again the gels washed twice in sterile DPBS for five minutes. After washing, 200µl of fresh supplemented DMEM medium was added to each well and the gels immediately imaged using a Zeiss Olympus upright microscope at 10x magnification using the calcein and ethidium homodimer pre-set filters. A total of 6 images were taken per gel, yielding 36 images per condition (there were six replicates per condition). The total number of living (green) and dead (red) cells were counted for each image and the percentage viability compared to the cell only negative control.

2.5 Statistical Analysis

2.5.1 Two way ANOVA

Data was presented ± 95% confidence limits and statistical significance analysed using a two-way ANOVA. Significant differences between the means of test groups (particle doses ranging from 0.5µm^3-50µm^3 wear debris per cell) and controls were determined using Tukey's Post hoc analysis. A p value < 0.05 was indicative of a significant difference. For data that was not normally distributed an arc sine transformation was performed to generate accurate confidence limits.

Chapter 3

Generation, Isolation and Characterisation of Cobalt Chrome and Stainless Steel Particles

3.1 Introduction

In order to determine the impact that the design and biomaterial selection of a total disc replacement has on its wear performance and consequently the host biological response to the TDR device (Vital & Boissiere, 2014), wear simulators with increasing levels of complexity and varying kinematic parameters have been used, ranging from pin-on-plate (Tipper et al., 1999; Germain et al., 2003; Papageorgiou et al., 2014), pin-on-disc (Chiba et al., 2007; Saikko, 2015) to whole joint, spine, simulators (O'Leary et al., 2005; Kurtz et al., 2012; Vicars et al., 2010; Colle et al., 2013; Hyde et al., 2015; Pasko et al., 2016).

It is important to consider the appropriate biomaterial when simulating wear using a joint simulator or a pin-on-plate simulator. Previous studies have utilised both wrought and cast cobalt chrome molybdenum alloys, with varying carbon content. Kretzer et al. (2009) using a hip simulator found steady state and run in wear rates from cobalt chromium molybdenum alloy were lowest when using low carbon CoCrMo on low carbon CoCrMo. Conversely, Firkins et al. (2001) using four 28mm femoral heads and acetabular cups made of medical grade wrought cobalt chromium molybdenum studied the effect of varying the carbon content of the cobalt chromium molybdenum alloy, <0.07% for low carbon and >0.2% for high carbon, and tested their wear performance using a hip simulator and 25% Bovine serum as the lubricant. Firkins et al. (2001) found than the high carbon on high carbon devices produced round to oval wear particles that had a mean length between 25nm and 36nm in length which were significantly larger than wear particles produced by the low carbon on low carbon articulations. The particles from high carbon cobalt chrome articulation were in the appropriate size range for metal particles observed *in vivo* following failed total hip replacements. Unlike Kretzer et al. (2009), Firkins et al. (2001) found the wear rates for the low carbon on low carbon articulations were largest at 0.51mm^3. million $cycles^{-1}$ which is significantly larger than the 0.18mm^3. million $cycles^{-1}$ observed with high carbon on high carbon articulations. Kinbrum & Unsworth. (2008) also found high carbon wrought cobalt chrome molybdenum alloy to have superior wear properties to low carbon wrought alloys (Kinbrum & Unsworth, 2008). Tipper et al (1999) used medical grade wrought cobalt chrome alloy, and using a

six-station pin-on-plate wear simulator and 25% bovine serum as the lubricant, used uniaxial and biaxial simulations to assess the effect of carbon content and type of motion on the wear performance of cobalt chromium molybdenum bearing surfaces and on the characteristics of the wear particles produced. Similarly to the results presented by Firkins et al (2001), Tipper et al. (1999) found that the low carbon on low carbon bearings both with uniaxial and biaxial motion demonstrated the highest wear rates of 0.53 $mm^3.km^{-1}$ and 0.15$mm^3.km^{-1}$ respectively. This material coupling also produced the largest particles (90nm for uniaxial motion and 87nm for biaxial motion). The high carbon cobalt chromium molybdenum on high carbon cobalt chromium molybdenum articulations generated the smallest particles (76nm and 56nm respectively) and demonstrated the lowest wear rates (0.12 $mm^3.km^{-1}$ and 0.11 $mm^3.km^{-1}$) with both uniaxial and biaxial motion. These results highlight the importance of the addition of multi-directional motion and the articulating surface. Biaxial motion produced particles, which more closely modelled the particles observed in hip simulations and *in vivo* from around failed metal-on-metal total hip replacements, thus this more simplistic method of wear production can be used to generate clinically relevant metallic wear particles. Previous *in vitro* investigations have utilised metallic particles, which weren't clinically relevant in size. The use of high carbon wrought cobalt chrome and 316L stainless steel was implemented to generate clinically relevant wear particles.

Germain et al. (2003) utilised a six-station pin-on-plate wear simulator to generate nanoscale cobalt chromium particles for use in cell culture studies. Here water, not serum or medium, was used as the lubricant. The particles produced were between 30nm and 50nm in size, thus simulation using high carbon wrought cobalt chromium molybdenum pins and plates in a six-station pin-on-plate wear rig using a stroke length of 28mm with 30° rotation, with biaxial motion and a load of 80N at a rate of 1Hz in water generated cobalt chromium particles in the nanoscale size range which would be appropriate for use in cell culture studies as they were similar in size to particles observed in metal-on-metal total hip replacements. Thus these parameters were also utilised for the generation of clinically relevant wear particles in this part of the study.

The aim of this part of the study was to generate clinically relevant cobalt chromium and stainless steel particles using a six-station pin-on-plate wear simulator in water, using high carbon wrought cobalt chrome molybdenum and 316L stainless steel pins and plates. These particles will subsequently be filtered and characterised in terms of particle morphology and size, heat sterilised and utilised in cell culture studies to determine the response of cells of the spinal cord to cobalt chromium and stainless steel wear particles.

3.2 Materials

The specification for the pins and plates used in the production of the cobalt chromium and stainless steel wear particles are shown in Table 3.1. The elemental compositions of medical grade 316L stainless steel and high carbon cobalt chrome used in this study are shown in Tables 3.2 and 3.3, respectively.

Table 3.1 Material specifications for pins and plates used to generate metallic wear debris in the six-station pin-on-plate wear simulator (all pins and plates were made in house in the School of Mechanical Engineering at the University of Leeds). Bar stocks were provided by DePuy Synthes Joint Reconstitution, UK.

Material	Surface Roughness	Pin Dimensions	Plate Dimensions (L x W)
High Carbon Cobalt Chrome Molybdenum ASTM F75	Ra ≤0.01μm	Height 12mm Width 11.975mm 100° radius	58 x 24.12mm
Stainless Steel 316L	Ra ≤0.01μm	Height 12mm Width 11.975mm 100° radius	58 x 24.12mm

The cobalt chromium and stainless steel pins and plates were manufactured in house in the School of Mechanical Engineering, the University of Leeds. The pins and plates were manufactured from high carbon (0.27% w/w) wrought cobalt-28 chromium-6 molybdenum, which is the alloy used in the production of surgical implants, or 316L medical grade stainless steel (see Figure 3.1 for pin dimensions and Figure 3.2 for plate dimensions). To generate clinically-relevant cobalt chrome and stainless steel wear particles the pins and plates were manufactured with a smooth contact face with a mean R_a value of ≤ 0.01μm (in accordance with ISO 5832). The pin was produced with a 100° radius.

For identification, all pins and plates were engraved with a number; on the non-contact face of the pin and on the non-contact front of the plate. This numbering system enabled continuity of orientation within the wear simulator. Prior to use in the six-station wear simulator the pins and plates were sonicated in isopropanol 70% (v/v) for 15 minutes to ensure the components were thoroughly cleaned. From this point on the components were handled with clean gloves to ensure no grease or oil from the simulator contaminated the contact surfaces, gloves were changed regularly throughout the set up of

the wear simulator to avoid this.

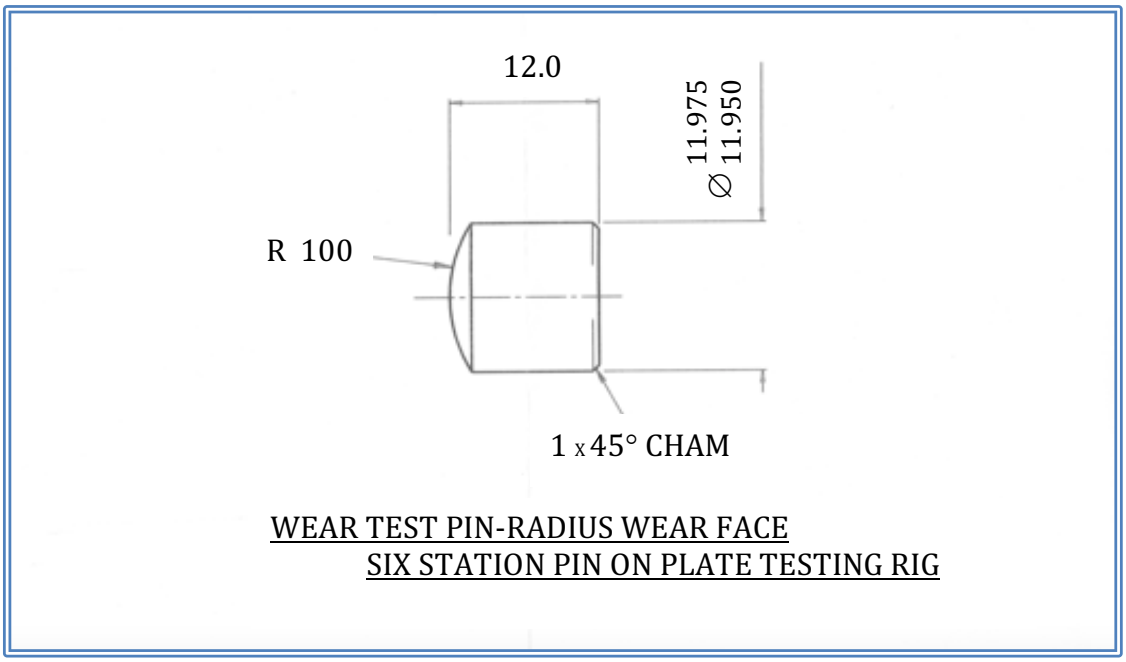

Figure 3.1 The dimensions of the cobalt chromium and stainless steel pins used in the six-station pin-on-plate wear simulator for the generation of clinically-relevant metallic wear debris. Highlighting the height of the pin 12mm and the degree of curvature of the contact surface; 100° radius.

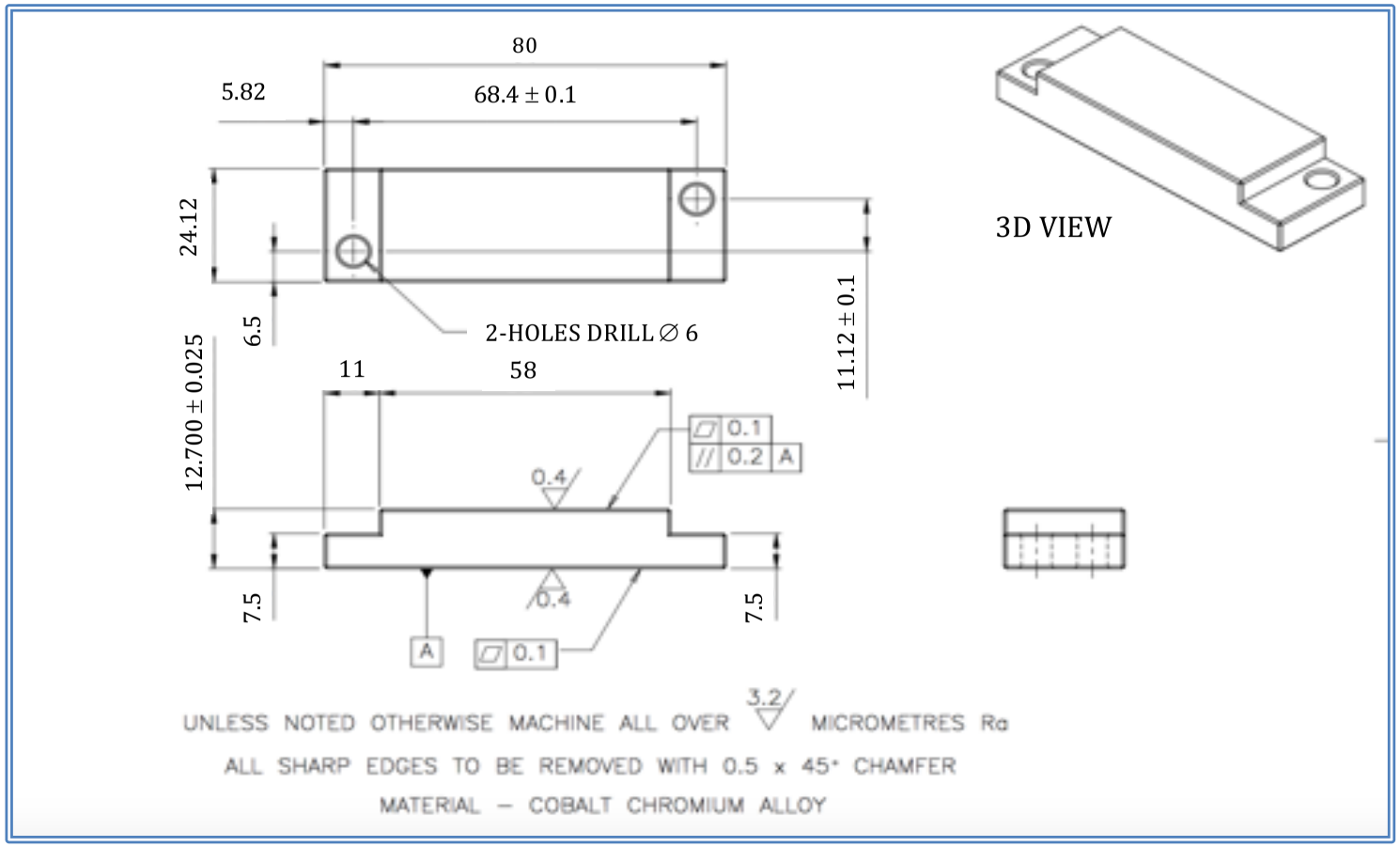

Figure 3.2. The dimensions of the standard cobalt chrome and stainless steel plates used in the six-station wear simulator. All dimensions in the image are in mm.

Table 3.2. Percentage (%) elemental composition of medical grade 316L stainless steel.

Grade		Fe	C	Mn	Si	P	S	Cr	Mo	Ni	N
316L	Min	62.045	0.03	2	0.75	0.045	0.03	16	2	10	0.1
	Max	72						18	3	14	

The stainless steel alloy used in this body of work comprised of Iron (Fe), Carbon (C), Manganese (Mn), Silicon (Si), Phosphrous (P), Sulphur (S), Chromium (Cr), Molybdenum (Mo), Nickel (Ni) and Nitrogen (N).

Table 3.3 Percentage elemental composition of medical grade high carbon (>0.2% w/w) wrought cobalt chrome molybdenum alloy (meets ASTM F75 for cobalt chrome alloy).

Grade		Cr	Mo	Ni	Fe	C	Si	Mn	W	P	S	N	Al	Ti	B	Co
High C CoCrMo	Min	27	5	<0.5	<0.75	<0.35	<1	<1	<0.2	<0.02	<0.01	<0.25	<0.1	<0.1	0.01	Bal
	Max	30	7													

The wrough medical grade cobalt chrome molybdenum alloy used in this body of work comprised of Chromium (Cr), Molybdenum (Mo), Nickel (Ni), Iron (Fe), Carbon (C), Silicon (Si), Manganese (Mn), Tungsten (W), Phosphorous (P), Sulphur (S), Nitrogen (N), Aluminium (Al), Titanium (Ti), Boron (B) and Cobalt (Co), The remaining percentage composition balance was referred to as Bal.

3.3 Methods

3.3.1 Generation of cobalt chrome and stainless steel wear debris using a six-station pin-on-plate wear simulator.

Clinically-relevant cobalt chrome and stainless steel wear particles were generated in water using the six-station pin-on-plate wear simulator using wrought high carbon, smooth (Ra 0.01μm) cobalt chrome or smooth 316L stainless steel pins and plates (section 3.2). The materials used in the generation of particles were the same as those used in the manufacture of orthopaedic implants. Once generated these metallic particles were cultured with spinal cord cells in 2D and 3D cell culture systems to investigate the biological response of cells of the CNS to metal wear particles.

3.3.1.1 Machining and preparation of cobalt chrome and stainless steel pins and plates for generation of clinically-relevant metallic wear debris.

Prior to the generation of cobalt chrome and stainless steel wear particles using the six-station pin-on-plate wear simulator, high carbon cobalt chrome and 316L stainless steel pins and plates were polished to produce a smooth surface finish (Ra 0.01μm) this was performed in house at the School of Mechanical Engineering at the University of Leeds.

3.3.1.2 Parameters for generation of cobalt chrome and stainless steel wear particles using a six-station pin-on-plate wear simulator.

The stroke length for this wear simulation was set at 28mm with ± 30° of rotation and a load of 80N at a frequency of 1Hz. Deionised water was used as the lubricant and the simulator operated for a total of 80 hours (Germain et al., 2003). The calibration of the stroke length and reciprocating speed was performed by a mechanical engineering lab technician prior to each 80-hour test. The load was calibrated prior to the start of each test (section 3.3.1.3).

3.3.1.3 Load calibration

To ensure that an 80N load was transferred to the pin accurately, prior to each test, a load calibration was performed in accordance with the standard operating procedure, SOP 01.3 revision 4 provided by the School of Mechanical Engineering at the University of Leeds. For all six stations the bridges were assembled into position and the load cell was placed into the cavity where the pin holder would sit (starting with station one first and repeating for all six stations). The lever arms were fixed into position and the screws removed, it is at this location on the lever (via the screw) that the load is transferred to the pin from the lever arm through a linear bearing mechanism (these were all replaced after

calibration). The same "calibration" screw was used for all six stations. Using a magnetic spirit level, the screw was adjusted to ensure the lever arm was level and the weight added to provide a load of 80N. Readout from the load cell was generated and recorded. If the load was incorrect by ± 5N, a technician was consulted and the test was not performed until the load was corrected by a technician.

3.3.1.4 Assembly of the six-station pin-on-plate wear simulator.

The components required for the set up of the six-station pin-on-plate wear simulator are described below in Table 3.4:

Table 3.4. The components required for the assembly of the six-station pin-on-plate wear simulator.

Assembly of pin/plate/load	Six-station pin-on-plate wear simulator components
Equipment for assembly of the plate in the bath.	Six stainless steel baths, six stainless steel bath inserts (cobalt chromium and stainless steel plates were fixed into these for the duration of the test), six polymer baffles, six stainless steel toothed racks and six plastic sheets.
Equipment for assembly of the pin in the holder.	Six polymer gear wheels, four stainless steel bridges (spans all six stations, two large bridges were designed to connect together two stations and two smaller bridges covered one station), six stainless steel pin holders (collets), six pin holder (collet) outer sleeves, six threaded nuts and six 9mm stainless steel spacers.
Screws, pins and bearings.	12 large stainless steel screws, 12 short, small stainless steel screws, 24 long, small stainless steel screws, six pivot pins, 12 split pins, six ball bearing assemblies and six linear bearings.
Additional equipment.	Six polyethylene connecting rods, six cantilever arms, six weights, black PVC tape, scalpel holder, curved scalpel blade, a range of Allen keys to fit four different sized screws, spirit level, adjustable wrench, tissue paper, 50ml syringe, sterile deionised water (50ml per bath), 150ml sterile collection pot (to collect lubricant after each 40 hour period).

3.3.1.4.1 Preparation of the linear bearing tray

Prior to the assembly of the six-station wear simulator the six numbered pins and plates were assigned to a station and recorded. The appropriately labeled bath insert (for example bath insert 1) was placed inside the corresponding stainless steel bath (stainless steel bath number 1). The assigned cobalt chrome or stainless steel plate was screwed into position within the bath using two of the large screws.

The corresponding polymer baffle was placed into the bath ensuring a snug fit. The baffle was secured into position using two layers of PVC tape. The two layers of tape provided a tight seal between the baffle and the stainless steel well, which prevented any lubricant loss. The two screw holes (where the toothed rack connected to the bath) were exposed using a curved edge scalpel blade, care was taken not to remove too much tape, thus keeping the seal intact. The toothed rack was secured onto the left hand side of each well using two small screws. A plastic sheet was fitted between the well and the linear bearing platform to prevent lubricant loss. The well was then secured onto the linear bearing platform using four of the small long screws. This process was repeated for each of the six plates.

3.3.1.4.2 Preparation of the pin holders

A 9mm high stainless steel spacer (Figure 3.3) was placed into the collet before fixing the pin into place (smooth side facing outward numbered face in contact with the spacer). It was important to ensure that the pin protruded out of the holder by approximately 5mm (Figure 3.4).

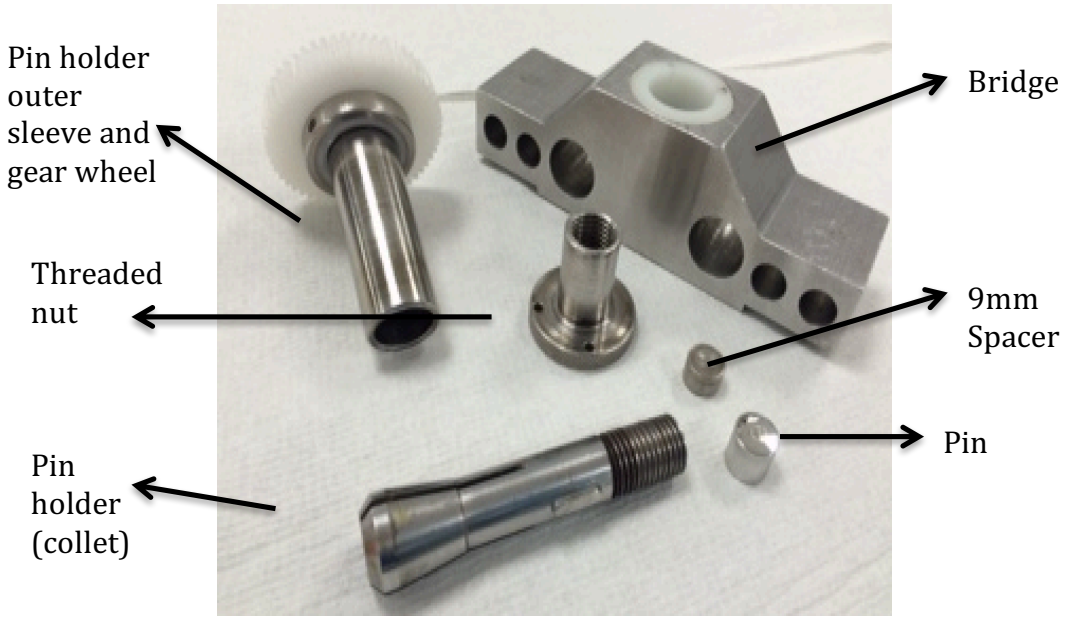

Figure 3.3 The components of the pin holder, collet and bridge.

The collet was then placed into the outer pin holder sleeve, ensuring correct alignment between the key and the taper. The pin holder was then passed through the corresponding numbered bridge section and the threaded nut screwed in place, fixing the pin into position in the collet. The polymer gear wheel was fixed onto the top of the pin holder apparatus.

The bridge apparatus was placed into the support brackets in the simulator. The polymer wheel connected to the toothed rack at the side of the stainless steel well and it was this connection that allowed rotation. At this point in the assembly the connection between the gear wheel and the toothed rack was checked to ensure smooth motion between the two bearings.

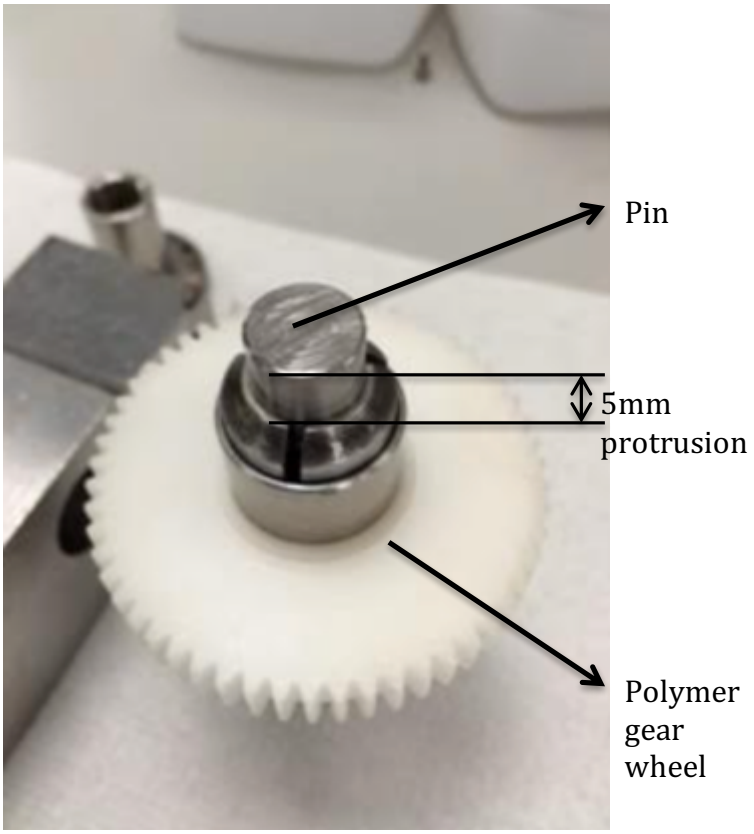

Figure 3.4 Protrusion of the pin out of the holder.

At this point the stroke length was also checked by a technician to ensure it was set to 28mm. The bridge was secured into position by tightening the clamps. Clearance distances were checked, ensuring there was approximately 3mm between the threaded nut and the bridge, 5mm between the bridge and the gear wheel and that the pins connected with the plates and were free to move vertically. This procedure was repeated for all six stations.

3.3.1.4.3 Final assembly of the six-station pin-on-plate wear simulator

Using a syringe, 50ml of sterile deionised water was added to each bath. This volume filled the bath to approximately 3mm above the superior surface of the plate. The pin was moved vertically to ensure the lubricant passed between the pin and the plate.

The polymer connecting rods were screwed into position, connecting the linear bearing trays to the scotch yolk mechanism. The numbered cantilever arms were fixed into position using two split pins per arm and a pivot pin. Using a spirit level and spanner the screws on the cantilever arms were adjusted until the levers were parallel to the plate and perpendicular to the pin.

A ball bearing assembly was positioned on top of each threaded nut and a bearing placed on top. These bearings provided a point where the load could be applied to the pin in a smooth manner (allowing for the ± 30° rotation). The frequency counter was set to zero and the motor turned on. The speed was adjusted to 1Hz, meaning that the simulator performed 60 cycles per minute. The weights were positioned at the 80N marker on the cantilever arm. The simulator was turned off after 8 hours continuous operation per day and the level of lubricant checked three times per day. If the level of water fell below 3mm above the superior surface of the plate it was topped up with sterile deionised water.

3.3.1.4.4 Dismantling the wear simulator and cleaning the components.

After 80 hours (eight hours per day for ten days) the wear simulator was dismantled. The weights were removed from each station and the speed reduced until the components stopped moving, the motor was then turned off. The number of cycles was recorded. The cantilever arms were removed and returned to their position in the storage rack.

The polymer connecting rods were un-screwed, this disconnected the linear bearing trays from the scotch-yolk mechanism. The ball-bearing assemblies atop the threaded nuts were removed, the bridges were released and the threaded nuts carefully unscrewed. The pin holders and polymer gear assemblies were then uncoupled from the bridge (the pin holder was kept in the upright position to ensure the pin was not released and damaged). The cobalt chrome or stainless steel pins and spacers were carefully removed from the pin holder and stored in medical wipes to prevent contamination with grease from the simulator and damage. The collet was released from the pin holder.

The six baths were detached from the linear bearing platforms and the plastic sheets taken from the platform. The toothed rack, PVC tape and polymer baffle were disconnected from

the wells. The polymer baffles were placed above the bath and left to drain for approximately 10 minutes to ensure all lubricant on the baffles was drained into the bath and collected. After draining, the lubricant was collected into 150ml pots. To ensure all debris was collected, each bath was rinsed with an additional 50ml of sterile deionised water and collected in the 150ml labeled pots (name, date and material) each pot was taped closed to prevent loss of lubricant. The lubricant was stored at -20°C until required. The cobalt chromium or stainless steel plate and bath insert was removed from each well, taking care not to damage the surface upon removal.

All components were cleaned thoroughly after use. Immediately after the simulator was dismantled all the components were washed in warm water with household detergent. The metal components were thoroughly cleaned with a hard bristled brush. A softer bristled brush was used to clean the polymer components. After this initial cleaning procedure, all components were rinsed thoroughly with distilled water to eliminate the detergent. Finally all the components were soaked in 1% (v/v) Trigene solution for 20 minutes. The components were rinsed with distilled water and dried. The cobalt chromium and stainless steel pins, plates and all the screws were placed in 70% (v/v) isopropanol and sonicated for 15 minutes. The pins and plates were dried using medical wipes to avoid further damage to the contact surfaces and stored in medical wipes. The pins and plates were re-polished after 80 hours use.

3.3.1.5 Recovery of the cobalt chrome and stainless steel wear particles using sequential filtration.

The “as generated” cobalt chrome and stainless steel wear particles were sequentially filtered through 5μm 1μm, 0.1μm, and 0.015μm polycarbonate filters to recover particles in order to generate a size distribution and to determine the morphology of the metallic wear debris.

The stainless steel and cobalt chromium wear particles (as generated) were stored at -20°C. Prior to filtration or generation of particle stocks, the samples were thawed at room temperature. Prior to use all glass filtration equipment was thoroughly cleaned. The apparatus was first washed in household detergent with a hard bristled brush and warm water. The equipment was then rinsed once with tap water and then three times with deionised water. The apparatus was left to dry.

3.3.1.5.1 Preparation of a known concentration (1mg.ml^{-1}) of cobalt chromium and stainless steel particle stock solutions.

After the cobalt chromium and stainless steel wear debris was generated in water using the six-station pin-on-plate wear simulator, the lubricant was collected from each bath and stored at -20°C until required for size distribution, particle morphology and elemental composition analysis or cell culture studies.

To generate the stock solutions, the samples of wear debris were thawed slowly at room temperature allowing the debris to settle to the bottom of the 250 ml storage pot. The cobalt chrome debris was passed through a 0.1μm polycarbonate filter to remove large platelet-like particles prior to the generation of the stock solution, this was not done for the stainless steel wear particles. The debris was collected from the bottom of the pot and transferred to a pre-weighed glass bottle. The sample was then placed in the oven at 190°C for four hours to sterilise the debris and remove endotoxin, derived from the cell membrane of gram-negative bacteria, ready for culture with cells. The bottle was reweighed. The initial weight was subtracted from the final weight yielding a value for the mass of debris. The appropriate volume of deionised water was added to generate a 1mg.ml^{-1} stock of particles.

3.3.1.5.2 Sequential filtration of as generated cobalt chrome and stainless steel wear particles through 5μm, 1μm 0.1μm and 0.015μm pore size polycarbonate filters.

The apparatus was assembled in a class I laminar flow hood (to reduce airborne contamination). A volume of 1ml of the "as generated" stock sample of stainless steel or cobalt chrome particles in water (1mg.ml^{-1}) was diluted in a further 5ml of deionised water for the cobalt chromium particles and 10ml of deionised water for the stainless steel particles and sequentially filtered through 25mm diameter; 5μm 1μm, 0.1μm, and 0.015μm pore size polycarbonate filters (for generation of stock solutions see section 3.3.1.5.1). The filters were handled with care, using tweezers, on the edge of the filter. Each filter was thoroughly cleaned by filtering 10ml 70% (v/v) ethanol, then 10ml ultra-pure water. This process also ensured there was a tight seal formed between the glass reservoir, the filter and the glass filter tray, ensuring the vacuum was strong enough to draw the liquid through the filter. The sample was then placed in the glass reservoir and the vacuum pump turned on and set to a pressure of 1 Bar, drawing the sample through each filter. Once the samples had passed through the filter, the filters were carefully transferred, using tweezers, to sterile petri dishes, one filter per petri dish, and allowed to dry under an infra-red lamp for a minimum of 4 hours inside the class I hood. The glass

filter tray was cleaned with pyrogen free water between each filtration. Prior to and after imaging using field emission gun scanning electron microscopy (FEGSEM) the filters were stored under vacuum in the presence of silica gel to minimise exposure to moisture.

3.3.1.6 Preparation of filters for field emission gun scanning electron microscopy. (FEGSEM) and energy-dispersive X-ray spectroscopy (EDX) analysis.

All filters; 5μm, 1μm, 0.1μm, and 0.015μm were mounted onto aluminium stubs (the filters and stubs were the same diameter; 25mm) using an adhesive carbon tab (double sided). To reduce charging of the sample, the circumference of each filter was painted with a viscous black carbon paste. The filters were coated, to a thickness of 3nm, with either platinum (using a sputter coater) or carbon rod evaporation. The samples were imaged immediately using a high-resolution scanning electron microscope.

3.3.1.7 Scanning electron microscopy of, as generated, stainless steel and cobalt chromium wear particles

The cobalt chromium and stainless steel particles generated in the six-station pin-on-plate wear simulator were imaged using scanning electron microscopy in order to determine their morphology and size distribution.

3.3.1.7.1 Imaging protocol for cobalt chromium and stainless steel wear particles using the Hitachi SU8230 FEGSEM

After the filters had been mounted and coated, the samples were imaged using a Hitachi SU8230 FEGSEM, the samples were viewed at a voltage of 1Kv and a working distance of 3mm. For each filter three fields of view were selected per magnification. The magnifications used were x 30K (x 30,000 magnification), x 60K, x 90K, and x 150K. At least two images per magnification (high magnification) were obtained for each filter.

3.3.1.8 EDX analysis of cobalt chrome and stainless steel wear particles

Energy dispersive x-ray spectroscopy (EDX) was used to determine the elemental composition of the particles collected on the 25mm polycarbonate filters. EDX analysis was performed at the same time as SEM imaging. Numerous EDX detection points were selected from metallic wear particle agglomerates (EDX was performed when the particles were coated with carbon, as the platinum coating contaminated the samples when performing the elemental analysis). Numerous fields of view (3-5) were selected for each filter and between 3-6 spectra obtained for each field of view.

3.3.1.9 Particle characterisation and image analysis using Image Pro Plus®

To generate a size distribution of the cobalt chromium and stainless steel particles the scanning electron microscopy images were analysed using Image Pro Plus® version 6.0 image analysis software. For this body of work, between one and five images were captured for each filter, The number of images taken was dependent on the number of particles available for counting in that particular field of view, a particle was only analysed if the entire perimeter of the particle could be observed and draw around. The imaging protocol was designed so a minimum of 300 particles could be analysed per material. Measurements from all filter sizes were combined and analysed to generate a size distribution. Each particle was sized manually by drawing around the particle. Every particle from each image (High magnifications only) from all filters were included in the size distribution, providing the entire perimeter of the particle could be observed and drawn around. If any region of the particle was obscured by another particle, for instance in agglomerates, this particle was not included. The measurements from each filter were pooled and exported into an excel spreadsheet. For each particle, the particle area, perimeter, width, length, aspect and roundness was measured. Initially the sample was viewed at a low magnification (x 35) to ensure the sample was of an appropriate quality to image and to make sure the surface was evenly dispersed with particles. High-resolution images were taken at x 30K, x 60K, x 90K and (sample permitting) x 150K magnification. A minimum of 300 particles were analysed for each material (cobalt chromium and stainless steel). The data was organised into incremental size categories. The size range, 0-500nm was separated into 10nm increments, the remaining particles were categorised as 500nm-1μm and >1μm and each particle allocated to a category depending on its length. This was achieved in excel using "countifs" formula. The results are presented as a percentage of the total number of particles sized.

3.4 Results

3.4.1 Production of cobalt chromium and stainless steel wear particles using the six-station pin-on-plate wear simulator.

The aim of this body of work was to generate sufficient volumes of cobalt chromium and stainless steel wear particles, to be used in cell culture studies, where cell lines and primary cells were cultured with metallic wear particles and the biological effects on cells of the central nervous system (CNS) determined.

3.4.2 Isolation of, as generated, cobalt chrome and stainless steel particles using a filter sequence of 5μm, 1μm, 0.1μm and 0.015μm polycarbonate filters.

FEGSEM images were taken of the cobalt chrome and stainless steel wear particles on all four polycarbonate filters and the particles analysed using Image Pro Plus® 6.0 imaging software. A 2Kv voltage and working distance between 8mm and 8.2mm was used to obtain images at low magnification on the larger 5μm and 1μm filters A voltage of 1Kv and a working distance of 3mm was used to obtain high resolution images at high magnifications on the 0.1μm and 0.015μm filters The morphologies of the cobalt chrome particles collected on each polycarbonate filter can be seen in Figures 3.5, 3.6, 3.7 and 3.8 and the stainless steel particles in Figures 3.12, 3.13, 3.14 and 3.15.

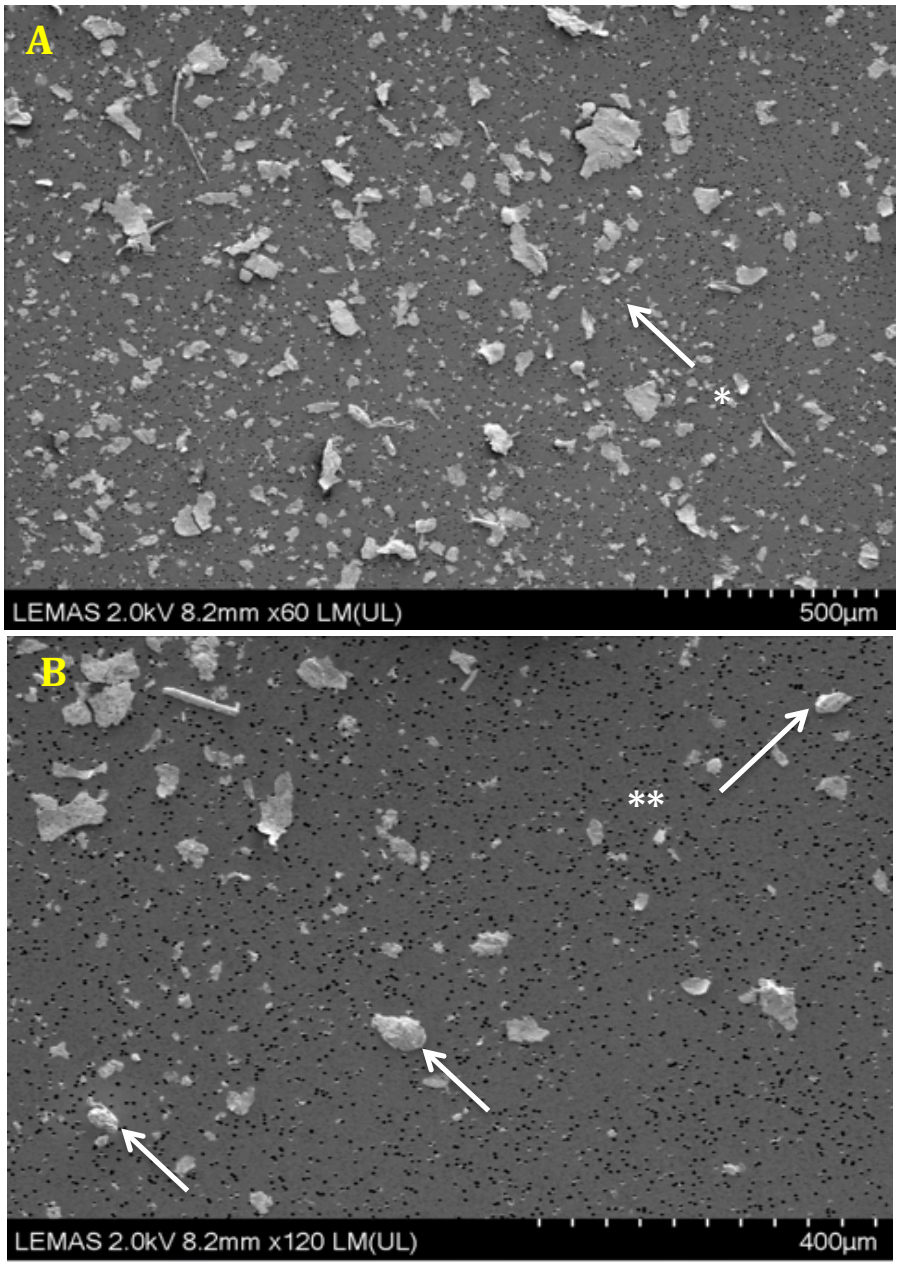

Figure 3.5 Cobalt chromium aggregates and micron-sized cobalt chromium wear particles generated in a six-station pin-on-plate wear simulator. The particles were collected on a 5µm filter analysed using high resolution FEGSEM at low magnification x 60 (A) and x 120 respectively (B). *= Large, irregular micron-sized particles, **= Agglomerates of sub-micron cobalt chrome particles.

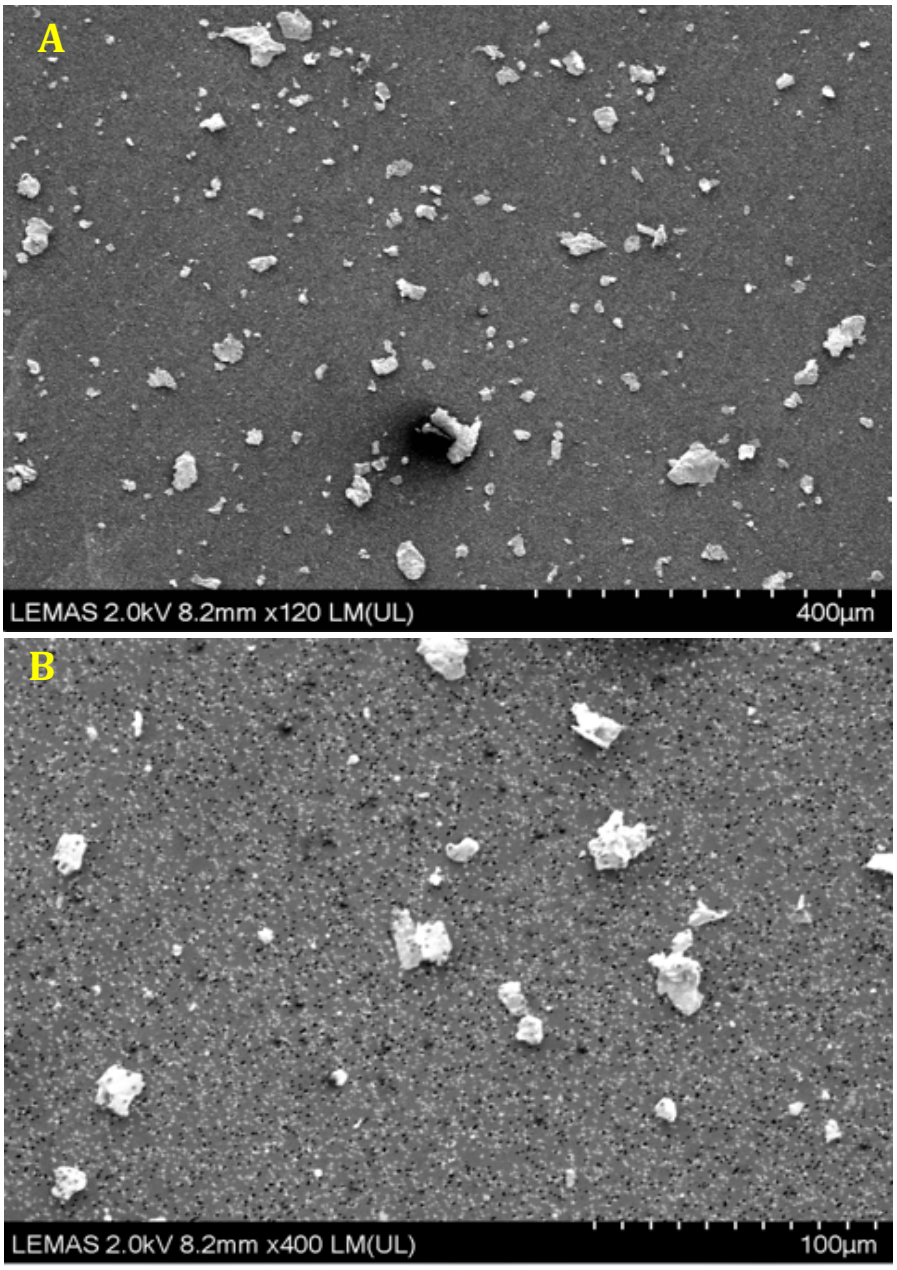

Figure 3.6 Cobalt chromium aggregates and micron-sized cobalt chromium wear particles generated in a six-station pin-on-plate wear simulator. The particles were collected on a 1µm filter analysed using high resolution FEGSEM at low magnification x 120 (A) and x 400 (B) respectively.

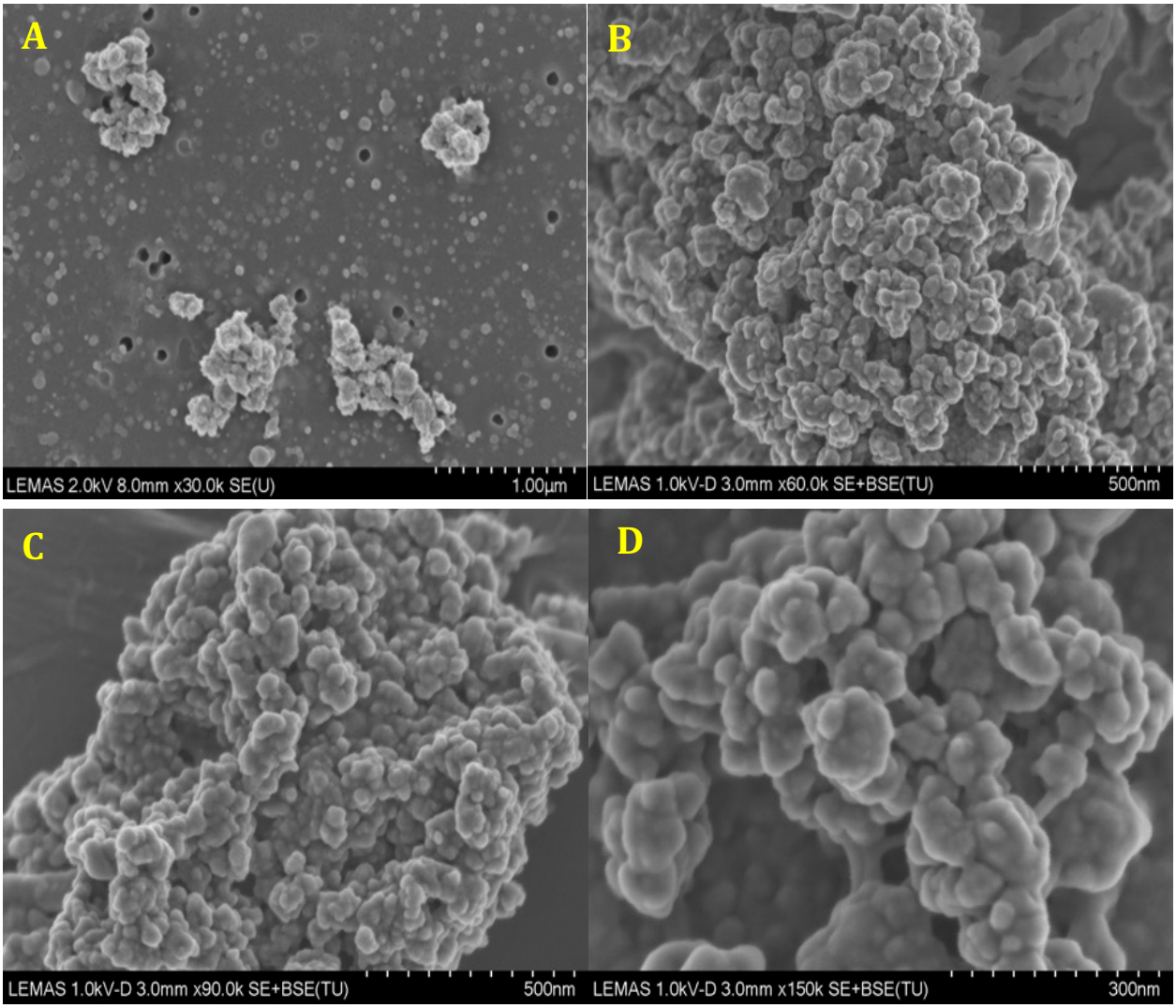

Figure 3.7 Aggregates of nanoscale cobalt chromium wear particles generated in a six-station pin-on-plate wear simulator. The particles were collected on a 0.1µm filter analysed using a high resolution FEGSEM at high magnification x 30K (A) and x 60K (B) x 90K (C) and x 150K (D) respectively.

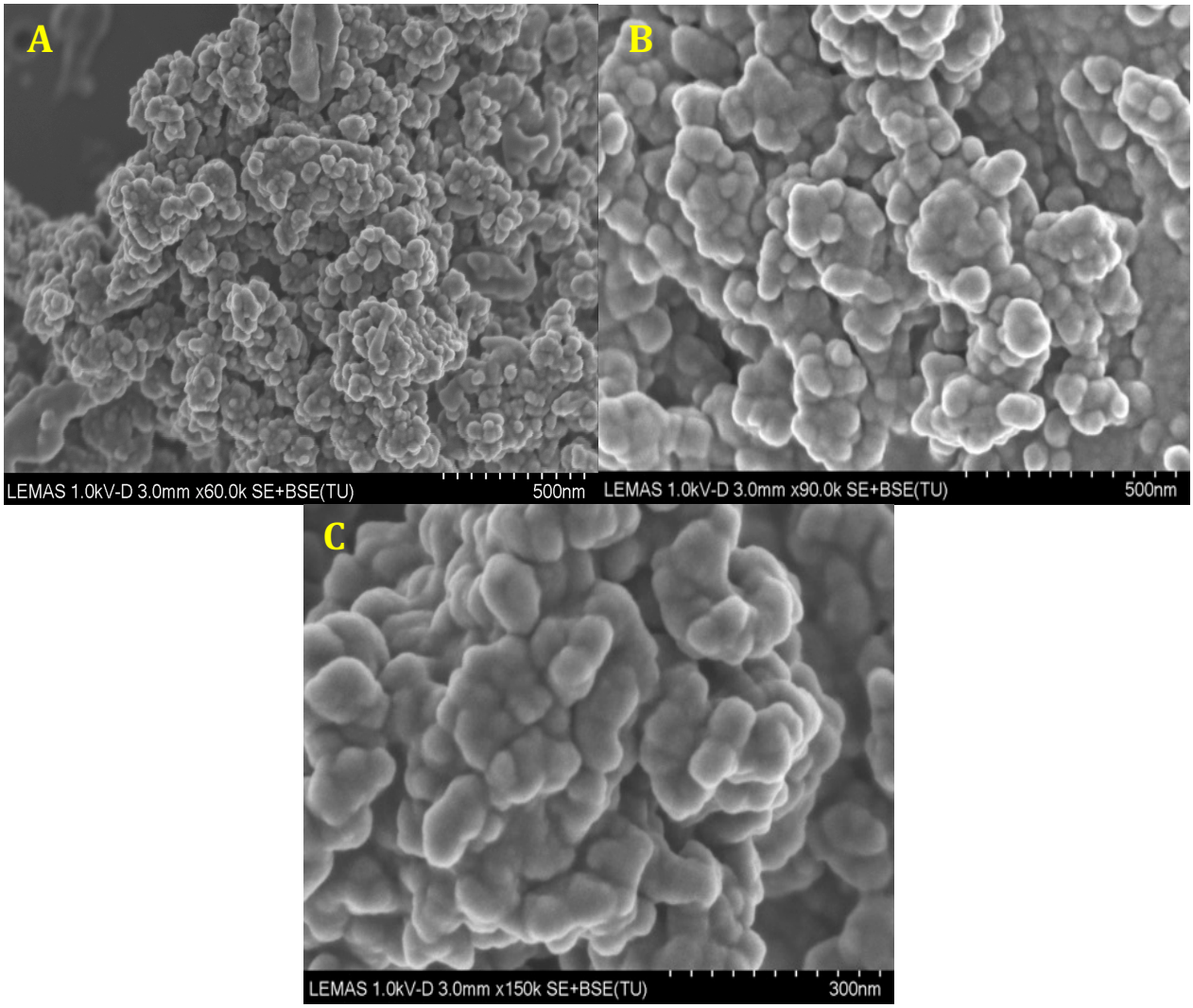

Figure 3.8 Aggregates of nano-scale cobalt chrome wear particles generated in a six-station pin-on-plate wear simulator collected on a 0.1μm filter analysed using high resolution FEGSEM at high magnification x 60K (A) x 90K (B) and x 150K (C) respectively.

Using the FEGSEM at low magnifications (x 60, x 120, x 200 and x 400 respectively) granular micron sized cobalt chrome particles were observed on the 5μm and 1μm polycarbonate filters (Figures 3.8 and 3.9). Using high magnification (x 60k, x 90k and x 150k) 0.1μm filter it was observed that many of these irregular particles were agglomerates of smaller sub-micron or nano-scale cobalt chromium particles (Figure 3.10 and Figure 3.11).

Furthermore on the smaller pore sized filters (0.1μm and 0.015μm) at high magnification x 30K, x 60K, x 90K and x 150K, large quantities of round to oval nano-scale cobalt chromium particles were observed (Figures 3.10 and 11).

The size distribution of particles collected on all four sized filters were obtained using Image Pro Plus® 6.0 image analysis software. The percentage (of the total number of particles) of cobalt chromium particles that were <50nm in length was 55.5%, 25.8% of cobalt chromium particles were between 50nm and 99nm in length, 14.8% of cobalt chromium particles were between 100nm and 499nm in length, 1.5% of cobalt chromium particles were between 500nm and 1μm in length and finally 2.6% of cobalt chromium particles were >1μm in length (Table 3.5). The mode size distribution of cobalt chromium particles was in the 30nm-39nm size range (Figure 3.9).

Table 3.5 The percentage of cobalt chromium particles generated in the six-station pin-on-plate wear simulator which were 0-49nm, 50nm-99nm, 100nm-499nm, 500nm-1μm and greater than 1μm.

Cobalt chrome particle length (nm)	Percentage (%) of total number of particles
0-49nm	55.5%
50nm-99nm	25.8%
100nm-499nm	14.8%
500nm-1μm	1.5%
>1μm	2.6%

The elemental composition of the particles collected on each filter was determined using EDX analysis, as described previously in section 3.3.1.8. EDX detection points were taken from within particle agglomerates (Figure 3.10) or were taken from particles >100nm (Figure 3.11). The EDX analysis revealed peaks of excitation for carbon, cobalt, chromium, oxygen and phospherous in both nano-scale particles (Figure 3.10B) and micron-sized cobalt chrome particles (figure 3.11B). The carbon peak was present, as the samples were coated with carbon for SEM imaging and EDX analysis. No contamination was detected on any filter.

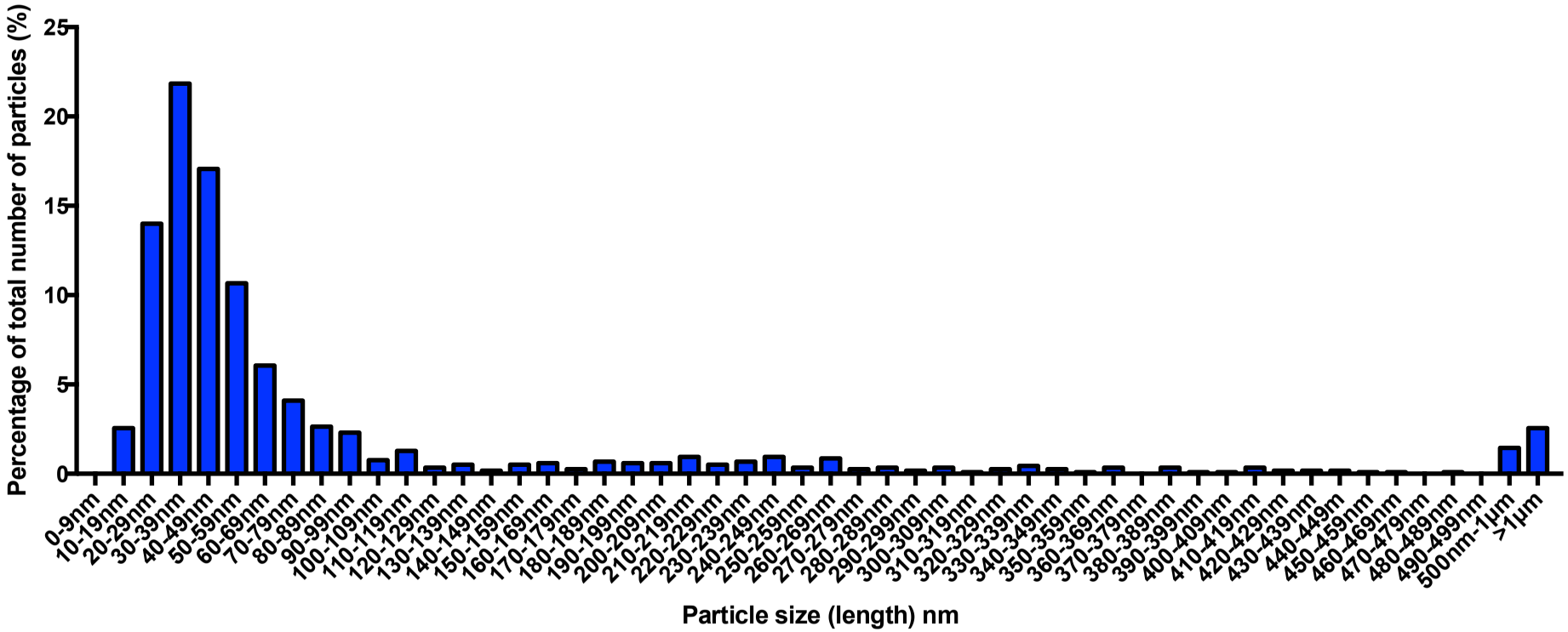

Figure 3.9 The size distribution of cobalt chromium wear debris generated in a six-station pin-on-plate wear simulator.

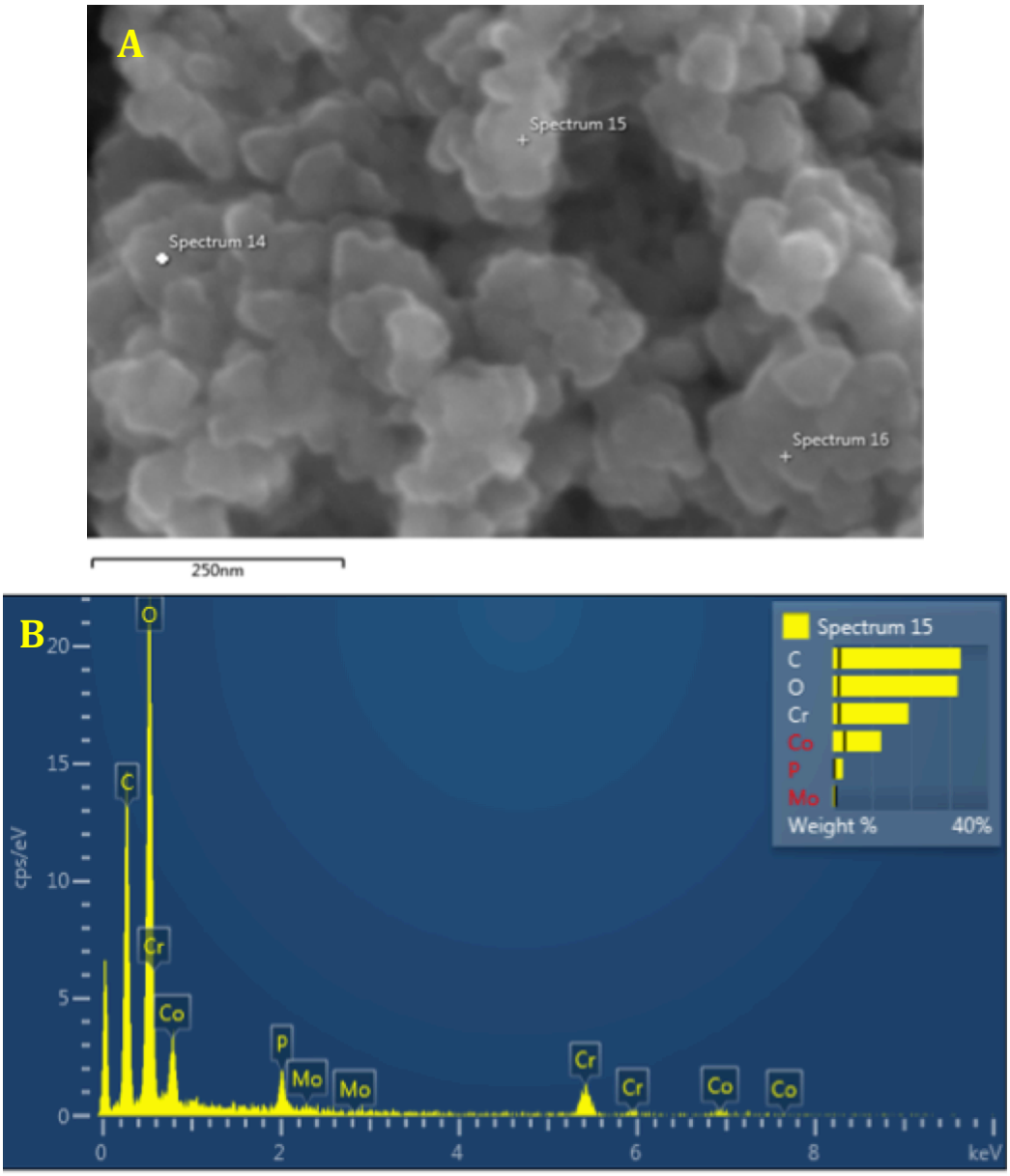

Figure 3.10 A) SEM image and **B)** energy dispersive X-ray (EDX) traces of cobalt chrome particles captured on a 0.015µm filter

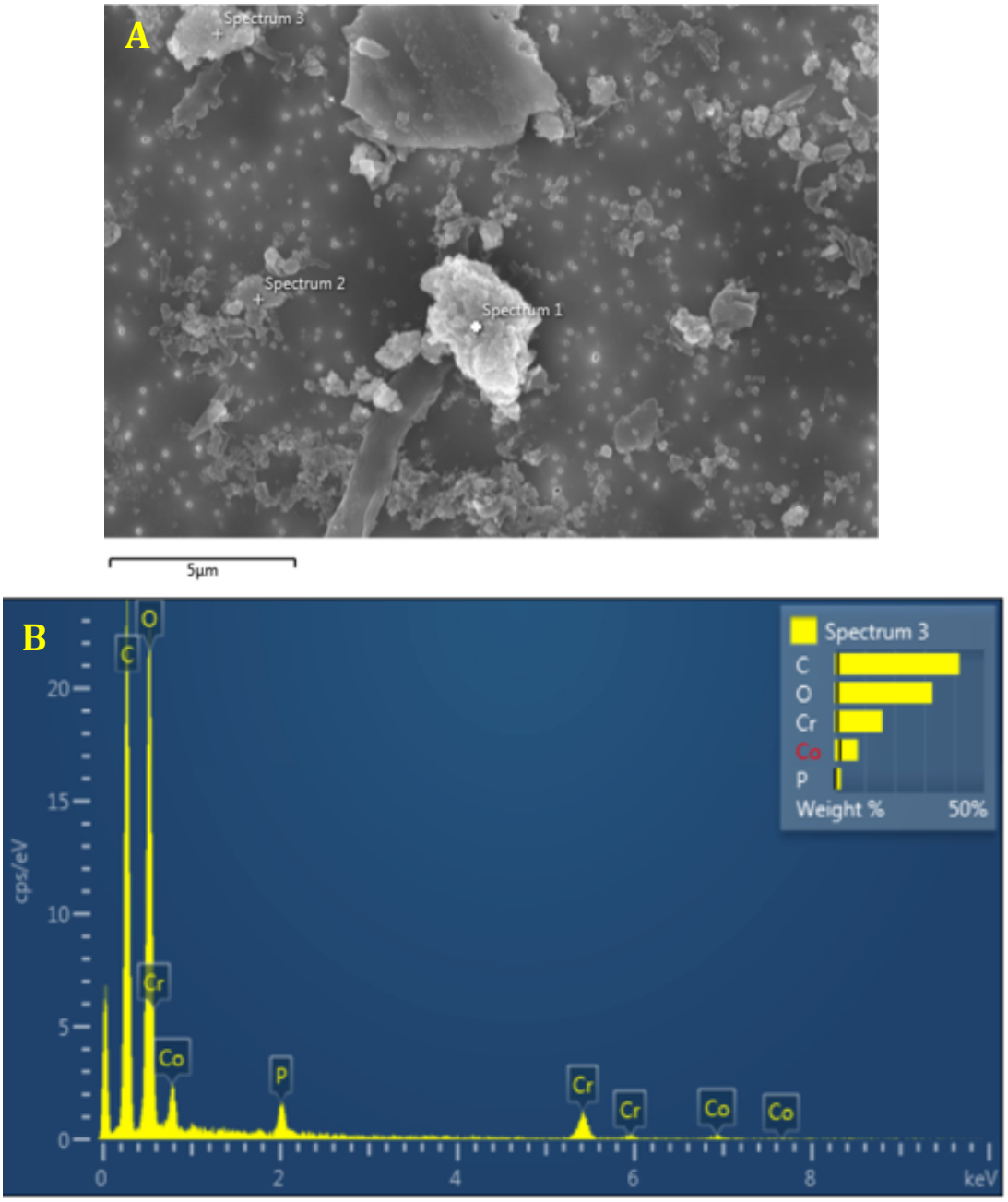

Figure 3.11 A) SEM image and **B)** energy dispersive X-ray (EDX) traces of cobalt chrome particles captured on a 0.1µm filter

When observed at low magnifications large, granular micron-sized stainless steel wear particles were observed on the 5μm and 1μm polycarbonate filters (Figures 3.12 and 3.13). These large irregular particles were more numerate for the stainless steel debris than observed with cobalt chrome.

Furthermore, on the smaller pore sized filters (0.1μm and 0.015μm) at high magnification x 30K, x 60K, x 90K and x 150K, large quantities of round nano-scale stainless steel particles were observed (Figures 3.14 and 3.15).

The mode of the size distribution for the stainless steel particles generated in the six-station pin-on-plate wear simulator was between 30nm and 39nm in length, a second peak was observed between 160nm and 169nm, and a final peak at >1μm. (Figure 3.17) The stainless steel particles were more widely distributed than the cobalt chrome wear particles. The size distribution of particles collected on all four sizes of filters was obtained using Image Pro Plus® 6.0 image analysis software. The percentage of stainless steel particles that were <50nm in length was 30.7%, 22.0% of stainless steel particles were between 50nm and 99nm in length, 41.5% of stainless steel particles were between 100nm and 499nm in length, 0.9% of stainless steel wear particles were between 500nm and 1μm in length and finally 5.0% of the stainless steel particles were >1μm in length (Table 3.6).

Table 3.6 The percentage of stainless steel particles generated in the six-station pin-on-plate wear simulator which were 0-49nm, 50-100nm, 100-499nm, 500nm-1μm and greater than 1μm.

Stainless steel particle length (nm)	Percentage (%) of total number of particles
0-49nm	30.7%
50nm-99nm	22.0%
100nm-499nm	41.5%
500nm-1μm	0.9%
>1μm	5.0%

The elemental composition of the stainless steel particles collected on each filter was determined using EDX analysis (Figure 3.16) this protocol was identical to the EDX analysis for cobalt chrome debris (section 3.3.1.8). Dominant peaks on the EDX spectrum were observed for carbon, oxygen, iron and a small peak for nickel (Figure 3.16). Upon comparison of these findings to Table 3.2 in section 3.2, which outlines the elemental composition of medical grade 316L stainless steel, iron comprises 62.045%-72% of the elemental composition, nickel comprises 10%-14% and carbon makes up 0.03%. Thus the peaks observed as part of the EDX analysis were as expected. As carbon was used to coat the samples prior to SEM imaging and EDX analysis this explains the high carbon peak. No contamination was observed upon analysis.

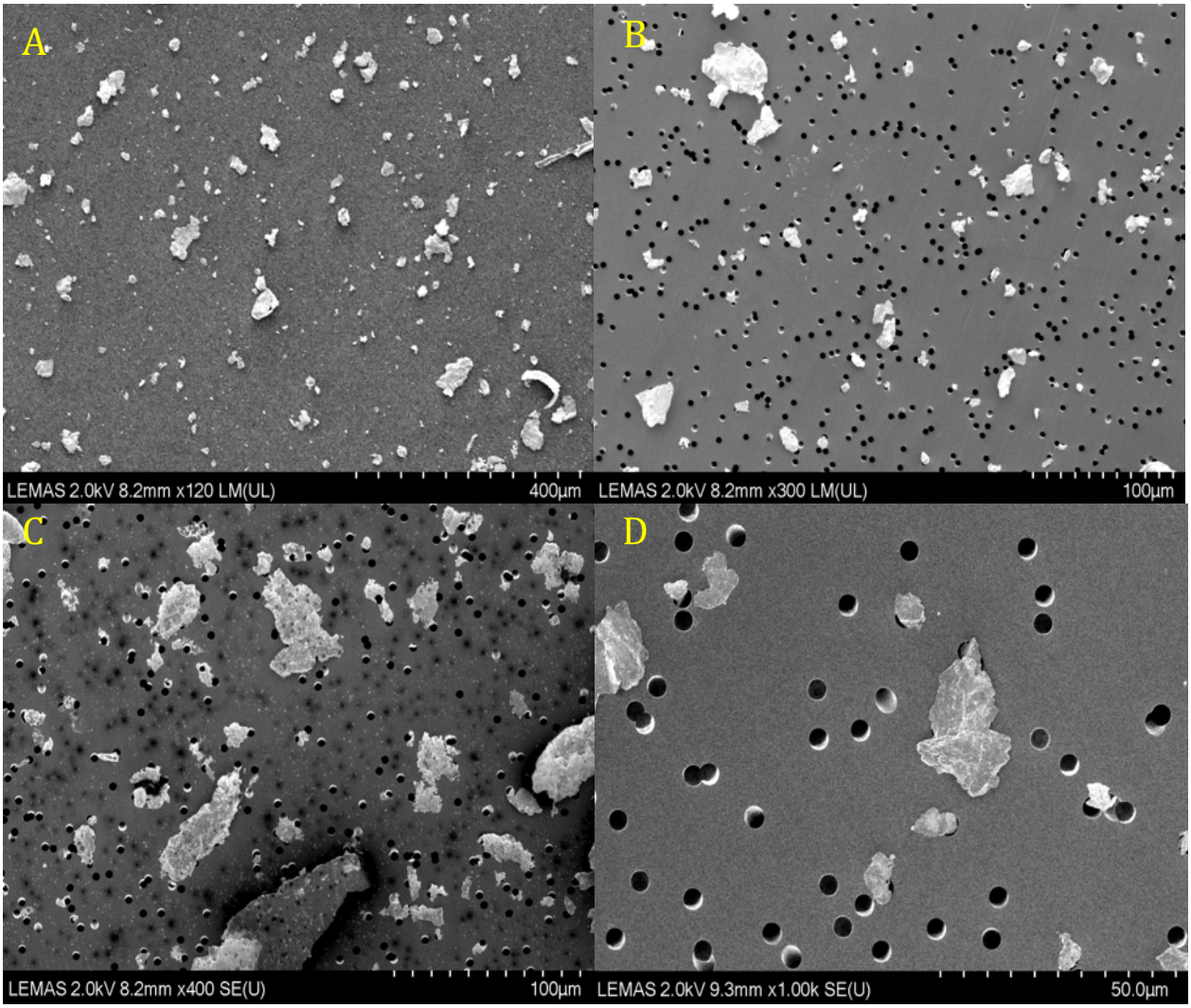

Figure 3.12 Stainless steel wear particles generated in a six-station pin-on-plate wear simulator. The particles were collected on a 5µm filter analysed using a high resolution FEGSEM at low magnification x 120 (A), x 300 (B), x 400 (C) and x 1K (D) respectively.

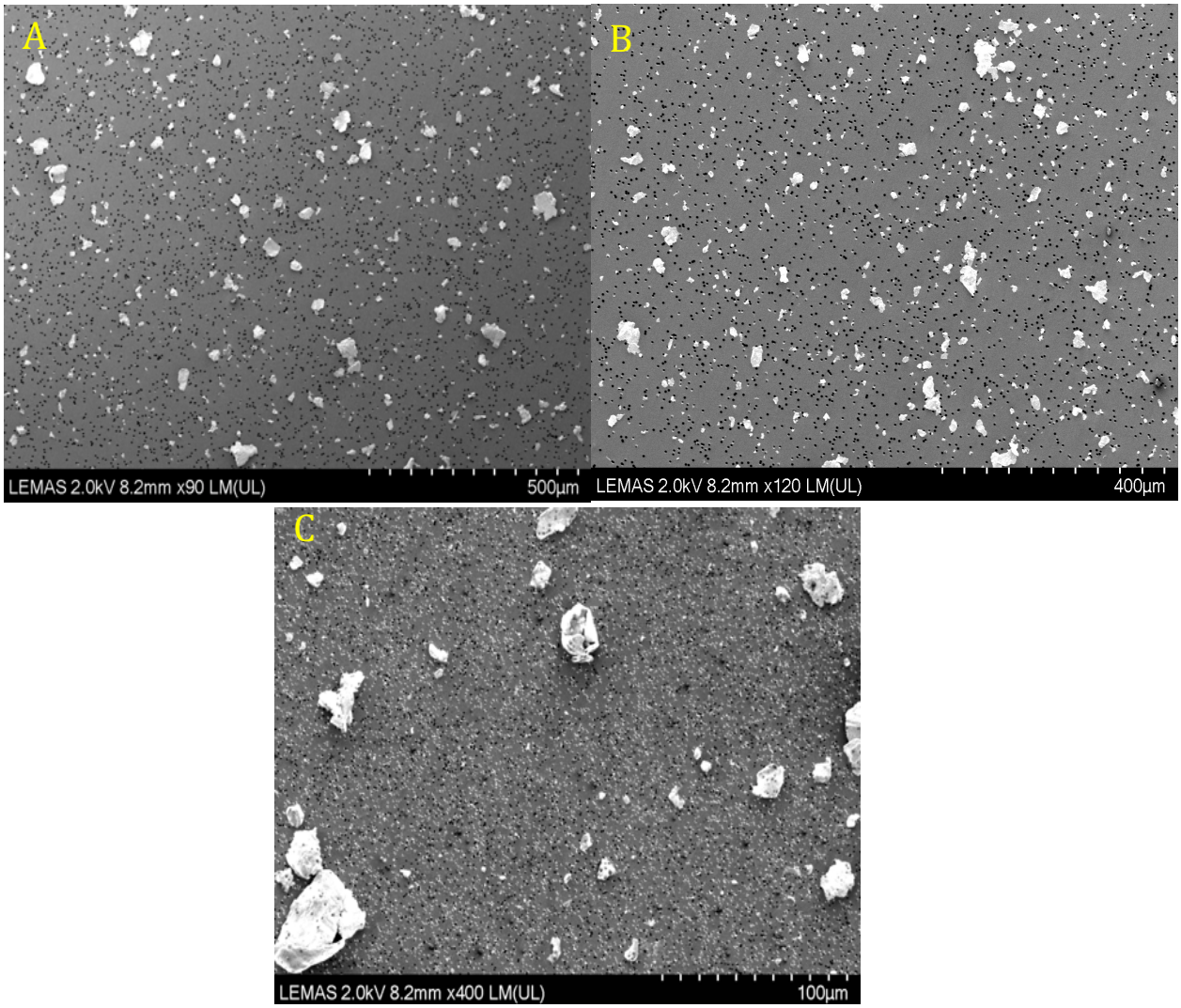

Figure 3.13 Stainless steel wear particles generated in a six-station pin-on-plate wear simulator. The particles were collected on a 1µm filter analysed using a high resolution FEGSEM at low magnification x 90 (A), x 120 (B) and x 400 (C) respectively.

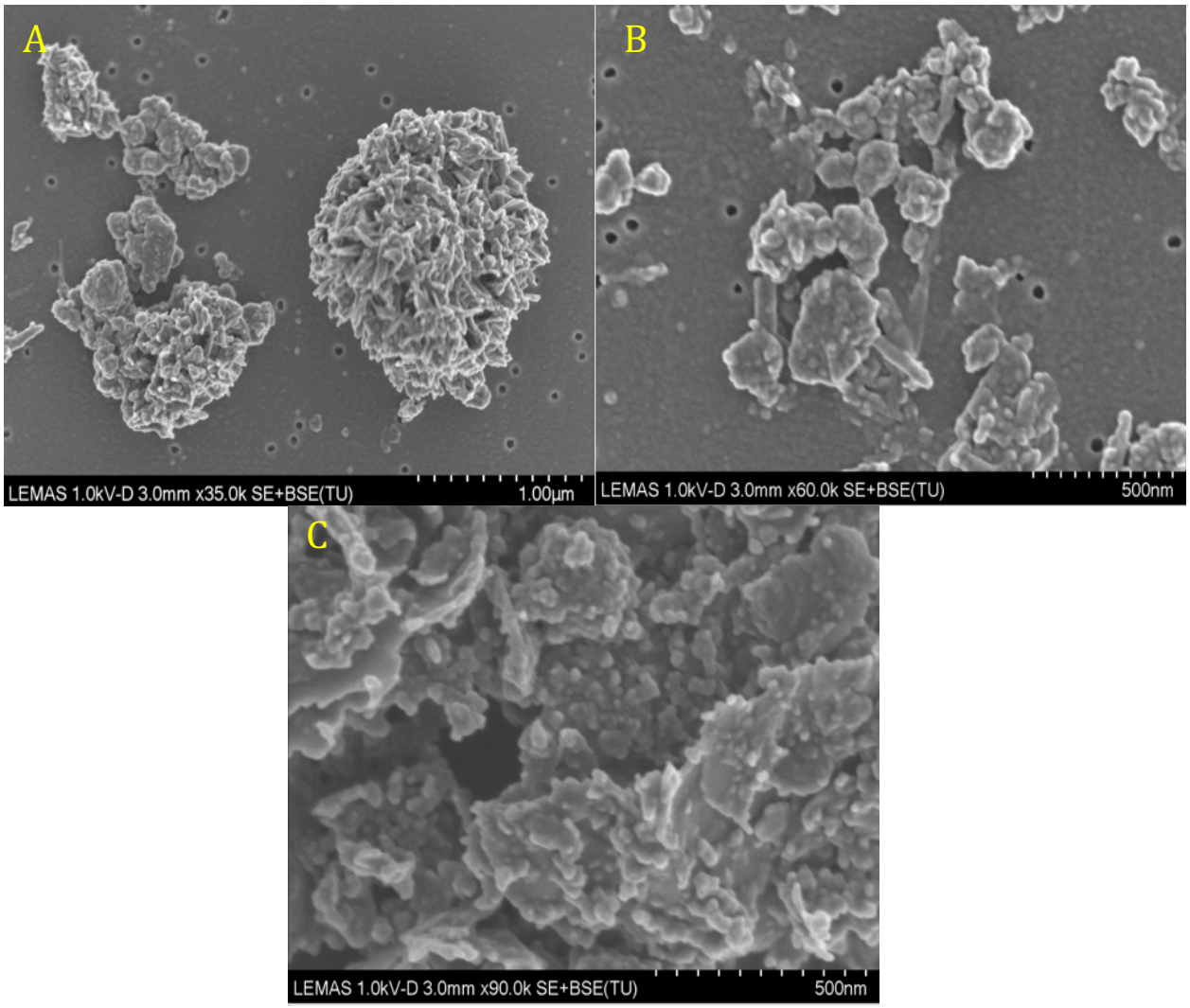

Figure 3.14 Stainless steel wear particles generated in a six-station pin-on-plate wear simulator. The particles were collected on a 0.1µm filter analysed using a high resolution FEGSEM at high magnification x 35K (A), x 60K (B) and x 90K (C) respectively.

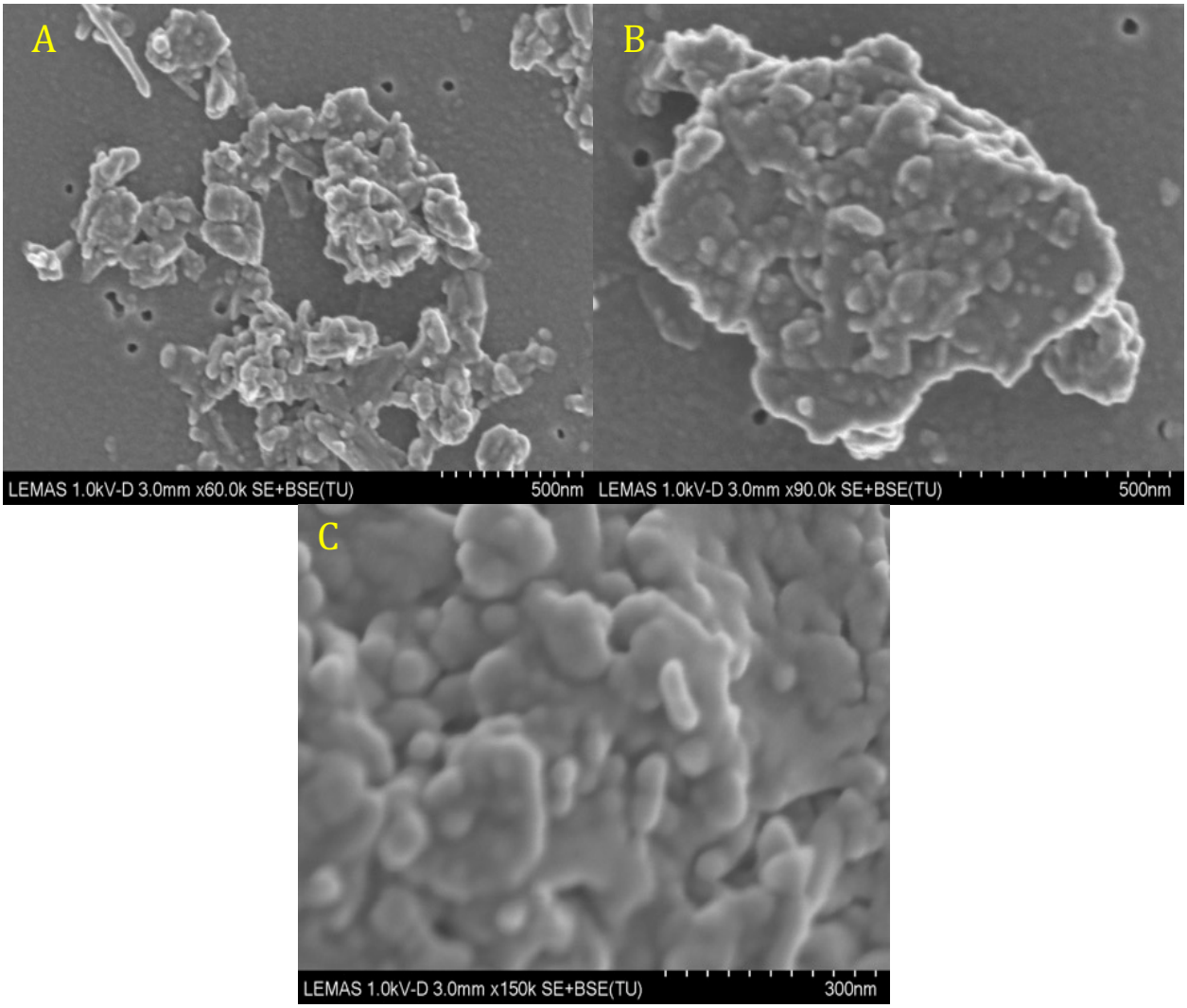

Figure 3.15 A) Stainless steel wear particles generated in a six-station pin-on-plate wear simulator. The particles were collected on a 0.015µm filter analysed using a high resolution FEGSEM at high magnification x 60K (**A**), x 90K (**B**) and x 150K (**C**) respectively.

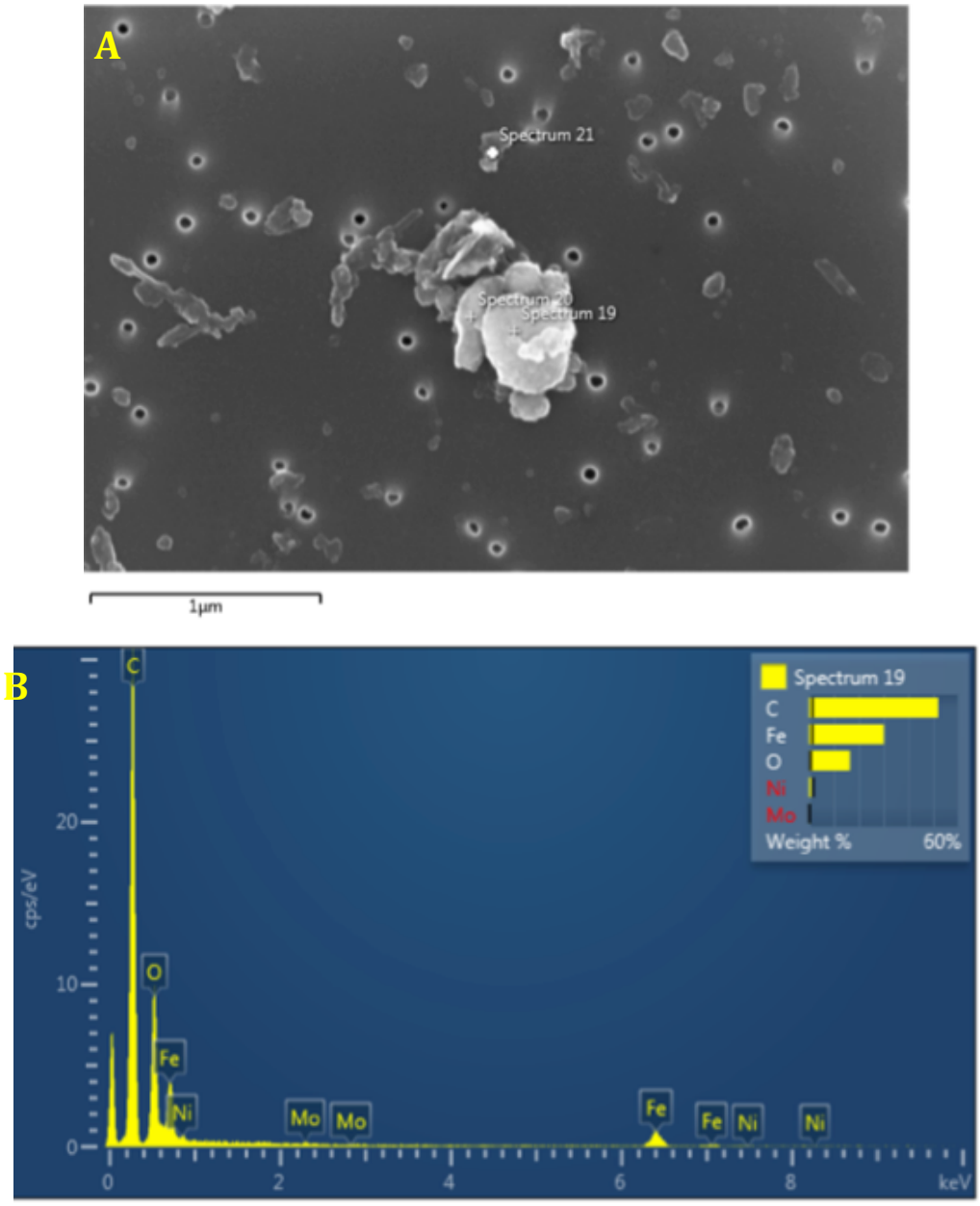

Figure 3.16 A) SEM image and **B)** energy dispersive X-ray (EDX) traces of stainless steel particles captured on a 0.1µm filter

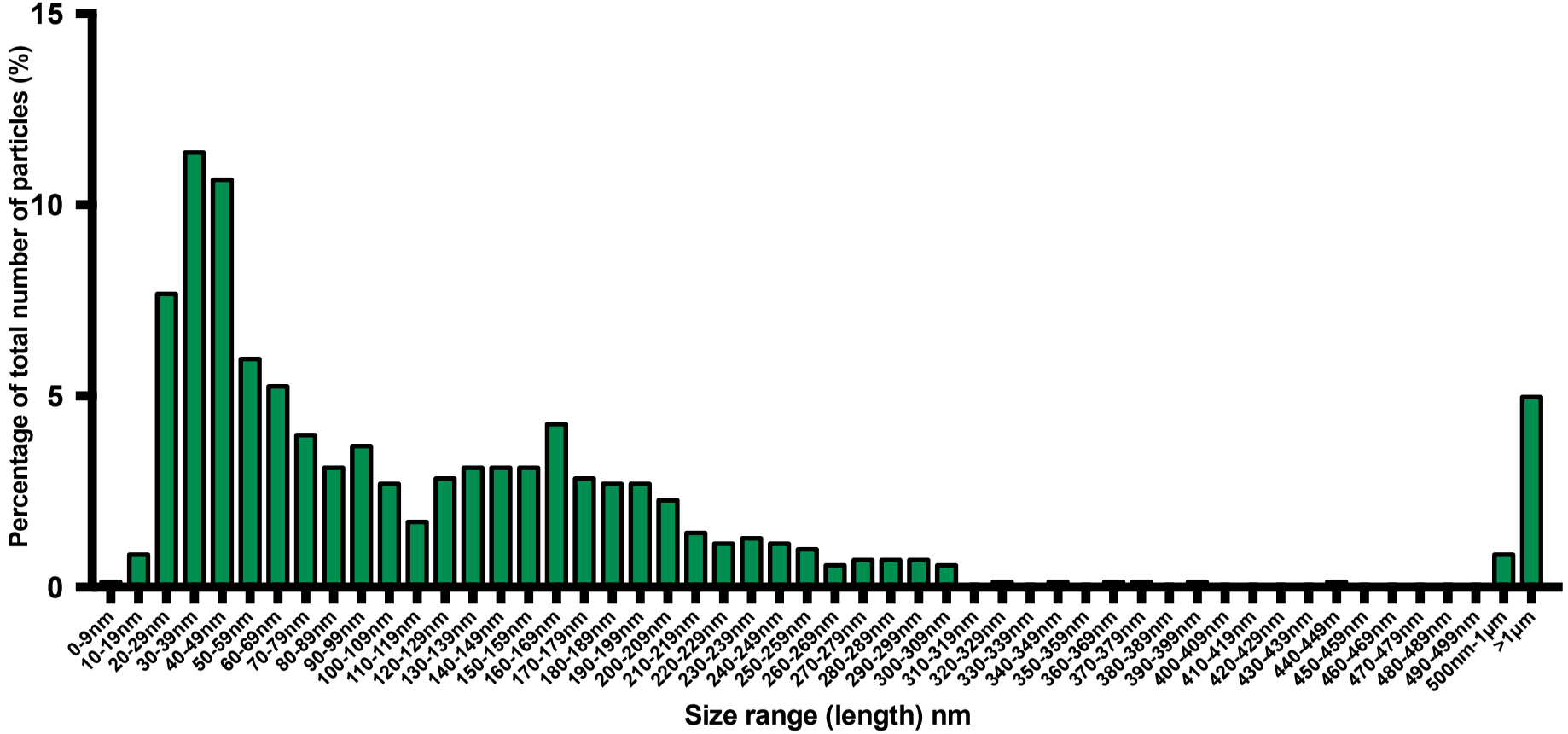

Figure 3.17 The size distribution of stainless steel wear debris generated in a six-station pin-on-plate wear simulator.

3.5 Discussion

For this part of the study a six-station pin-on-plate wear simulator was used to generate cobalt chromium and stainless steel wear debris, using smooth (Ra ≤0.01) wrought high carbon cobalt chromium molybdenum and 316L medical grade stainless steel pins and plates, using deionized water as a lubricant. Here, six metal pins articulated against six metal plates using multi-directional motion. Particles were generated over an 80-hour time period, articulating at a frequency of 1Hz under a load of 80N.

The cobalt chromium particles generated in this part of the study had a mode size of 30nm-39nm in length. The stainless steel wear particles generated using a six-station pin-on-plate wear simulator also had a mode length of 30nm-39nm, though these particles were more widely distributed than the cobalt chromium wear particles. Both stainless steel and cobalt chromium particles were of a comparable size to those observed from around failed metal-on-metal hip replacements (in the nanoscale size range) (Doorn et al., 1998) and could be compared to those observed in the limited amount of literature regarding simulation of wear of metal-on-metal total disc replacement in terms of size and morphology (Pasko et al., 2016).

These cobalt chrome and stainless steel particles were to be used at a later date in both 2D and 3D cell culture studies. To determine the effect of metallic wear debris on cells of the spinal cord, the cobalt chromium and stainless steel debris was sterilised and a 1mg.ml^{-1} stock generated for each material.

Due to the presence of large irregular shaped cobalt chrome particles present in the pooled cobalt chrome particle stock, identified using SEM, prior to culture with cells, the pooled cobalt chrome particles were passed through a 0.1µm polycarbonate filter. However SEM images and size distribution analysis was only carried out on the "as generated" cobalt chrome particle stock. Ideally additional SEM images would have been acquired and EDX analysis would have been performed on the filtered particles to precisely determine the size range of the particles cultured with the glial cells in 2D and 3D culture, however this was not performed. The additional filtration step was not performed on the stainless steel particles.

It is important to note that in order to begin evaluating the host response to metal particles a thorough morphological and chemical composition characterisation of the debris is required as the biological response to implant wear debris is dependent on particle volume, size, shape and chemical composition (Nine et al., 2014). There are numerous requirements of a reproducible, efficient isolation process, this includes

minimal alteration to particle size, morphology and chemical composition as well as isolating particles that are residue and contaminant-free (Billi et al., 2009).

A particle isolation protocol can generally be considered to comprise four aspects; isolation, display and image acquisition, characterization and analysis.

Acid and alkaline digestion protocols for particles generated in serum have been reported to alter the size and chemical composition of the metallic wear debris (Catelas et al., 2001) and enzymatic digestion does not enable a direct retrieval of all of the debris in the sample (efforts need to be made to improve the efficiency of enzymatic digestion protocols) and may leave a protein residue on metal particles making morphological analysis difficult (Brown et al., 2007) as a result the particles in this part of the study were generated in water. Particles generated in serum have been shown the have very similar size and morphology to those generated in water (Hailey et al., 1996).

Direct isolation from water by filtration, was employed in this part of the study as it is a simple technique for collecting all particles on a support. The polycarbonate filter can be mounted easily onto stainless steel stubs and imaged using scanning electron microscopy. Problems may arise with vacuum filtration due to agglomeration. As the particles are being forced to pass through a pore via a path that is not straight (a funnel-effect), this means the particles become concentrated around the pores. In addition particles larger in size than the size of the pores may cause a blockage, which would reduce the area for filtration and may cause more agglomeration. By sequentially filtering particles through four different sized polycarbonate filters (5μm, 1μm, 0.1μm and 0.015μm) blockage of filters is avoided. Care was taken when selecting the size of the filter pores to maximise capture of all sized particles.

The two main methods for image acquisition are scanning electron microscopy (SEM) and transmission electron microscopy (TEM), which work in fundamentally different ways. For analysis using TEM, particles are embedded in resin and cut into thin sections (80nm thick). TEM works by passing an electron beam through the sample being analysed, the image produced is the projection of the particles in the path of the beam, this makes TEM very difficult for use in size and morphology analysis of sub-micron particles as aggregates would appear as one large particle. Problems with this technique also arise when considering the orientation of the beam and the sample as the angles between the two may cause long fibril-like particles to appear short and round depending on their positioning, by cutting sections every 80nm this may also slice through particles thus underestimating the particle size. As an accurate analysis of particle size and morphology

was required for this study, scanning electron microscopy was used for the image acquisition. The Hitachi SU8230 SEM at the University of Leeds is capable of generating high resolution images and EDX analysis of both micron and sub-micron metal particles. The resolution of this SEM was <1nm. However, when nanoparticles exist in solution they move under Brownian motion, due to the high surface area to volume ratio of nanoparticles they behave as highly reactive colloidal particles and have a tendency to form aggregates, this makes individual particles difficult to see and thus sizing becomes more awkward.

Morphological and chemical characterisation has been performed differently by individual research groups, using numerous parameters as descriptors of particle morphology. Schmiedberg et al. (1994) imaged titanium and cobalt chromium debris using SEM and used length and width as the two parameters to size cobalt chromium molybdenum and titanium wear debris from intervertebral disc prostheses. The length of the particle was defined as the longest axis through the debris and the width was the shorter length of the particle perpendicular to the length. Schmiedberg et al. (1994) found titanium particles ranging from <1μm to >30μm in length. Cobalt chromium wear debris <5μm and >30μm in size were produced from the articulation of a novel dynamic intervertebral disc prosthesis when tested using a spine simulator.

Doorn et al. (1998) isolated cobalt chrome particles from tissue from around failed metal-on-metal hip prosthesis (isolated from patients who were undergoing revision surgery) using an enzymatic digestion technique and TEM to image the particles. These authors observed nanoscale cobalt chrome debris, which was round-oval in morphology. Doorn et al. (1998) used the length to define the particle size using TEM. When using TEM the measured size of the particle is limited to the thickness of the tissue section, which in this study was 80nm, and the orientation of the particle within that section. Thus this method of image acquisition may underestimate the actual particle size. Doorn et al. (1998) found the cobalt chromium molybdenum particles were predominantly <50nm (6-834nm). Unlike Doorn, Catelas et al (2003) used the ratio of the length and width to determine a quantitative measure of morphology. The length of the particle was defined as the maximum dimension of the particle and the width the maximum orthogonal dimension, similar to Schmiedberg et al in their definition of the size parameters.

Brown et al. (2007) used maximum diameter measurements taken from 150 particles per sample to assess the size distribution of metal-on-metal and ceramic-on-ceramic wear particles produced under differing hip simulator conditions. Brown et al. (2007) aimed to characterize metal wear from metal on metal and metal on ceramic hip implants using

standard and micro-separation, adverse hip wear conditions. Using an enzymatic digestion procedure to limit the alterations to the size and chemical composition of the cobalt chromium particles during isolation, accurate particle characterisation was performed. Brown et al. (2007) found cobalt chromium particles with a mean length of <50nm with a rounded, irregular morphology. Significant differences in size and morphology of particles were not observed between bearing couples and simulator conditions.

In this part of the study, the length was used to define particle size. The mode length of the cobalt chrome size distribution was 30-39nm (Figure 3.9) and the mode length of the stainless steel debris generated was 30-39nm (Figure 3.17). The percentage of the total number of particles >1μm for cobalt chrome debris was 2.6% (Table 3.5) and for stainless steel debris was 5% (Table 3.6) suggesting more larger particles were produced by stainless steel. This was supported by the fact that approximately 2.6% of the CoCr particles were >1μm, whereas 5% of the stainless steel particles were >1μm. The percentage of the total number of particles <100nm for cobalt chrome debris was 81.23% (Table 3.5) and for stainless steel debris was 52.7% (Table 3.6). Upon comparison of these particles to the metallic nanoparticles observed around failed total hip replacements it can be see that the cobalt chrome particles match what has been seen in the literature (Doorn et al., 1998; Firkins et al., 2001; Germain et al., 2003; Papageorgiou et al., 2014; Pourzal et al., 2011;). Though there is a lack of literature detailing the size of metal particles produced *in vivo* by total disc replacements there is evidence that these particles will be similar in size to those observed in the articulation of metal-on-metal hips, In the nanoscale size range (Punt et al., 2011). Upon comparison of cobalt chrome wear particles generated in this part of the study to those produced in a spine simulator in The School of Mechanical Engineering at The University of Leeds and cobalt chrome wear debris generated in the six-station pin-on-plate wear simulator there is no significant difference in size distribution and particle morphology (Pasko et al., 2016).

3.6 Conclusion

Cobalt chrome and stainless steel wear particles for use in cell culture studies were generated in water in a six-station pin-on-plate wear simulator. The size and morphology of this metallic wear debris was similar to that generated by articulating cobalt chrome molybdenum total disc replacement components in a spine simulator at the University of Leeds (Pasko et al., 2016) and to those observed in metal-on-metal total hip replacements. The cobalt chrome and stainless particles were isolated via vacuum filtration and

characterized using SEM and their elemental composition confirmed using EDX analysis. Sufficient wear debris had been generated to complete cell studies with cell lines and primary cells to determine the effect of stainless steel and cobalt chrome wear particles on cells of the spinal cord.

Chapter 4

The effect of cobalt chrome and stainless steel wear particles on the viability and DNA integrity of glial cells in a 2D cell culture system.

4.1 Introduction

Wear generation, corrosion and re-passivation of metal-on-metal implants can cause an accumulation of metal particles and ions within the body, which may be toxic to the host. With increasing reports within the literature of adverse tissue reactions and the formation of pseudotumors associated with the wear products of metal-on-metal total disc replacements (Cavanaugh et al., 2009; Berry et al., 2010; Guyer et al., 2011; Cabraja et al., 2012) and with growing evidence that nanoscale cobalt chrome particles (20-60nm) are capable of altering the structural integrity of the dura mater, (Papageorgiou et al., 2014) it can be hypothesised that the protective barrier surrounding the spinal cord may be breached by metal nanoparticles generated by metal-on-metal total disc replacements. It is therefore essential to investigate the response of the periprosthetic tissue to such wear products, with particular focus on the spinal cord cellular response to cobalt chrome and stainless steel wear products, the two leading materials selected in the design of total disc replacements.

Numerous *in vitro* studies have been performed to determine the effect of cobalt chrome (Allen et al., 1997; Germain et al., 2003; Williams et al., 2003; Papageorgiou et al., 2007 Posada et al., 2014) and stainless steel (Bailey et al., 2005) wear particles on cell viability using 2D monolayer culture. A variety of cell types including; osteoblast, monocyte, macrophage, fibroblast and glioma cell lines and primary cells have previously been utilised. However, only a limited number of studies have been performed to determine the effects of metallic wear particles on cells of the CNS. Primarily, within the literature the effect of wear products on glial cells and neuronal cells has been investigated (DeGuzman & VandeVord, 2007; Behl et al., 2013). These studies have been performed using porcine dural cells or C6 (astrocytic) and PC12 (neuronal) cell lines to assess the effects of bulk and particulate materials used in the production of orthopaedic implants on cell viability. A high quality study using physiologically relevant particle volumes and clinically relevant particle sizes is still required.

The cobalt chrome and stainless steel wear particles were generally found to have a toxic effect on cells at varying concentrations and time points tested (Allen et al., 1997; Germain

et al., 2003; Bailey et al., 2005; De Guzman & VandeVord, 2007; Posada et al., 2014). However the cobalt chrome particles utilised in these studies were often >1μm and the stainless steel particles were 1-100μm in length which were not comparable to the nanoscale particles observed around failed metal-on-metal total hip replacements (Doorn et al., 1998) and metal-on-metal total disc replacements (Pasko et al., 2016). Furthermore, the use of large wear particles to establish the cytotoxicity of CoCr particles may reduce the release of potentially cytotoxic ions from the wear particles, as a result of a smaller exposed surface area of the particles, and may no longer represent the *in vivo* condition accurately. In many of the *in vitro* investigations commercially available cobalt chrome particles were used; these particles often possessed a different morphology and chemical composition to particles generated using either a pin-on-plate wear simulator, hip simulator or spine simulator and to those found *in vivo*. In numerous instances the particle doses that the cells were challenged by were extremely high and would not be clinically relevant. Thus to more accurately understand the biological response of cells of the CNS to metallic wear products produced by total disc replacements, model CNS cells such as C6 glial, PC12 neuronal cell lines and rat primary astrocytes and microglia in co-culture should be cultured with clinically relevant cobalt chrome and stainless steel wear particles at physiologically relevant particle doses.

The use of *in vitro* models offers numerous advantages over *in vivo* models. They enable the investigation of the role of a single cell type in the biological response to wear particles and the study of the possible deleterious or protective roles of specific molecules or compounds, without the complexity and cost that has been associated with *in vivo* animal models (Schlachetzki et al., 2013). In the development of new biomaterials and in the testing of existing ones for orthopaedic applications, it would be of great interest to quantitatively screen the genotoxic and cytotoxic responses of cells to wear particles *in vitro.*

The use of the neuronotypic PC12 model cell line has been widely reported in the literature (Slotkin et al., 2014). This cell line has been used as a model cell type to investigate neurological disorders such as; Alzheimer's disease, Huntington's disease, Parkinson's disease and amyotrophic lateral sclerosis (ALS) also known as Lou Gehrig's disease. C6 astrocytic cells have been reported in the literature as a model glial cell which has been used for numerous applications such as CNS repair (Assis et al., 2014), the study of glioblastoma growth and invasion (Grobben et al., 2002), therapeutic targeting and screening (Quincozes-santos et al., 2013) and drug delivery mechanisms (Tang et al., 2015), as these cells behave in similar ways to primary astrocytes in terms of molecular

mechanisms, apoptotic pathways and cytokine expression (Grobben et al., 2002). These cell lines were ideally suited for a preliminary investigation into the biological response of CNS cells to metallic wear particles in this study.

When selecting a specific cell line for determining the biological response to metallic wear debris it is of the utmost importance to select a cell type that will be capable of modelling the response or phenomenon that is likely to be incurred by the particulate stimuli *in vivo* (Jones and Grainger, 2009*).*

The C6 cell line is commonly selected for *in vitro* investigations on the basis that these cells behave in a similar manner to astrocytes. Astrocytes are a dynamic cell type and have numerous roles within the CNS, predominantly in maintaining homeostasis within the CNS. Astrocytes have also been implicated in the regulation of the brain microenvironment, maintenance of the blood-brain barrier, guidance of neuronal migration, immune function and in the onset of glial scar formation following spinal cord injury (Markiewicz & Lukomska, 2006). The glial scar comprises reactive, ramified, hypertrophic astrocytes, which have undergone numerous cellular changes, referred to as astrogliosis. Astrogliosis can be characterized by and up-regulation of intermediate filament protein; glial fibrillary acidic protein (GFAP). However, the C6 cell line does not express glial fibrillary acidic protein (GFAP) at detectable levels, unlike primary astrocytes (Pentreath & Mead, 2004; Jacobs et al., 2011). Therefore the amount of information that can be determined from the use of C6 glial and PC12 neuronal cell lines is limited to understanding the effects of cobalt chrome and stainless steel on the viability of these cell types, thus the use of more physiologically relevant primary astrocytes and microglia is necessary for a more in depth study into the biological response.

An ATP Lite™ assay was used to assess cell viability. This assay was selected as it was a highly sensitive, reproducible assay and was able to detect as few as five cells in 100µl medium. An alkaline comet assay was chosen to assess the effect of cobalt chrome and stainless steel wear particles on the integrity of primary astrocyte and microglia and primary astrocyte DNA. Previously the alkaline comet assay has been used extensively to assess the genotoxic effect of nanoparticles (Papageorgiou et al., 2007; Karlsson et al., 2008; Singh et al., 2009; Gajski et al., 2014). Alternative methods to assess genotoxicity have also been reported within the literature such as the use of chromosome painting, the chromosome aberration test and the micronucleus assay. The comet assay is a versatile and sensitive method for quantitatively measuring single and double strand breaks in DNA. It has been reported that the alkaline comet assay is more sensitive than the more

traditionally used micronucleus assay and was therefore selected for this application (He et al., 2000).

4.1.1. Aims

The first aim of this part of the study was to determine whether increasing physiologically relevant particle volumes (0.05μm^3, 0.5μm^3, 5μm^3 and 50μm^3) of clinically relevant cobalt chrome and stainless steel wear particles, generated using a six-station pin-on-plate wear simulator with a mode size of 30nm-39nm, for both materials, had a toxic effect on C6-glial, PC12-neuronal cell lines and primary rat astrocytes and microglia after 24 hours, three and five days in 2D culture.

The second aim was to determine whether increasing concentrations of stainless steel and cobalt chrome particles (0.5μm^3, 5μm^3 and 50μm^3) caused significant DNA damage in primary astrocytes and microglia in co-culture and primary astrocytes in isolation after 24hours, 48 hours and five days.

The effect of cobalt chrome and stainless steel wear particles on cell viability was assessed using an ATP-Lite™ cell viability assay. An alkaline comet assay was used to assess the effect of cobalt chrome and stainless steel wear particles on DNA integrity.

4.2 Materials

4.2.1 Rat C6 glial cell line. This cell line was cloned from a rat glial tumor, induced by N-nitrosomethylurea. This cell type was donated to the University of Leeds, for the study by Dr. James Phillips, University College London, UK.

4.2.2 Rat PC12 neuronal cell line. This cell line was derived from a transplantable rat adrenal pheochromocytoma and was donated to the University of Leeds, for the study by Dr. James Phillips, University College London, UK.

4.2.3 Primary astrocytes and microglia. These cells were isolated from P2 Wistar rat cortices. The cortices were obtained in accordance with UK Animals (Scientific Procedures) Act 1986 under the Home Office Schedule One procedure (Home Office Project license: PPL70/8085). The primary astrocytes and microglia were isolated and cultured according to the protocol first described by East et al. (2009) detailed in section 2.4.1.6. Primary astrocytes and microglia were separated into individual cell populations in accordance with the protocol outlined in Chapter 2, section 2.4.1.6.4.

4.3 Methods

The effects of cobalt chrome and stainless steel wear particles, generated using a six-station pin-on-plate wear simulator, on the viability of C6 glial cells, PC12 neuronal cells and on the viability and DNA integrity of primary astrocytes and microglia, in co-culture, in a 2D cell culture system, were investigated in this chapter.

4.3.1 Particle preparation

4.3.1.1 Generation of cobalt chrome and stainless steel wear particles using a six-station pin-on-plate wear simulator.

Cobalt chrome and stainless steel wear particles were generated using a six-station pin-on-plate wear simulator manufactured in house in the School of Mechanical Engineering at the University of Leeds. Smooth cobalt chrome or stainless steel pins articulated against smooth cobalt chrome or stainless steel plates using water as the lubricant, as described in Chapter 3, section 3.3.1.4. Cobalt chrome and stainless steel stock solutions ($1mg.ml^{-1}$) in deionized water were generated in accordance with the protocol outlined in Chapter 3, section 3.3.1.5.1 and stored at -20°C until required for cell culture experiments.

4.3.1.2 Determination of the mass of cobalt chrome particles for culture with C6, PC12 cell lines and primary astrocytes and microglia.

The quantity of particles cultured with each cell type was expressed as a particle volume (μm^3) to cell number ratio. A ratio of 50:1 (the largest particle volume assessed) equated to $50\mu m^3$ of debris per cell. The largest particle volume to cell number ratio used in this study was 50:1 and the smallest was 0.05:1.

To calculate the volume of the cobalt chrome particle stock solutions ($1mg.ml^{-1}$) required for each cobalt chrome particle dose, the following equations were applied, where the density of cobalt chrome is equal to $7.7g/cm^3$ and the density of stainless steel is equal to $7.99g/cm^3$. The same equations were used to calculate the volume of stainless steel stock solution required for each particle dose.

$$\text{Density} = \text{Mass (M)} / \text{Volume}$$

$$\text{Therefore; Mass (M)} = \text{Density} \times \text{Volume}$$

4.3.1.3 Worked example for 50μm³ cobalt chrome debris per cell using a seeding density of 1 x 10⁴ cells per well.

Applying the above equation for a particle volume of 50μm³ cobalt chrome debris per cell, a density of 7.7g/cm³ for cobalt chrome and a seeding density of 1 x 10⁴ cells per well with six replicates for each test condition:

Density= Mass (M)/ Volume

$1cm^3=1000mm^3$

$1mm^3$ CoCr= 7.7mg

$1mm^3=1x10^9\mu m^3$

therefore $1\mu m^3= 7.7 x10^{-9}$ mg

For a dose of 50μm³ cobalt chrome of debris per cell and a seeding density of 1 x 10⁴ cells per well

$50\mu m^3$ x 7.7 $x10^{-9}$ mg= Mass of cobalt chrome needed per cell

= 3.85 x 10^{-7} mg per cell

1 x 10^4 x 3.85 x 10^{-7} mg= Mass of cobalt chrome needed per well

=3.85 x 10^{-3}mg debris per well

=3.85μg per well

Therefore 3.85μl of the 1mg.ml^{-1} cobalt chrome stock solution was required per well. This volume was multiplied by six to give sufficient volume for six repeats per condition. The volume was scaled up further so a 1 in 10 dilution could be made for lower doses 5μm³, 0.5μm³ and 0.05μm³ cobalt chrome debris per cell.

4.3.2 The effect of cobalt chrome and stainless steel particles on C6 glial cell, PC12 neuronal cell and primary astrocytes and microglia viability

Each cell type, C6, PC12 and primary astrocytes and microglia in co-culture (seeding density 1 x 10⁴ cells per well) were cultured *in vitro* in 2D culture with cobalt chrome and stainless steel wear particles of increasing particle concentrations (0.05μm³, 0.5μm³, 5μm³ and 50μm³ wear debris per cell) for five days and the effect on viability assessed using an APT Lite™ assay after 24 hours, three days and five days in culture.

4.3.2.1 The effect of cobalt chrome and stainless steel wear particles on the viability of cells in 2D culture assessed using an ATP Lite™ assay.

In 2D culture the effect of cobalt chrome and stainless steel wear particles on cell viability was determined using an ATP Lite™ assay (PerkinElmer, USA). The ATP Lite™ assay relies upon the principal that living, metabolically active cells produce ATP (Adenosine triphosphate). The level of ATP is significantly reduced when a cell undergoes apoptosis or necrosis. When ATP from lysed cells interacts with the added D-Luciferin and Luciferase (in the provided ATP substrate) light is produced. The level of light generated is proportional to the concentration of ATP and thus is an indicator of cell viability.

C6 glial, PC12 neuronal cells and primary astrocytes and microglia (in co-culture) were passaged and a cell count performed as outlined previously in Chapter 2, section 2.4.1.4. After passaging it was ensured that each cell type had a viability of at least 90% (the cell lines were passaged a maximum of eight times for this part of the study to reduce phenotypic changes in these cell types). The primary astrocytes and microglia were passaged only once to reduce the likelihood of changes to the cells characteristics. The C6, rat glioma cell line was cultured in supplemented Ham's F12 medium (Chapter 2, section 2.3.2). The PC12 rat neuronal cell line was cultured in supplemented RPMI1640 medium (Chapter 2, section 2.3.16). Primary astrocytes and microglia were cultured with supplemented DMEM culture medium (Chapter 2, section 2.3.20). In a class II cabinet, using aseptic technique, the cells were seeded into 96-well plates (flat bottom for the adherent C6 glial cell line and primary astrocytes and microglia, U bottomed for the PC12 neuronal suspension cells). The flat-bottom 96-well plates were pre-coated with poly-d lysine for the primary astrocytes and microglia to enhance cellular adherence. A seeding density of 1 x 10^4 cells per well in 100µl of the appropriate supplemented medium (see Chapter 2, sections 2.3.2, 2.3.16 and 2.3.20, respectively) was used for all cell types (6 replicates per test condition).

After seeding, the cells were exposed to cobalt chrome and stainless steel wear particles (taken from a pre-prepared 1mg.ml^{-1} stock) at varying particle concentrations ranging from 0.05µm^3 debris per cell to 50µm^3 debris per cell (suspended in 100µl of supplemented medium), the volume of particle stocks used for each material and each dose was calculated using the equations detailed in section 4.3.1.2.

Camptothecin (2µg.ml^{-1} in 200µl supplemented medium) was used as a positive control for this study, the preparation of camptothecin was outlined previously in Chapter 2, section 2.3.6. A volume of 200µl of medium only acted as a blank (six repeats per condition) to determine the baseline spectrophotometric reading of the medium used. A cell only negative control was included as well as a particle only control. The plate set up, detailing each test condition and controls is shown in Figure 4.1. The cells were cultured with the particles for 24 hours, three days and five days at 37°C in 5% (v/v) CO_2 in air.

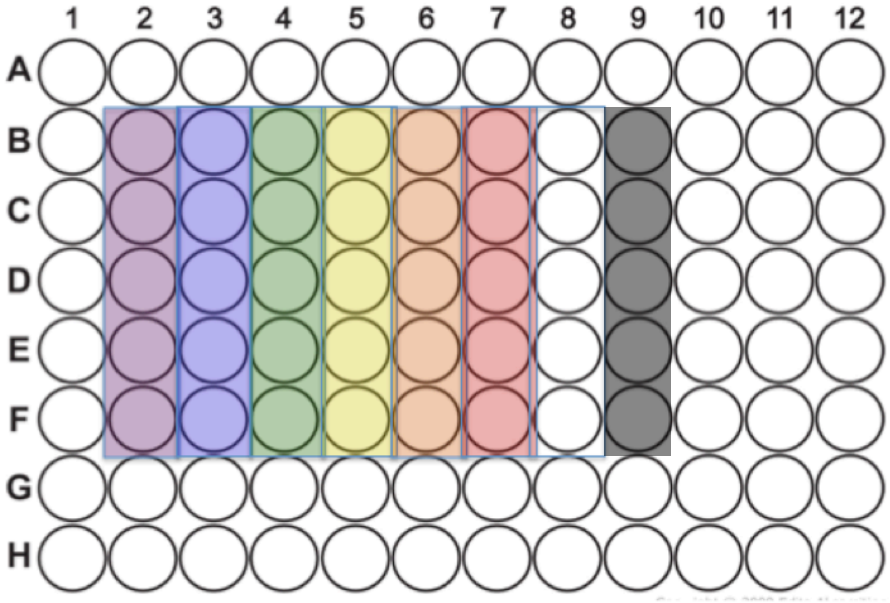

Figure 4.1 96-well plate set up for ATP Lite™ assay. Purple= cells cultured with 50µm^3 wear debris per cell. Blue= cells cultured with 5µm^3 wear debris per cell. Green= cells cultured with 0.5µm^3 wear debris per cell. Yellow= cells cultured with 0.05µm^3 wear debris per cell. Orange= cell only negative control where cells were not treated with wear debris. Red= blank (200µl supplemented medium). White= particle only control, CoCr or stainless steel particles equivalent to the highest particle dose suspended in 200µl supplemented medium. Grey= positive control, cells treated with Camptothecin (2 µg.ml^{-1}).

At the appropriate time point, 24 hours, three days or five days, the ATP-Lite™ assay was performed in accordance with the protocol outlined in Chapter 2, section 2.4.2.1. The output for this assay was presented as average luminescence counts per second (CPS).

4.3.2.2 Statistical analysis for cell viability data.

The raw data generated by the spectrophotometer was transferred into a Microsoft Excel document for analysis. The data was analysed and expressed as an average counts per second reading and as a percentage of the cell only negative control. Prior to analysis the

percentage data was transformed using an arcsine transformation to enable a two-way ANOVA to be performed. A two-way ANOVA was used to determine whether there was a significant difference ($p<0.05$) between the test conditions and the cell only negative control. The two-way ANOVA reports significant differences between groups, it does not detail which groups differed significantly, and therefore a post-hoc test was performed. Significant differences in the cell viability between the test conditions and the cell only negative control were determined using a Tukey post-hoc analysis test.

4.3.3 The effect of cobalt chrome and stainless steel particles on primary astrocytes and microglia DNA integrity.

To determine the effect of cobalt chromium and stainless steel wear particles on the integrity of primary astrocyte and microglia (in co-culture) and primary astrocyte (in isolation) DNA, in 2D culture, an alkaline comet assay was used. An alkaline comet assay kit (Trevigen, Maryland, USA) was utilised to assess DNA damage in primary astrocytes and microglia. The Olive tail moment was used as a measure of DNA damage. The Olive tail moment is the product of the length of the tail of the comet and the fraction of the total DNA located within the tail.

4.3.3.1.The effect of cobalt chrome and stainless steel wear particles on the integrity of CNS cell DNA.

An alkaline comet assay was used to determine the effect of cobalt chrome and stainless steel on the integrity of the DNA of primary astrocytes and microglia in co-culture and primary astrocytes in isolation. The comet assay was a simplistic test to measure DNA strand breaks. The assay utilises the principle that when cells are embedded in agarose gels and are lysed with detergent in a high salt environment, this will result in the formation of nucleoids containing supercoiled DNA. If there were single or double stranded breaks in the DNA, the supercoiling is lost leaving the negatively charged genetic material free to move towards the anode and a comet is formed (Figure 4.2). The amount of movement of genetic material is dependent on the size of the DNA strand and the number of breaks in the DNA. In-tact DNA does not lose its supercoiling and thus the DNA remains in the nucleoid. This effect can be visualised using SYBR gold to stain the genetic material and the results analysed using the Comet IV Lite software package.

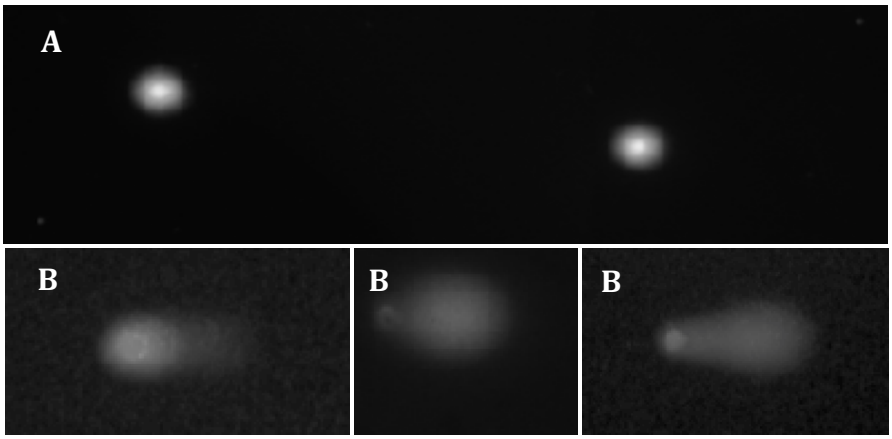

Figure 4.2 Comet images. A) No DNA damage, DNA remains in the nucleoid B) DNA damage, the negatively charged fragmented genetic material is able to move through the agarose gel towards the anode and a comet is formed.

4.3.3.2 Preparation of cells prior to the comet assay.

Prior to the comet assay, primary astrocytes and microglia in co-culture and primary astrocytes in isolation were cultured using a 2D monolayer cell culture system with increasing particle doses of cobalt chrome and stainless steel wear particles (0.5μm^3-50μm^3 debris per cell) for 24 hours, 48 hours and five days. Hydrogen peroxide (100µM), a known inducer of single stranded and double stranded DNA breaks, was used as a positive control. The cells were seeded into 24-well plates pre-coated with PDL to encourage cell adhesion at a seeding density of 1.5 x 10^5 cells (in 1.25ml supplemented medium) per well for the 24hours and two-day assays. A seeding density of 1 x 10^5 cells (in 1.25ml supplemented medium, Chapter 2, section 2.3.20) per well was used for the longer-term assay (over five days) to avoid cell crowding.

The cells were cultured with increasing particle volumes of cobalt chrome and stainless steel (particle volume re-suspended in 1.25ml supplemented medium) in 24-well plates, pre-coated with PDL. Supplemented DMEM, Chapter 2 section 2.3.20, was used to culture the primary astrocytes and microglia and primary astrocytes in isolation. The mass of cobalt chrome and stainless steel particles needed to provide the necessary volume doses was calculated using the method previously outlined in Chapter 4, section 4.3.1.2

4.3.3.3 Preparation of solutions and equipment for the alkaline comet assay.

Prior to commencing the comet assay, the lysis solution was cooled to 4°C. Using a Bunsen burner, in a beaker of boiling water, the LMP agarose was melted, allowed to cool slightly for five minutes, and transferred to a 37°C water bath. The CometSlides™ were labelled with the test conditions, the date and slide ID and transferred to a 37°C incubator until

ready for use. Each CometSlide™ was supplied with two windows allowing two agarose gels to be prepared on each slide. As there were four repeats per condition 2 slides were prepared per condition (Figure 4.3).

The alkaline electrophoresis buffer (preparation outlined in Chapter 2, section 2.3.1) and DNA unwinding solutions were prepared (Chapter 2, section 2.3.10). When the alkaline electrophoresis solution was thoroughly mixed, the solution was transferred into an electrophoresis tank at 4°C for one-hour prior to use. The DNA unwinding solution was prepared and allowed to cool to room temperature, for 30 minutes, prior to use.

A volume of 500ml of pre-prepared sterile PBS, without calcium and magnesium, was placed on ice prior to commencing the comet assay.

Figure 4.3 The design of the CometSlide™ with two windows per slide. Two slides were used per test condition (4 repeats per condition).

4.3.3.4 Preparation of agarose gels and protocol for the alkaline comet assay

After all the solutions and necessary equipment were prepared as described in section 4.3.3.3 above, the agarose gels were produced. The 24-well plates containing cells plus particles were removed from the incubator after the appropriate incubation period and in a class II safety cabinet the supplemented medium was removed from each well and discarded.

The cells were washed twice with 500µl sterile DPBS (without calcium and magnesium) and 300µl 0.5% with EDTA of trypsin was added to each well. The 24-well plate was incubated for 10 minutes on a rocker at 80rpm at 37°C in 5% (v/v) CO_2 in air to detach the cells from the tissue culture plastic.

After the 10 minute incubation, the 24-well plate was gently tapped to detach the cells from the bottom of each well. The cells were observed using an inverted microscope to ensure all cells had detached from the base of the well. If this was not the case then the 24-well plate was incubated at 37°C in 5% (v/v) CO_2 in air for an additional two minutes. The trypsin was inhibited with 800µl of supplemented DMEM medium, described in Chapter 2, section 2.3.20. The contents of each well were mixed thoroughly by pipetting up and down and transferred to pre-labelled sterile 1.5ml eppendorfs. The 24-well plate was again observed using an inverted microscope to ensure that the cells had been removed.

The cells were centrifuged at 200g for 10 minutes at 4°C. The supernatant was removed taking extra care to ensure the pellet was not dislodged. The cell pellet was re-suspended in 150µl ice cold PBS and thoroughly mixed by aspiration. The cells were placed on ice, to prevent any DNA repair, and a cell count performed for each condition using the trypan blue exclusion assay (see Chapter 2, section 2.4.1.4). The cells were diluted further with ice cold PBS (without calcium and magnesium) to a concentration of 1 x 10^5 cells per ml. This ensured sufficient cells would be visualised in each window on the comet slides and that sufficient cells would be analysed using the Comet IV Lite Software. The cells were incubated on ice in the dark until the agarose gels were prepared.

Cells were added to the LMP agarose at a ratio of 1:10 (v/v). Here, 6µl of cell suspension (approximately 600 cells) was combined with 60µl LMP agarose and carefully mixed to ensure the cells were evenly distributed throughout the gel. Immediately after mixing, 50µl of the cell: LMP agarose mixture was pipetted onto the corresponding CometSlide™ (this step was carried out at speed so that the agarose gel did not set in the pipette tip or in the eppendorf where it was mixed). The viscous cell, agarose mixture was manipulated using a pipette tip to ensure there was an even distribution of the gel over the slide window. To confirm the presence of an appropriate concentration of cells in each window each slide was observed using an inverted light microscope. The slides were then placed in the dark at 4°C for 10 minutes to ensure the gels were set.

After all the gels were prepared, the positive control, hydrogen peroxide, slides were immersed in a coplin jar containing 30ml of 100µM hydrogen peroxide for five minutes at 4°C. This was a sufficient length of time to cause DNA damage in primary astrocytes and microglia. After five minutes the slides were thoroughly rinsed in sterile PBS (without calcium and magnesium), to remove residual hydrogen peroxide, to prevent contamination of the remaining slides in the subsequent steps. All slides were flooded in

pre-cooled (4°C) lysis solution (provided as part of the Trevigen Comet assay kit) for 30 minutes.

After the 30-minute incubation period, any excess lysis solution was drained and discarded and the slides were immersed in alkaline DNA unwinding solution (Chapter 2, section 2.3.10), in the dark, at room temperature for 20 minutes. The excess DNA unwinding solution was discarded and the slides placed in an electrophoresis tank containing the alkaline electrophoresis solution at 4°C. Care was taken to ensure the slides were equidistant from the electrodes. The orientation of the slides was noted for later analysis. The power pack was set to 1 Volt.cm^{-1} length. As the length of the tank was 30cm, it was set to 30V. The mAMP was adjusted to 300 ± 5mAMP, this was achieved by the addition or removal of electrophoresis solution. The samples were electrophoresed in the dark at 4°C for 20 minutes. The slides were then removed from the electrophoresis tank and washed twice with distilled water in the dark for five minutes. Finally, the slides were immersed in 70% (v/v) ethanol for five minutes in the dark. Following this the slides were incubated at 37°C in 5% (v/v) CO_2 in air for 10 minutes to dry. The CometSlides™ were stored in plastic trays containing desiccant beads in the dark at room temperature prior to imaging. The imaging was always performed 24 hours after the comet assay for continuity.

4.3.3.5 Staining and imaging of CometSlides™

A volume of 100µl pre-prepared SYBR gold solution (see Chapter 2, section 2.3.25) was added to each window of all CometSlides™ ensuring each agarose gel was completely immersed in SYBR gold solution. The slides were incubated at 37°C in 5% (v/v) CO_2 in air for 30 minutes in the dark. After the required incubation period, any excess SYBR gold solution was removed and discarded. The slides were washed three times with distilled water to remove any residual SYBR gold. Any excess water on the slides was removed with blue tissue roll, taking care not to disrupt the agarose gels. The gels were then allowed to dry in the dark at 37°C in 5% (v/v) CO_2 in air (for approximately 2 hours), which brought all the cells into the same focal plane.

The slides were imaged using a Zeiss upright microscope. To ensure uniformity of imaging for each experiment the following settings were utilised.

- The HXP 120V power source was set to 10.
- A x 10 objective lens was used for all windows on all sides.
- The EGFP channel was used for all images (emission wavelength 509nm).
- The exposure time was set to 1500ms

- The Zen software was used so numerous images were taken of each gel. A 7x7 grid was selected creating 49 tiles in total for imaging. A 4 x 3 grid was placed over the tiles to generate set points. Each set point was checked to ensure all areas of the gel were in focus. Then the 49 tiles were sewn into one image. The image intensity was set to maximum to ensure all the comets were clear. This was uniform for all images in all experiments. This was necessary as the software detecting the comets used tail intensity as a key measurement. This would be different if the same settings were not adhered to for all images.

The olive tail moment was used to detect DNA damage over time. The olive tail moment is a product of tail length and the fraction of the total DNA located in the tail.

4.3.3.6 Image processing using Comet IV Lite Software.

Prior to image processing all images were orientated such that the heads of the comet were positioned to the left hand side in the field of view and the tail to extend out of the right hand side of the head. This made sure all comets, regardless of the direction of electrophoresis, were aligned in the same direction. This ensured the software would accurately detect the comets and the readings for tail moment would all be in a uniform direction.

Overlapping comets, comets located on the edge of the image so part of the comet had been removed, comets surrounded by cellular debris or too close together for the software to detect individual comets, were not included in the measurements. All the well-separated cells were counted in each window, this ranged between 10 and 150 cells per window. A minimum of 50 cells per condition (0.5μm^3 debris per cell, 5μm^3 debris per cell, 50μm^3 debris per cell, cell only and hydrogen peroxide positive control) were measured and processed.

4.3.3.7 Statistical analysis of comet assay data.

When imaging the agarose gels, a minimum of 50 cells were analysed for each test condition. The number of cells counted per window was different for each test condition meaning that the number of comets analysed for each test condition was not equal. In order to compare means of each test condition and determine whether or not significant DNA damage had been caused in relation to the cell only negative control, a two-way ANOVA was performed. However the calculations performed as part of the two-way ANOVA assume equal group sizes, adjustments were made to accommodate for the varying group sizes.

4.4 Results

4.4.1 The effect of cobalt chrome and stainless steel wear particles on the viability of C6 glial, PC12 neuronal cell lines and primary astrocytes and microglia.

4.4.1.1 The effect of cobalt chrome particles on the viability of C6 glial cells.

An ATP Lite™ cell viability assay was used to determine the effect of increasing volumes of cobalt chrome particles (0.05μm³, 0.5μm³, 5μm³, and 50μm³ per cell) on the viability of C6 glial cells in 2D culture. The average luminescence values, indicative of cellular metabolic activity and thus viability, for the cell only negative control continued to rise over the course of the five day culture period (Figure 4.4) demonstrating an approximately 10-fold increase over five days.

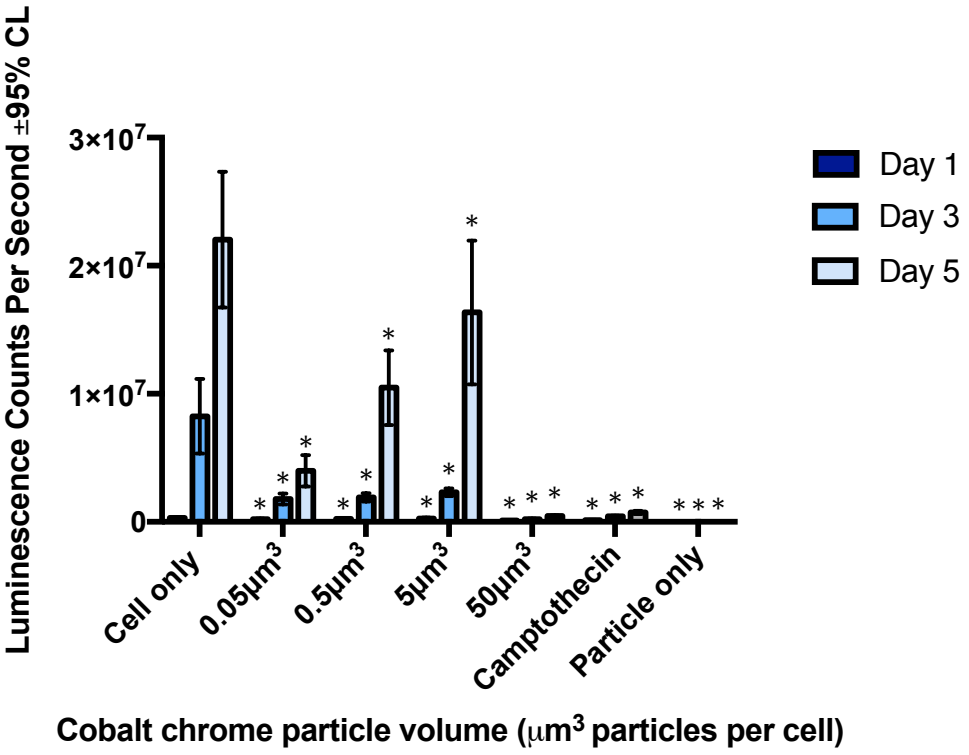

Figure 4.4 The effect of cobalt chrome particles on the viability of C6 glial cells in 2D monolayer culture after 24 hours, three days and five days in culture. Data is presented as the mean (n=6) ± 95% confidence limits. A single asterisk depicts a significant decrease, between means ($p < 0.05$) when compared to the cell only negative control (Two-way ANOVA and Tukey posthoc analysis).

C6 cells, which received the highest cobalt chrome particle dose, 50μm³ cobalt chrome debris per cell, demonstrated significant reductions in viability at all three time points tested when compared to the cell only negative control (Figure 4.4). A 65% reduction in

viability was observed after 24 hours, 97.5% reduction after three days and 98% after 5 days in culture (Figure 4.5).

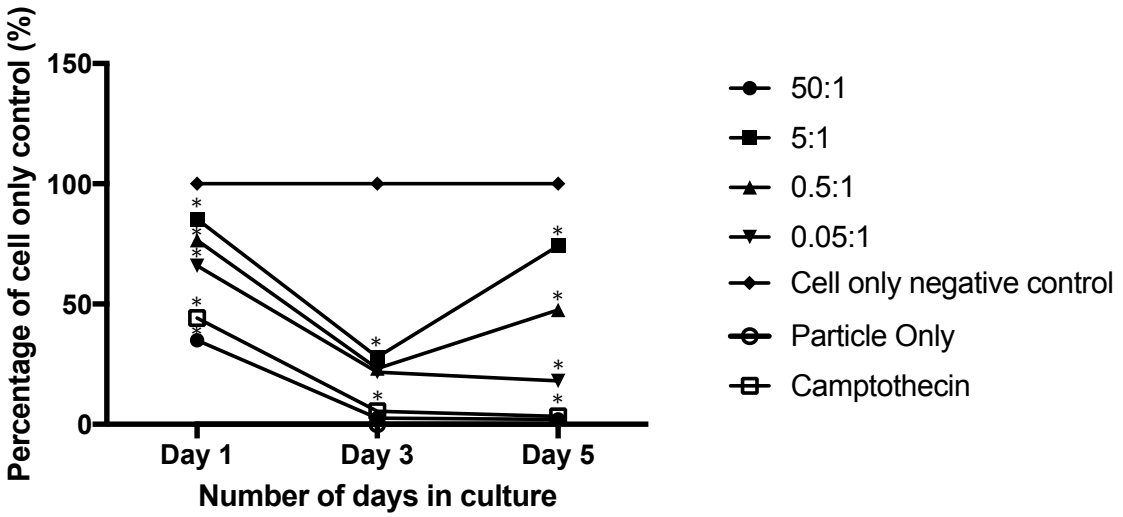

Figure 4.5 The effect of cobalt chrome particles on the viability of C6 glial cells in 2D monolayer culture over five days, expressed as a percentage of the cell only negative control. Data is presented as the mean (n=6). A single asterisk depicts a significant reduction in viability.

The C6 cells cultured with cobalt chrome at a particle volume of 5μm^3 exhibited a significant reduction in viability at all time points tested with a 14.7% reduction in viability observed after 24 hours. After three days in culture a significant, 72.1%, reduction was observed when C6 cells were cultured with 5μm^3 cobalt chrome debris per cell. After five days in culture a significant 25.8% reduction in viability was observed.

Upon culture with a particle volume of 0.5μm^3 the C6 glial cells demonstrated a decrease in viability when compared with the cell only negative control at all time points tested. A significant 23.4% reduction in viability was observed after 24 hours and a significant 76.8% reduction after three days. After five days in culture a significant 52.5% reduction in viability was observed when compared to the cell only negative control.

When C6 glial cells were cultured with 0.05μm^3 cobalt chrome debris per cell a significant decrease in viability was observed at all time points when compared with the cell only negative control, with a significant 34% reduction observed after 24 hours and a significant 78.4 % decrease after three days. After five days in culture a significant 82% reduction in viability was observed when compared to the cell only negative control.

Camptothecin, significantly reduced the viability of the C6 glial cells over the course of the investigation, here a 55.8% significant reduction was observed after 24 hours, 94.6% reduction after three days and 96.7% reduction after five days. The cobalt chrome, particle only control, did not interfere with the luminescence readings for this assay. A summary of the effects of cobalt chrome on the viability of C6 glial cells is provided in Table 4.1

4.4.1.2 The effect of stainless steel on the viability of C6 glial cells.

The effects of stainless steel on the viability of C6 glial cells are shown in Figure 4.6. The average luminescence counts per second value for the cell only negative control continued to rise for the duration of the cell culture experiment with a 10-fold increase in average luminescence counts per second seen over five days.

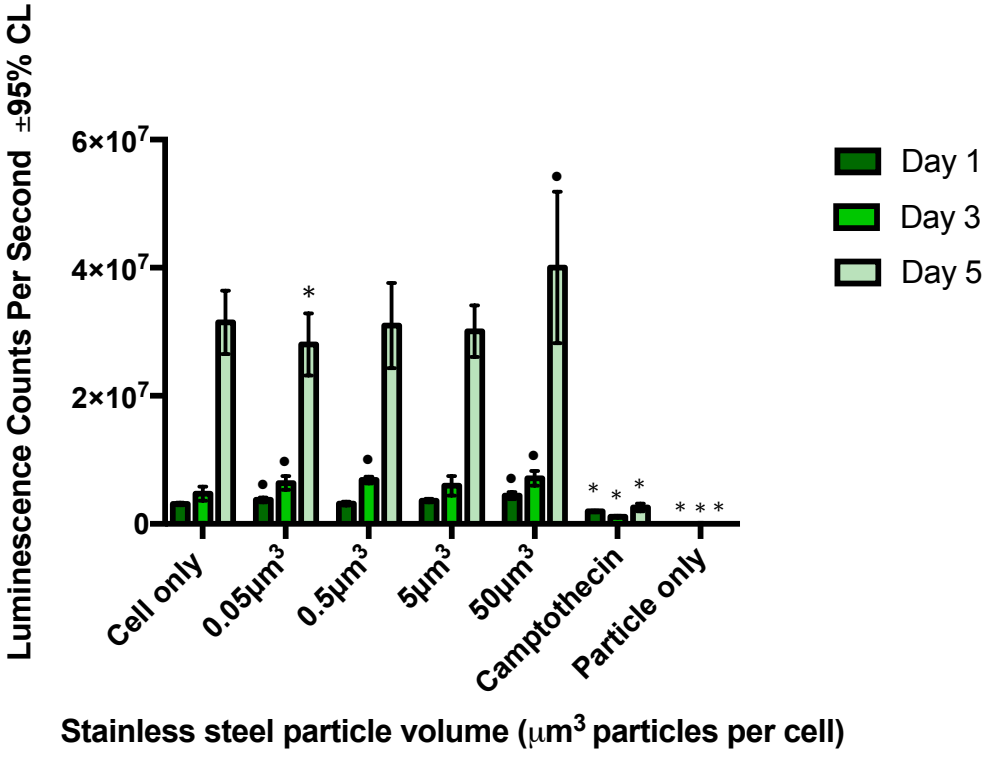

Figure 4.6 The effect of stainless particles on the viability of C6 glial cells in 2D monolayer culture after 24 hours, three days and five days in culture. Data is presented as the mean (n=6) ± 95% confidence limits. A single asterisk depicts a significant reduction in viability (p value of <0.05) when compared to the cell only negative control. An • is indicative of a significant increase in viability when compared to the cell only negative control.

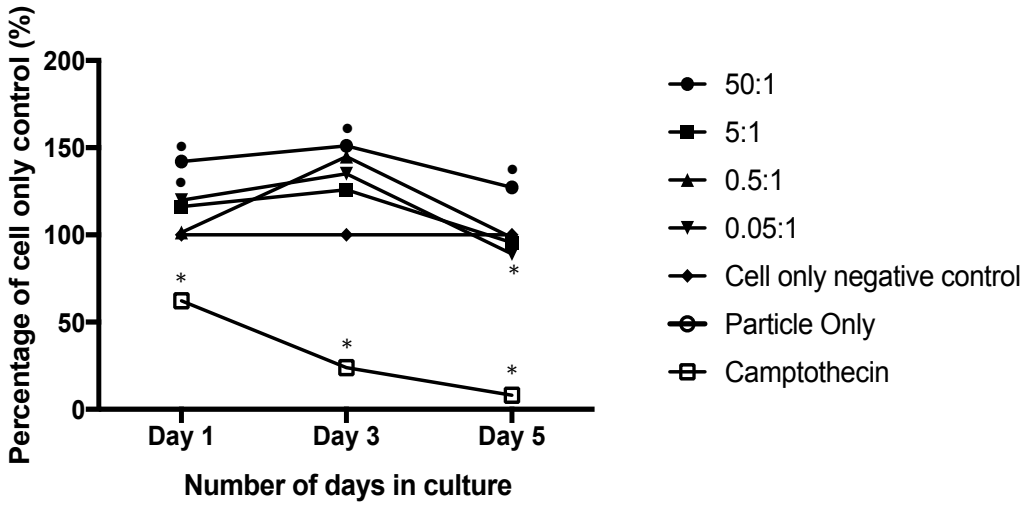

Figure 4.7 The effect of stainless steel particles on the viability of C6 glial cells in 2D monolayer culture over five days expressed as a percentage of the cell only negative control. Data is presented as the mean (n=6). A single asterisk depicts a significant reduction in viability. An • is indicative of a significant increase in viability when compared to the cell only negative control.

When C6 glial cells were cultured with the highest dose of stainless steel wear debris, 50μm^3 stainless steel debris per cell, no adverse effect on C6 cell viability was observed at any time point. Conversely a significant increase in viability was detected at all time points when compared to the cell only negative control (Figure 4.6 and Figure 4.7).

The C6 Glial cells cultured with 5μm^3 for five days were not adversely affected in terms of cell viability when compared to the cell only negative control at any time point tested.

After 24 hours the 0.05μm^3 per cell dose of stainless steel particles significantly increased the viability of C6 cells and on the third day in culture both 0.5μm^3 and 0.05μm^3 doses of stainless steel were observed to significantly increase the viability of C6 Cells. This effect was no longer observed at day five. After five days in culture the lowest stainless steel dose, 0.05μm^3debris per cell, significantly reduced the viability of C6 glial cells by 11%.

When the C6 cells were cultured with camptothecin for five days a continuous significant decline in viability was observed, with a significant 37.7% reduction observed after 24 hours, 76.1 % decrease after three days and 91.9% after five days.

The stainless steel wear particles suspended in supplemented medium did not interfere with the luminescence count for the ATP Lite™ assay. A summary of the effects of stainless steel on the viability of C6 glial cells is provided in Table 4.1.

Table 4.1 The effect of cobalt chrome and stainless steel wear particles on the viability of C6 glial cells. A significant decrease in viability ($p<0.05$) compared to the cell only negative control is indicated with an asterisk. Conditions marked with an • are indicative of a significant increase in cell viability relative to the cell only control.

	C6 and Cobalt chrome particles					C6 and stainless steel particles				
	0.05μm³	0.05μm³	5μm³	50μm³	Camp.	0.05μm³	0.5μm³	5μm³	50μm³	Camp.
Day 1	*	*	*	*	*	•			•	*
Day 3	*	*	*	*	*	•	•		•	*
Day 5	*	*	*	*	*	*			•	*

4.4.1.3 The effect of cobalt chrome particles on the viability of PC12 neuronal cells.

The effects of cobalt chrome wear particles on the viability of PC12 neuronal cells are shown in Figure 4.8. The PC12 neuronal suspension cells continued to grow and multiply for the duration of the investigation, indicated by a continuing rise in the level of ATP over the five day time period.

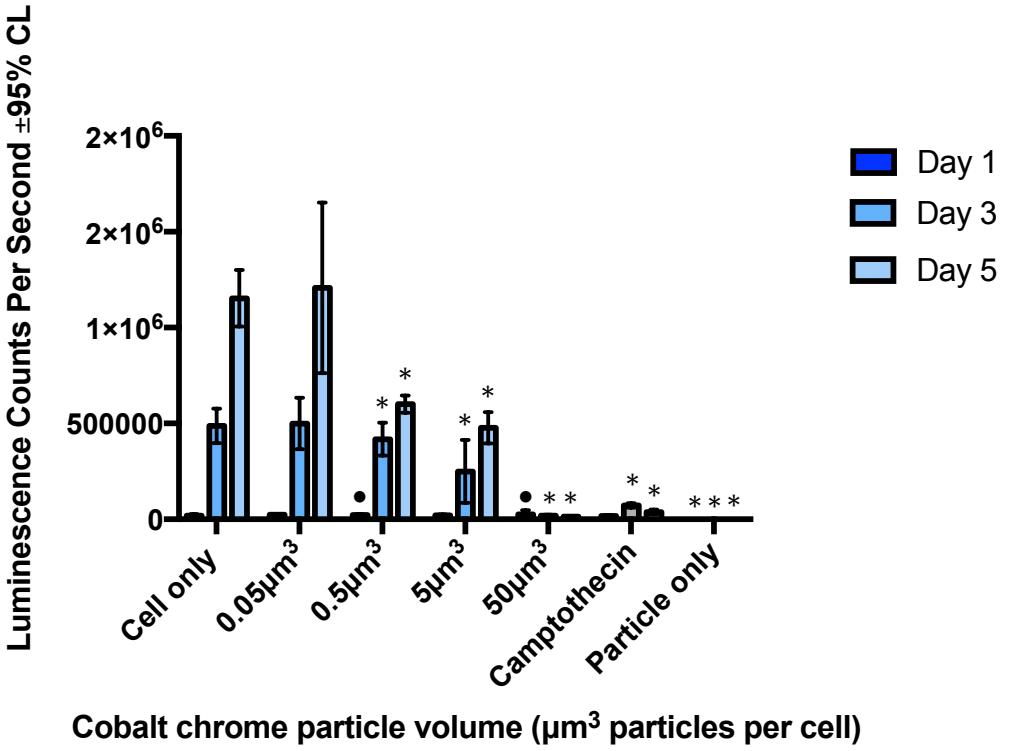

Figure 4.8 The effect of cobalt chrome particles on the viability of PC12 glial cells in 2D monolayer culture after 24 hours, three days and five days in culture. Data is presented as the mean (n=6) ± 95% confidence limits. A single asterisk depicts a significant reduction in viability (p value of <0.05) and an • is indicative of a significant increase in viability when compared to the cell only negative control.

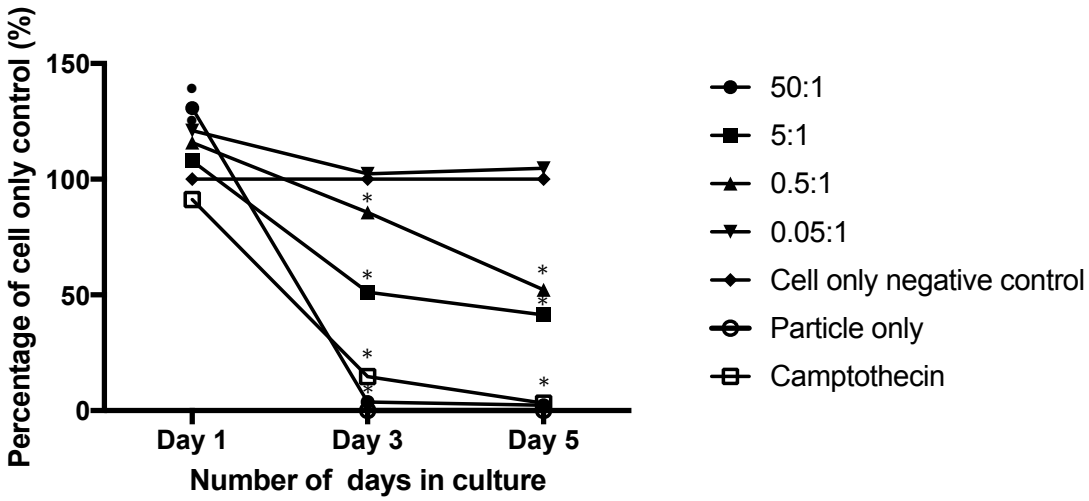

Figure 4.9 The effect of cobalt chrome particles on the viability of PC12 glial cells in 2D monolayer culture after five days in culture, expressed as a percentage of the cell only negative control. Data is presented as the mean (n=6). A single asterisk depicts a significant reduction in viability an • is indicative of a significant increase in viability when compared to the cell only negative control.

After 24 hours the highest dose of cobalt chrome did not have a significant adverse effect on the viability of PC12 cells (Figure 4.8). Interestingly, after 24 hours in culture the cobalt chrome particles had a beneficial effect on the PC12 viability at this dose, but after three and five days in culture a significant reduction in cell viability was observed, with a 96.2% reduction evident after three days and a 97.7% reduction after five days (Figure 4.9).

When PC12 cells were cultured with 5μm^3 cobalt chrome debris per cell. After 24 hours in culture there were no adverse effects on the cell viability of PC12 neuronal cells, however after three days in culture a significant 48.8% reduction was observed, and after five days the viability decreased by 58.6% which was significant when compared to the cell only negative control ($p<0.05$).

The PC12 neuronal cells cultured with 0.5μm^3 cobalt chrome debris per cell were not adversely affected in terms of cell viability when compared to the cell only negative control after 24 hours. After the PC12 cells were cultured with 0.5μm^3 cobalt chrome debris per cell for three and five days, significant 14.3 % and 47.8% reductions in viability were observed respectively.

The PC12 cells cultured with particle volume (μm^3) to cell number ratio of 0.05:1 of cobalt chrome particles were not adversely affected in terms of viability when compared to the cell only control at any time point tested.

When the PC12 cells were cultured with the camptothecin positive control for five days a continuous decline in viability was observed, with an 8.8% reduction observed after 24 hours, which was not significant when compared to the cell only negative control. A significant 85.2% decrease in viability was observed after three days in culture and a significant 96.7% reduction after five days. The cobalt chrome wear particles suspended in supplemented medium did not interfere with the luminescence readings for the ATP Lite™ assay. A summary of the effects of cobalt chrome on the viability of PC12 neuronal cells can be seen in Table 4.2.

4.4.1.4.The effect of stainless steel particles on the viability of PC12 neuronal cells.

The effect of increasing stainless steel particle volumes (0.05μm^3-50μm^3 stainless steel debris per cell) on the viability of PC12 neuronal cells was assessed using the ATP Lite™ cell viability assay over five days in culture. Over the course of the five day culture period

the cell only negative control continued to proliferate with an approximately four-fold increase in ATP production from day one to day five (Figure 4.10).

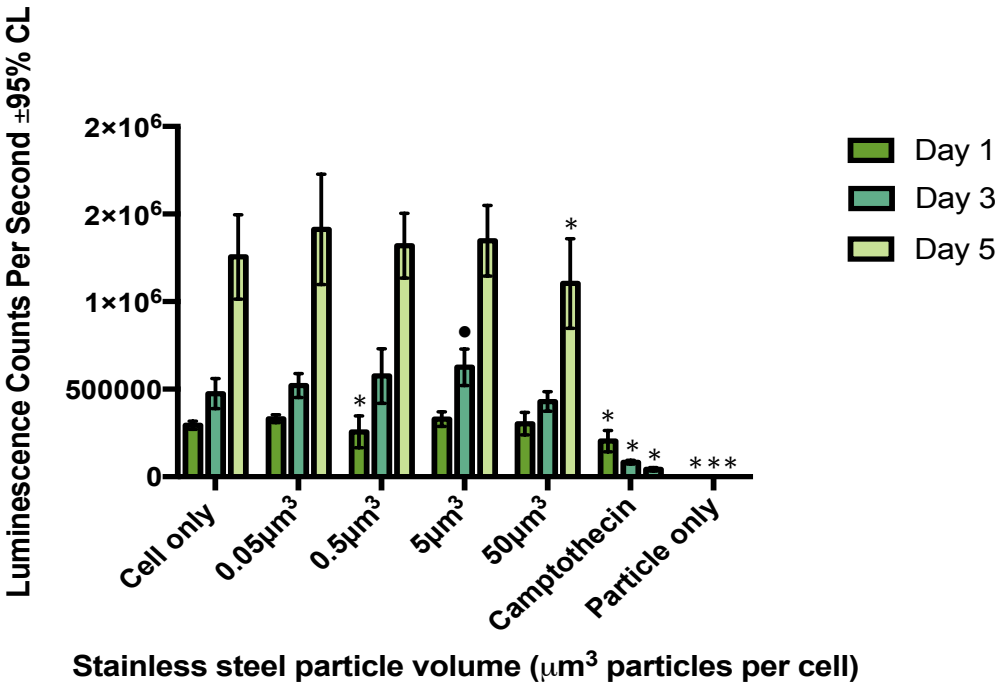

Figure 4.10 The effect of stainless steel wear particles on the viability of PC12 glial cells in 2D monolayer culture after 24 hours, three days and five days in culture. Data is presented as the mean (n=6) ± 95% confidence limits. An asterisk depicts a significant decrease in viability (p value <0.05) compared to the cell only negative control. An • is indicative of a significant increase in viability when compared to the cell only negative control.

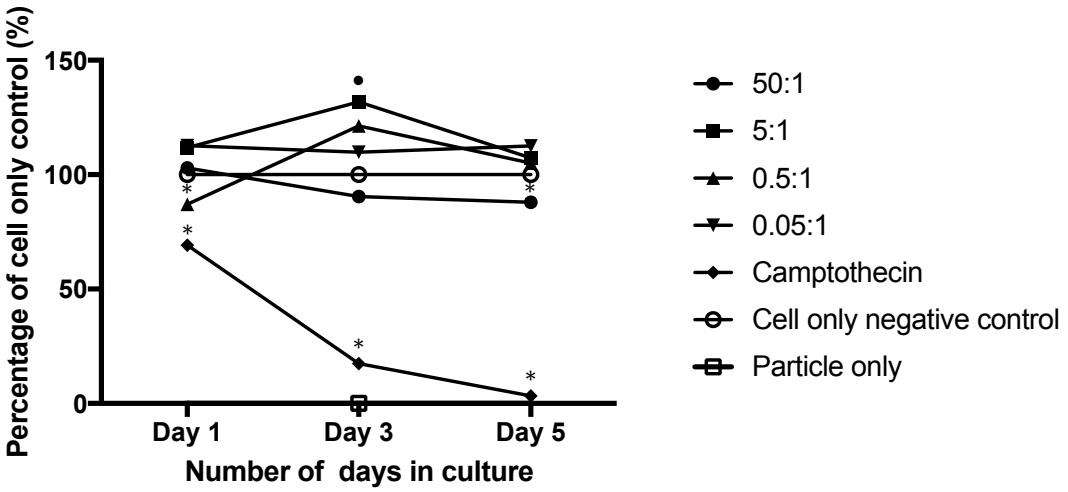

Figure 4.11 The effect of stainless steel on the viability of PC12 glial cells in 2D monolayer culture after five days as a percentage of the cell only negative control. Data is presented as the mean (n=6). An asterisk depicts a significant decrease in viability (p value <0.05) compared to the cell only negative control. Conditions marked with an • are indicative of a significant increase in viability when compared to the cell only negative control.

No adverse effect on viability was observed when PC12 cells were cultured with 50μm^3, 5μm^3 and 0.05μm^3 stainless steel debris per cell after 24 hours in culture (Figure 4.10 and Figure 4.11). The 0.5μm^3 stainless steel dose did trigger a significant 12.9% reduction at this time point.

Interestingly after three days in culture a significant increase in viability was observed when the PC12 cells were cultured with 5μm^3 stainless steel debris per cell. At this time point the 50μm^3, 0.5μm^3 and 0.05μm^3 stainless steel debris per cell did not adversely effect PC12 viability.

After five days in culture the 50μm^3 stainless steel debris per cell dose adversely affected PC12 cells, with a 12.1 % reduction in viability observed.

The camptothecin positive control elicited a significant reduction in PC12 viability over the course of the experiment when compared to the cell only negative control. A 30.9% reduction in viability observed after 24 hours, 82.6% reduction after three days and a 96.6% decrease after five days. A two-way ANOVA and Tukey post-hoc test was used to determine whether the reduction in viability was significant ($p<0.05$).

The luminescence readings were not disrupted by the presence of stainless steel wear particles. A summary of the effects of stainless steel on the viability of PC12 cells is provided in Table 4.2

Table 4.2 The effect of cobalt chrome and stainless steel wear particles on the viability of PC12 neuronal cells. A significant decrease in viability ($p<0.05$) compared to the cell only negative control is indicated with an asterisk. Conditions marked with an • are indicative of a significant increase in cell viability relative to the cell only control.

	PC12 and Cobalt chrome particles					PC12 and stainless steel particles				
	0.05µm³	0.5µm³	5µm³	50µm³	Camp.	0.05µm³	0.5µm³	5µm³	50µm³	Camp.
Day 1		•		•			*			*
Day 3		*	*	*	*			•		*
Day 5		*	*	*	*				*	*

4.4.1.5. The effect of cobalt chrome particles on the viability of primary astrocytes and microglia.

The effect of increasing cobalt chrome volume doses of particles on the viability of primary astrocytes and microglia in co-culture was assessed using the ATP Lite™ assay over time. Over the course of the investigation the primary astrocytes and microglia continued to proliferate (Figure 4.12).

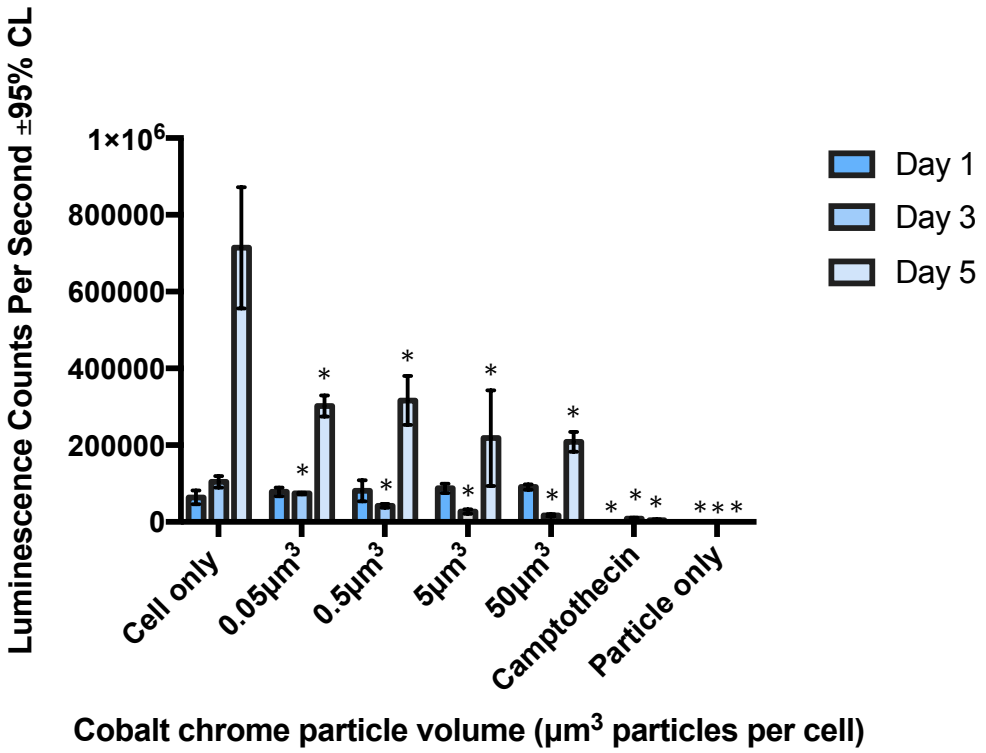

Figure 4.12 The effect of cobalt chrome particles on the viability of primary astrocytes and microglia in co-culture in 2D monolayer culture after 24 hours, three days and five days. Data is presented as the mean (n=6) ± 95% confidence limits. An asterisk depicts a significant decrease in viability (p value <0.05) when compared to the cell only negative control.

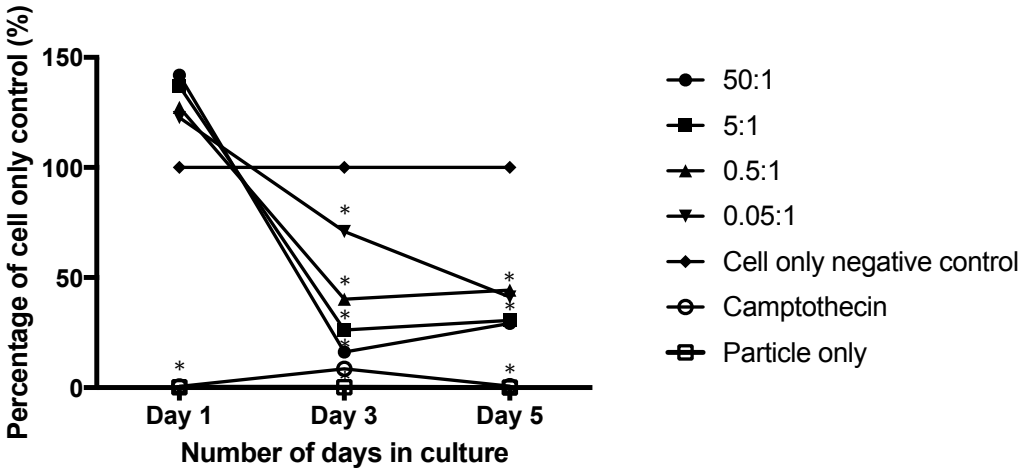

Figure 4.13 The effect of cobalt chrome particles on the viability of primary astrocytes and microglia in 2D monolayer culture after five days, expressed as a percentage of the cell only negative control. Data is presented as the mean (6 replicates per condition). An asterisk depicts a significant decrease in viability (p value <0.05) when compared to the cell only negative control.

The culture of primary astrocytes and microglia with 50μm³, 5μm³, 0.5μm³ and 0.05μm³ cobalt chrome wear particles did not elicit an adverse effect on cell viability after 24 hours in culture (Figure 4.12). However after three and five days in culture with cobalt chrome wear particles, a significant reduction in the viability of primary astrocytes and microglia was observed for all particle doses (50μm³, 5μm³, 0.5μm³ and 0.05μm³). When primary astrocytes and microglia in co-culture were cultured with the highest cobalt chrome particle dose of 50μm³, an 83.8% and 70.8% decrease in viability was observed after three and five days, respectively, compared to the cell only negative control (Figure 4.13). The viability of primary astrocytes and microglia in co-culture was significantly reduced after three and five days when cultured with 5μm³ cobalt chrome debris per cell. After three days in culture, a significant 73.9% reduction in viability was observed and a 69.4% decrease was observed after five days when compared to the cell only negative control. The viability of primary astrocytes and microglia in co-culture was significantly reduced when cultured with 0.5μm³ cobalt chrome debris per cell after three and five days in culture. After three days a 59.8% decrease was observed and after 5 days a 55.7% decline was recorded. Primary astrocytes and microglia cultured with 0.05μm³ cobalt chrome debris per cell revealed a gradual decline in viability over the course of the investigation. After three days in culture a 29% reduction in viability was observed and a 58.8% reduction in viability after five days.

When primary astrocytes and microglia were cultured with the camptothecin positive control a rapid decline in cell viability occurred over the five-day study. After 24 hours in culture with camptothecin the viability of primary astrocytes and microglia was significantly reduced by 99.5%. After three days the viability was significantly reduced by 91.4% and significantly reduced by 99.3% after five days.

The luminescence readings were not disrupted by the presence of cobalt chrome wear particles for this assay. A summary of the effects of cobalt chrome on the viability of primary astrocytes and microglia can be seen in Table 4.3.

4.4.1.6. The effect of stainless steel particles on the viability of primary astrocytes and microglia.

The effect of increasing stainless steel particles volumes on the viability of primary astrocytes and microglia in co-culture was assessed using the ATP Lite™ assay over time. When primary astrocytes and microglia were cultured with 50μm³, 5μm³ and 0.5μm³ stainless steel debris per cell for 24 hours a significant reduction in viability was observed

for all three doses when compared to the cell only negative control (38.8%, 38.9% and 24.9% reductions respectively) (Figures 4.14 and 4.15).

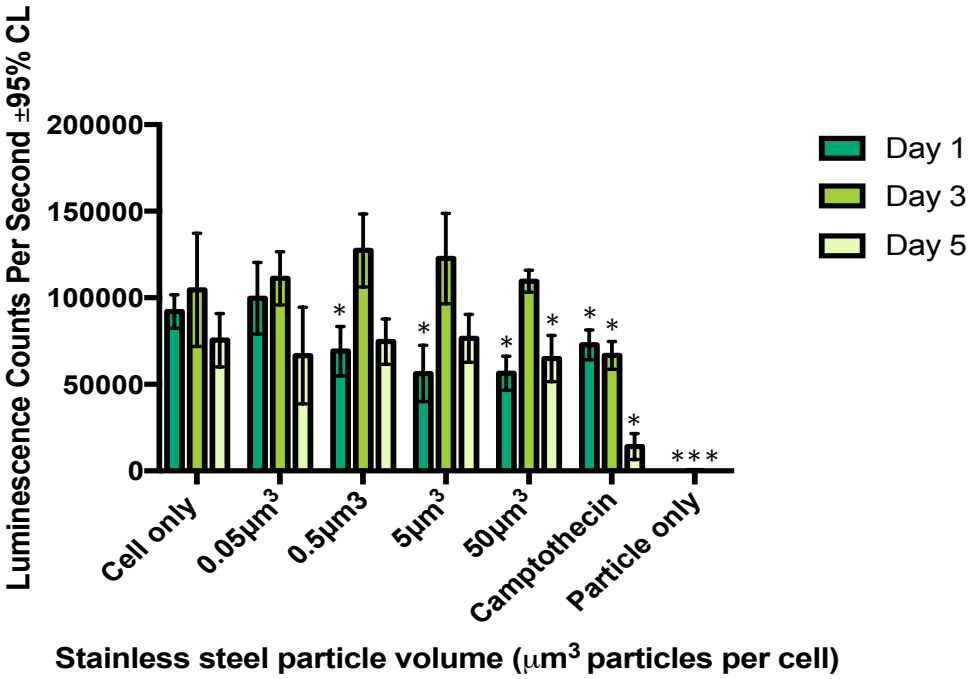

Figure 4.14 The effect of stainless steel particles on the viability of primary astrocytes and microglia over 24 hours, three days and five days in 2D monolayer culture. Data is presented as the mean (n=6) ± 95% confidence limits. An asterisk depicts a significant decrease in viability (p value of <0.05) when compared to the cell only negative control.

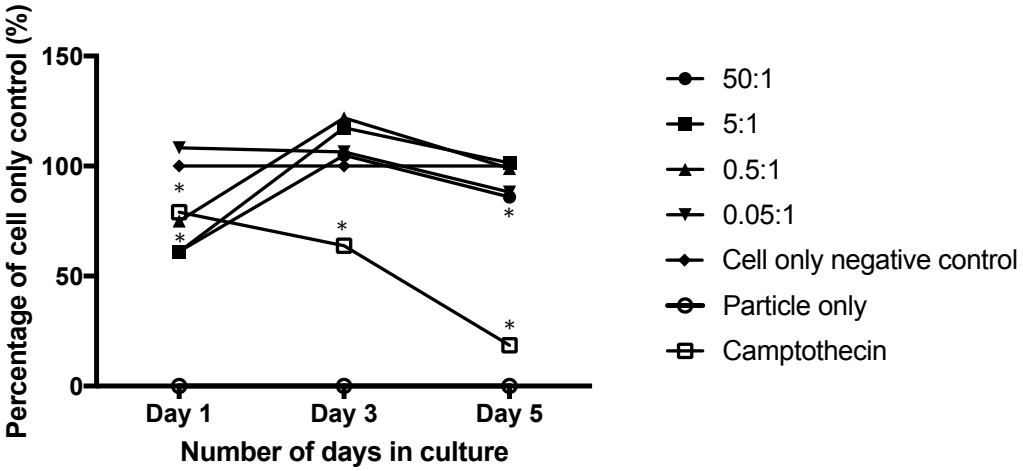

Figure 4.15 The effect of stainless steel particles on the viability of primary astrocytes and microglia after five days in 2D monolayer culture system, expressed as a percentage of the cell only negative control. Data is presented as the mean (6 replicates per condition). An asterisk depicts a significant decrease in viability (p value <0.05) when compared to the cell only negative control.

Primary astrocytes and microglia cultured with the lowest 0.05µm³ stainless steel per cell particle dose were not adversely affected in terms of viability, when compared to the cell only negative control after 24 hours in culture (Figure 4.15).

No significant differences in cell viability were observed when primary astrocytes and microglia were cultured with 5µm³, 0.5µm³ and 0.05µm³ stainless steel debris per cell at the three and five day time points. After five days in culture primary astrocytes and microglia cultured with the highest stainless steel particle dose of 50µm³ a significant reduction in viability of 14.1% was observed.

The primary astrocytes and microglia cultured with camptothecin showed progressive reductions in viability, 20.9%, 36.2%, 81.5% after one, three and five days, respectively, when compared to the cell only negative control.

The stainless steel wear particles did not interfere with the luminescence counting for this assay. A summary of the effects of stainless steel on the viability of primary astrocytes and microglia can be seen in Table 4.3

Table 4.3 The effect of cobalt chrome and stainless steel wear particles on the viability of primary astrocytes and microglia. A significant decrease in viability $p<0.05$ compared to the cell only negative control is indicated with an asterisk.

	Primary A +M and CoCr particles					**Primary A+M and SS particles**				
	0.05µm³	0.5µm³	5µm³	50µm³	Camp.	0.05µm³	0.5µm³	5µm³	50µm³	Camp.
Day 1					*		*	*	*	*
Day 3	*	*	*	*	*					*
Day 5	*	*	*	*	*				*	*

4.4.2. The effect of cobalt chrome and stainless steel wear particles on the integrity of primary astrocyte and microglia DNA.

4.4.2.1. The effect of cobalt chrome wear particles on the integrity of primary astrocyte and microglia DNA.

Primary astrocytes and microglia in co-culture and primary astrocytes in isolation were cultured in a 2D monolayer cell culture system with increasing particle volumes of cobalt chrome and stainless steel (0.5μm^3, 5μm^3 and 50μm^3 debris per cell). An alkaline comet assay was used to determine the effect of these particle doses on the integrity of primary astrocyte and microglia DNA.

When primary astrocytes and microglia were cultured in a 2D monolayer system low levels of DNA damage were detected over the duration of the investigation. After 24 hours a tail moment of 0.95 was observed, 0.56 after two days and, 1.16 after five days. The level of DNA damage in response to increasing cobalt chrome wear particle doses was compared to the cell only negative control at each time point tested using a Two-way ANOVA and Tukey post hoc analysis (Figure 4.16).

When primary astrocytes and microglia were cultured with the highest cobalt chrome particle volume (50μm^3 cobalt chrome debris per cell) for 24 hours, two days and five days the level of DNA damage was significantly greater than that observed in the cell only negative control. After 24 hours a tail moment of 2.63 was recorded and after two days in culture the tail moment was 2.16, after five days in culture a tail moment of 1.65 was recorded.

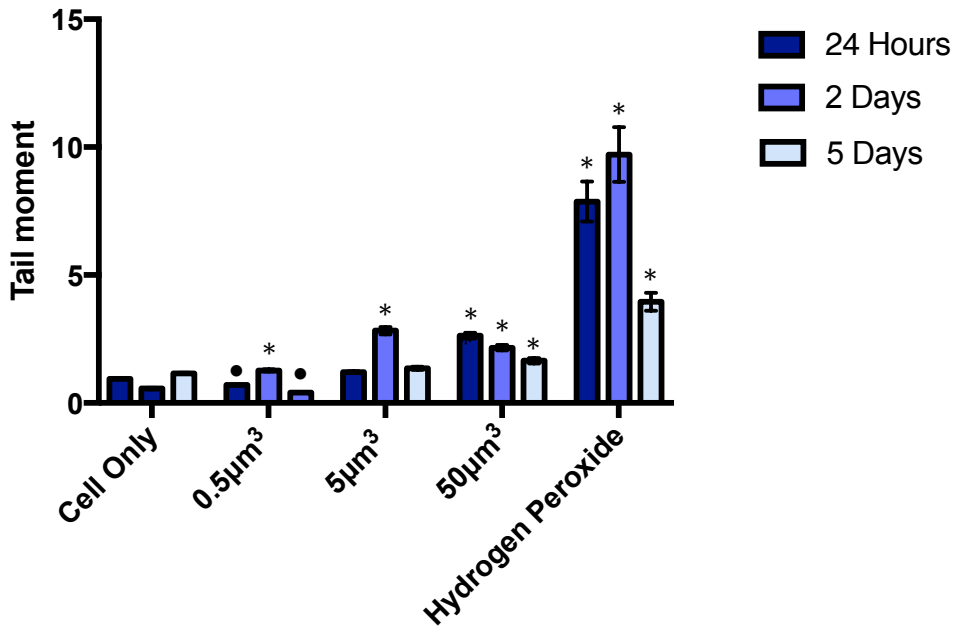

Figure 4.16 The effect of increasing cobalt chrome particle volumes on the integrity of primary astrocytes and microglia DNA after 24 hours, two and five days in culture, mean tail moment ± 95% confidence intervals (six replicates per condition). Hydrogen peroxide was used as a positive control. An asterisk indicates a significant increase in the level of DNA damage expressed as a value for tail moment ($p<0.05$) when compared with cell only negative control using a Two-way ANOVA. An • indicates a significant decrease in the level of DNA damage expressed as a value for tail moment ($p<0.05$) when compared with cell only negative control using a Two-way ANOVA.

When primary astrocytes and microglia were cultured with 5µm^3 cobalt chrome debris per cell, no significant DNA damage was observed after 24 hours in culture. After two days, this particle dose induced significantly greater levels of DNA damage when compared to the cell only negative control. At this time point a tail moment of 2.83 was recorded. This effect was no longer significant at the five-day time point (Figure 4.16).

The lowest cobalt chrome particle concentration of 0.5µm^3 cobalt chrome caused significant DNA damage after 48 hours in culture with a tail moment of 1.27 compared to a tail moment of 0.56 observed in the cell only gels. Interestingly after 24 hours and five days, the level of DNA damage of primary astrocytes and microglia was significantly lower at this dose, when compared to the cell only negative control (Figure 4.16). This was denoted by a • symbol in Figure 4.16

At all time points tested the hydrogen peroxide positive control caused significant DNA damage when compared to the cell only negative control. After 24 hours in culture a tail moment of 7.87 was recorded. This level of DNA damage increased further to 9.71 after two days, almost 20 times the level observed in the cell only control. At the five-day time point a tail moment of 3.95 was recorded.

4.4.2.2. The effect of cobalt chrome wear particles on the integrity of primary astrocyte DNA.

When primary astrocytes in isolation were cultured in a 2D monolayer system, low levels of DNA damage were observed throughout the duration of the investigation. The levels of DNA damage observed, expressed as a tail moment value, were 4.71, 1.74 and 1.99 after 24 hours, two days and five days, respectively (Figure 4.17).

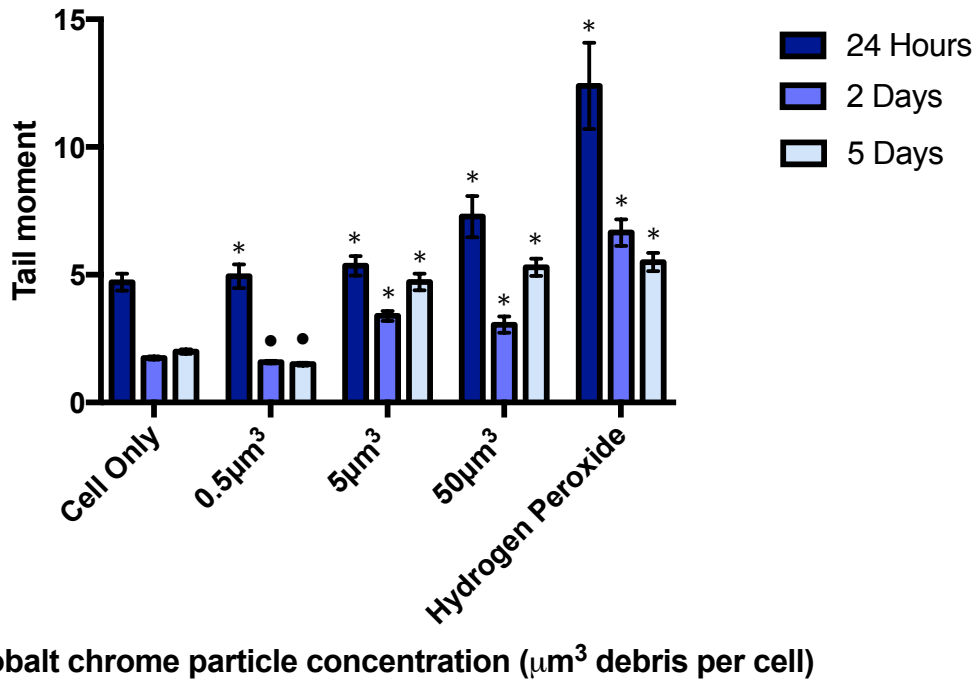

Figure 4.17 The effect of increasing cobalt chrome particle volumes on the integrity of primary astrocyte DNA after 24 hours, two and five days in culture, mean tail moment ± 95% confidence intervals (six replicates per condition). Hydrogen peroxide was used as a positive control. An * indicates a significant increase in level of DNA damage expressed as a value for tail moment ($p<0.05$) when compared with cell only negative control using a Two-way ANOVA. An • indicates a significant decrease in level of DNA damage expressed as a value for tail moment ($p<0.05$) when compared with cell only negative control using a Two-way ANOVA.

When primary astrocytes in isolation were cultured with the highest cobalt chrome particle concentration, 50μm^3 cobalt chrome debris per cell, significant increases in DNA damage, when compared to the cell only negative control, were observed at all three time points tested. The tail moments recorded were 7.28, 3.05 and 5.29 after 24 hours, two days and five days, respectively.

At all time points tested, 24 hours, two days and five days, the 5μm^3 cobalt chrome particle volume dose triggered significant levels of DNA damage. The levels of DNA damage recorded, expressed as a tail moment value, were 5.35, 3.39 and 4.72 after 24 hours, two days and five days, respectively (Figure 4.17).

When primary astrocytes in isolation were cultured with the lowest cobalt chrome particle concentration of 0.5μm^{3}cobalt chrome debris per cell a significant level of DNA damage was observed after 24 hours with a tail moment of 4.94. The level of DNA damage was not significantly greater than the cell only control at any other time point, in fact after 48 hours and five days the level of DNA damage with this particle dose was significantly lower than the cell only control.

The hydrogen peroxide positive control caused significant DNA damage for the duration of the investigation when compared to the cell only negative control. The tail moment values recorded after 24 hours, two days and five days were 12.40, 6.65 and 5.50, respectively.

A summary of the effects of increasing cobalt chrome particle volumes (0.5μm^3 -50μm^3 cobalt chrome debris per cell) on the integrity of primary astrocyte and microglia DNA can be seen in Table 4.4 below.

Table 4.4 The effects of increasing cobalt chrome particle concentrations on the integrity of primary astrocyte and microglia DNA. Cells with significantly increased levels of DNA damage $p<0.05$ (two-way ANOVA with Tukey post hoc analysis) compared to the cell only negative control were indicated with an *. An • Indicates a significant decrease in level of DNA damage expressed as a value for tail moment ($p<0.05$) when compared with cell only negative control using Two-way ANOVA.

	Astrocytes and microglia				Astrocytes in isolation			
	0.5µm³	5µm³	50µm³	H_2O_2	0.5µm³	5µm³	50µm³	H_2O_2
Day 1	•		*	*	*	*	*	*
Day 2	*	*	*	*	•	*	*	*
Day 5	•		*	*	•	*	*	*

4.4.2.3. The effect of stainless steel wear particles on the integrity of primary astrocyte and microglia DNA.

When primary astrocytes and microglia in co-culture were cultured using a 2D monolayer system, low levels of DNA damage were observed throughout the five-day investigation. The DNA damage expressed as a tail moment value, were 7.94, 1.85 and 1.0 after 24 hours, two days and five days, respectively (Figure 4.18).

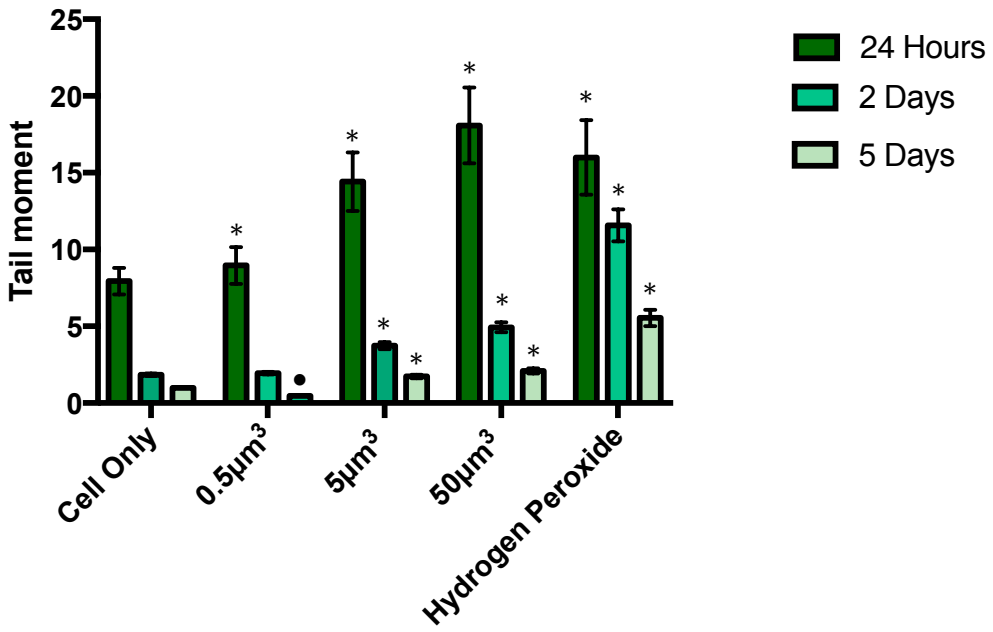

Figure 4.18 The effect of increasing stainless steel particle volumes on the integrity of primary astrocytes and microglia in co-culture DNA after 24 hours, two and five days in culture, mean tail moment ± 95% confidence intervals (six replicates per condition). Hydrogen peroxide was used as a positive control. An * indicates a significant increase in the level of DNA damage expressed as a value for tail moment ($p<0.05$) when compared with cell only negative control using Two-way ANOVA. An • indicates a significant decrease in level of DNA damage expressed as a value for tail moment ($p<0.05$) when compared with cell only negative control using Two-way ANOVA.

When primary astrocytes and microglia were cultured with the highest stainless steel particle concentration (50µm^3 stainless steel debris per cell) the level of DNA damage was significant when compared to the cell only negative control at all time points tested. After 24 hours in culture with the highest stainless steel particle volume the level of DNA damage, expressed as a tail moment value was 18.08. After two days the tail moment observed was 4.94. After five days the tail moment was 2.09.

The 5µm^3 stainless steel particle dose also triggered significant DNA damage in primary astrocytes and microglia at all time points tested. The level of DNA damage induced was recorded as a value of tail moment. The mean tail moments recorded after 24 hours, two days and five days were 14.42, 3.74 and 1.73, respectively.

The lowest stainless steel particle dose 0.5μm^3 stainless steel debris per cell induced significant levels of DNA damage after 24 hours in culture with a tail moment of 8.96 compared to the 7.94 tail moment of the cell only negative control. This effect was no longer significant after 48 hours and after 5 days the level of DNA damage was significantly lower than the cell only negative control.

When primary astrocytes and microglia were cultured with the hydrogen peroxide positive control, significant levels of DNA damage were detected at all time points. After 24 hours the level of DNA damage caused by the hydrogen peroxide, recorded as a tail moment value, was 15.99. At the two and five day time points tail moments of 11.57 and 5.55, respectively were recorded.

4.4.2.4. The effect of stainless steel wear particles on the integrity of primary astrocyte DNA.

When primary astrocytes in isolation were cultured in a 2D monolayer system, low levels of DNA damage were observed at all time points tested. The level of damage to primary astrocyte DNA, expressed as a tail moment value, was 11.57, 7.93 and 0.95 after 24 hours, two days and five days respectively (Figure 4.19).

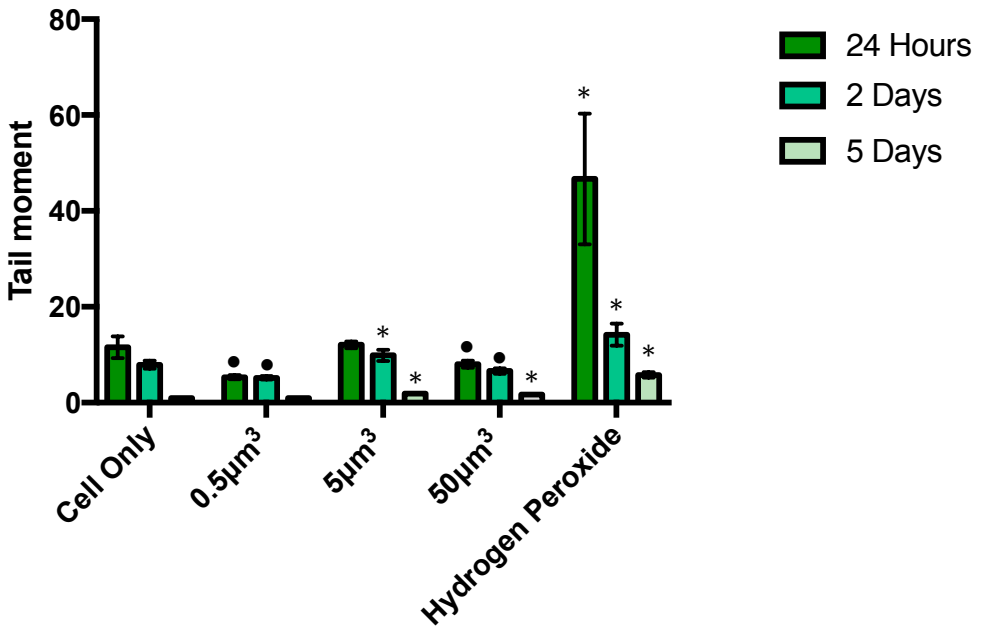

Figure 4.19 The effect of increasing stainless steel particle volumes on the integrity of primary astrocyte DNA after 24 hours, two and five days in culture, mean tail moment ± 95% confidence intervals (six replicates per condition). Hydrogen peroxide was used as a positive control. An * indicates a significant increase in DNA damage ($p<0.05$) when compared with cell only negative control using a Two-way ANOVA. An • indicates a significant decrease in level of DNA damage expressed as a value for tail moment ($p<0.05$) when compared with cell only negative control using a Two-way ANOVA.

When primary astrocytes in isolation were cultured with the highest stainless steel particle dose (50µm^3 stainless steel wear debris per cell) significant adverse effects on cellular DNA were observed after five days in culture only. After the five-day time point a tail moment of 1.69 was recorded. Interestingly after 24 hours and two days the level of DNA damage caused by this particle dose was significantly lower than the level of damage seen in the cell only control.

After 48 hours and five days, the mid particle volume of 5µm^3, induced significant levels of DNA damage in primary astrocytes in a 2D monolayer cell culture system. The level of DNA damage expressed as a tail moment value was 9.87 after two days and 1.93 after five days in culture with this particle dose.

Primary astrocytes in isolation did not exhibit significant increased levels of DNA damage when compared to the cell only negative control at any time point tested when cultured

with the lowest 0.5μm³ stainless steel debris per cell. Interestingly at the 24 hour and two-day time points, the levels of DNA damaged induced by this particle dose in primary astrocytes was significantly lower than the cell only negative control.

The hydrogen peroxide positive control induced significant levels of DNA damage at all three time points tested. After 24 hours the level of DNA damage caused by the hydrogen peroxide, recorded as a tail moment value was 46.69, approximately four times the level of damage seen in the cell only negative control. At the two-day and five-day time points tail moments of 14.19 and 5.79, respectively were recorded.

The effects of increasing stainless steel particle volumes (0.5μm³-50μm³) on the integrity of primary astrocyte and microglia DNA are summarised in Table 4.5 below.

Table 4.5 The effects of increasing stainless steel particle volumes on the integrity of primary astrocyte and microglia DNA. Cells with significantly increased levels of DNA damage $p<0.05$ (two-way ANOVA with Tukey post hoc analysis) compared to the cell only negative control were indicated with an *. An • indicates a significant decrease in level of DNA damage expressed as a value for tail moment ($p<0.05$) when compared with cell only negative control using Two-way ANOVA.

	Astrocytes and microglia				Astrocytes in isolation			
	0.5μm³	5μm³	50μm³	H_2O_2	0.5μm³	5μm³	50μm³	H_2O_2
Day 1	*	*	*	*	•		•	*
Day 2		*	*	*	•	*	•	*
Day 5	•	*	*	*		*	*	*

4.5 Discussion

The use of total disc replacements to reduce pain and instability associated with degenerative disc disease has been an instrumental intervention for the spinal surgeon. Motion preservation devices such as total disc replacements are increasingly being implanted into younger, more active patients with high subjective expectations regarding their postoperative performance (Siepe et al., 2007). Such intentions to return to previous activity levels poses a significant challenge to surgical techniques and implant design (Burnett, 2010). In the design of total hip replacements such high demands lead to the use of metal-on-metal hip prostheses for younger individuals. The use of metals, predominantly stainless steel and cobalt chrome for total disc replacements has raised substantial concerns regarding the long-term health implications and risks including; adverse reactions to metal debris and elevated levels of metal ions in blood and urine. Limited investigations have been performed to understand the adverse biological outcomes to intervertebral disc prostheses. With numerous instances of pseudotumors being developed in association with metal-on-metal total disc replacements (Cavanaugh et al., 2009; Berry et al., 2010; Guyer et al., 2011 Cabraja et al., 2012) and with evidence of metal nanoparticles breaching the dura mater in an organ culture model there is an overwhelming need to investigate the response of cells of the CNS to metallic wear products.

The aim of this study was to determine the effect of increasing particle volumes (0.05μm^3, 0.5μm^3, 5μm^3 and 50μm^3) of cobalt chrome and stainless steel (mode size 30-39nm for both cobalt chrome and stainless steel) on the viability of C6-glial, PC12-neuronal cell lines and primary astrocytes and microglia after 24 hours, three days and five days in 2D culture and the effects of 0.5μm^3, 5μm^3 and 50μm^3 cobalt chrome and stainless steel particles on the DNA integrity of primary astrocytes and microglia in co-culture and primary astrocytes in isolation after 24 hours, 48 hours and five days.

4.5.1. The effect of cobalt chrome and stainless steel wear particles on the viability of C6 glial, PC12 neuronal cell lines and primary astrocytes and microglia in co-culture using a 2D cell culture system.

When C6 glial cells were cultured with cobalt chrome wear particles significant adverse effects on cell viability were observed at all time points with all particle doses tested (0.05μm^3, 0.5μm^3, 5μm^3 and 50μm^3 cobalt chrome debris per cell). Similarly when the PC12 neuronal cell line was cultured with increasing particle volumes (0.05μm^3, 0.5μm^3, 5μm^3 and 50μm^3) of cobalt chrome wear particles significant adverse effects on PC12 cell

viability were observed after three and five days in culture with the 0.5μm^3, 5μm^3 and 50μm^3 cobalt chrome debris per cell particle doses. Interestingly, after 24 hours in culture the 0.5μm^3 and 50μm^3 cobalt chrome per cell had a significant beneficial effect on the viability of PC12 cells. When primary astrocytes and microglia in co-culture were cultured with cobalt chrome wear particles of increasing doses no adverse effects on cell viability were observed after 24 hours in culture with any dose tested. However, after three and five days in culture significant reductions in viability were observed with all particle doses (0.05μm^3, 0.5μm^3, 5μm^3 and 50μm^3).

When C6-glial cells were cultured with stainless steel wear particles, for the first three days in culture no adverse effects on cell viability were observed. After five days in culture adverse effects on C6 cell viability were reported when cultured with 0.05μm^3 stainless steel debris per cell. When PC12 cells were cultured with stainless steel for 24 hours a significant reduction in cell viability was observed with 0.5μm^3 stainless steel debris per cell. After five days in culture the highest stainless steel particle dose, 50μm^3 debris per cell, adversely affected the viability of PC12 neuron-like cells. Finally when primary astrocytes and microglia in co-culture were exposed to increasing particle volumes of stainless steel after just 24 hours in culture significant reductions in viability were observed with the 50μm^3, 5μm^3 and 0.5μm^3 particle doses, these adverse effects on viability did not persist for the duration of the investigation. After five days in culture, only the highest particle dose of 50μm^3 stainless steel debris per cell significantly reduced primary astrocyte and microglia cell viability. Interestingly, the stainless steel particles also had beneficial effects on the viability of the C6 and PC12 cells. Positive effects on the viability of C6 cells were observed at all time points when cultured with the highest particle dose of 50μm^3 stainless steel debris per cell. After three days in culture the 0.5μm^3 stainless steel per cell dose had a beneficial effect on C6 cell viability. After 24 hours and three days in culture the lowest particle dose 0.05μm^3 stainless steel debris per cell significantly increased the viability of C6 cells. Similarly, after three days in culture a significant increase in cell viability was observed when PC12 cells were cultured with 5μm^3 stainless steel debris per cell.

Interestingly when C6 glial cells were cultured with increasing doses of clinically relevant cobalt chrome wear particles, though significant adverse effects on cell viability were reported with all particle doses, a noteworthy pattern in the cellular response was observed. The highest particle dose (50μm^3 cobalt chrome debris per cell) reduced C6 viability by 65%, 97.5% and 98% after 24 hours, three days and five days, respectively

(when compared to the cell only negative control). However the adverse effect observed with the lower particle doses (0.05μm³ -5μm³ cobalt chrome debris per cell) was not dose dependent, in fact the inverse of this statement was true. The lowest particle dose (0.05μm³) appeared to have most prominent adverse effect on C6 glial cell viability when compared to the 0.5μm³ and 5μm³ dose, with the lowest counts per second reading being recorded for the 0.05μm³ particle dose (discounting the reading for highest particle dose, 50μm³). This observation remained true for all time points tested. The C6 glial cell line selected for this part of the study was representative of astrocytes. *In vivo* when the CNS becomes damaged as a result of injury, infection, ischemia or as part of an autoimmune response a process referred to as astrogliosis ensues. Here astrocytes become reactive and rapidly proliferate in response to stressful stimuli and a series of morphological and molecular expression profile alterations within these cells is triggered. In this instance at the lower particle doses (0.05μm³, 0.5μm³ and 5μm³ cobalt chrome debris per cell), rapid cellular proliferation may have been responsible for the elevated ATP level observed with the 5μm³ compared to the 0.5μm³ particle dose, therefore a dose dependent astrocyte reactivity response may be a possible explanation for this unusual observation. The protein GFAP is up-regulated in the process of astrogliosis however due to this cells inability to express this marker at detectable levels this could not have been investigated to determine whether or not this process was occurring. By coupling the ATP lite™ assay with a cellular proliferation assay such as CytoTrack™, flow cytometry (using BrdU to detect proliferating cells) or a live dead assay more information could have been provided to further understand this effect. Without the support of an additional assay the possibility that stimulatory effect on proliferation by cobalt chrome particles could not be eliminated.

Although, throughout this part of the study there may have been statistically significant increases or decreases in cell viability when compared to the cell only negative control, the cobalt chrome and stainless steel particle volumes were considered to have a significant effect on cell viability when a consistent decrease in ATP emerged over the five day period (evidenced by a continuous decline in counts per second readings). Isolated changes in cell viability relative to the cell only negative control even when significant could not be considered truly meaningful. An example of this phenomenon can be seen when the C6 glial cell line was cultured with 5μm³ cobalt chrome debris per cell. At all three time points tested the average counts per second reading was significantly lower than that of the cell only control, however over the five day time period the counts per second reading

continuously increased. A possible explanation for this result may be that the cells are not actually dying but are simply dividing at a lower rate.

There are numerous methodologies reported in the literature to quantitatively assess cell viability, most assays involve the addition of a dye which is either; included, excluded or converted (normally via an enzymatic process) within living cells and quantified colorimetrically or fluorescently (Jones & Grainger, 2009). These assays include; MTT (De Guzman & VandeVord, 2007; Papageorgiou et al., 2007; Papageorgiou et al., 2008; Li et al., 2014; Posada et al., 2014; Kaja et al., 2015), XTT (Vetten et al., 2013), MTS (Chueh et al., 2014), ATP-Lite™, (Germain et al., 2003; Behl et al., 2013; Liu et al., 2015), LDH (Allen et al., 1997; Papageorgiou et al., 2007), fluorescein diacetate (Sruthi & Mohanan, 2015), propidium iodide (Radzium et al., 2011), live dead (De Guzman & VandeVord, 2007), trypan blue (Tsaousi et al., 2010) and alamar blue (Bonnier et al., 2015). The most commonly used cytotoxicity assay is the MTT assay (Nogueira et al., 2014). For this part of the study the ATP lite™ assay was used to quantitatively determine the effect of increasing doses of cobalt chrome and stainless steel wear particles on C6, PC12 and primary astrocyte and microglia cell viability. The principle for this assay is outlined in Chapter 2, section 2.4.2. The ATP Lite™ assay is more sensitive than the MTT assay with a detection limit of 5 cells in 100µl medium, which was more appropriate for this part of the study. There have been reports in the literature where nano-particles have interfered with the readings for MTT, by reducing MTT to formazan in the particle only control; hence the ATP Lite™ assay was preferable (Fisichella et al., 2009).

Attempts were made to utilise the MTT assay for this part of the study, however the detection limit of this assay is $1x10^4$ cells, below this quantity the MTT is no longer efficient in detecting subtle differences in cell number. Due to significant reductions in viability when C6, PC12 and primary astrocyte and microglia cells were cultured with cobalt chrome and stainless steel wear particles, this assay could not be utilised reliably.

For this part of the study camptothecin was used as a positive control, as it is a known inducer of apoptosis. There have been numerous reports in the literature of the use of camptothecin for this purpose (Germain et al., 2003; Williams et al., 2004; De Guzman & VandeVord, 2007; Behl et al., 2013; Suner et al., 2014). Morris & Geller. (1996) found camptothecin to inhibit the activity of the enzyme topoisomerase I. The function of the topoisomerase enzyme is to relax DNA supercoiling during DNA transcription and replication. Camptothecin binds to the topoisomerase I-DNA complex and causes a single strand break in the DNA. Attempts made by the cell to enter the S phase of the cell cycle

fail leading to a late S phase-G2 arrest and subsequently trigger apoptosis (Morris & Geller, 1996). It is thought that the cytotoxic effect of metallic wear particles and their subsequent ions is due to apoptosis as opposed to necrosis (Rana & Vir, 2008) as a result camptothecin was selected as an appropriate positive control for this part of the study.

Using 2D monolayer *in vitro* cell culture investigations cobalt chrome has been found to be toxic to numerous cell types; U937 macrophages, L929 fibroblasts, porcine dural epithelial cells, porcine dural fibroblasts, human fibroblasts and C2C12 myotubes; (Germain et al., 2003; Williams et al., 2003; Papageorgiou; 2007; Tsaousi et al., 2010; Behl et al., 2013; Rovetta et al., 2013; Posada et al., 2014). Williams et al. (2003) found that 50μm^3, 5μm^3 and 0.5μm^3 cobalt chrome debris per cell were sufficient particle volumes to trigger significant reductions in U937 cell viability after four days in culture. However, L929 fibroblasts were less sensitive and only the highest cobalt chrome particle dose tested, 50μm^3, caused significant cytotoxic effects with this cell type. These results were similar to the findings presented by Germain et al. (2003) who found nanoscale (5nm-200nm) cobalt chrome particles triggered a significant reduction in the viability of U937 macrophages and L929 fibroblasts when both cell types were cultured with 50μm^3 and 5μm^3 cobalt chrome debris per cell. An adverse effect on viability was reported after two days in culture with the U937 cells and persisted for the duration of the investigation, whereas the significant reduction in viability of L929 was detected earlier after just 24 hours in culture and persisted for the duration of the investigation. Similarly, Posada et al. (2014) reported that the viability of U937 macrophages was significantly reduced by 5mg cobalt chrome debris after five days in culture. The findings of the study conducted by Williams et al. (2003) were comparable to the results presented here as part of this study with similar particle doses causing cell death. Interestingly, C6 cells and primary astrocytes and microglia appear to be more sensitive than macrophages as an even lower dose of 0.05μm^3 stimulated significant reductions in viability with these cell types. It is important to note that the particles utilised by Germain et al. (2003) Williams et al. (2003) and Posada et al. (2014) were generated by articulation and thus were clinically relevant in terms of size and morphology.

Behl et al. (2013) found that nanoscale cobalt chrome wear particles caused a significant reduction in the viability of porcine dural epithelial cells after 24 hours when these cells were cultured with 6.05μm^3, 60.5μm^3 and 121μm^3 cobalt chrome debris per cell. This adverse effect on viability persisted until the final time point of four days in culture. Interestingly no adverse effect on porcine dural fibroblasts was reported with any particle

dose at any time point tested. Once again these findings are comparable to the particle doses that were toxic to C6, PC12 and primary astrocytes and microglia presented here. Papageorgiou et al. (2007) reported that nanoscale cobalt chrome particles had a dose dependent and progressive adverse effect on the viability of human fibroblasts over a five day culture period. The highest cobalt chrome particle dose 50μm^3 cobalt chrome debris per cell triggered a significant reduction in human fibroblast viability when compared to the cell only negative control after just 24 hours in culture. The 5μm^3 particle dose caused a significant reduction in viability after three days in culture and this adverse effect persisted to the end of the investigation. Finally the 0.5μm^3 particle dose caused a significant adverse effect on viability after five days in culture.

Though there is a paucity of literature regarding the use of C6 and PC12 cell lines to investigate the toxicity of wear particles from orthopaedic biomaterials, De Guzman & VandeVord, (2007) used the C6 cell line as a model astrocyte cell type to determine the neurotoxicity of numerous biomaterials used in the orthopaedic industry e.g. titanium, UHMWPE, cobalt chromium and PMMA, at increasing particle doses, 0$mg.ml^{-1}$, 0.3125$mg.ml^{-1}$, 0.625$mg.ml^{-1}$, 1.25$mg.ml^{-1}$, 2.5$mg.ml^{-1}$ 5$mg.ml^{-1}$ and measured their effect on viability using an MTT assay and a live dead stain. Similarly to the results presented here, De Guzman & VandeVord. (2007) observed significant reductions in viability when C6 cells were cultured with cobalt chrome wear particles after 48 hours with 2.5$mg.ml^{-1}$ and 5$mg.ml^{-1}$ particle doses. Interestingly, these authors also observed an increase in proliferation of C6 cells when cultured with lower doses of cobalt chrome particles; 0.3125$mg.ml^{-1}$ and 0.625$mg.ml^{-1}$ after 48 hours in culture. However, the particles utilised in the study conducted by De Guzman & VandeVord. (2007) were approximately 100 times larger than would be observed *in vivo* from total disc replacements, with cobalt chrome particles with an average size of 5.7μm tested (range of 1μm -20μm) and the particle doses were not clinically relevant, when considering the wear rates on metal-on-metal total disc replacements reported in the literature. The particles used in this part of the study (30nm-39nm in length) had a more severe adverse effect on viability, with significant adverse effects on viability observed with all doses, 0.05μm^3, 0.5μm^3, 5μm^3 and 50μm^3, at all time points, 24 hours, three days and five days, when compared to the findings of De Guzman & VandeVord. (2007).

Though there is limited information in the literature regarding the effect of stainless steel wear products on cell viability, a small number of studies have been performed to determine the effect of bulk and particulate stainless steel on RAW macrophage and

MC3T3 mouse osteoblast cells. Bailey at al. (2005) observed a reduction in the viability of RAW macrophages when cultured with 316L stainless steel particles 1-100μm in size after 24 hours in culture. The particle dose of stainless steel particles was not reported for this particular investigation and the effect on cell viability only qualitatively measured using a live dead stain. Conversely, Li et al. (2014) did not report any adverse effects on viability when MC3T3 mouse osteoblast cells were cultured with bulk 316L stainless steel. This is similar to the results reported here in this part of the study, where C6 glial cells were not adversely affected by stainless steel wear particles, and PC12 neuronal cells and primary astrocytes and microglia were only adversely affected by the highest particle dose, 50μm^3 stainless steel debris per cell.

This part of the study revealed that there were clear differences in the cellular responses to nanoscale cobalt chrome and stainless steel wear particles. It is well documented that these two orthopaedic biomaterials have very different elemental compositions, (Chapter 2, section 3.2). Medical grade 316L stainless steel has 16-18% chromium content, whereas high carbon cobalt chrome molybdenum has a 27-30% chromium content. Furthermore cobalt chrome molybdenum is composed of ~60% cobalt, whereas cobalt is not present in medical grade 316L stainless steel. Cobalt ions have been found to induce more cytotoxic effects than chromium (Sansone et al., 2013; Kanaji et al., 2014). Chromium exerts a more genotoxic effect on cells this may explain the different effects on cell viability seen with the two biomaterials. Within the literature the effects of cobalt and chromium ions on cell viability and genotoxicity have focused on osteoblasts and macrophages, there is limited literature on the effects on CNS cells.

Within the literature it has been found that metallic particles 200nm or smaller, with a preference for 50nm metal particles which are taken up into cells faster and more extensively than smaller (≥ 14nm) and larger (≤ 500nm) particles (Chithrani et al., 2006; Gratton et al., 2008; Billi & Campbell, 2010). With a greater proportion of cobalt chrome particles (55.5%) being less than 50nm compared to stainless steel particles (30.7%) this may also account for the differing biological response observed between the two biomaterials.

In addition to causing adverse effects on cell viability, orthopaedic metals including cobalt chrome are considered complex genotoxins (Papageorgiou et al., 2007). Hexavalent chromium (Cr VI) is known to cause single and double strand DNA breaks as well as DNA cross -links (O'Brien et al., 2003; Ha et al., 2004; Depault et al., 2006). Trivalent chromium is also a genotoxic intermediate and can cause cellular apoptosis. Cobalt is also a known

toxin to cells and can produce reactive oxygen species (Kopera et al., 2004) and acts as a poison to topoisomerase II (Baldwin et al., 2004)

4.5.2.The effect of cobalt chrome and stainless steel wear particles on the DNA integrity of primary astrocytes and microglia in co-culture and primary astrocytes in isolation.

For this part of the study hydrogen peroxide (100μM) was used as the positive control. Hydrogen peroxide has been used previously as a known inducer of single and double strand DNA breaks (Nakamura et al., 2003; Daroui et al., 2004; Driessens et al., 2009). In the Fenton reaction, ferrous iron reduces hydrogen peroxide to reactive free radicals, which are known to cause DNA strand breaks.

When primary astrocytes and microglia in co-culture were exposed to increasing particle volumes of cobalt chrome debris (0.5μm^3 to 50μm^3 cobalt chrome debris per cell) after 24 hours the highest particle dose only (50μm^3 cobalt chrome debris per cell) triggered significant levels of DNA damage in primary astrocytes and microglia. After five days in culture once again only the highest particle dose 50μm^3 cobalt chrome debris per cell caused significant DNA damage when compared to the cell only negative control. When primary astrocytes in isolation were cultured with increasing particle doses of cobalt chrome debris, all particle doses triggered significant levels of DNA damage after 24 hours in culture when compared to the cell only negative control. After two and five days in culture; the 50μm^3 and 5μm^3 particle doses of cobalt chrome only caused significant DNA damage in primary astrocytes when compared to the cell only negative control. Primary astrocytes cultured with the lowest particle dose (0.5μm^3 debris per cell) exhibited significantly less DNA damage after two and five days in culture.

When primary astrocytes and microglia in co-culture were exposed to increasing particle volumes of stainless steel debris (0.5μm^3 to 50μm^3 debris per cell) after 24 hours culture all particle doses triggered significant levels of DNA damage when compared to the cell only negative control. Similar levels of DNA damage were also observed after two and five days in culture however the lowest particle dose 0.5μm^3 stainless steel debris per cell no longer cause significant DNA damage when compared to the cell only negative control. Dissimilarly after five days in culture the lowest stainless steel particle dose caused significantly less DNA damage when compared to the cell only negative control. When primary astrocytes in isolation were cultured with increasing particle doses of stainless steel debris, after 24 hours in culture no significant DNA damage was observed when

compared to the cell only negative control. After two days in culture the mid, 5μm^3 particle dose triggered significant DNA damage. Finally after five days in culture; the 50μm^3 and 5μm^3 particle doses of stainless steel caused significant DNA damage in primary astrocytes when compared to the cell only negative control.

Unlike the results presented in this part of the study, Gajski et al in 2014 investigated the *in vitro* genotoxicity of medical implant materials; titanium, cobalt chrome and UHMWPE in human lymphocytes. Human lymphocytes were cultured with 10μg.ml^{-1} (particles were <10μm in size and generated by milling) for 24 hours and the effect on DNA integrity assessed using an alkaline comet assay. In this investigation no significant DNA damage was observed with any biomaterial tested.

Papageorgiou et al in 2007, cultured human fibroblasts with increasing particle doses (0.005μm^3-5000μm^3 debris per cell) of nano-scale, 29.5nm and micron, 2.904μm, sized cobalt chrome particles for five days in culture. Papageorgiou found that the nanoparticles caused statistically more DNA damage than the micron-sized particles in primary human fibroblasts after 24 hours. After 24 hours all particle doses of nano-scale cobalt chrome triggered significant DNA damage in human fibroblasts, this adverse effect deceased with time as after three days in culture only the 0.005μm^3, 0.5μm^3 and 50μm^3 cobalt chrome particle doses caused significant DNA damage. These findings were comparable to the results presented in this part of the study. The results presented by Papageorgiou highlighted the role of particle size on the induction of DNA damage with micron-sized particles causing significantly less DNA damage.

Similarly Parry et al in 2010 investigated the effect of increasing particle doses of cobalt chrome 0.00018mg/cm^2, 0.00036 mg/cm^2, 0.0036 mg/cm^2 and 0.036 mg/cm^2 on the integrity of human fibroblast DNA after 24 hours in culture using the alkaline comet assay. Parry found that all doses triggered significant DNA damage after just 24 hours in culture. The particle doses tested by Parry et al were similar to the doses utilised in this part of the study and the same adverse effect observed.

Finally Tsaousi et al in 2010 determined the genotoxic effects of cobalt chrome on primary human fibroblasts. Cobalt chrome of increasing particle volumes,1-10mg/T-75 flask were cultured with primary human fibroblasts for five days and the effect on DNA damage assessed using the micronucleus assay. After 24 hours in culture significant increases in micronucleated bionucleated cells were observed in a clear dose dependent manner.

Tsaousi et al. (2010) observed that the 1 mg/T-75,2 mg/T-75 and 5 mg/T-75 particle doses caused significant DNA damage after 24 hours in culture.

Interestingly similar levels of DNA were observed in this part of the study with both cellular conditions and both biomaterials tested. Intriguingly when primary astrocytes and microglia in co-culture and primary astrocytes in isolation were cultured with stainless steel wear particles of increasing particle volume significant DNA damage was observed but this did not translate to cell death.

As mentioned previously, PC12 neuronal and C6 glial cell lines have been used in the literature as model CNS cells (Grobben et al., 2002; Assis et al., 2014; Slokin et al., 2014; Tang et al., 2015) though there are numerous advantages for the use of immortalised cell lines such as; unlimited supply of pure cells providing a consistent sample and yields reproducible results, they are easier to maintain than primary cells, cost effective, bypass ethical concerns regarding the use of animals or human tissue. Cell lines should fundamentally express and maintain functional features as closely to primary cells as is possible to achieve. Due to the fact that cell lines have been genetically manipulated their phenotype, response to stimuli and characteristic functions may be altered. Also repeated passaging of cells may alter cell line phenotype over time resulting in heterogeneity of cultures (Kaur & Dufour, 2012). Though the cell lines were important in preliminary investigations as a means of determining lethal and sub-lethal particle doses of both cobalt chrome and stainless steel wear particles it was imperative to move forward and use more physiologically relevant primary rat astrocytes and microglia.

However, when primary cells are isolated from tissue and cultured in 2D phenotypic changes have been observed. The cell shape becomes flatter, and their division rate alters (Bonnier et al., 2015). In simplistic 2D monolayer culture astrocytes adopt a reactive phenotype, which is characterised by an up-regulation of glial fibrillary acidic protein. In 3D culture, astrocytes do not present this phenotype unless stimulated to do so, highlighting the superior control over the environment in 3D culture, (East & Phillips, 2008). The wider aims of the study were to determine the biological response of CNS cells in terms of cellular reactivity, DNA damage and cytokine release. As primary astrocytes already adopt a reactive phenotype in 2D culture, it would be difficult to discern whether or not the cellular response of primary astrocytes and microglia in co-culture, and primary astrocytes in isolation, to metallic wear particles was due to the particle doses they were challenged with or just a consequence of the culture environment they were in. Thus, moving forward, a 3D culture system was deemed to be critical.

When culturing primary astrocytes and microglia and primary astrocytes in isolation in 3D culture a greater cell seeding density is required, which increases the number of particles required in each experiment. So as to minimise wastage of particles and reduce the number of primary cells utilised only three of the four particle doses (0.5μm^3, 5μm^3 and 50μm^3 debris per cell) used in this part of the study and shown to exert adverse effects of the C6 glial, PC12 neuronal and primary cells and were taken forward into 3D culture.

4.5.3 Key findings

- In 2D culture cobalt chrome and stainless steel wear particles had differing effects on the viability of C6 glial, PC12 neuronal cells and primary astrocytes and microglia. Cobalt chrome wear particles adversely affected the viability of C6 glial cells at all particle doses and all time points tested whereas cobalt chrome particles (the 0.5μm^3, 5μm^3 and 50μm^3 particle per cell doses) only adversely affected PC12 and primary astrocyte and microglia viability after three and five days in culture.
- Stainless steel wear particles only caused significant adverse effects on the viability of C6 glial and PC12 neuronal cells after five days (0.05μm^3 debris per cell) in culture and one (0.5μm^3 debris per cell) and five days (50μm^3 debris per cell) in culture respectively, interestingly, stainless steel particles caused significant adverse effects on primary astrocyte and microglia viability after just 24 hours in culture (the 0.5μm^3, 5μm^3 and 50μm^3 particle per cell doses) and after five days in culture with the highest particle dose (50μm^3 debris per cell).
- Significant levels of DNA damage were observed when primary astrocytes and microglia in co-culture were cultured with the highest cobalt chrome particle dose (50μm^3 debris per cell) at all time points tested. The mid 5μm^3 cobalt chrome debris per cell dose only caused significant DNA damage after 48 hours in culture. The highest (50μm^3 debris per cell) and mid (5μm^3 debris per cell) particle doses caused significantly high levels of DNA damage in primary astrocytes in isolation at all time points tested. The lowest particle dose (0.5μm^3 debris per cell) triggered significant DNA damage after just 24 hours in culture but this effect did not last for the duration of the investigation.
- Significant levels of DNA damage were observed when primary astrocytes and microglia were cultured with the highest and mid stainless particle doses (50μm^3 debris per cell and 5μm^3 debris per cell respectively) at all time points tested. The lowest stainless steel particle dose, 0.5μm^3, caused significant levels of DNA

damage after just 24 hours in culture. DNA damage was induced in primary astrocytes in isolation after 48 hours in culture with 5μm^3 stainless steel debris per cell and when cultured with 50μm^3 and 5μm^3 stainless steel debris per cell after five days in culture.

- The differences in cellular response to the two biomaterials may be attributed to the differing elemental compositions.

Chapter 5

The Biological Effects of Cobalt Chrome and Stainless Steel Wear Particles on Primary Astrocytes and Microglia in Co-Culture and Primary Astrocytes in Isolation in a 3D Cell Culture System.

5.1 Introduction

Metallic wear particles generated in total disc replacements have the potential to interact with, and alter the structural integrity of the dura mater by disrupting the underlying collagen matrix (Papageorgiou et al., 2014). Such alterations in the barrier function of the meninges have the potential to pose significant clinical problems, as evidenced by increasing cases of adverse soft tissue reactions to wear products being reported within the literature (Cavanaugh et al., 2009; Berry et al., 2010; Guyer et al., 2011; Cabraja et al., 2012). A limited number of studies have been performed to investigate how clinically relevant cobalt chrome and stainless steel wear particles interact with cells of the central nervous system (Mohanty et al., 2003; De Guzman & VandeVord, 2007).

There are certain criteria, which should be considered when designing an *in vitro* model to investigate the biological response of CNS cells to metallic wear products from total disc replacements. The particles utilised must be clinically relevant in terms of size, shape and chemical composition. The particle volumes the cells are subjected to should be physiologically relevant and not be in excess of what is possible within the *in vivo* environment. The cell type selected should be physiologically relevant and behave in a manner that is representative of the response experienced upon stimulation *in vivo.* Finally, it is of paramount importance that cells are cultured in a spatial arrangement that is, as close as possible, reflective of the *in vivo* environment.

The use of model CNS cells; C6 glial and PC2 neuronal enabled a preliminary investigation into the effect of clinically relevant metallic wear particles on CNS cell viability, however due to an inability to express key markers of cellular reactivity at detectable levels without prior stimulation, specifically glial fibrillary acidic protein, more applicable rat primary astrocytes and microglia were utilised for this part of the study.

The spinal cord is comprised of numerous different cell types including neurons and neuroglia; whose primary role is in the protection of neurons. The CNS possesses four different types of neuroglia; astrocytes, oligodendrocytes, microglia and ependymal cells. This study focused on the effects of cobalt chrome and stainless steel wear particles on

the viability, cellular reactivity and cytokine production of primary astrocytes and microglia in co-culture and astrocytes in isolation. Astrocytes are star-shaped glial cells and possess extensions or processes**.** Astrocytes are the predominant cell type involved in the formation of a glial scar following trauma, injury, inflammation, autoimmune responses or ischemia. Microglia are the least numerate and smallest neuroglia of the CNS and are referred to as the resident macrophages of the brain and the spinal cord, continually scavenging the CNS for infectious agents, plaques and damaged neurons. Under normal conditions in the brain and spinal cord these cells appear to be inactive. Upon activation by an infectious agent, these cells rapidly proliferate to mount a response to the potential harmful agent. These cells are extremely sensitive to brain and spinal cord homeostasis (Gehrmann et al., 1995). As the resident macrophage of the CNS it was important to investigate the biological response of this cell type to metallic wear particles.

The culture of primary astrocytes and microglia from P2 rat cortices yields a high proportion of astrocytes in comparison to microglia (85% astrocytes to 15% microglia). Though the cellular physiologies, functions and responses of astrocytes and microglia upon activation are profoundly different, microglia can perform cellular functions that astrocytes cannot and minimal numbers of microglia can occasionally be responsible for the effects observed in cultures where astrocytes are the dominant cell type (Saura, 2007). If the involvement of both astrocytes and microglia in co-culture and astrocytes in isolation are not investigated separately the effects of particles, toxins or external stimuli can be erroneously attributed to the predominant astrocyte cell type. Thus for this part of the study it was important to investigate the effects of cobalt chrome and stainless steel wear particles on astrocytes and microglia in co-culture and astrocytes in isolation.

Much of the current understanding regarding the biological response to cobalt chrome and stainless steel wear particles has utilised cell lines or primary cells cultured in a simplistic 2D monolayer environment. This some-what primitive method of culture is not representative of the *in vivo* environment, where cells are arranged in much more complex matrices.

Additionally *In vivo* multiple cell types are capable of interaction with one-another and with the extracellular matrix itself. This is not accurately mimicked by monolayer culture (Haycock et al., 2011). Primarily, the goal of 3D cell culture is to bridge the gap between monolayer culture and complex animal models. A simple starting point in recreating a growth environment, which closely models that of the native tissue is the culture of cells in a porous biocompatible scaffold. The decision to move from 2D culture to a more

complex 3D culture environment required careful consideration of cell adhesion, interaction, proliferation and waste removal.

In vivo, in the undamaged CNS astrocytes express low levels of glial fibrillary acidic protein (GFAP) (Cancilla et al., 1992; East et al., 2009). However following injury or inflammation they demonstrate a reactive hypertrophic phenotype evidenced by an up-regulation of GFAP, vimentin and chondroitin sulphate proteoglycans (Calvo et al., 1991; Silver & Miller, 2004). Difficulties may arise when primary astrocytes are cultured on stiff matrices, as they are in 2D culture. Here the primary astrocytes exhibit a reactive, ramified phenotype. As a result of this phenomenon any cellular reactivity observed could incorrectly be regarded as a response to variations in experimental parameters and not simply a product of the spatial environment the cells are cultured in. Within 3D culture, type I collagen gels, primary astrocytes possess a rounded, unreactive morphology resembling their morphology in the physiological environment, which would be much more appropriate for this application whereby the effect of metallic wear particles on cellular reactivity was to be investigated.

Type I collagen, has been used extensively for the culture of cells in a 3D environment for a wide range of applications especially in the fields of; tissue engineering, drug delivery (Obarzanek-Fojt et al., 2016), toxicology and spinal cord injury repair (Han et al., 2010; Macaya et al., 2013; Altinova et al., 2014). This material is capable of supporting numerous cell types and is highly adaptable to mimic *in vivo* conditions. In recent years collagen gels have been used to enable cells of the CNS such as neurons and glial cells; astrocytes, microglia and oligodendrocytes to interact and behave as they would *in vivo* by creating an environment similar to that of the CNS (East et al., 2009).

5.1.2. Aims

There is a paucity of literature regarding the effect of wear products from biomaterials utilised in the orthopaedic industry on the viability of cells of the CNS in 3D culture thus it was the aim of this part of the study to investigate the effect of cobalt chrome and stainless steel wear particles (and ions) on the viability of primary astrocytes and microglia in co-culture and primary astrocytes in isolation and to determine whether or not the effects of the metallic particles on viability are different between 2D and 3D culture systems. Though it is important to understand the effect of lethal doses these materials on cell viability it is also key to understand some of the sub-lethal effects. Therefore the effect of cobalt chrome and stainless steel particles on cellular activation and cytokine release were also studied using a physiologically relevant 3D collagen gel

cell culture system. An up-regulation in the expression of GFAP was selected as a marker of astrocyte reactivity and assessed using immunocytochemistry. The effect of metallic wear products on the release of TNF-α was established using an enzyme linked immunosorbent assay.

5.2. Materials

Materials used in addition to those stated previously in Chapter 2, section 2.1 include the reagents and antibodies detailed in Table 5.1 and 5.2 respectively.

Table 5.1. Assay kits used to determine the effect of cobalt chrome and stainless steel particles on cell viability and cytokine release.

Material	Supplier
Live dead® cytotoxicity kit for mammalian cells. Calcein AM and Ethidium homodimer-1	ThermoFisher Scientific. Massachusetts, USA.
Rat TNF-α sandwich ELISA kit	2B Scientific, Oxfordshire UK.

Table 5.2 Antibodies and stains used to determine the effect of cobalt chrome and stainless steel on primary astrocyte cellular reactivity.

Antibody	Primary antibody dilution	Secondary antibody dilution	Secondary antibody
Glial fibrillary acidic protein (GFAP)	1:300	1:300	DyLight® 549 Anti-rabbit IgG
Hoescht 33258	1:1000		-

5.3 Methods

The aspects of the biological response that were investigated as part of this study were; cell viability (response to metallic particles and ions), cellular reactivity and TNF-α cytokine release. A live dead assay was used to determine the effect of cobalt chrome and stainless steel wear particles on cell viability, immunocytochemistry to determine the effects of metallic particles on cellular reactivity and an enzyme linked immunosorbent assay used to determine the effects on TNF-α release.

5.3.1. Cell viability assays

A live dead assay was used to determine the effects of cobalt chromium and stainless steel wear particles on the viability of primary astrocytes and microglia in co-culture and primary astrocytes in isolation.

5.3.1.1.The effects of cobalt chrome and stainless steel debris on cell viability in an advanced 3D cell culture system using a live dead assay.

The live dead assay comprised two fluorescent dyes; ethidium homodimer-1 and calciein AM. The calcien fluorescent dye stained living cells green and the ethidium homodimer-1 stained dead cells red. Primary astrocytes and microglia were isolated and cultured in co-culture and astrocytes in isolation in accordance with the protocol outlined previously in Chapter 2, section 2.4.1.6.

Primary astrocytes and microglia in co-culture and primary astrocytes in isolation were seeded into collagen gels at a seeding density of 1 x 10^5 cells per 100μl gel and cultured with all doses of stainless steel or cobalt chromium particles (0.5μm^3 - 50μm^3 debris per cell, 6 repeats per condition) for 48 hours and five days at 37°C in 5% (v/v) CO_2 in air. A volume of 100μl DMSO was used as a positive control to induce cell death.

After the appropriate incubation period with cobalt chrome or stainless steel wear debris, a live dead assay was performed. The assay was performed in accordance with the protocol outlined in Chapter 2, section 2.4.2.2. The gels were imaged immediately after the live dead assay was performed using a Zeiss Olympus upright microscope at x 10 magnification using the calcein and ethidium homodimer pre-set filters (617nm and 514nm emission wavelengths, respectively). A total of six images were taken for each gel, and with six gels per test condition, a total of 36 images were captured for each test condition. The number of living (green) and dead (red) cells was totalled for each image using image J and the cell counter analysis tool within the software and a percentage of

living cells recorded. A mean percentage of living cells was calculated for each condition by calculating a mean of all 36 images. A two-way ANOVA and Tukey post-hoc analysis was used to determine whether the effects of the particles on cell viability were significant when compared to the cell only negative control.

5.3.1.2 Image acquisition protocol.

A precise, well defined, protocol was developed to image each collagen gel after the appropriate incubation period with the live dead fluorescent dyes to determine the effect that the cobalt chrome and stainless steel wear particles had on the viability of primary astrocytes and microglia in co-culture and primary astrocytes in isolation. This protocol was specifically designed to avoid areas of the gel where the primary astrocytes would demonstrate a reactive phenotype in response to tissue culture plastic so as to avoid false positive results. The areas of the gel that were not imaged included the edge of the gel where the cells would be in contact with tissue culture plastic and the surface of the gel. Upon setting, the gels naturally formed a meniscus, the tension in this area leads to cellular reactivity and therefore this area was omitted from analysis.

After performing the live dead assay at the appropriate time point (after two days and five days in culture) the collagen gels were imaged using a Zeiss upright microscope. For each experiment the same settings were selected on the microscope.

For all images the x 10 objective lens was used to view the gels. Initially the gel was positioned so the objective lens was aligned directly over the centre of the gel. By adjusting the Z plane and noting where the cells moved in and out of focus, the top and bottom of the gel was located and the co-ordinates noted. These reference points were utilised to find the centre of the gel and an image taken at this point (acquisition of image one). Further images were taken around this central point (see Figure 5.1).

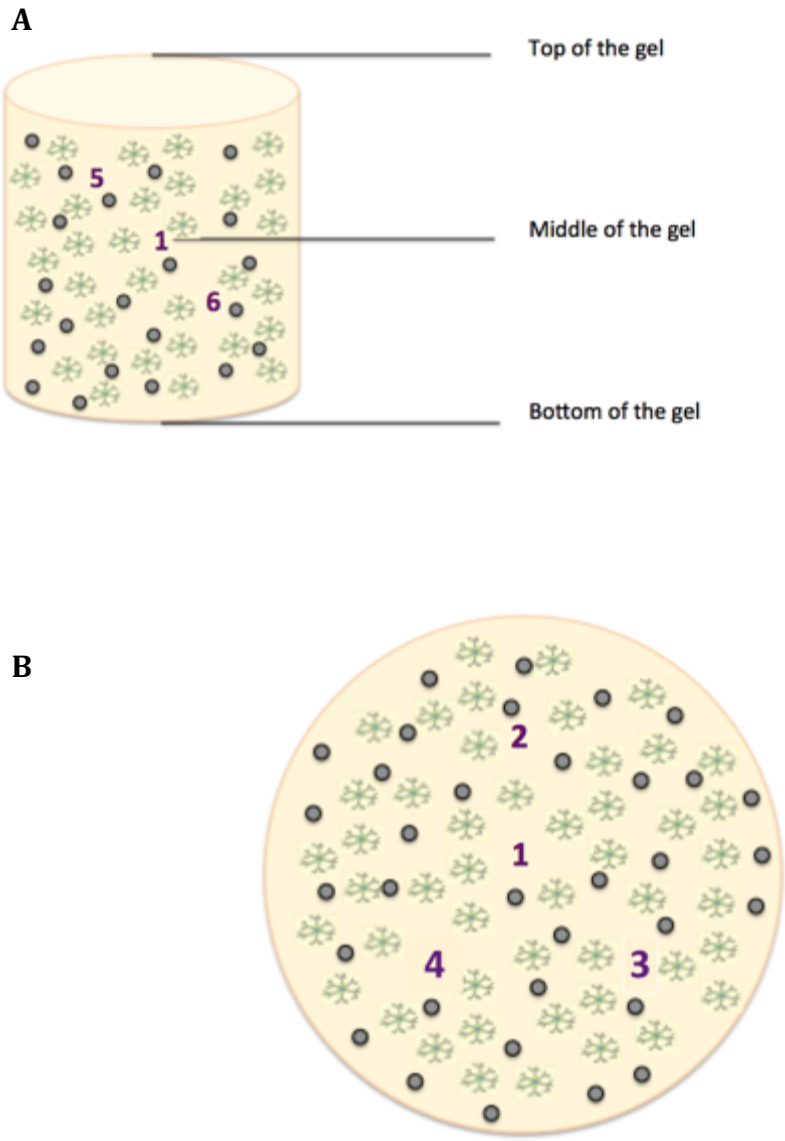

Figure 5.1. Gel imaging protocol **A)** The location of image 5, 1 and 6 points. These points were selected to avoid the meniscus at the surface and to be equidistant from the centre to obtain representative images of the gel. **B)** Images 1,2,3 and 4 were taken in the same Z plane half way through the gel. Image 1 was taken directly at the centre of the gel and images 2, 3 and 4 at equidistant locations around this central point.

A total of six images were taken and analysed for each gel and six gels were produced for each condition (0.5-50μm^3 cobalt chromium or stainless steel debris per cell, cell only negative control, DMSO positive control, particle only control and blank). Using point one as a reference point, a further three images were acquired in the same Z plane, images two, three and four. Imagining the gel as a clock, image two was taken at the 12 o'clock position, image three at the 4 o'clock position and four at the 8 o'clock position. Image five was taken closer to the top of the gel and to the left of the central point. Image six was

acquired towards the bottom of the gel, to the right of the central point. The rationale behind taking six images per gel was to obtain a holistic view of the cellular response in all non-reactive regions of the gel.

5.3.1.3 Image analysis using Image J

Image J software was used to count living (green) and dead (red) cells as a quantitative measure to assess the effect of metallic wear particles on the viability of primary astrocytes and microglia in co-culture and primary astrocytes in isolation. For each test condition all 36 images were included in analysis. All cells, living and dead (in and out of focus), were counted for each image using the cell counter analysis tool within the Image J software. For each image the number of viable cells was expressed as a percentage and an average percentage over all 36 images calculated for each test condition, this was compared to the cell only negative control using a two-way ANOVA and Tukey post hoc analysis.

5.3.1.4 Statistical analysis for live dead data.

As the data generated from the live dead images was presented in percentages, prior to any statistical analysis, the data was adjusted to account for the fact the data was not normally distributed, and an arcsine transformation also known as the angular transformation performed. A histogram of the percentage data for each condition was produced to ensure the data was not normally distributed. Upon transformation of the original percentage data using the arcsine transformation the distribution closely approximated a normal distribution. A two-way ANOVA and Tukey post-hoc analysis (whose formulas and assumptions rely on normally distributed data) were performed on the transformed data. In reporting the mean for each condition, the data was back-transformed back to percentages for graphical purposes.

5.3.2 Primary astrocyte reactivity.

In vivo astrocytes are rounded in morphology and unreactive, in response to trauma astrocytes exhibit a reactive phenotype, of which the up-regulation of the intermediate filament protein, glial fibrillary acidic protein (GFAP) is a marker. *In vivo* primary astrocytes do not constitutively express this protein, this only occurs in adverse environmental conditions.

5.3.2.1 Immunocytochemistry to detect glial fibrillary acidic protein (GFAP).

To determine the effect of cobalt chromium and stainless steel wear particles on the reactivity of primary astrocytes and microglia in co-culture and primary astrocytes in

isolation, cells were cultured with increasing particle volumes (0.5μm^3 - 50μm^3 metallic wear debris per cell). After the appropriate incubation period, two and five days, the gels were fixed using 4% PFA (v/v) and immunocytochemistry used to determine the effect on GFAP expression.

5.3.2.2 Antibodies used for labelling of glial fibrillary acidic protein

The primary antibody was polyclonal rabbit anti-glial fibrillary acidic protein (GFAP) diluted 1:300 in PBS without calcium and magnesium.

The secondary antibody was DyLight® 549 anti-rabbit IgG (H+L) diluted 1:300 in PBS. In addition, Hoechst 33258 was used to identify nuclear DNA diluted 1:1000 (1μg/ml) in PBS.

The PFA was discarded and the gels (100μl collagen gels in 96-well plates) were washed three times for five minutes with PBS (without calcium and magnesium). Following the PBS washes, 100μl of 0.1% (v/v) Triton X-100 (Chapter 2, section 2.3.28) was added to each gel and incubated at room temperature for 30 minutes. After the incubation period, the Triton X-100 was removed and the gels washed three times in PBS for five minutes. During the washes a 5% (v/v) goat serum block (Chapter 2, section 2.3.12) and primary GFAP antibody solution was prepared.

After the PBS washes, cells were blocked with 100μl of 5% (v/v) goat serum to prevent any non-specific binding of the primary antibody. The gels were incubated for 30 minutes at room temperature. The gels were then washed with PBS three times for five minutes each and 100μl of the primary GFAP antibody (1:300 primary antibody diluted in PBS) was added to each gel. The 96-well plate was wrapped in foil and stored overnight at 4°C.

After the overnight incubation the primary antibody was removed from each gel and three, 10 minute washes with PBS performed at room temperature. During the PBS washes the combined secondary antibody and Hoechst 33258 solution was prepared (1:300 dilution of the secondary antibody in PBS with 1:1000 Hoescht 33258). A volume of 100μl of the secondary antibody Hoecht solution was added to each well and incubated at room temperature in the dark for 90 minutes. The secondary antibody Hoescht solution was removed and three, five-minute washes with PBS were performed at room temperature. The gels were stored in PBS at 4°C and imaged the same day according to the previously outlined protocol (section 5.3.1.2). A negative control was not used for the antibody staining.

5.3.2.3 Immunocytochemistry image acquisition protocol.

The imaging protocol was identical to the procedure outlined in section 5.3.1.2, where the effects of cobalt chrome and stainless steel wear debris on the viability of primary astrocytes and microglia were investigated. However the Hoescht and red pre-set channels were selected. The laser settings used were Laser Diode 405: 405nm (Hoechst) and HeNe1: 543nm (for the detection of GFAP). A total of six images were taken per gel in the same orientation as outlined previously in section 5.3.1.2 and six gels were produced per test condition. This yielded a total of 36 images per test condition.

Each image was analysed for the expression of GFAP (stained red). When the cells expressed GFAP, red staining was present, the image was labeled with a +, When no GFAP expression was observed, no red staining, the image was labeled -. The number of + and – images for each test condition was recorded, the mode grade for each test condition was determined and compared to the cell only negative control.

5.3.3 TNF-α Cytokine release

5.3.3.1 A solid phase sandwich Enzyme Linked Immunosorbent Assay to determine the effect of cobalt chrome and stainless steel wear particles on TNF-α production in primary astrocytes and microglia.

A solid phase sandwich enzyme linked immunosorbent assay (ELISA) was used to determine the concentration of TNF-α produced by primary astrocytes and microglia in co-culture and primary astrocytes in isolation when cultured with metallic (cobalt chrome and stainless steel) wear debris.

Rat astrocytes do not constitutively produce TNF-α but upon mechanical injury or biological stimulation are known to release TNF-α. TNF-α production, a marker of systemic inflammation, was measured using a solid phase sandwich enzyme linked immunosorbent assay (ELISA). Supernatants stored from previous cytotoxicity investigations were used for this part of the study. Lipopolysaccharide was used as the positive control in this investigation. Lipopolysaccharide ($2ng.ml^{-1}$), is a component of endotoxin, originating from the cell walls of gram-negative bacteria is know to induce TNF-α production in primary rat astrocytes (Brahmachari et al., 2006). The lipopolysaccharide stimulated positive control gels (100μl gels, with a seeding density of $1x10^5$ cells per 100μl gel) were produced in a separate investigation to the cytotoxicity studies, the supernatant was collected and stored at -80°C until required. An alternative positive control was also investigated. In 2D monolayer culture, primary astrocytes

exhibit a reactive phenotype and up-regulate the expression of GFAP. Glial fibrillary acidic protein is a marker of astrogliosis, an abnormal proliferation of primary astrocytes in response to a biological or mechanical stimulus. One of the key detrimental effects of astrogliosis is the release of pro-inflammatory cytokines such as TNF-α. Thus primary astrocytes were cultured in a 2D monolayer cell culture system for 48 hours, the supernatant was removed and stored at -80°C for use in this part of the study for an additional positive control.

Pre-coated plates, already coated with a monoclonal capture antibody specific for rat TNF-α, were used in this study. The supernatants from previous cytotoxicity experiments (time points two and five days) were collected and stored at -80°C. The required samples were thawed at room temperature for approximately 2 hours prior to commencing the ELISA. During the thawing process the wash buffer, standard diluent buffer and biotinylated anti-rat TNF-α were prepared (Chapter 2, sections 2.3.31, 2.3.23 and 2.3.4, respectively).

Initially the standards for generation of the standard curve were prepared in the pre-coated 96-well plate. To prepare the standards the vial provided in the kit was reconstituted in the recommended volume (1.19ml) of standard diluent, immediately prior to use. By reconstituting the vial in 1.19ml of standard diluent a stock solution of 1000pg.ml^{-1} of rat TNF-α was produced. This solution was mixed thoroughly by inverting the vial. Serial dilutions of rat TNF-α were prepared directly in the pre-coated 96-well plate. The standard dilutions ranged from 31.25-1000pg.ml^{-1} of rat TNF-α. Immediately after reconstitution 200µl of indicated standard was added to wells A1 and A2 providing the highest concentration on the standard curve (1000pg.ml^{-1}). A volume of 100µl of standard diluent was added to the remaining standard wells, B1 and B2 to F1 and F2. A volume of 100µl was taken from A1 and A2 and added to B1 and B2, respectively yielding the second standard, 500pg.ml^{-1}. The contents of B1 and B2 were mixed thoroughly by aspiration. The 1:1 dilution was continued using 100µl from wells B1 and B2 through to wells F1 and F2. The excess 100µl was discarded from wells F1 and F2 and 100µl of antibody diluent added to wells G1 and G2 to provide the zero standard concentration. A volume of 100µl of the thawed supernatant samples were added to the remaining wells of the pre-coated 96-well plate in accordance with Figure 5.2.

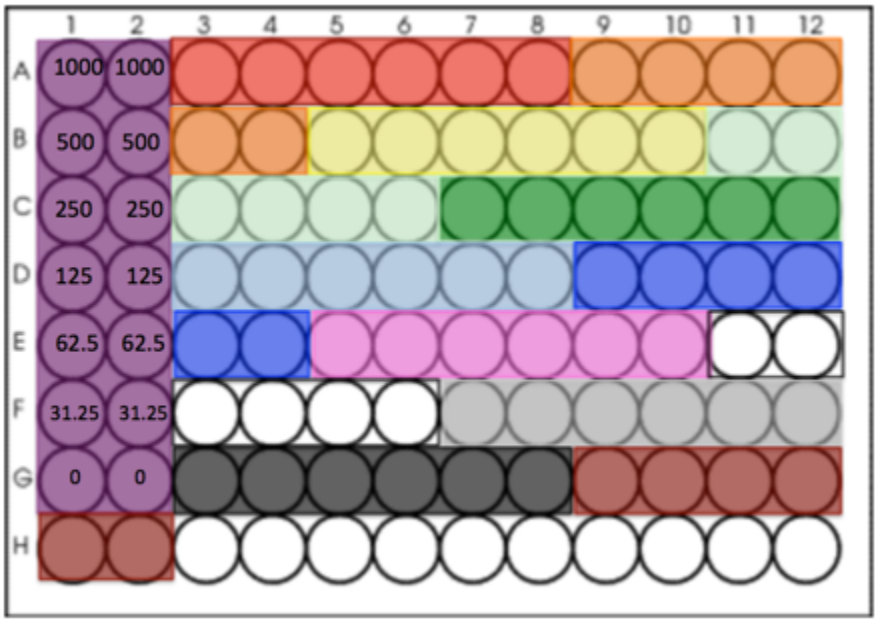

Figure 5.2 The positioning of supernatant samples in the pre-coated 96-well plate in the enzyme linked immunosorbent assay. Purple= Standards ranging from 0-1000pg.ml^{-1}. Red=Primary astrocytes and microglia in co-culture cultured with 50µm^3 CoCr debris for two days. Orange= Primary astrocytes and microglia in co-culture cultured with 5µm^3 CoCr debris for two days. Yellow= Primary astrocytes and microglia in co-culture cultured with 0.5µm^3 CoCr debris for two days. Light green= Primary astrocytes and microglia in co-culture for two days (cell only negative control). Dark green=Primary astrocytes and microglia and reactive cell supernatant from 2D monolayer culture two days. Light Blue= Primary astrocytes and microglia with LPS (2ng.ml^{-1}) two days. Dark Blue= Primary astrocytes and microglia in co-culture cultured with 50µm^3 stainless steel debris for two days. Pink= Primary astrocytes and microglia in co-culture cultured with 5µm^3 stainless steel debris for two days. White= Primary astrocytes and microglia in co-culture cultured with 0.5µm^3 stainless steel debris for two days. Grey= Primary astrocytes and microglia in co-culture for two days (cell only negative control). Black= Primary astrocytes and microglia and reactive cell supernatant two days. Brown= Primary astrocytes and microglia with LPS (2ng.ml^{-1}) two days.

After the samples were added to the 96-well plate, 50µl of biotinylated anti-Rat TNF-α was added to all wells. The plate was covered with a micro-plate sealing film and incubated at room temperature for three hours. During this three-hour incubation period the Streptavidin-HRP solution was prepared (Chapter 2, section 2.3.24). The Streptavidin-HRP solution was diluted, 150µl of Streptavidin-HRP in 10mls of Streptavidin-HRP diluent (the recommended dilution for a 96-well plate).

After the three-hour incubation period all wells were washed with 300µl the wash buffer solution. Initially the contents of each well were aspirated over the sink and approximately 300µl of wash buffer solution was added to each well. After 30 seconds the contents were once again aspirated. This wash step was repeated three times ensuring all wash buffer was removed after each step.

A volume of 100µl of Streptavidin-HRP solution was added to each well. The 96-well plate was covered with a plastic micro-plate sealing film and the plate incubated at room temperature for 30 minutes. After the 30-minute incubation period each well was washed three times with PBS (as previously outlined). The ready-to-use TMB substrate (100µl) provided in the kit was added to each well. The plate was covered with a micro-plate sealing film, wrapped in foil and incubated at room temperature for 20 minutes. After this time wells containing TNF-α developed a blue colouring. The ready-to-use stop solution was added to each well in the 96-well plate (100µl per well). The addition of the stop solution converted the blue solution to a yellow solution. The plate was then read using a spectrophotometer using 450nm as the primary wavelength and 630nm as the reference wavelength, providing an optical density value for each sample.

An average optical density value was calculated for the standard samples, all test samples and controls. Using the average optical densities for the standards a linear standard curve was generated. Here the mean optical density value for each standard was plotted against the corresponding TNF-α concentration. The concentration of TNF-α (measured in $pg.ml^{-1}$) for each test sample was derived from the standard curve using the average optical density value.

5.4 Results

5.4.1.The effect of cobalt chrome wear particles on the viability of primary astrocytes and microglia in co-culture and primary astrocytes in isolation.

To determine the effect of cobalt chrome wear particles on the viability of cell of the CNS. Primary astrocytes and microglia in co-culture and primary astrocytes in isolation were cultured with increasing particle volumes ($0.5\mu m^3$ – $50\mu m^3$) and their effect on viability determined using a live dead assay.

5.4.1.1 The effect of cobalt chrome wear particles on the viability of primary astrocytes and microglia in co-culture.

Primary astrocytes and microglia were cultured with increasing particle volumes ($0.5\mu m^3$ CoCr debris per cell to $50\mu m^3$ CoCr debris per cell) for two and five days (Figure 5.3). Following this incubation period the live dead assay was performed in accordance with the protocol outlined in Chapter 2, section 2.4.2.2. Live dead images showing the effect of cobalt chrome wear particles on the viability of primary astrocytes and microglia after 48 hours and five days in culture can be seen in Figures 5.4 and 5.5 respectively

When primary astrocytes and microglia in co-culture were cultured with increasing concentrations of cobalt chrome particles for two and five days in culture, the cell only negative control maintained a high percentage of living cells at 77.8% and 82.7%, respectively after two and five days in culture (Figure 5.3).

After the primary astrocytes and microglia were cultured with the largest cobalt chrome particle dose of $50\mu m^3$ CoCr debris per cell, at two and five days a significant decrease in viability was observed when compared to the cell only negative control with only 41.8% of cells being viable after two days and 54.2% of cells being viable after five days.

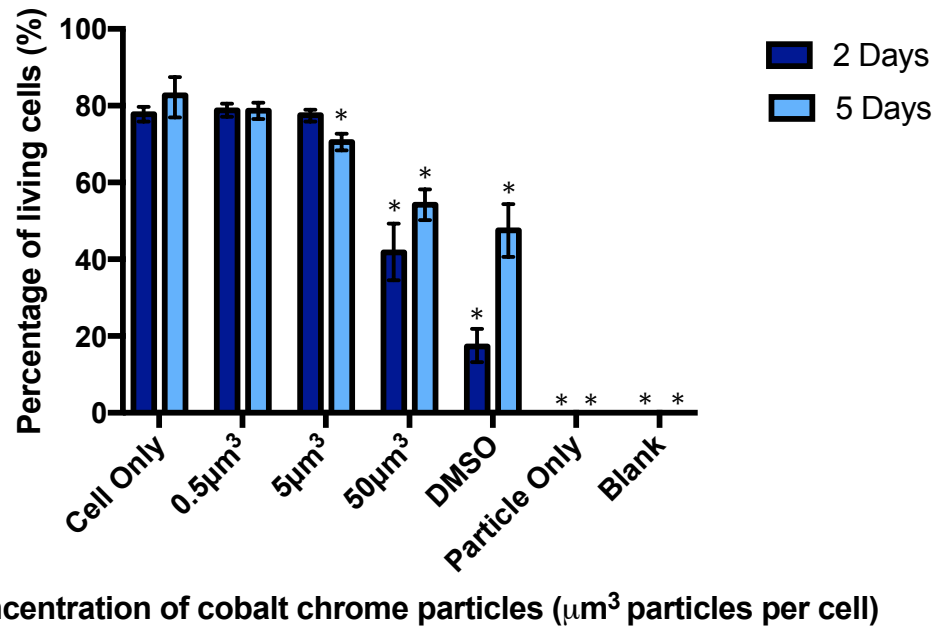

Figure 5.3 The effect of increasing particle volumes (0.5µm³-50µm³) of cobalt chrome on the viability of primary astrocytes and microglia in co-culture after two and five days. Mean percentage of living cells ± 95% confidence intervals (six replicates per condition). DMSO was used as a positive control, a particle only negative control was also used. An asterisk indicates a significant reduction in viability ($p<0.05$) when compared with cell only negative control using a Two-way ANOVA.

When the primary astrocytes and microglia were cultured in 3D collagen gels with 5µm³ cobalt chrome debris per cell no significant adverse effect on cell viability was observed after two days, however, a significant decline in viability was seen after five days in culture, with only 70.5% viable cells recorded at this time point, compared to 82.7% in the cell negative only control.

After two and five days in culture with the lowest cobalt chrome particle dose of 0.5µm³ CoCr debris per cell, no adverse effect on primary astrocyte and microglia viability was detected when compared to the cell only negative control.

When primary astrocytes and microglia were cultured with 100µl DMSO positive control, significant decreases in viability were observed at both two and five-day time points. After 48 hours in culture with the DMSO positive control only 17.3% of the cells were viable. After five days in culture 47.6% of primary astrocytes and microglia were viable. No fluorescence was emitted from the particle only gels, indicating the particles did not auto-fluoresce and interfere with the assay.

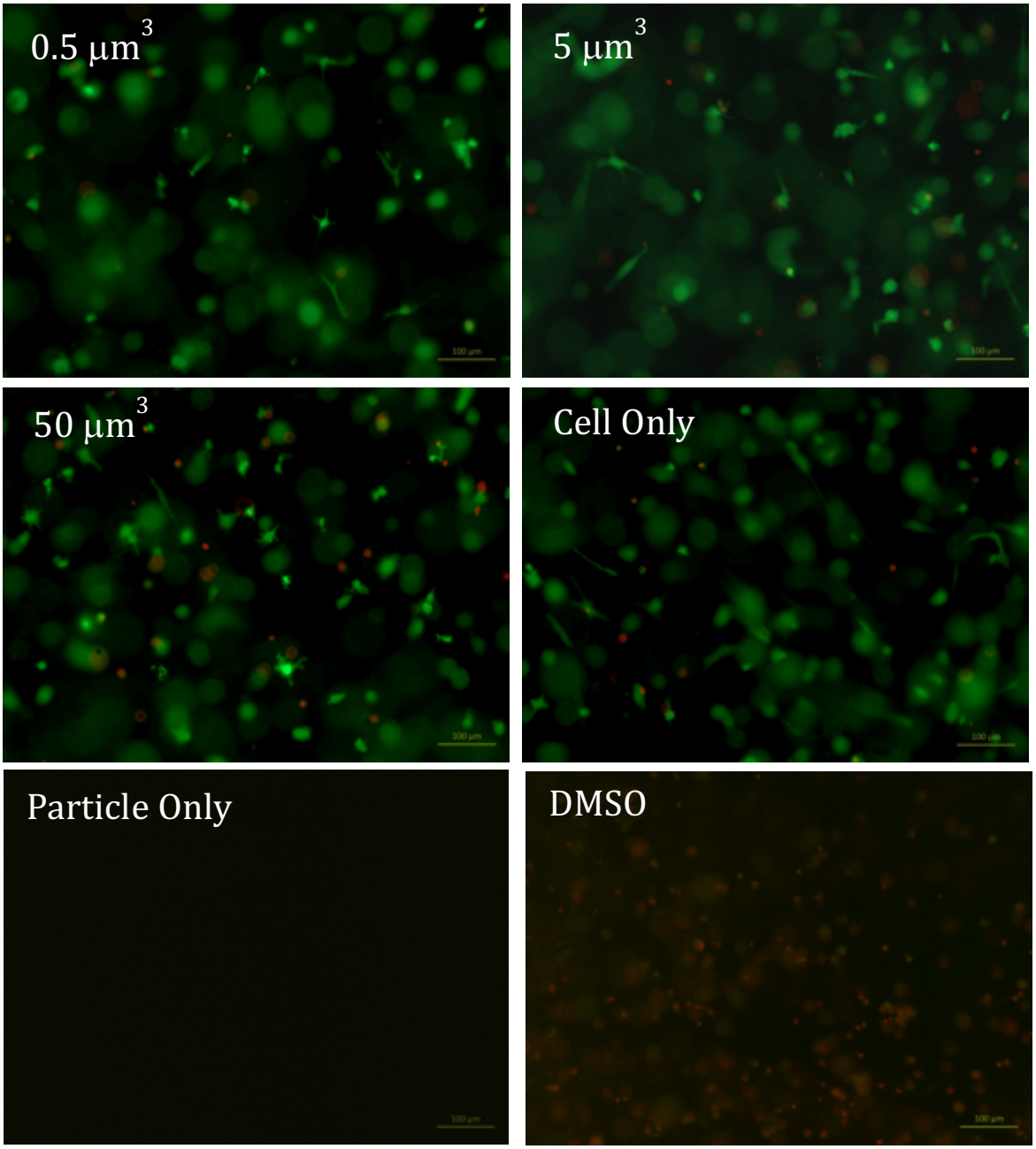

Figure 5.4 The effect of increasing cobalt chrome particle volumes (0.5µm³-50µm³ cobalt chrome particles per cell) on the viability of primary astrocytes and microglia in co-culture after 48 hours assessed using a live dead assay. The highest particle dose (50µm³ cobalt chrome particles per cell) was used as a particle only control. The green, calcein stain, stains living cells and the red, ethidium homodimer fluorescent dye, stained dead cells.

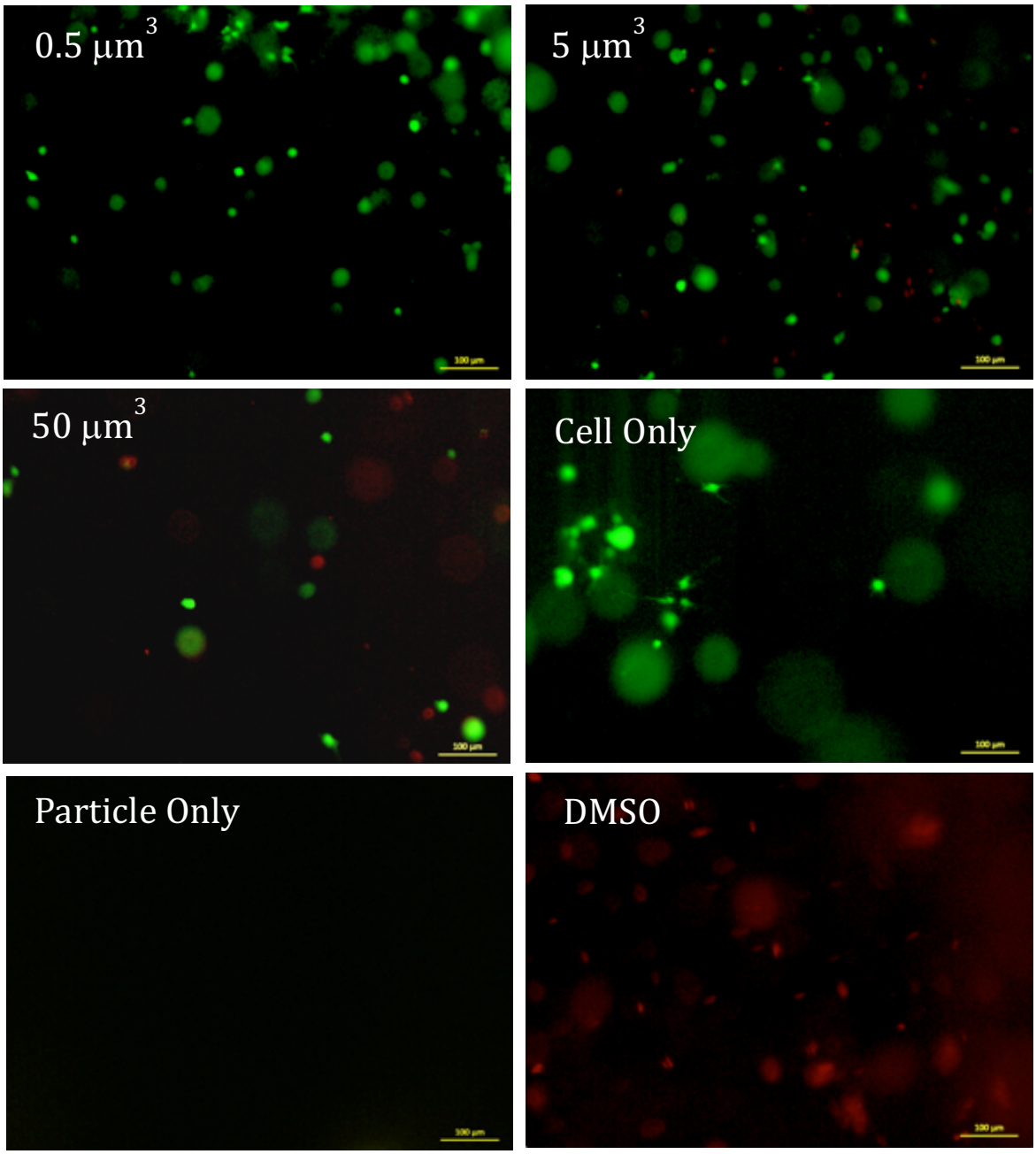

Figure 5.5 The effect of increasing cobalt chrome particle volumes (0.5µm^3-50µm^3 cobalt chrome particles per cell) on the viability of primary astrocytes and microglia in co-culture after five days assessed using a live dead assay. The highest particle dose (50µm^3 cobalt chrome particles per cell) was used as a particle only control. The green, calcein stain, stains living cells and the red, ethidium homodimer fluorescent dye, stained dead cells.

5.4.1.2 The effect of cobalt chrome wear particles on the viability of primary astrocytes in isolation.

The effect of cobalt chrome wear particles on the viability of primary astrocytes in isolation was determined using a live dead assay (Figure 5.6). Live dead images showing the effect of cobalt chrome wear particles on the viability of primary astrocytes in isolation after 48 hours and five days in culture can be seen in Figures 5.7 and 5.8 respectively.

Over the course of the investigation the primary astrocytes (in isolation) continued to grow and divide and maintained a high proportion of living cells; 84.4% living cells after two days and 94.3% after five days (Figure 5.6).

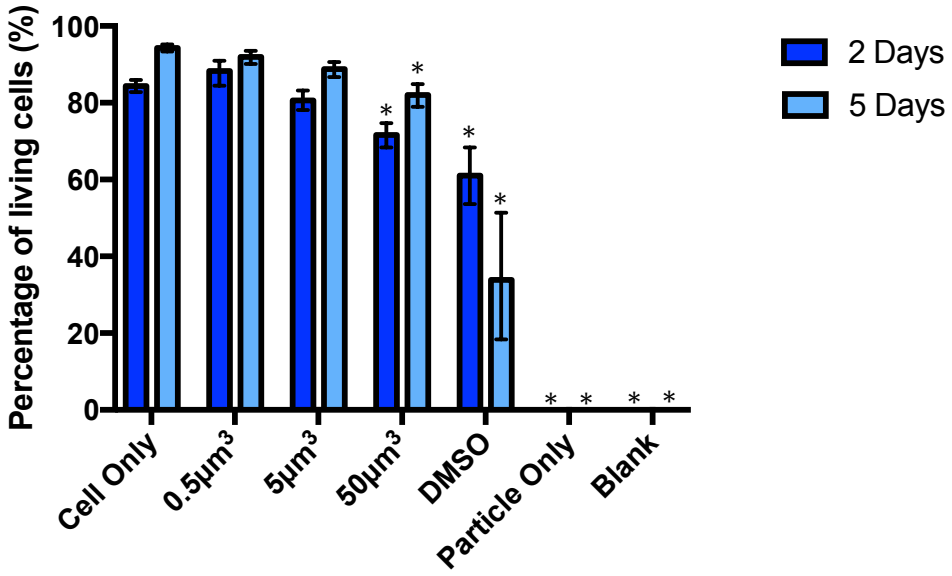

Figure 5.6 The effect of increasing particle volumes (0.5µm³-50µm³) of cobalt chrome on the viability of primary astrocytes in isolation after two and five days in culture. Mean percentage of living cells ± 95% confidence intervals (six replicates per condition). DMSO was used as a positive control, a particle only negative control was also used. An * Indicates a significant reduction in viability ($p<0.05$) when compared with cell only negative control using Two-way ANOVA.

Similar effects on cell viability were observed when primary astrocytes in isolation were cultured with cobalt chrome particles in a 3D collagen hydrogel for two and five days. Significant adverse effects on viability were observed when the primary astrocytes in isolation were cultured with the highest cobalt chrome particle dose of 50µm³ per cell, after two and five days in culture when compared to the cell only negative control. The

cell viability was reduced to 71.6% living cells after two days (compared to 84.4% living cells in the cell only control) and 82.0% after five days (compared to 94.3% living cells in the cell only control). No adverse effects on viability were observed when primary astrocytes were cultured with the 5μm^3 and 0.5μm^3 cobalt chrome per cell particle doses after two and five days in culture.

The DMSO positive control induced a significant reduction in viability of primary astrocytes at both time points. The percentage of living cells after two days fell to 61.1% from 84.4% viable cells in the cell only control and to 33.9% from 94.3% in the cell only control after five days.

No fluorescence was emitted from the particle only gels, indicating the particles did not auto-fluoresce and interfere with the assay.

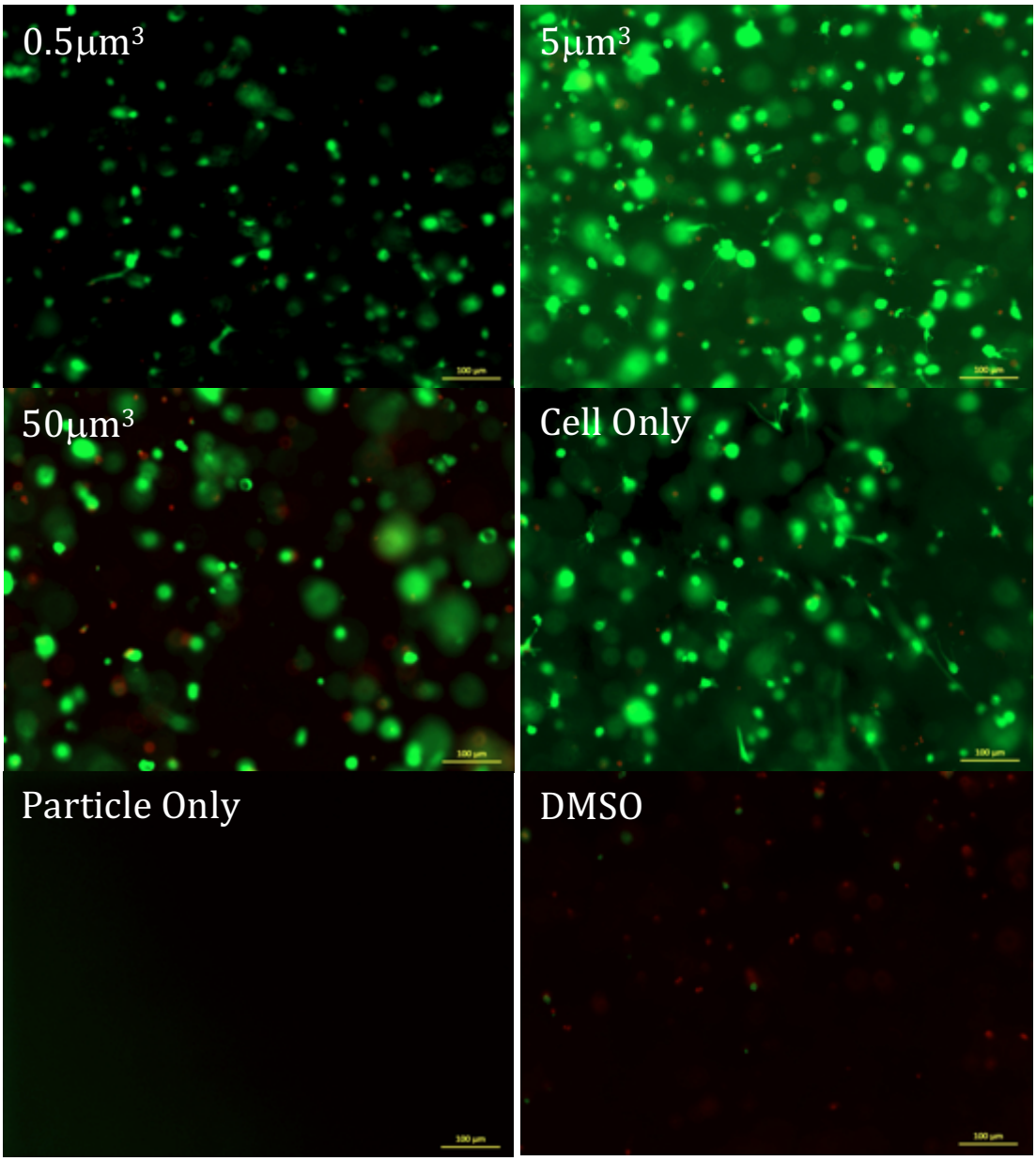

Figure 5.7 The effect of increasing cobalt chrome particle volumes (0.5µm³-50µm³ cobalt chrome particles per cell) on the viability of primary astrocytes in isolation after 48 hours assessed using a live dead assay. The highest particle dose (50µm³ cobalt chrome particles per cell) was used as a particle only control. The green, calcein stain, stains living cells and the red, ethidium homodimer fluorescent dye, stained dead cells.

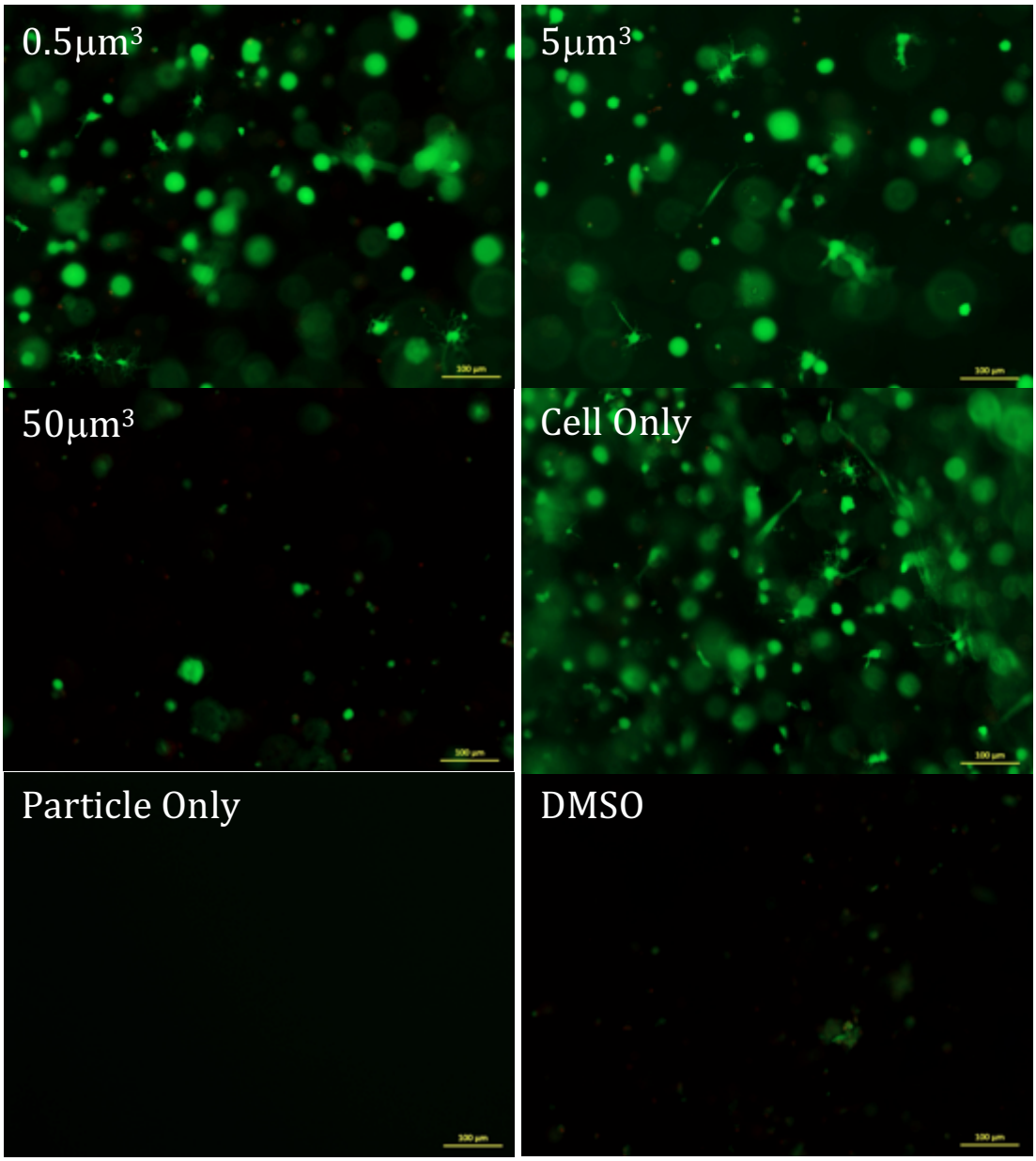

Figure 5.8 The effect of increasing cobalt chrome particle volumes (0.5µm³-50µm³ cobalt chrome particles per cell) on the viability of primary astrocytes in isolation after five days in culture assessed using a live dead assay. The highest particle dose (50µm³ cobalt chrome particles per cell) was used as a particle only control. The green, calcein stain, stains living cells and the red, ethidium homodimer fluorescent dye, stained dead cells.

A summary of the effects of cobalt chrome wear particles on the viability of primary astrocytes and microglia in co-culture and primary astrocytes in isolation in 3D culture after two and five days are presented in Table 5.3

Table 5.3 The effects of cobalt chrome wear particles on the viability of primary astrocytes and microglia in co-culture and primary astrocytes in isolation in an advanced 3D cell culture system assessed using a live dead assay. Cells with significantly decreased viabilities ($p<0.05$) compared to the cell only negative control were indicated with an asterisk.

	Astrocytes and microglia				**Astrocytes in isolation**			
	$0.5\mu m^3$	$5\mu m^3$	$50\mu m^3$	DMSO	$0.5\mu m^3$	$5\mu m^3$	$50\mu m^3$	DMSO
Day 2			*	*			*	*
Day 5		*	*	*			*	*

5.4.1.3.The effect of stainless steel wear particles on the viability of primary astrocytes and microglia in co-culture.

A live dead assay was used to determine the effect of stainless steel wear particles on the viability of primary astrocytes and microglia in a more physiologically relevant 3D cell culture system compared to 2D monolayer culture (Figure 5.9). Live dead images showing the effect of stainless steel wear particles on the viability of primary astrocytes and microglia in co-culture after 48 hours and five days in culture can be seen in Figures 5.10 and 5.11 respectively.

A high proportion of living cells were maintained for the primary astrocyte and microglia cell only negative control over the course of the investigation with 79.4% living cells after 48 hours and 88.6% after five days (Figure 5.9).

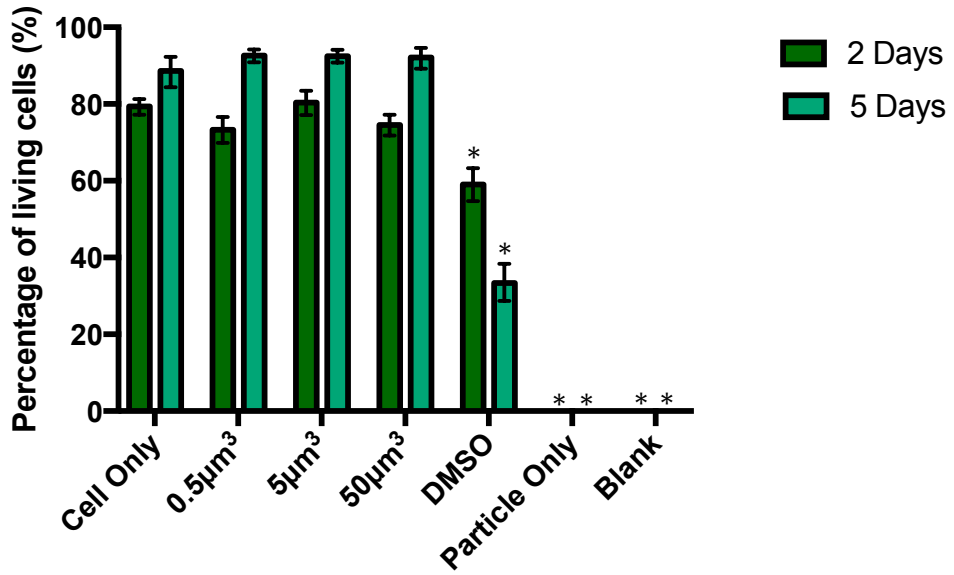

Figure 5.9 The effect of increasing particle volumes (0.5µm³-50µm³) of stainless steel on the viability of primary astrocytes and microglia in co-culture after two and five days in culture. Mean percentage of living cells ± 95% confidence intervals (six replicates per condition). DMSO was used as a positive control, a particle only negative control was also used. An asterisk indicates a significant reduction in viability ($p<0.05$) when compared with cell only negative control using Two-way ANOVA.

No adverse effects on viability were observed when primary astrocytes and microglia were cultured with 50µm³, 5µm³ and 0.5µm³ stainless steel debris per cell after 48 hours or five days in culture.

The DMSO positive control triggered a progressive reduction in viability of primary astrocytes and microglia over the course of the study. The percentage of living cells was reduced to 59.0% compared to 79.4% viable cells in the cell only gel after 48 hours and to 33.4% compared to 88.6% viable cells in the cell only gels after five days.

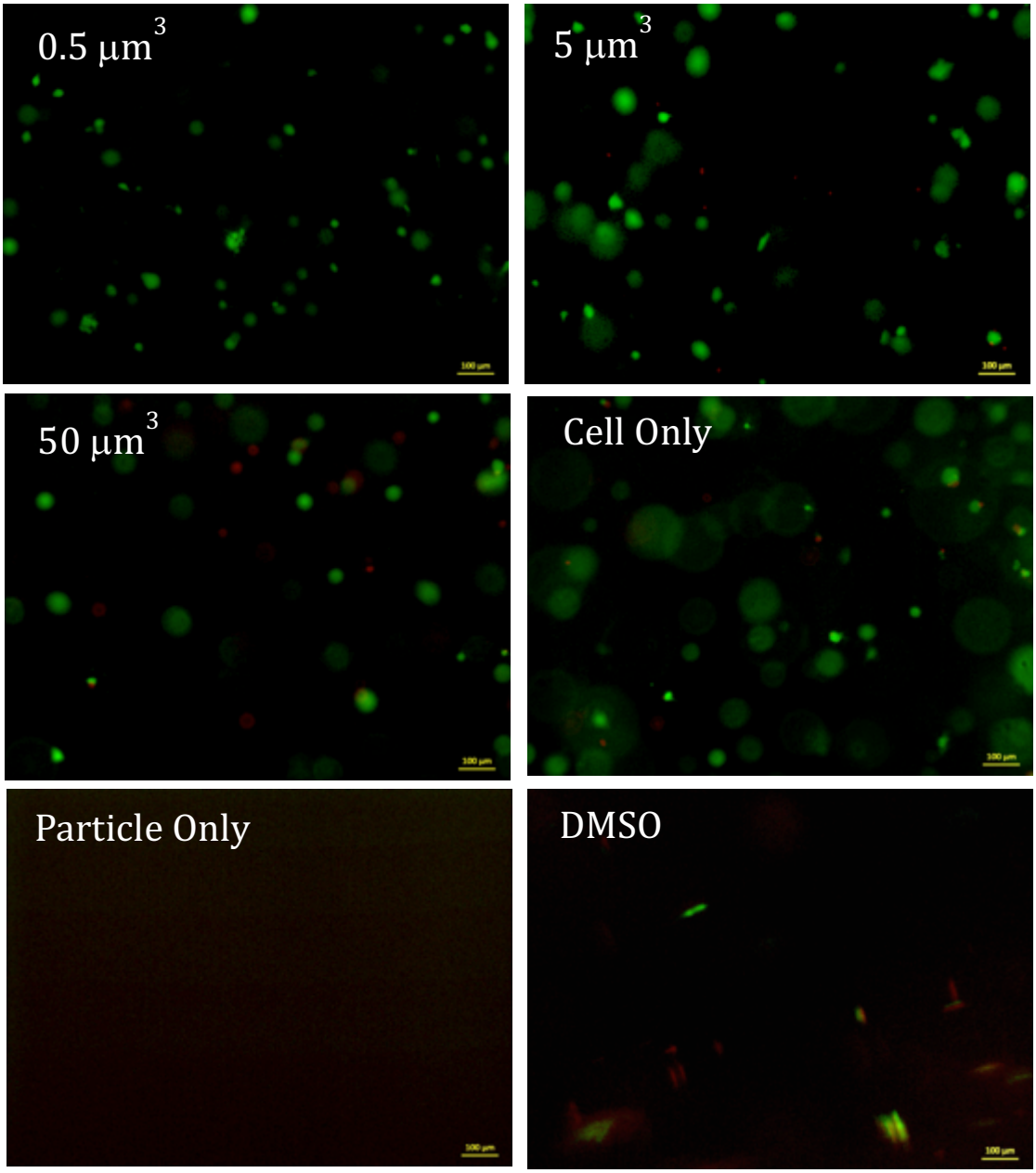

Figure 5.10 The effect of increasing stainless steel particle volumes (0.5µm³-50µm³ stainless steel particles per cell) on the viability of primary astrocytes and microglia in co-culture after 48 hours assessed using a live dead assay. The highest particle dose (50µm³ stainless steel particles per cell) was used as a particle only control. The green, calcein stain, stains living cells and the red, ethidium homodimer fluorescent dye, stained dead cells.

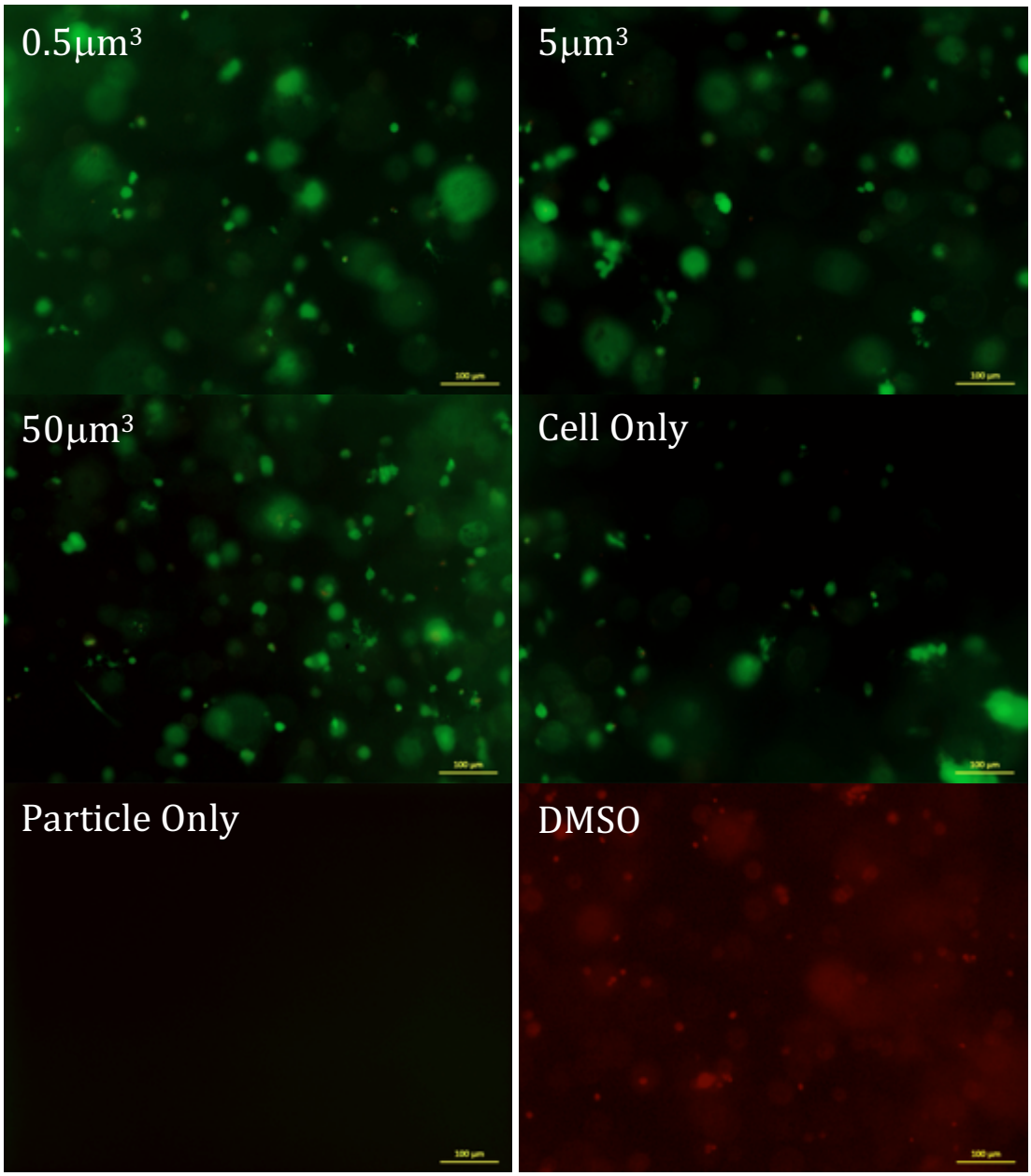

Figure 5.11 The effect of increasing stainless steel particle volumes (0.5µm³-50µm³ stainless steel particles per cell) on the viability of primary astrocytes and microglia in co-culture after five days in culture assessed using a live dead assay. The highest particle dose (50µm³ stainless steel particles per cell) was used as a particle only control. The green, calcein stain, stains living cells and the red, ethidium homodimer fluorescent dye, stained dead cells.

No fluorescence was observed in the particle only gels, indicating the particles did not auto-fluoresce.

5.4.1.4 The effect of stainless steel wear particles on the viability of primary astrocytes in isolation.

The effect of stainless steel wear particles on the viability of primary astrocytes in isolation was assessed using a live dead assay. The primary astrocytes were cultured with increasing particle volumes of stainless steel (0.5μm^3-50μm^3 stainless steel debris per cell) for two and five days (Figure 5.12). Live dead images showing the effect of stainless steel wear particles on the viability of primary astrocytes in isolation after 48 hours and five days in culture can be seen in Figures 5.13 and 5.14 respectively.

Over the five-day incubation period the primary astrocytes in isolation continued to proliferate with 92.2% viable cells after 48 hours and 93.7% living cells after five days (Figure 5.12).

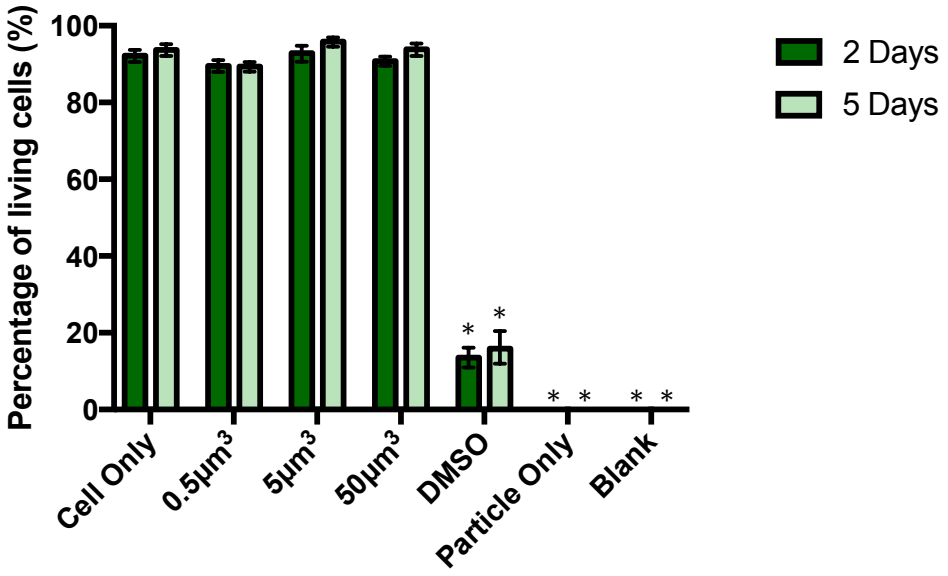

Figure 5.12 The effect of increasing particle volumes (0.5μm^3-50μm^3) of stainless steel on the viability of primary astrocytes in isolation after two and five days in culture. Mean percentage of living cells ± 95% confidence intervals (six replicates per condition). DMSO was used as a positive control, a particle only negative control was also used. An asterisk indicates a significant reduction in viability ($p<0.05$) when compared with cell only negative control using a Two-way ANOVA.

Once again the stainless steel wear particles did not trigger an adverse effect on the viability of primary astrocytes after 48 hours and 5 days in culture at any particle dose tested.

A progressive reduction in viability was detected when primary astrocytes in isolation were cultured with DMSO after 48 hours and five days. The percentage of living cells was reduced to 13.6% from 92.2% in the cell only negative control after 48 hours and to 15.9% from 93.7% in the cell only negative control after five days.

No fluorescence was observed in the particle only gels, indicating the particles did not auto-fluoresce.

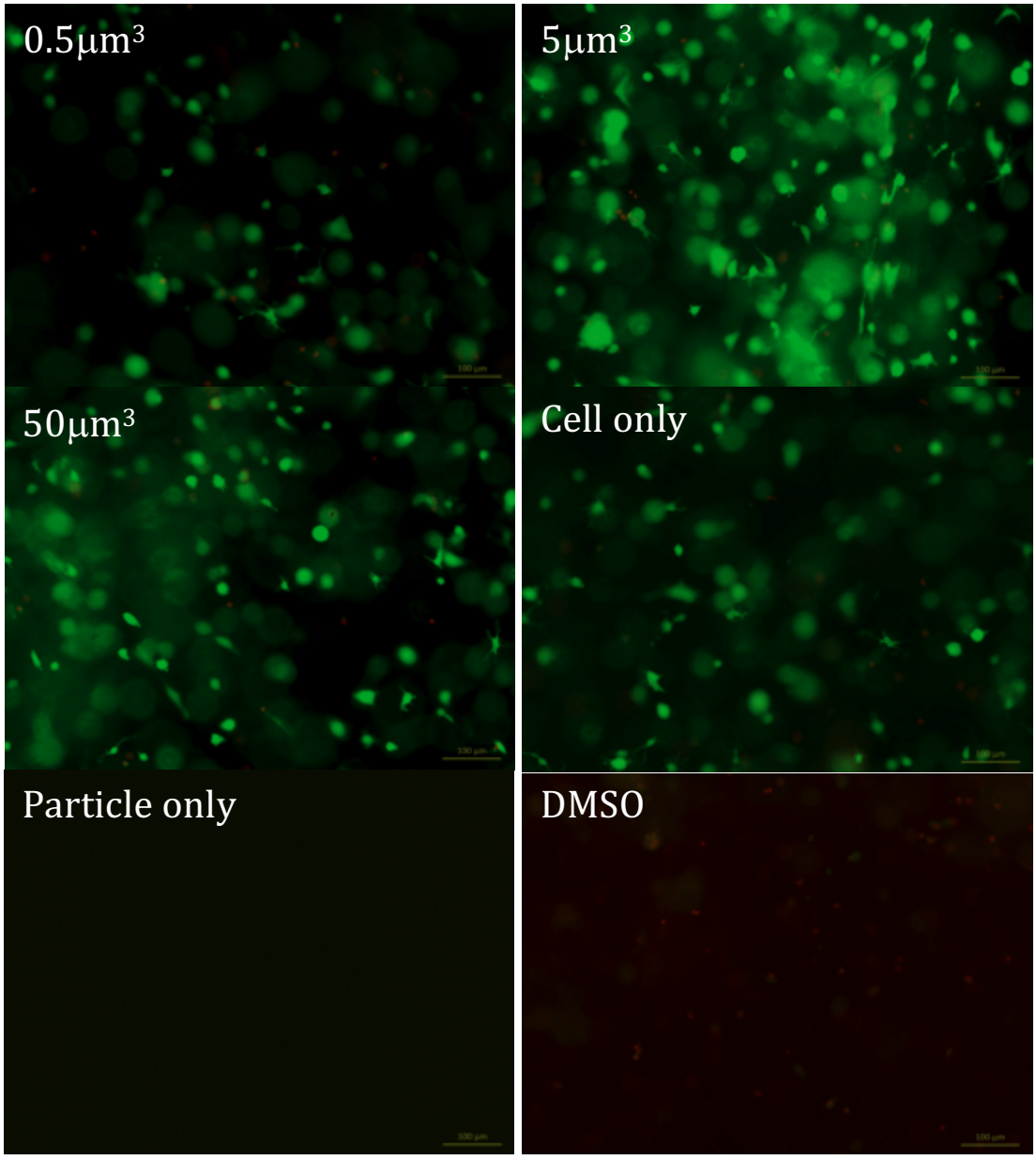

Figure 5.13 The effect of increasing stainless steel particle volumes (0.5µm³-50µm³ stainless steel particles per cell) on the viability of primary astrocytes in isolation after 48 hours assessed using a live dead assay. The highest particle dose (50µm³ stainless steel particles per cell) was used as a particle only control. The green, calcein stain, stains living cells and the red, ethidium homodimer fluorescent dye, stained dead cells.

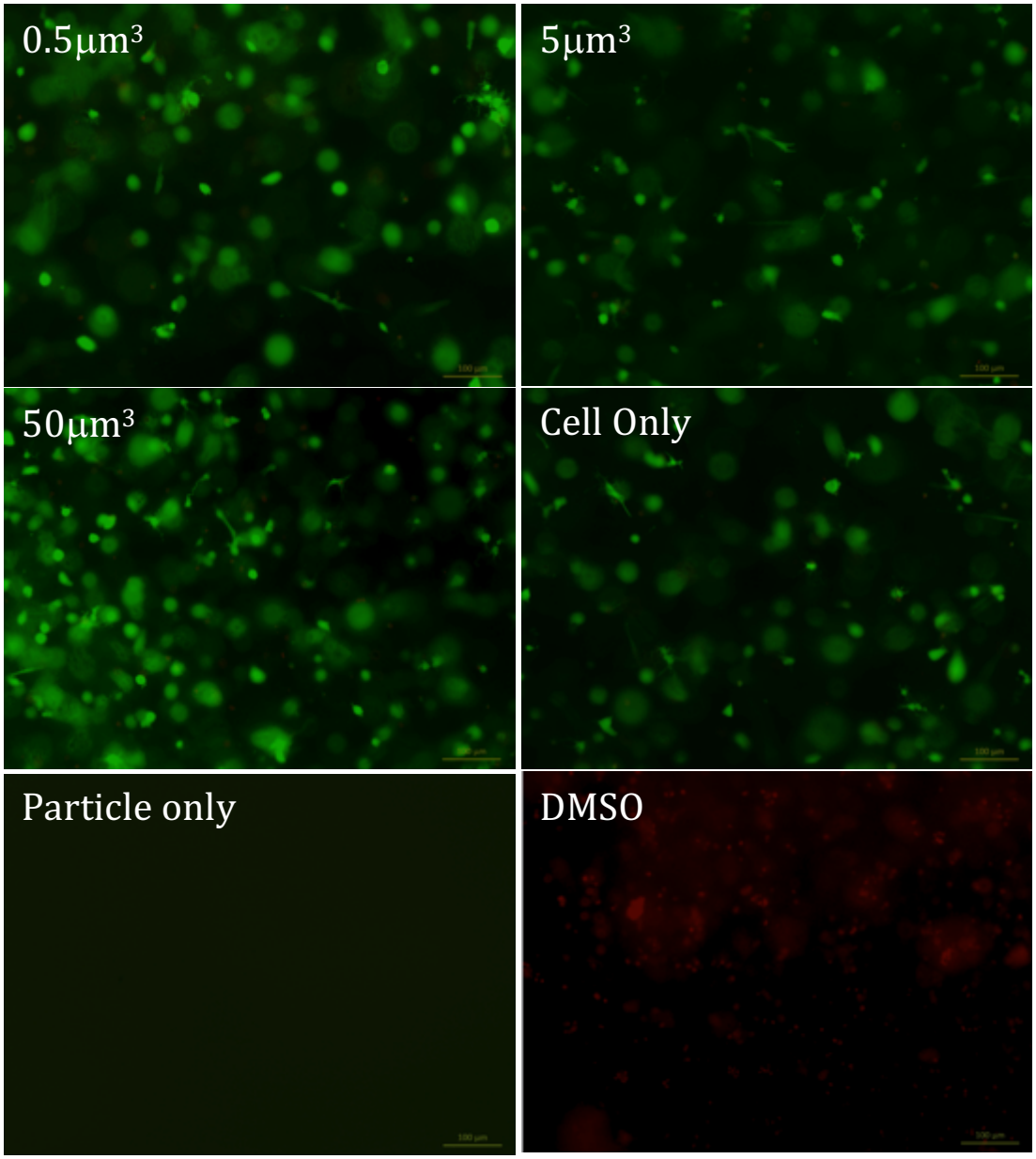

Figure 5.14 The effect of increasing stainless steel particle volumes (0.5µm^3-50µm^3 stainless steel particles per cell) on the viability of primary astrocytes in isolation after five days in culture, assessed using a live dead assay. The highest particle dose (50µm^3 stainless steel particles per cell) was used as a particle only control. The green, calcein stain, stains living cells and the red, ethidium homodimer fluorescent dye, stained dead cells.

A summary of the effects of stainless steel wear particles on the viability of primary astrocytes and microglia in co-culture and primary astrocytes in isolation in 3D culture after two and five days can be seen below in Table 5.4.

Table 5.4 The effect of stainless steel wear particles on the viability of primary astrocytes and microglia in co-culture and primary astrocytes in isolation using an advanced 3D cell culture system and assessed using a live dead assay. Cells with significantly decreased viabilities $p<0.05$ (Two-way ANOVA) compared to the cell only negative control were indicated with an asterisk.

	Astrocytes and microglia				Astrocytes in isolation			
	0.5μm³	5μm³	50μm³	DMSO	0.5μm³	5μm³	50μm³	DMSO
Day 2				*				*
Day 5				*				*

In conjunction with the live dead assay, attempts were made to validate the semi-quantitative live dead assay with the quantitative ATP Lite™ assay, however, due to the density of the viscous collagen gels it was extremely difficult to reliably and reproducibly determine the effects of cobalt chrome and stainless steel on cell viability using this method in an advanced 3D cell culture system. The ATP Lite™ assay was based on the generation of light as a result of the interaction with ATP and Luciferin, this was difficult to capture when the cells were embedded in a gel, therefore this part of the study proceeded with the use of the live dead assay only.

5.4.2 The effect of cobalt chromium ions and stainless steel ions on the viability of primary astrocytes and microglia in co-culture and primary astrocytes in isolation.

To determine the effect of ions from cobalt chrome and stainless steel particles on the viability of primary astrocytes and microglia in co-culture and primary astrocytes in isolation, particle doses ($0.5\mu m^3$ – $50\mu m^3$) of each material were suspended in supplemented DMEM media (Chapter 2, section 2.3.20) for 24 hours, after the 24 hour incubation period the medium-particle suspension was centrifuged to remove the particles and the supernatant added to both cell types in 3D culture. The effect of metallic ions on cell viability was determined using a live dead assay. The data was presented as percentage of living cells and prior to any statistical analysis the data was arcsine transformed. The data was back-transformed to percentages for graphical presentation.

5.4.2.1 The effect of cobalt chromium ions on the viability of primary astrocytes and microglia.

A live dead assay was used to determine the effect of cobalt chromium ions on the viability of primary astrocytes and microglia in co-culture using a 3D cell culture system (Figure 5.15). Live dead images showing the effect of ions from cobalt chrome wear particles on the viability of primary astrocytes in co-culture after 48 hours and five days in culture can be seen in Figures 5.16 and 5.17 respectively.

A continuously high proportion of cells in the cell only negative control were viable throughout the duration of the investigation. After two days in culture 84.5% of the primary astrocytes and microglia were viable and 90.5% were viable after five days (Figure 5.15).

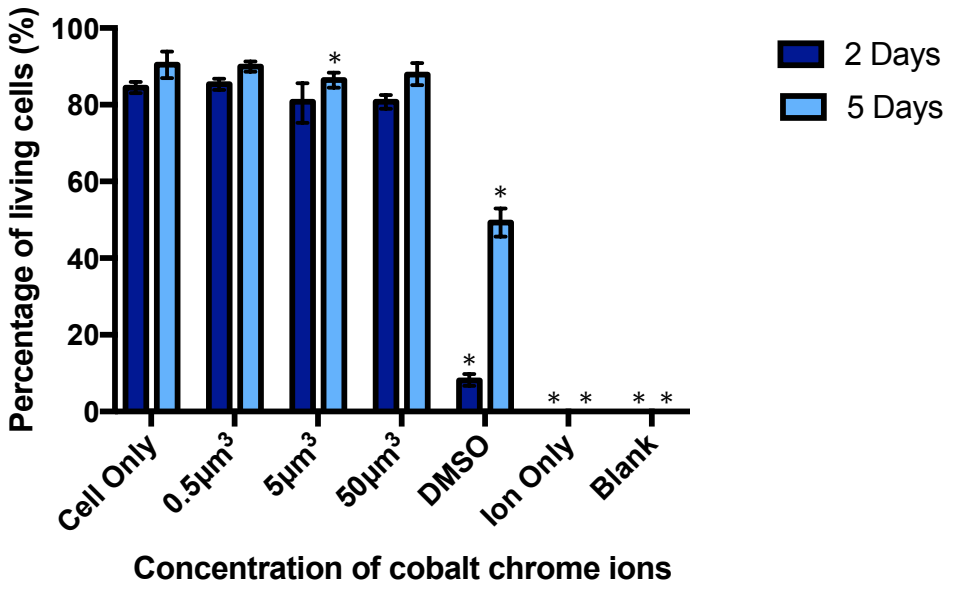

Figure 5.15. The effect of increasing concentrations of ions from wear particle doses (0.5µm³-50µm³) of cobalt chrome on the viability of primary astrocytes and microglia in co-culture after two and five days in culture. Mean percentage of living cells ± 95% confidence intervals (six replicates per condition). DMSO was used as a positive control, an ion only negative control was also used. An * Indicates a significant reduction in viability ($p<0.05$) when compared with cell only negative control using a Two-way ANOVA.

When the primary astrocytes and microglia were cultured with the highest ion concentration (the concentration of ions released from 50µm³ cobalt chrome wear particles per cell in a 24 hour incubation period) no significant effect on viability was observed at either time point tested.

Ions released from 5µm³ cobalt chrome wear particles did not adversely affect cell viability after 48 hours in culture, however a significant reduction in viability with this concentration of cobalt chrome ions was observed after five days in culture. The percentage of living cells was reduced from 90.5% in the cell only control to 86.5%.

The viability of primary astrocytes and microglia was not adversely affected by cobalt chromium ions when cultured with the lowest ion concentration, the concentration of cobalt chromium ions released from 0.5µm³ cobalt chrome wear debris at any time point tested.

After 48 hours the DMSO positive control had a dramatic effect on the viability of primary astrocytes and microglia, causing a significant level of apoptosis with only 8.2% viable cells at this time point. The effect was not as pronounced after five days in culture but the decline in viability was still significant with 49.3% viable cells.

No fluorescence was seen in the ion only control at either time point tested.

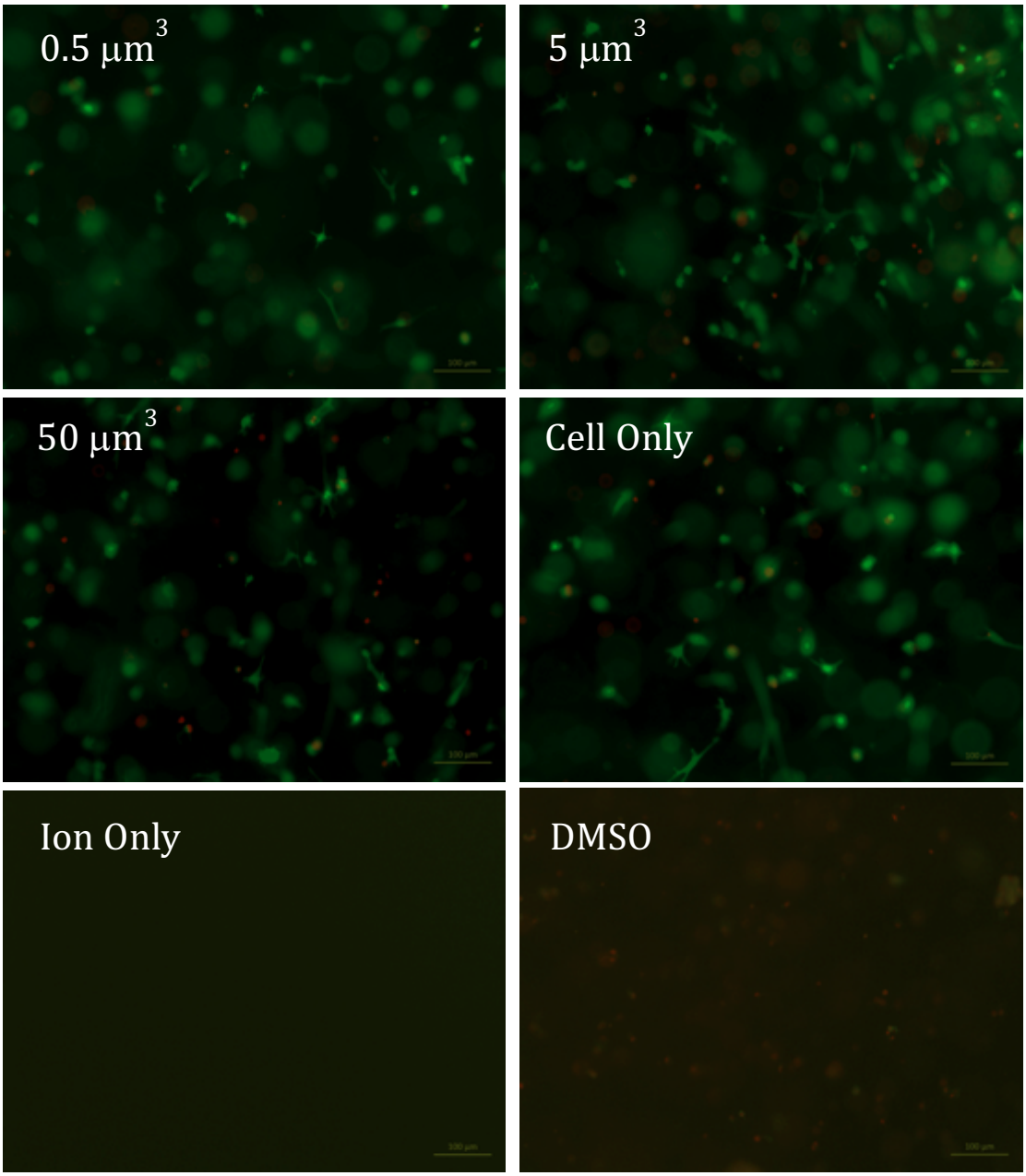

Figure 5.16 The effect of increasing doses of ions generated by increasing volumes (0.5µm³-50µm³) of cobalt chrome particles per cell on the viability of primary astrocytes and microglia in co-culture after 48 hours, assessed using a live dead assay. The ion only control was produced from the greatest cobalt chrome particle dose (50µm³ cobalt chrome debris per cell). The green, calcein, fluorescent dye stains living cells and the red, ethidium homodimer, stains dead cells red.

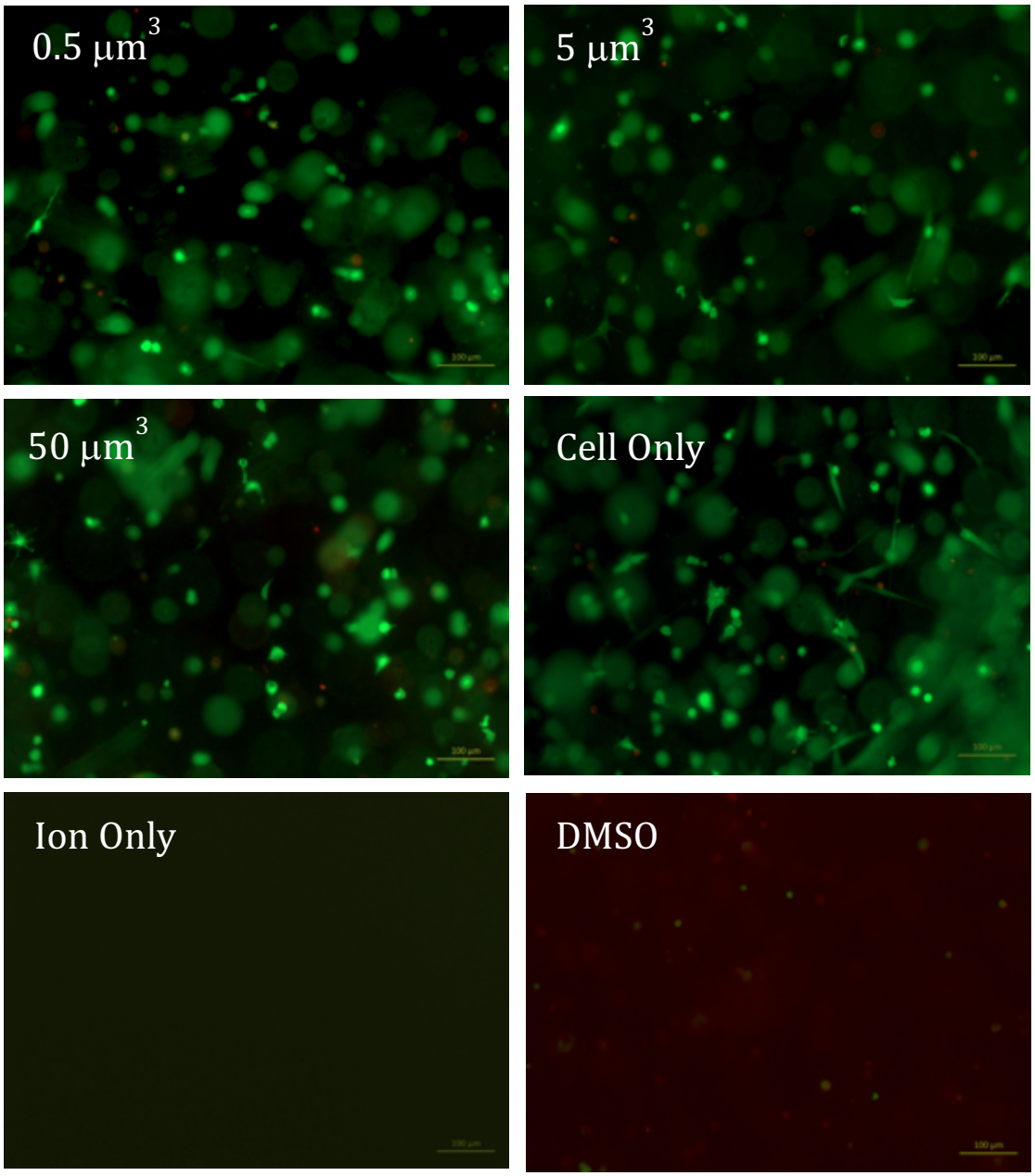

Figure 5.17 The effect of increasing doses of ions generated by increasing volumes (0.5µm^3-50µm^3) of cobalt chrome particles per cell on the viability of primary astrocytes and microglia in co-culture after five days in culture, assessed using a live dead assay. The ion only control was produced from the greatest cobalt chrome particle dose (50µm^3 cobalt chrome debris per cell). The green, calcein, fluorescent dye stains living cells and the red, ethidium homodimer, stains dead cells red.

5.4.2.2 The effect of cobalt chromium ions on the viability of primary astrocytes in isolation

Primary astrocytes in isolation were cultured with increasing concentrations of cobalt chromium ions over a five-day period (the cobalt chromium ions released from 50µm³, 5µm³ and 0.5µm³ cobalt chrome particle doses following a 24 hour incubation at 37°C in 5% (v/v) CO_2 in air). After 48 hours and five days a live dead assay was performed to determine the effect of cobalt chromium ions on primary astrocyte viability (Figure 5.18). Live dead images showing the effect of ions form cobalt chrome wear particles wear particles on the viability of primary astrocytes in isolation after 48 hours and five days in culture can be seen in Figures 5.19 and 5.20 respectively.

The primary astrocytes in isolation had similar proportions of viable cells after two and five days in culture, 88.2% and 87.7% living cells, respectively (Figure 5.18).

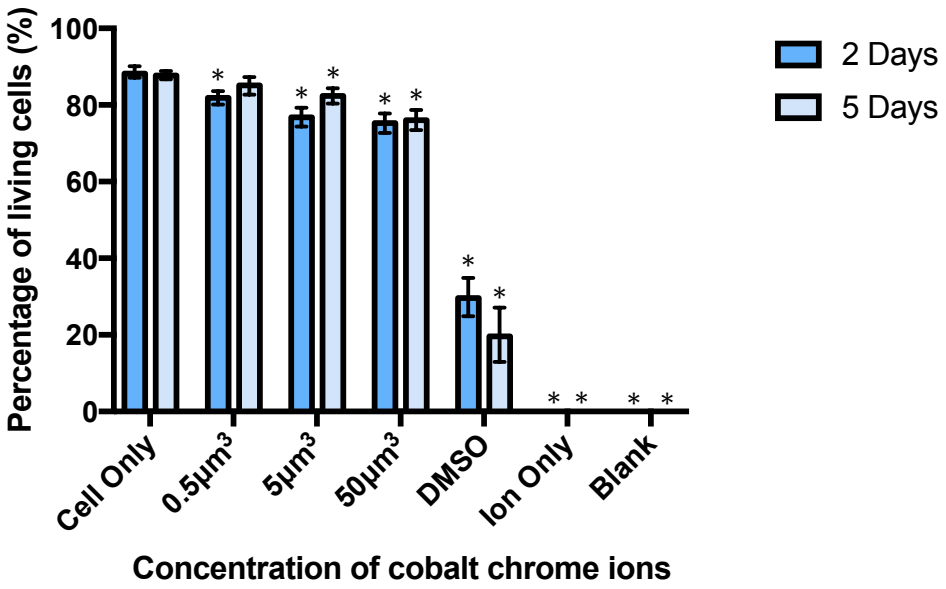

Figure 5.18 The effect of increasing concentrations of ions from wear particle doses (0.5µm³-50µm³) of cobalt chrome on the viability of primary astrocytes in isolation after two and five days in culture. Mean percentage of living cells ± 95% confidence intervals (six replicates per condition). DMSO was used as a positive control, an ion only negative control was also used. An asterisk indicates a significant reduction in viability ($p<0.05$) when compared with cell only negative control using Two-way ANOVA.

When primary astrocytes in isolation were cultured with the highest concentration of cobalt chromium ions (ions released from the highest cobalt chrome particle dose of 50µm³ debris per cell) a significant reduction in viability was observed at both the 48 hours and five-day time point when compared to the cell only negative control. After two

days in culture the percentage of viable primary astrocytes was reduced to 75.3% and was reduced to 76.1%, after five days.

Upon culture of primary astrocytes in isolation with the middle concentration of cobalt chromium ions (ions released from the 5μm^3 cobalt chrome debris per cell particle dose after a 24 hour incubation at 37°C in 5% (v/v) CO_2 in air) a significant reduction in viability was observed after two and five days in culture when compared to the cell only negative control. After 48 hours the percentage of living cells had fallen to 76.8% and to 82.4% after five days in culture

An adverse effect on viability was observed after 48 hours when primary astrocytes were cultured with the lowest concentration of cobalt chromium ions (the concentration of cobalt chromium ions released from 0.5μm^3 cobalt chrome wear particles per cell after 24 hours incubation) the percentage of viable cells fell to 81.9% at this time point, the effect was no longer significant after five days in culture.

In comparison with the cell only negative control, a continuing reduction in viability was seen when primary astrocytes were cultured with the DMSO positive control. After two days in culture with DMSO the percentage of living primary astrocytes had fallen to 29.7% living cells and was reduced further to 19.6% by five days.

No fluorescence was seen in the ion only control at either time point tested.

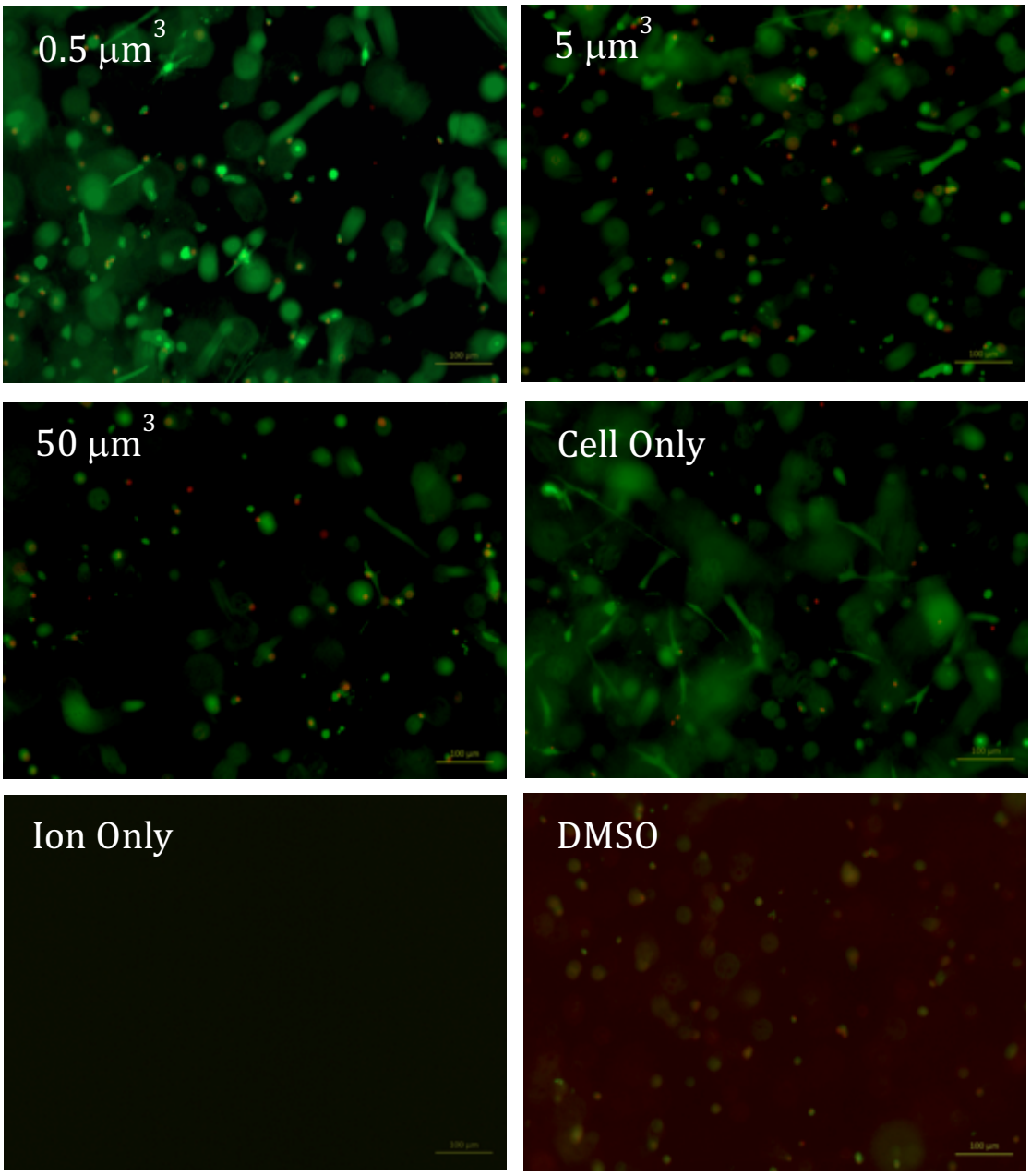

Figure 5.19 The effect of increasing doses of ions generated by increasing volumes (0.5μm³-50μm³) of cobalt chrome particles per cell on the viability of primary astrocytes in isolation after 48 hours, assessed using a live dead assay. The ion only control was produced from the greatest cobalt chrome particle dose (50μm³ cobalt chrome debris per cell). The green, calcein, fluorescent dye stains living cells and the red, ethidium homodimer, stains dead cells red.

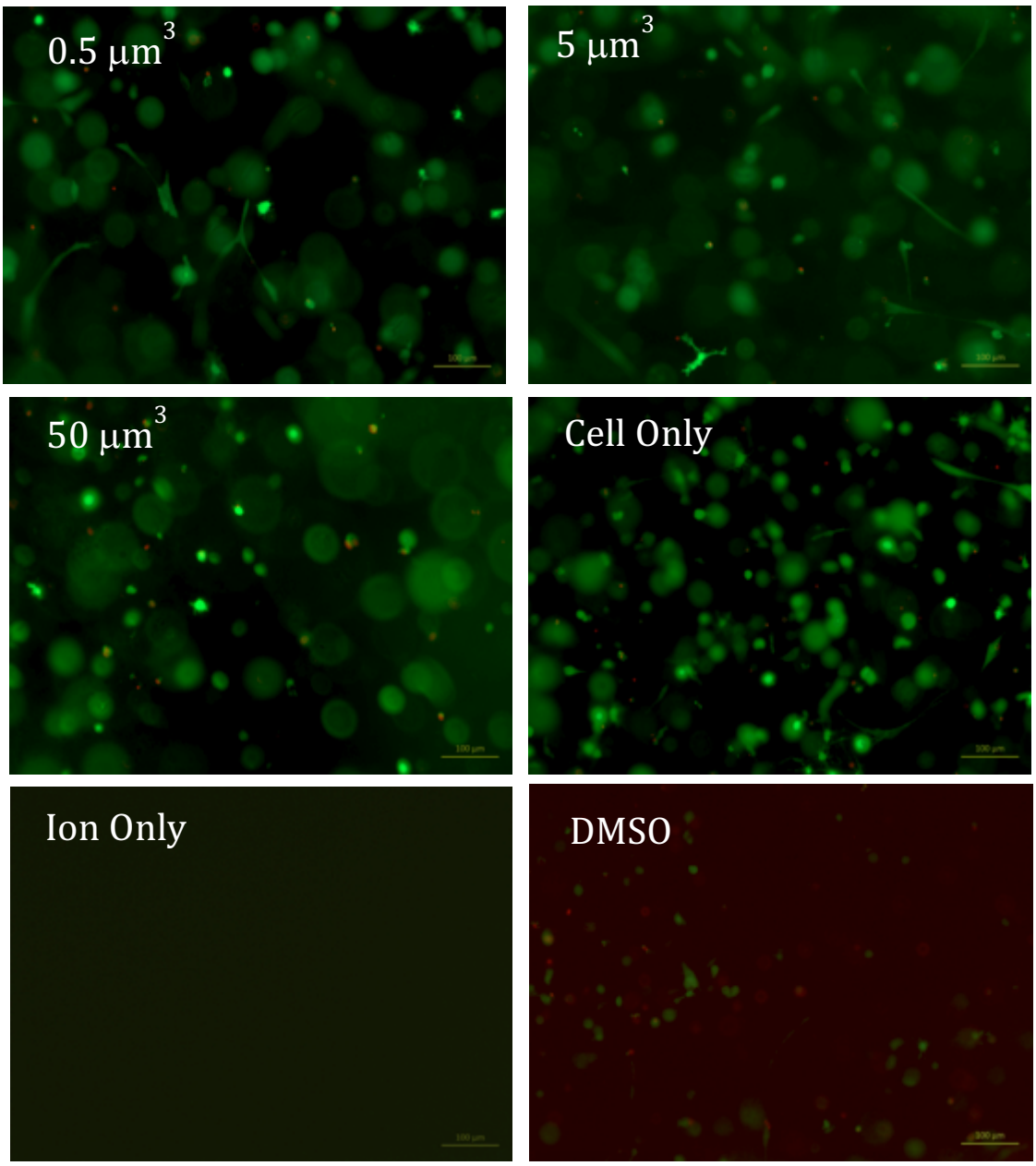

Figure 5.20 The effect of increasing doses of ions generated by increasing volumes (0.5μm³-50μm³) of cobalt chrome particles per cell on the viability of primary astrocytes in isolation after five days in culture, assessed using a live dead assay. The ion only control was produced from the greatest cobalt chrome particle dose (50μm³ cobalt chrome debris per cell). The green, calcein, fluorescent dye stains living cells and the red, ethidium homodimer, stains dead cells red.

A summary of the effects of cobalt chromium ions on the viability of primary astrocytes and microglia in co-culture and astrocytes in isolation is presented in Table 5.5.

Table 5.5 The effect of cobalt chromium ions on the viability of primary astrocytes and microglia in co-culture and primary astrocytes in isolation using an advanced 3D cell culture system and assessed using a live dead assay. Cells with significantly decreased viabilities (two-way ANOVA with Tukey post hoc analysis) $p<0.05$ compared to the cell only negative control are indicated with an asterisk.

	Astrocytes and microglia				**Astrocytes in isolation**			
	$0.5\mu m^3$	$5\mu m^3$	$50\mu m^3$	DMSO	$0.5\mu m^3$	$5\mu m^3$	$50\mu m^3$	DMSO
Day 2				*	*	*	*	*
Day 5		*		*		*	*	*

5.4.2.3 The effect of metallic ions released from stainless steel wear particles on the viability of primary astrocytes and microglia.

Primary astrocytes and microglia were cultured with increasing concentrations of ions released from increasing stainless steel particle volumes over a five-day period. A live dead assay was performed after two and five days in culture (Figure 5.21). Live dead images showing the effect of ions from stainless steel wear particles on the viability of primary astrocytes and microglia in co-culture after 48 hours and five days in culture can be seen in Figures 5.22 and 5.23 respectively.

Primary astrocytes and microglia in co-culture continued to increase in number for the duration of the study. After 48 hours in culture 78.1% of the cells were viable and after five days 91.5% of the cells were viable (Figure 5.21).

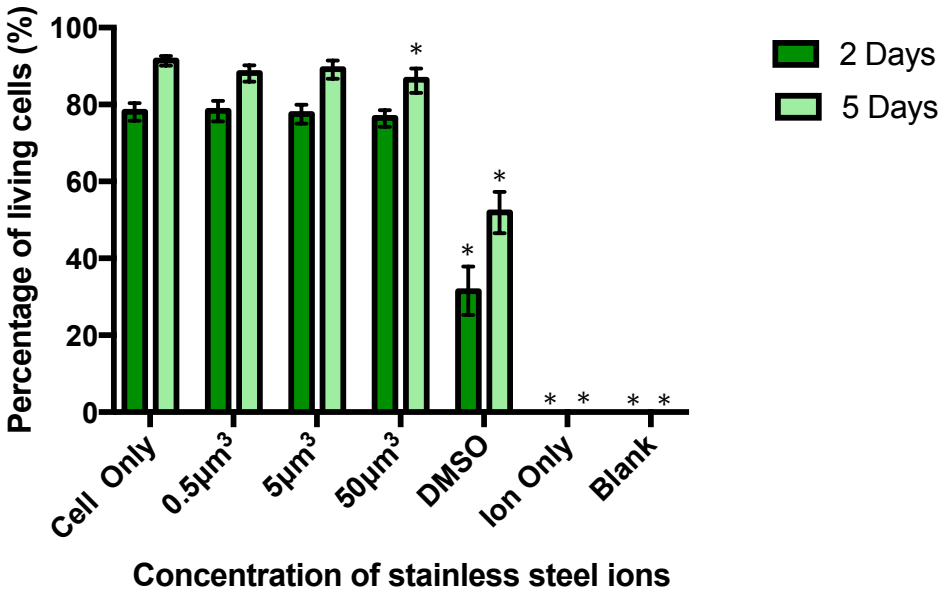

Figure 5.21 The effect of increasing concentrations of ions from wear particle doses (0.5µm³-50µm³) of stainless steel on the viability of primary astrocytes and microglia in co-culture after two and five days in culture. Mean percentage of living cells ± 95% confidence intervals (six replicates per condition). DMSO was used as a positive control, an ion only negative control was also used. An * Indicates a significant reduction in viability ($p<0.05$) when compared with cell only negative control using Two-way ANOVA.

No adverse effect on viability was observed after two days when primary astrocytes and microglia were cultured with the highest dose of stainless steel ions, ions released from the 50µm³ stainless steel wear particle volume. However, after five days in culture a significant reduction in viability was observed when primary astrocytes and microglia in

co-culture were cultured with the highest concentration of ions from stainless steel wear particles. A reduction in viability from 91.5% in the cell only control to 86.5% viable cells was observed at this time point.

No adverse effects on viability were observed after two and five days when primary astrocytes and microglia were cultured with the lower concentrations of ions released from increasing stainless steel wear particle volumes (5μm^3 and 0.5μm^3 stainless steel particle volumes) when compared to the cell only negative control.

The DMSO positive control adversely affected the viability of primary astrocytes and microglia cultured in a 3D collagen matrix over the five-day investigation. After two days in culture only 31.4% of the primary astrocytes and microglia were viable. After five days 51.9% of the cells were viable.

No fluorescence was seen in the ion only control gels at either time point tested.

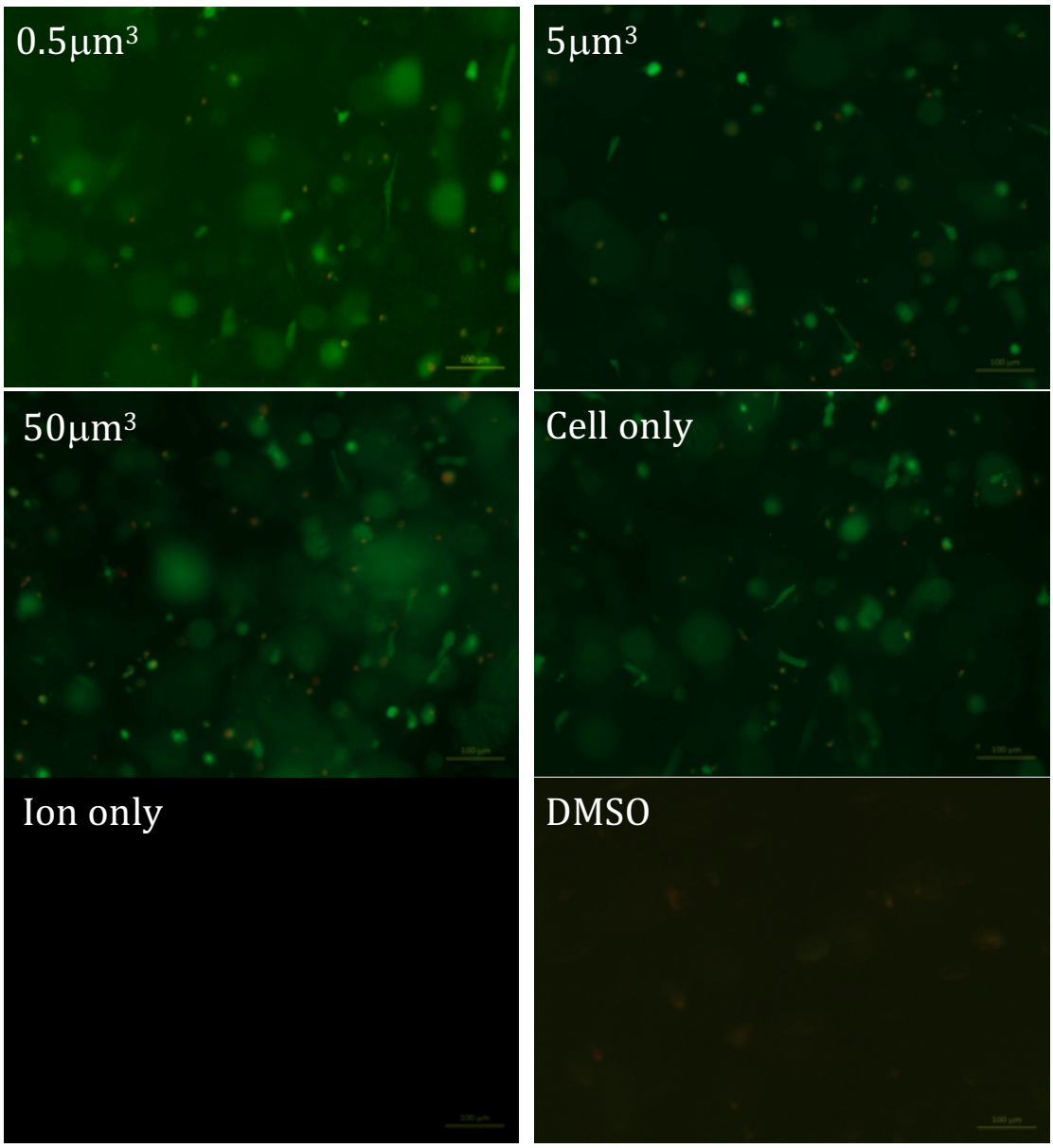

Figure 5.22 The effect of increasing doses of ions generated by increasing volumes (0.5µm^3-50µm^3) of stainless steel particles per cell on the viability of primary astrocytes and microglia in co-culture after 48 hours assessed using a live dead assay. The ion only control was produced from the greatest stainless steel particle dose (50µm^3 stainless steel debris per cell). The green, calcein, fluorescent dye stains living cells and the red, ethidium homodimer, stains dead cells red.

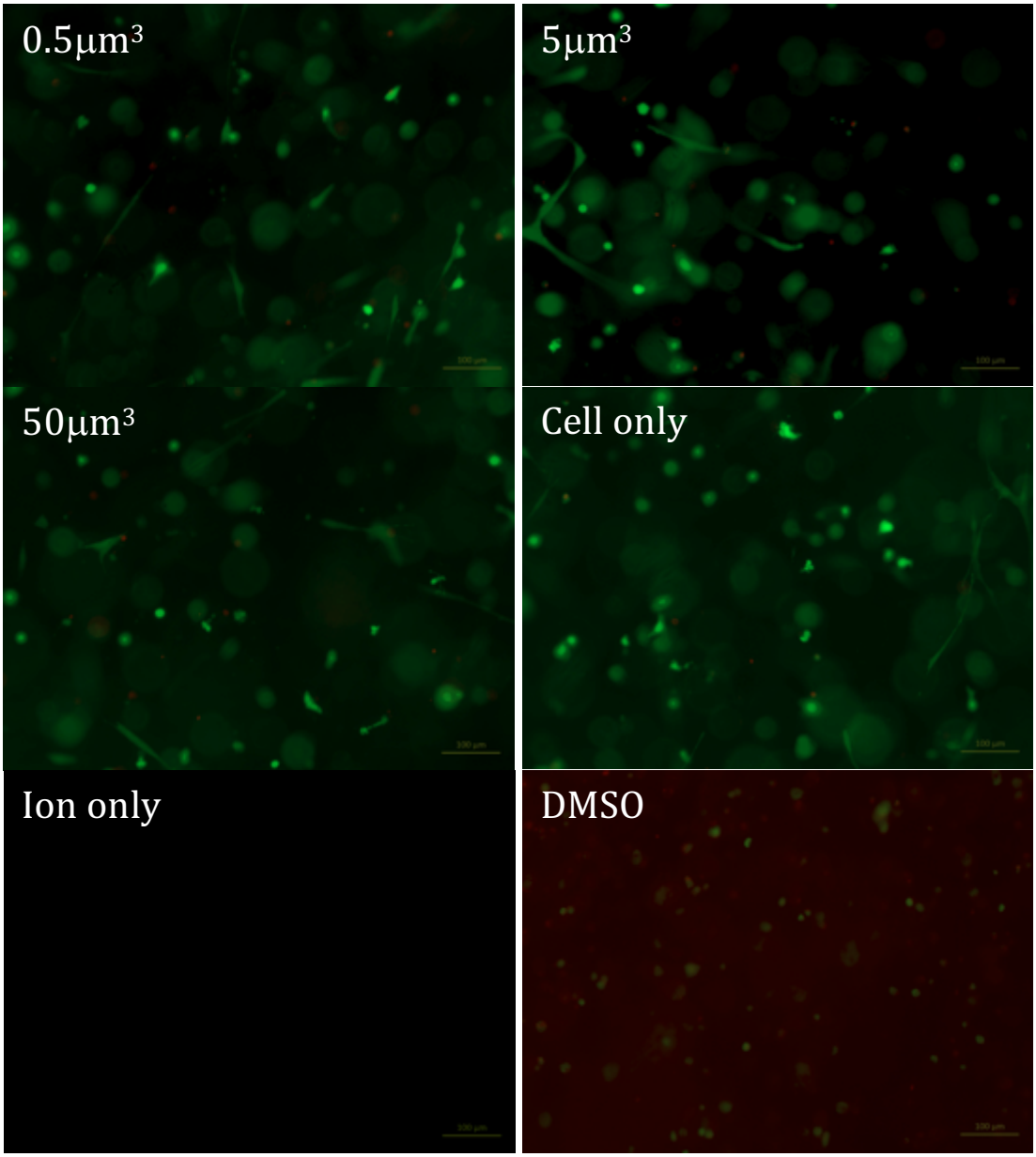

Figure 5.23 The effect of increasing doses of ions generated by increasing volumes (0.5µm³-50µm³) of stainless steel particles per cell on the viability of primary astrocytes and microglia in co-culture after five days in culture assessed using a live dead assay. The ion only control was produced from the greatest stainless steel particle dose (50µm³ stainless steel debris per cell). The green, calcein, fluorescent dye stains living cells and the red, ethidium homodimer, stains dead cells red.

5.4.2.4 The effect of metallic ions released from stainless steel wear particles on the viability of primary astrocytes in isolation.

Primary astrocytes in isolation were cultured with increasing concentrations of ions released from increasing stainless steel particle doses for five days in culture. A live dead assay was performed after two and five days in culture to assess the effect of ions on cell viability (Figure 5.24). The Live dead images showing the effect of ions from stainless steel wear particles wear particles on the viability of primary astrocytes in isolation after 48 hours and five days in culture can be seen in Figures 5.25 and 5.26 respectively.

The primary astrocytes in isolation maintained a high level of living cells for the duration of the experiment. After two days in culture in a 3D collagen hydrogel 86.5% of the primary astrocytes were viable, this level of viability remained constant as the percentage of living cells after five days in culture was a very similar 86.8% (Figure 5.24)

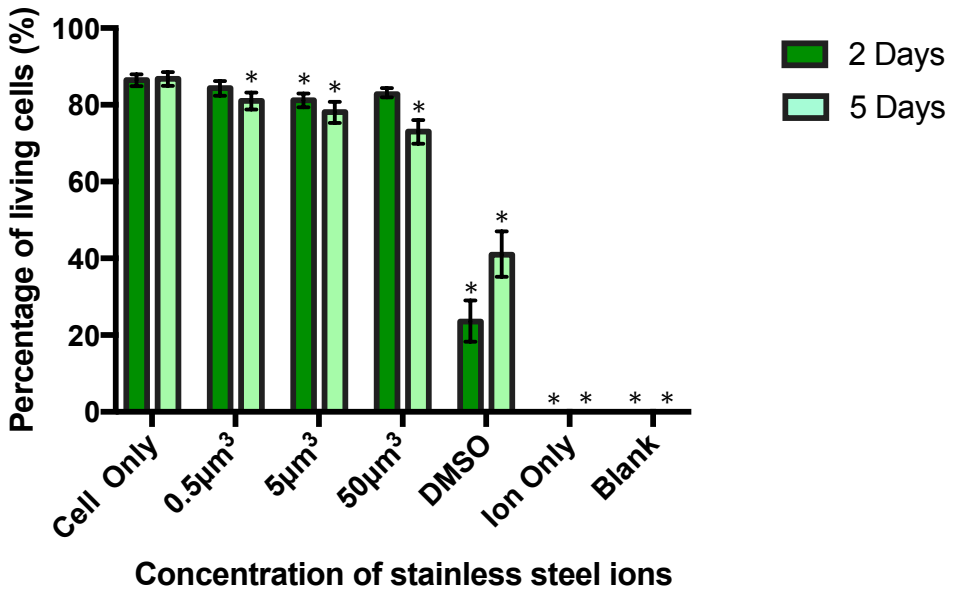

Figure 5.24 The effect of increasing concentrations of ions from wear particle doses (0.5µm³-50µm³) of stainless steel on the viability of primary astrocytes in isolation after two and five days in culture. Mean percentage of living cells ± 95% confidence intervals (six replicates per condition). DMSO was used as a positive control, an ion only negative control was also used. An * Indicates a significant reduction in viability ($p<0.05$) when compared with cell only negative control using Two-way ANOVA.

After 48 hours in culture with the ions released from the mid 5µm³ stainless steel particle dose an adverse effect on viability was observed. With the middle ion concentration (from the 5µm3 debris per cell dose), the percentage of viable cells was reduced from

86.5% in the cell only gels to 81.2%. No significant effect on viability was observed with the other ion concentrations at this time point.

Interestingly after five days in culture primary astrocytes in isolation cultured with the ions released from all particle doses demonstrated significant adverse effects on the cell viability when compared to the cell only negative control. Only 73.0% of the primary astrocytes cultured with the ions released from the highest stainless steel particle dose were viable, only 78.1% of cells were living when cultured with ions released from the 5μm^3 stainless steel debris per cell particle dose and only 81.1% of cells were living when cultured with ions released from the 0.5μm^3 stainless steel debris per cell particle dose when compared to 86.8% viable cells in the cell only negative control.

Significant reductions in the viability of primary astrocytes were detected when the cells were cultured with the DMSO positive control. After 48 hours only 23.5% of the cells were viable and after five days the percentage of viable cells was 41.0%.

No fluorescence was seen in the ion only control gels at either time point tested.

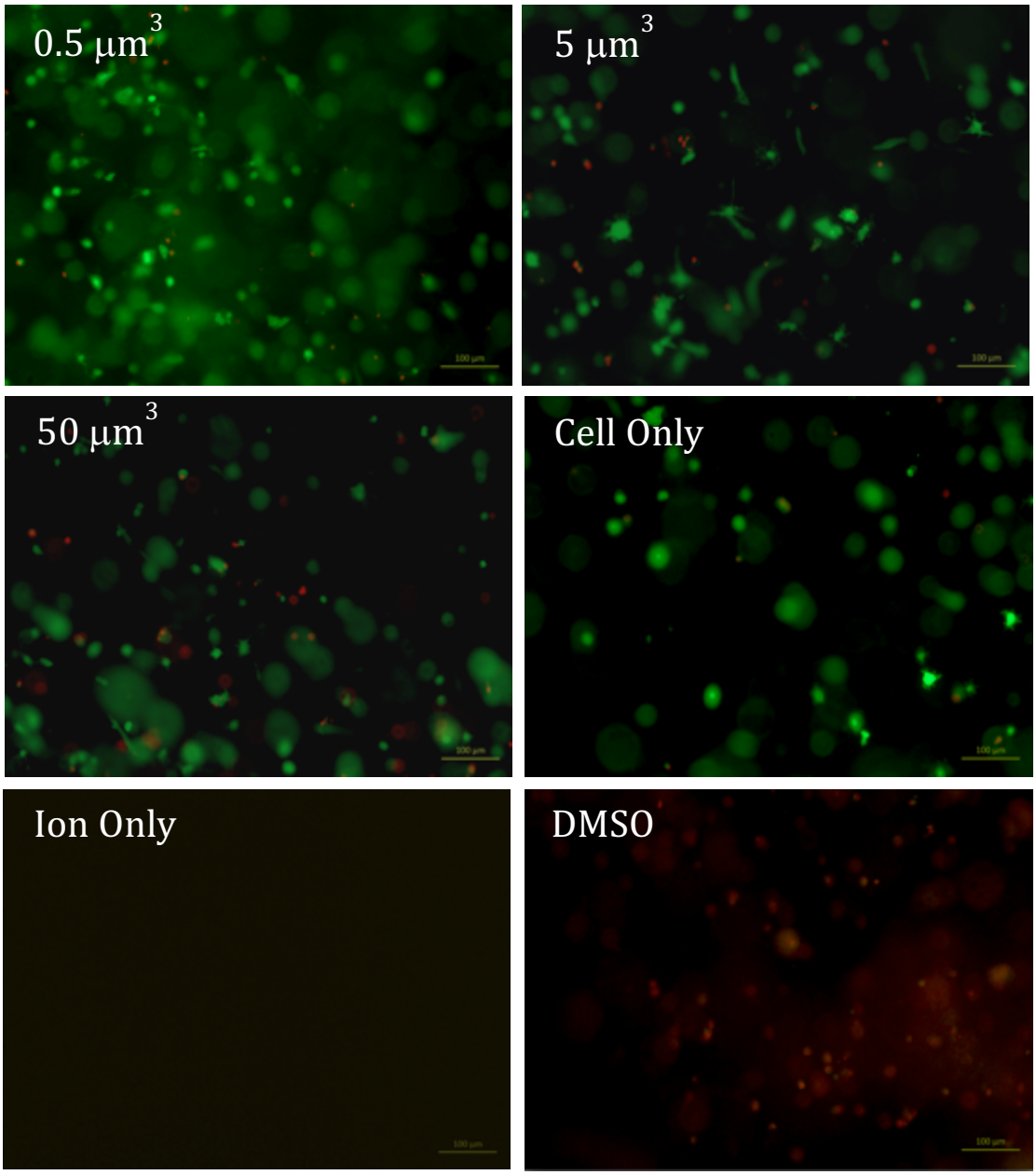

Figure 5.25 The effect of increasing doses of ions generated by increasing volumes (0.5µm^3-50µm^3) of stainless steel particles per cell on the viability of primary astrocytes in isolation after 48 hours in culture, assessed using a live dead assay. The ion only control was produced from the greatest stainless steel particle dose (50µm^3 stainless steel debris per cell). The green, calcein, fluorescent dye stains living cells and the red, ethidium homodimer, stains dead cells red.

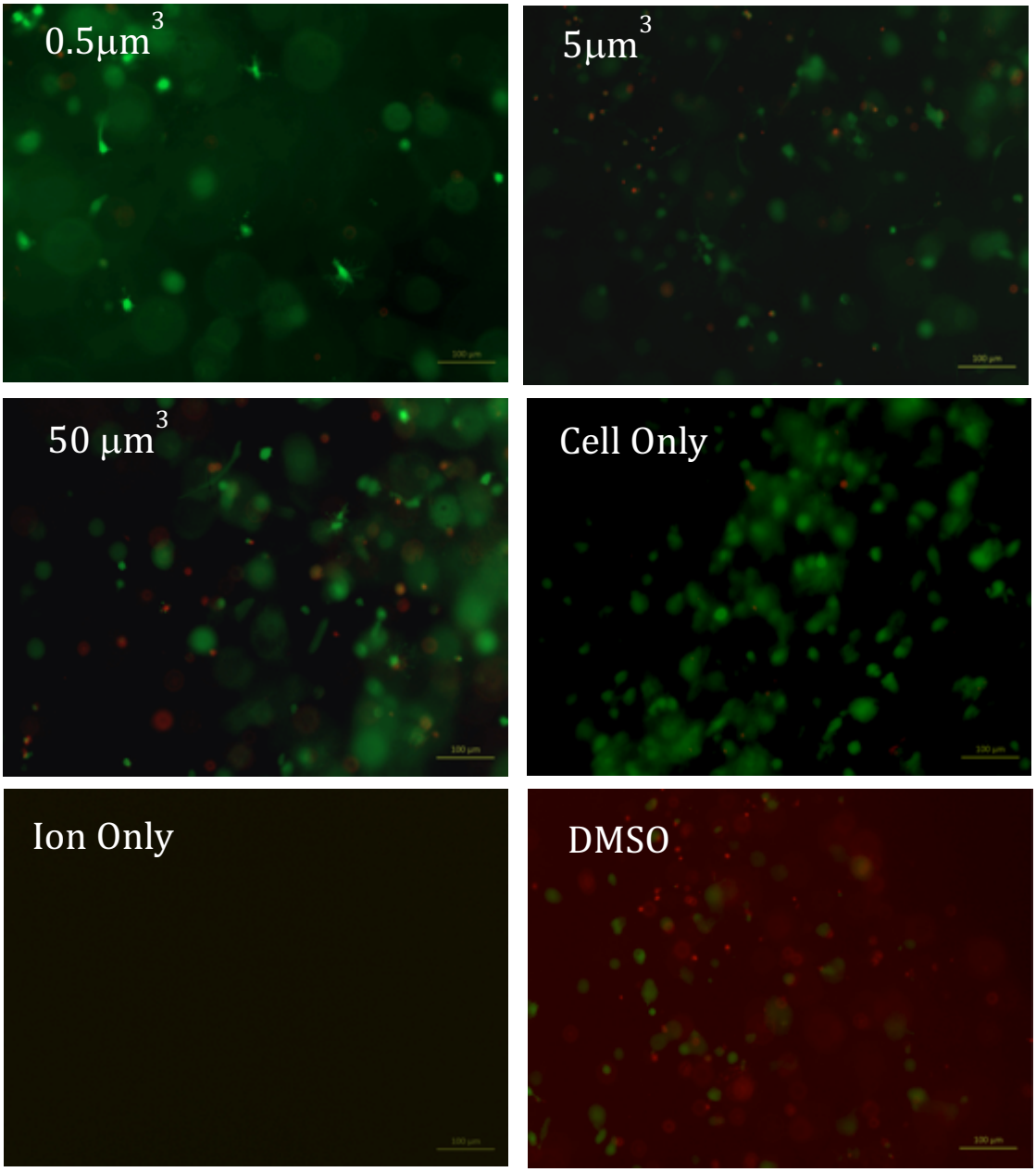

Figure 5.26 The effect of increasing doses of ions generated by increasing volumes (0.5µm^3-50µm^3) of stainless steel particles per cell on the viability of primary astrocytes in isolation after five days in culture, assessed using a live dead assay. The ion only control was produced from the greatest stainless steel particle dose (50µm^3 stainless steel debris per cell). The green, calcein, fluorescent dye stains living cells and the red, ethidium homodimer, stains dead cells red.

A summary of the effects of stainless steel ions on the viability of primary astrocytes and microglia can be seen in Table 5.6 below.

Table 5.6 The effect of ions released from increasing stainless steel particle volumes on the viability of primary astrocytes and microglia in co-culture and primary astrocytes in isolation using an advanced 3D cell culture system and assessed using a live dead assay. Cells with significantly decreased viabilities $p<0.05$ (two-way ANOVA with Tukey post hoc analysis) compared to the cell only negative control were indicated with an asterisk.

	Astrocytes and microglia				Astrocytes in isolation			
	0.5µm³	5µm³	50µm³	DMSO	0.5µm³	5µm³	50µm³	DMSO
Day 2				*		*		*
Day 5			*	*	*	*	*	*

5.4.3 The effect of cobalt chrome and stainless steel wear particles on glial fibrillary acidic protein (GFAP) expression by primary astrocytes in the presence and absence of microglia.

Primary astrocytes and microglia in co-culture and astrocytes in isolation were cultured with increasing doses of cobalt chrome and stainless steel wear particles (0.5μm^3, 5μm^3 and 50μm^3 wear debris per cell) for 48 hours and five days in a 3D collagen gel. Immunocytochemistry was used to determine the effects of metallic wear particles on the production of GFAP by primary astrocytes in the presence and absence of microglia. Images of GFAP expression profiles of the response of astrocytes and microglia in co-culture and astrocytes in isolation in response to cobalt chrome wear particles after two and 5 days can be seen in Figures 5.27, 5.28 and 5.29 and 5.30 respectively. Images of GFAP expression profiles of the response of astrocytes and microglia in co-culture and astrocytes in isolation in response to stainless steel wear particles after two and 5 days can be seen in Figures 5.31, 5.32 and 5.33 and 5.34 respectively.

A total of six images were taken per gel and six gels were produced for each test condition, yielding 36 images for each condition. Each image was graded depending on GFAP expression. A – grade was indicative of no GFAP expression and a + was indicative of the cells expressing GFAP. More detailed tables showing the grading of every image can be seen in Appendix 2 Tables A-H.

5.4.3.1 The effects of cobalt chrome wear particles on GFAP expression by primary astrocytes in the presence of microglia after two and five days.

When primary astrocytes and microglia were cultured with the highest cobalt chrome particle dose of 50μm^3 cobalt chrome per cell GFAP expression was observed (+) at both time points tested, this was compared to the cell only controls where no GFAP was expressed as the cells were not reactive. When primary astrocytes and microglia were cultured with 5μm^3 and 0.5μm^3 cobalt chrome particle concentrations no GFAP expression was observed after 48 hours, however GFAP (+) was expressed when primary astrocytes and microglia were exposed to both 5μm^3 and 0.5μm^3 cobalt chrome particle doses after five days. Once again the cell only negative control cells did not express GFAP (Table 5.7).

Primary astrocytes and microglia as the cell only negative control did not express GFAP at any time point tested. Primary astrocytes and microglia cultured with the TGF-β1 positive control expressed GFAP (+) after both two and five days in culture.

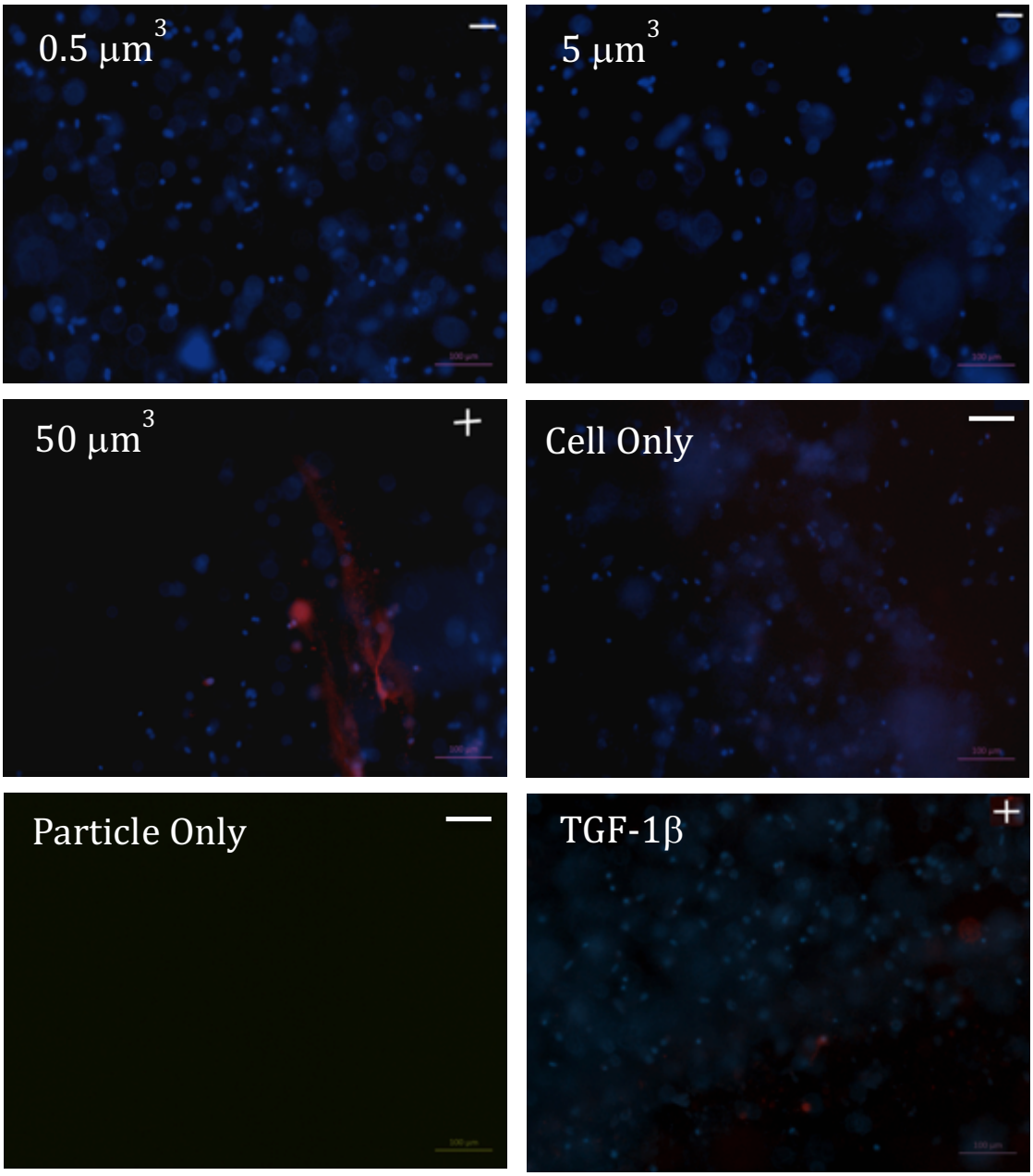

Figure 5.27 The effect of increasing cobalt chrome particle volumes (0.5μm³-50μm³ cobalt chrome particles per cell) on the expression of glial fibrillary acidic protein by primary astrocytes in the presence of microglia after 48 hours. The highest particle dose (50μm³ cobalt chrome particles per cell) was used as a particle only control. The genetic material is stained blue (Hoechst) and the intermediate filament protein, glial fibrillary acidic protein, stained red.

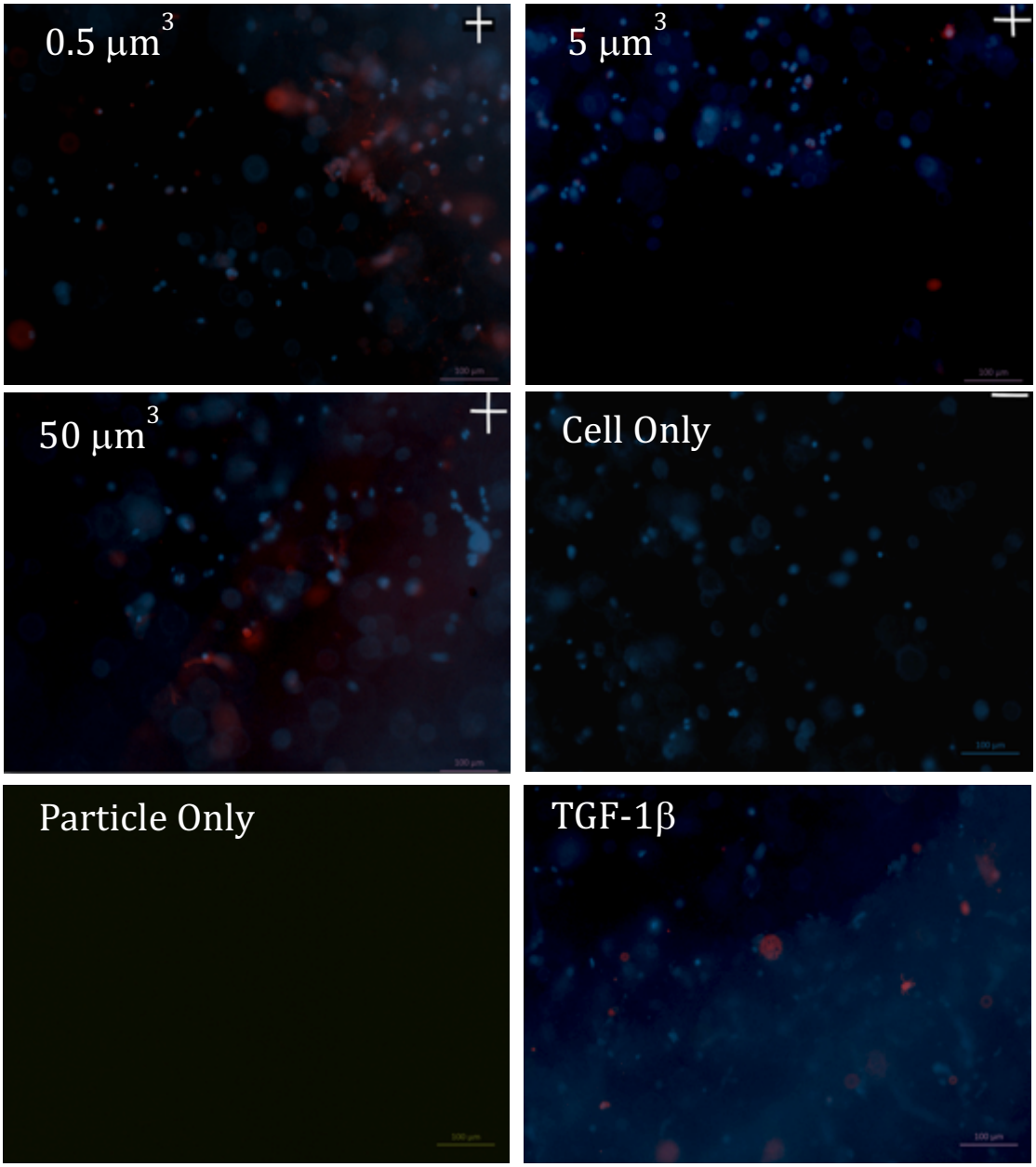

Figure 5.28 The effect of increasing cobalt chrome particle volumes (0.5µm^3-50µm^3 cobalt chrome particles per cell) on the expression of glial fibrillary acidic protein by primary astrocytes in the presence of microglia after five days in culture. The highest particle dose (50µm^3 cobalt chrome particles per cell) was used as a particle only control. The genetic material is stained blue (Hoechst) and the intermediate filament protein, glial fibrillary acidic protein, stained red.

5.4.3.2 The effects of cobalt chrome wear particles on GFAP expression by primary astrocytes in isolation.

When primary astrocytes were cultured in isolation with the highest cobalt chrome particle dose (50μm^3 cobalt chrome debris per cell) no GFAP expression was observed at either time point tested (Table 5.8).

Primary astrocytes cultured with the lower 5μm^3 and 0.5μm^3 did not express GFAP after 48 hours, however GFAP (+) was detected when primary astrocytes in isolation were exposed to both 5μm^3 and 0.5μm^3 cobalt chrome particle doses after five days. Once again the cell only negative control cells did not express GFAP (Table 5.8) at either time point tested. Primary astrocytes cultured with the TGF-β1 positive control expressed GFAP (+) after both two and five days in culture

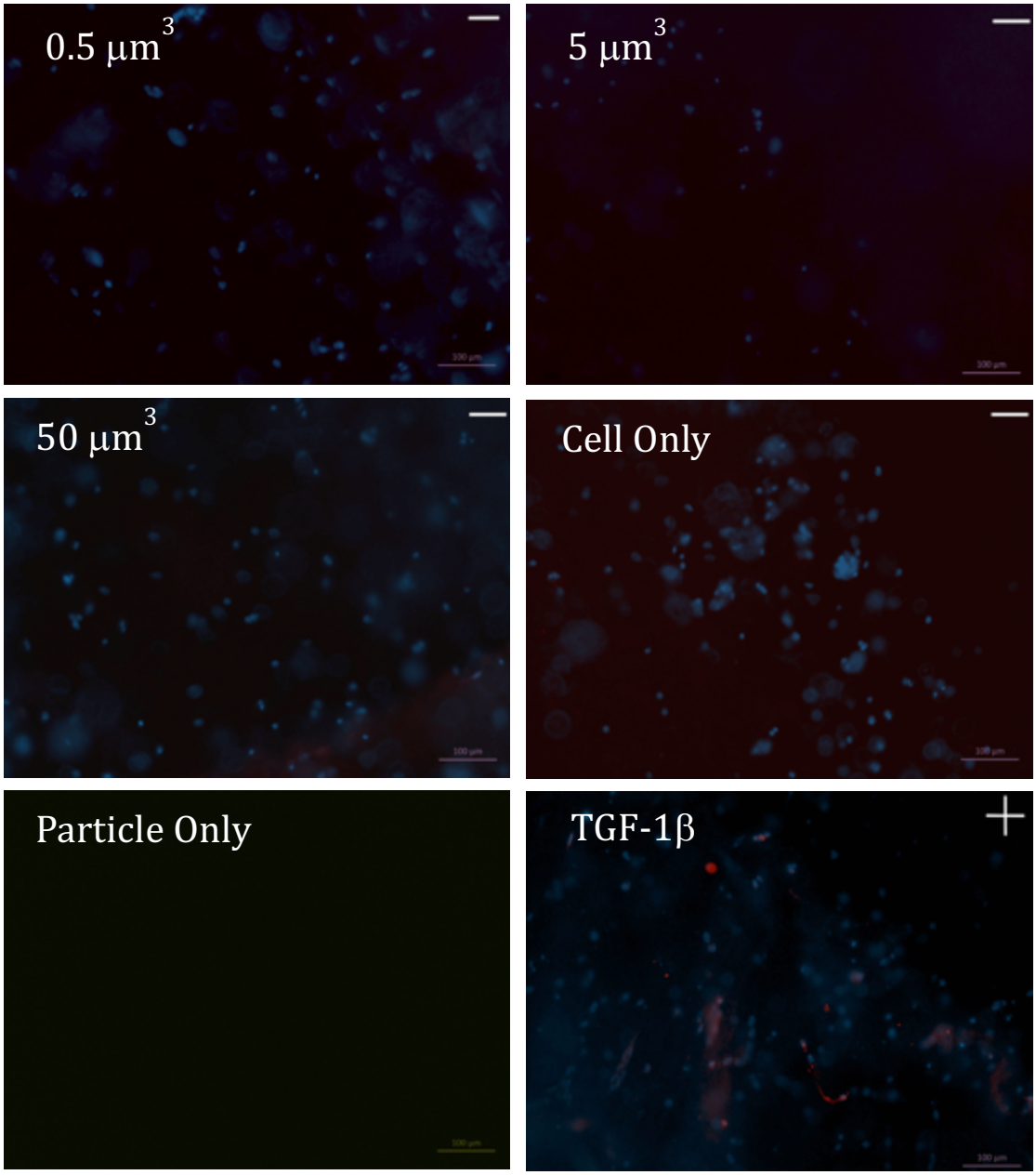

Figure 5.29 The effect of increasing cobalt chrome particle volumes (0.5μm³-50μm³ cobalt chrome particles per cell) on the expression of glial fibrillary acidic protein by primary astrocytes in the absence of microglia after 48 hours. The highest particle dose (50μm³ cobalt chrome particles per cell) was used as a particle only control. The genetic material is stained blue (Hoechst) and the intermediate filament protein, glial fibrillary acidic protein, stained red.

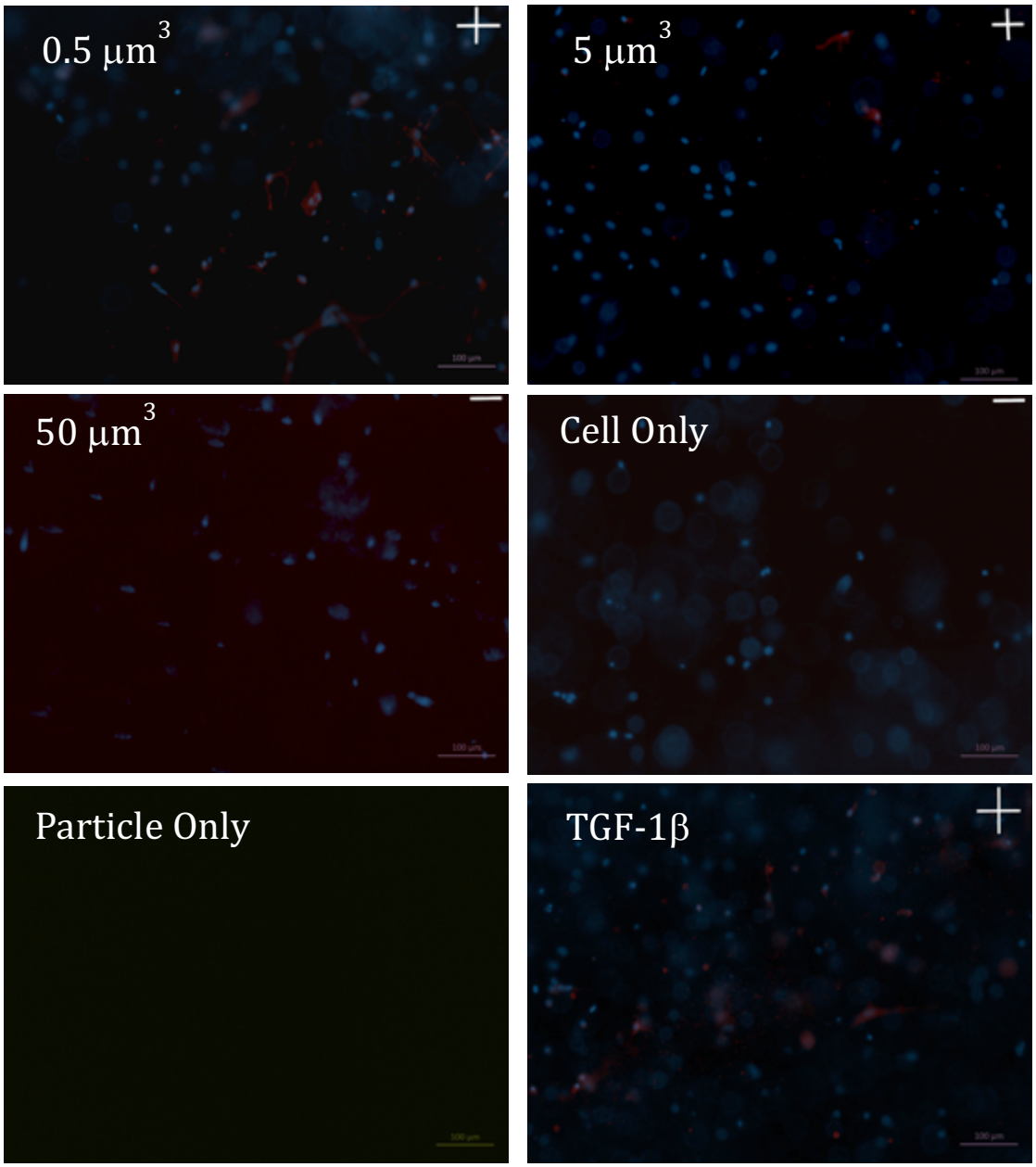

Figure 5.30 The effect of increasing cobalt chrome particle volumes (0.5μm^3-50μm^3 cobalt chrome particles per cell) on the expression of glial fibrillary acidic protein by primary astrocytes in the absence of microglia after five days in culture. The highest particle dose (50μm^3 cobalt chrome particles per cell) was used as a particle only control. The genetic material is stained blue (Hoechst) and the intermediate filament protein, glial fibrillary acidic protein, stained red.

5.4.3.3 The effects of stainless steel wear particles on glial fibrillary acidic protein GFAP expression by primary astrocytes in the presence of microglia.

No GFAP expression was observed when primary astrocytes and microglia were exposed to stainless steel particles (doses $0.5\mu m^3$, $5\mu m^3$ and $50\mu m^3$ stainless steel debris per cell) at any time points tested (Table 5.7).

There was no expression of GFAP in the cell only negative control gels, at any time point tested. Primary astrocytes and microglia cultured with the TGF-β1 positive control expressed GFAP (+) after both two and five days in culture. Images of GFAP expression profiles of the response of astrocytes and microglia in co-culture and astrocytes in isolation in response to stainless steel wear particles after two and five days can be seen in Figures 5.31, 5.32 and 5.33 and 5.34 respectively.

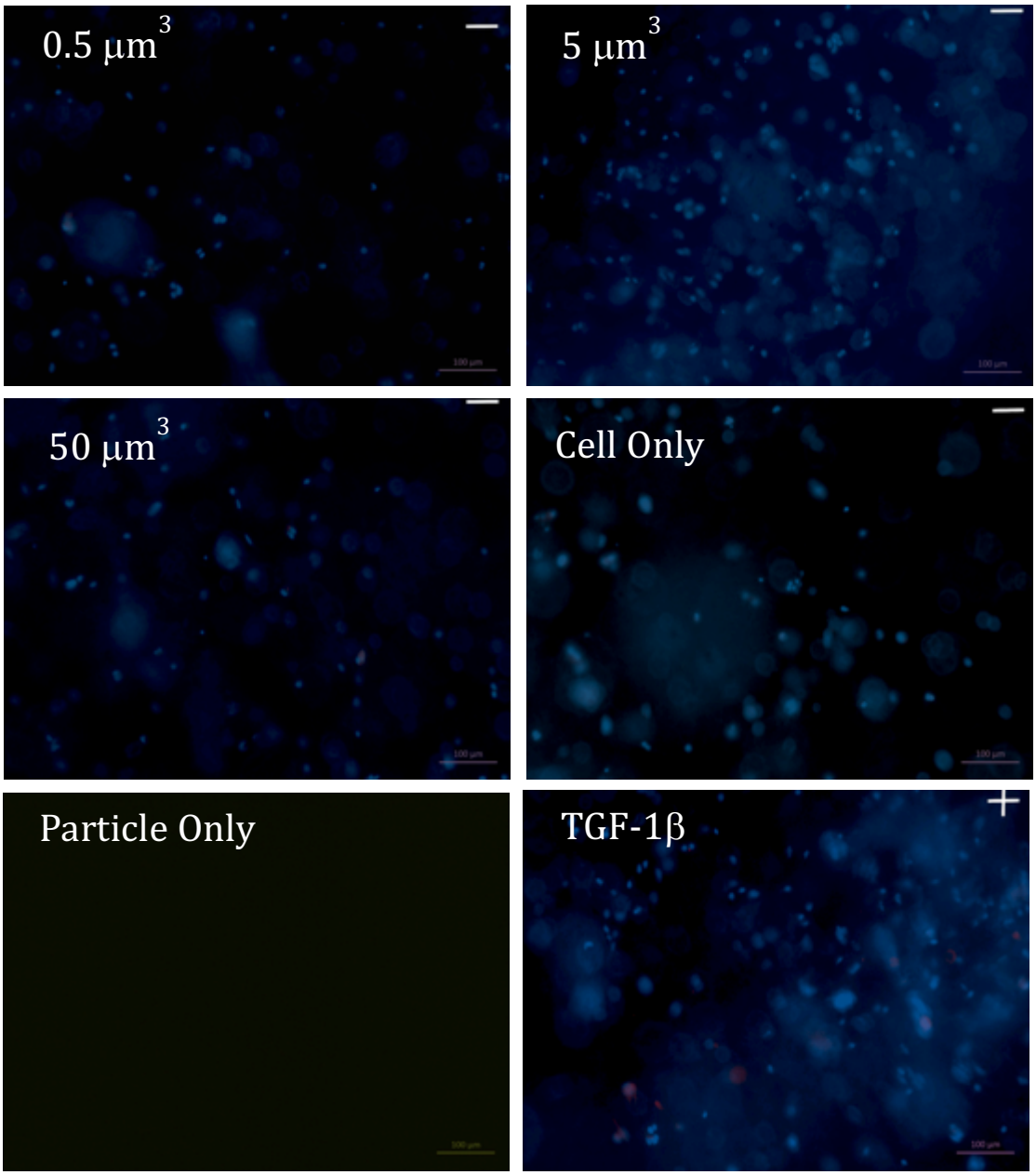

Figure 5.31 The effect of increasing stainless steel particle volumes (0.5μm^3-50μm^3 stainless steel particles per cell) on the expression of glial fibrillary acidic protein by primary astrocytes in the presence of microglia after 48 hours. The highest particle dose (50μm^3 stainless steel particles per cell) was used as a particle only control. The genetic material is stained blue (Hoechst) and the intermediate filament protein, glial fibrillary acidic protein, stained red.

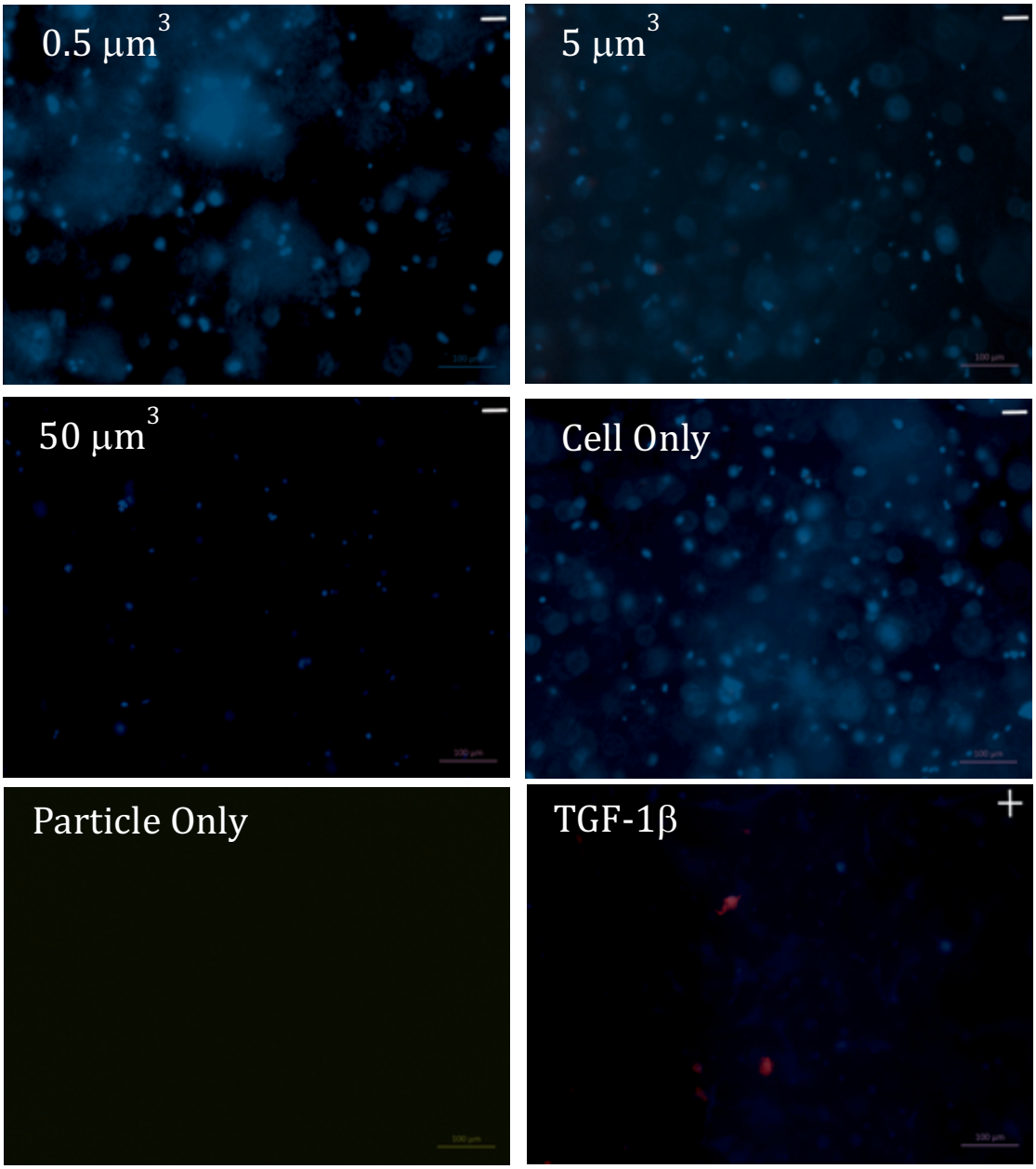

Figure 5.32 The effect of increasing stainless steel particle volumes (0.5μm^3-50μm^3 stainless steel particles per cell) on the expression of glial fibrillary acidic protein by primary astrocytes in the presence of microglia after five days in culture. The highest particle dose (50μm^3 stainless steel particles per cell) was used as a particle only control. The genetic material is stained blue (Hoechst) and the intermediate filament protein, glial fibrillary acidic protein, stained red.

5.4.3.4 The effects of stainless steel wear particles on glial fibrillary acidic protein GFAP expression by primary astrocytes in the absence of microglia.

Glial fibrillary acidic protein was not expressed when primary astrocytes in isolation were exposed to stainless steel particles (doses $0.5\mu m^3$, $5\mu m^3$ and $50\mu m^3$ stainless steel debris per cell) at any time point tested. The cell only negative control, primary astrocytes in isolation in supplemented media, did not express GFAP at either time point tested (Table 5.8).

Primary astrocytes in isolation cultured with the TGF-β1 positive control expressed GFAP (+) after both two and five days in culture.

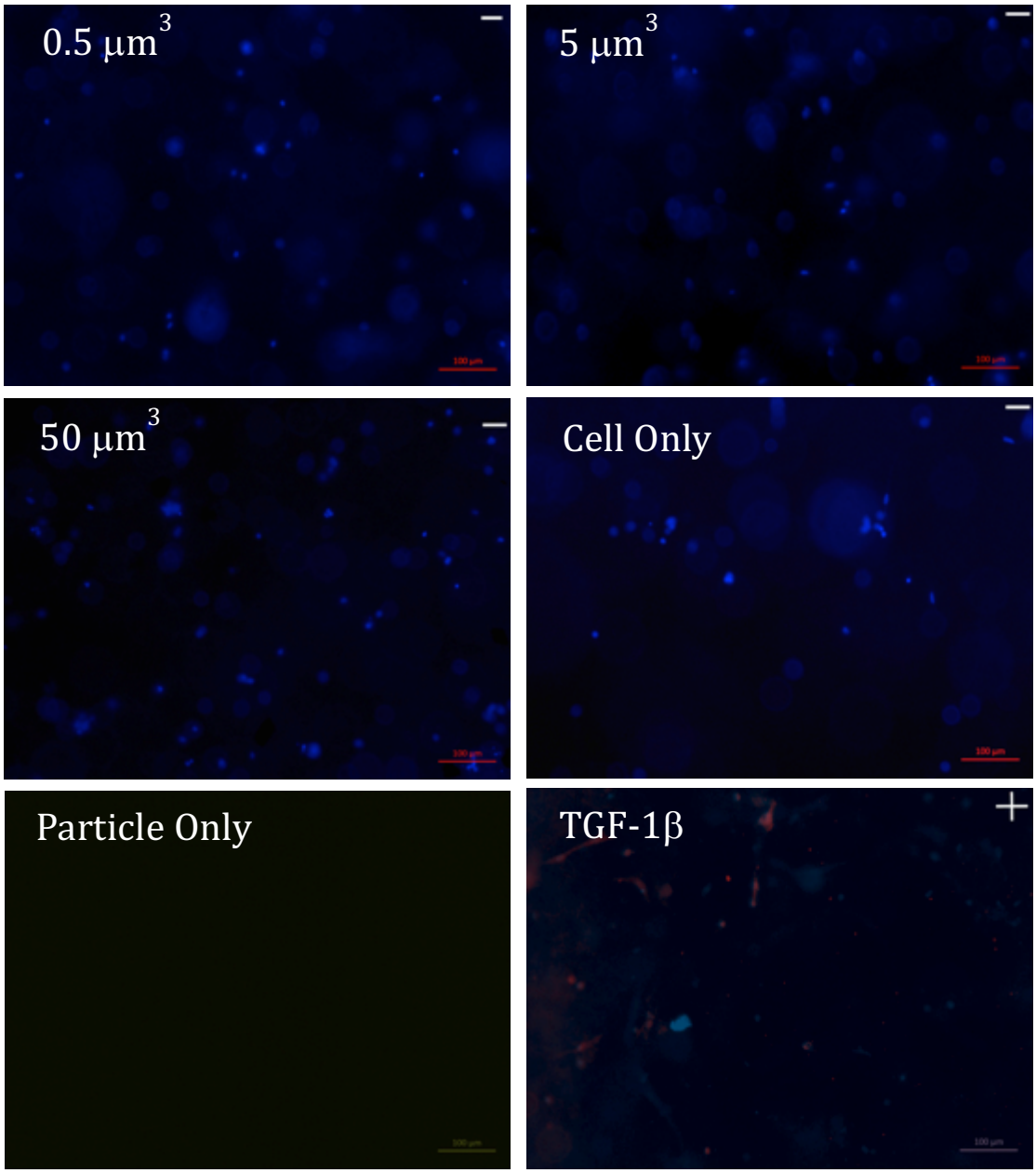

Figure 5.33 The effect of increasing stainless steel particle volumes (0.5µm³-50µm³ stainless steel particles per cell) on the expression of glial fibrillary acidic protein by primary astrocytes in the absence of microglia after 48 hours. The highest particle dose (50µm³ stainless steel particles per cell) was used as a particle only control. The genetic material is stained blue (Hoechst) and the intermediate filament protein, glial fibrillary acidic protein, stained red.

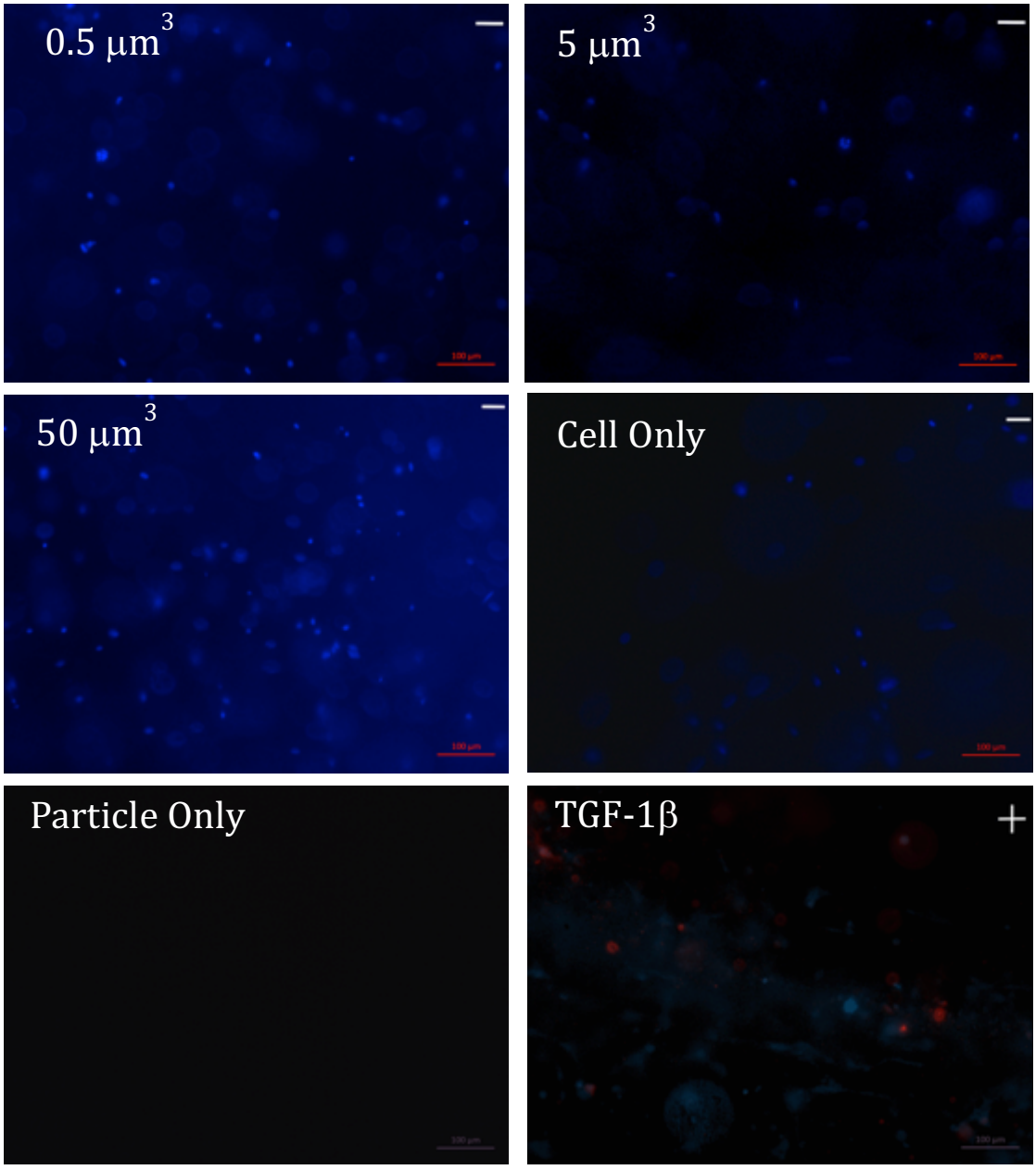

Figure 5.34 The effect of increasing stainless steel particle volumes (0.5µm³-50µm³ stainless steel particles per cell) on the expression of glial fibrillary acidic protein by primary astrocytes in the absence of microglia after five days in culture. The highest particle dose (50µm³ stainless steel particles per cell) was used as a particle only control. The genetic material is stained blue (Hoechst) and the intermediate filament protein, glial fibrillary acidic protein, stained red.

Table 5.7 The effects of cobalt chrome and stainless steel on the expression of GFAP by primary astrocytes in the presence of microglia after two and five days in culture.

Astrocytes and microglia	Cobalt chrome 2 days	Cobalt chrome 5 days	Stainless steel 2 days	Stainless steel 5 days
50 μm^3 debris per cell	+	+	-	-
5 μm^3 debris per cell	-	+	-	-
0.5 μm^3 debris per cell	-	+	-	+/- exactly 18 images expressing GFAP and 18 without
TGF-β1 Positive control	+	+	+	+
Cell only	-	-	-	-
Particle only	-	-	-	-
Blank	-	-	-	-

Note: The primary astrocytes and microglia were cultured with increasing particle volumes of cobalt chrome and stainless steel wear particles (0.5μm^3-50μm^3 particles per cell) for five days in culture. A cell only negative control was used. The highest particle dose (50μm^3 particles per cell) was used as a particle only control and acellular 100µl gels used as a blank reference control (6 replicates per condition).

Table 5.8 The effects of cobalt chrome and stainless steel on the expression of GFAP by primary astrocytes without microglia after two and five days in culture.

Astrocytes only	Cobalt chrome 2 days	Cobalt chrome 5 days	Stainless steel 2 days	Stainless steel 5 days
50 μm^3 debris per cell	-	-	-	-
5 μm^3 debris per cell	-	+	-	-
0.5 μm^3 debris per cell	-	+	-	-
TGF-1β Positive control	+	+	+	+
Cell only	-	-	-	-
Particle only	-	-	-	-
Blank	-	-	-	-

Note: The primary astrocytes in isolation were cultured with increasing particle volumes of cobalt chrome and stainless steel wear particles (0.5μm^3-50μm^3 particles per cell) for five days in culture. A cell only negative control was used. The highest particle dose (50μm^3 particles per cell) was used as a particle only control and acellular 100µl gels used as a blank reference control (6 replicates per condition).

Primary astrocytes with no particle stimulation did not express GFAP at any time point tested. Primary astrocytes exposed to the TGF-β1 positive control expressed low levels of GFAP (+) after both two and five days in culture.

5.4.4 Cytokine release by primary astrocytes and microglia and primary astrocytes

The aim of this section of the study was to compare the cellular responses of primary astrocytes and microglia in co-culture and primary astrocytes in isolation to cobalt chrome and stainless steel wear particles in terms of cytokine release.

5.4.4.1 The effect of cobalt chrome and stainless steel particles on TNF-α cytokine release by primary astrocytes and microglia in co-culture.

When primary astrocytes and microglia were cultured with increasing cobalt chrome particle volumes (0.5μm^3 - 50μm^3 cobalt chrome debris per cell) for 48 hours no TNF-α release was observed for any particle volume. The average optical density values for each condition were below the average optical density for the 0 $pg.ml^{-1}$ standard. No TNF-α production was observed in the cell only negative control. A concentration of 213.3$pg.ml^{-1}$ TNF-α was produced when primary astrocytes and microglia were cultured with the LPS positive control.

When primary astrocytes and microglia were cultured with the highest stainless steel particle volume, 50μm^3 stainless steel debris per cell, for 48 hours, 29.9$pg.ml^{-1}$ TNF-α was produced.

TNF-α was not secreted when primary astrocytes and microglia were cultured with 5μm^3 and 0.5μm^3 stainless steel debris per cell. No TNF-α production was observed in the cell only negative control. A concentration of 288.7$pg.ml^{-1}$ TNF-α was produced when primary astrocytes and microglia were cultured with the LPS positive control.

5.4.4.2 The effect of cobalt chrome and stainless steel particles on TNF-α cytokine release by primary astrocytes in the absence of microglia.

When primary astrocytes in isolation were cultured with increasing particle volumes of cobalt chrome (0.5μm^3 -50μm^3 cobalt chrome debris per cell) for 48 hours no TNF-α release was observed for any particle volume. The average optical density values for each test condition was below the average optical density for the 0 $pg.ml^{-1}$ standard. No TNF-α production was observed in the cell only negative control. A concentration of 143.6$pg.ml^{-1}$ TNF-α was produced when primary astrocytes were cultured with the LPS positive control.

TNF-α was not secreted when primary astrocytes were cultured with increasing particle volumes of stainless steel, 50μm^3, 5μm^3 and 0.5μm^3 debris per cell. No TNF-α production

was observed in the cell only negative control. A concentration 176.4pg.ml^{-1} TNF-α was produced when primary astrocytes in isolation were cultured with the LPS positive control.

5.5 Discussion

An *in vitro* model designed for the purpose of analysing the biological response of cells to particulate stimuli should create a spatial environment whereby the cells cultured within the matrix scaffold are able to behave as they would *in vivo.* Using a 3D, type I collagen gel primary astrocytes and microglia in co-culture and primary astrocytes in isolation resembled glial cells in their physiological environment. Primary astrocyte and microglia cellular responses to particulate stimuli could be more accurately analysed with this model, than in 2D where astrocytes exhibit a reactive phenotype. The high level of activity demonstrated by primary astrocytes in 2D culture inhibited the further study of cellular reactivity upon simulation with cobalt chrome and stainless steel wear particles as the baseline levels of activity were too high (East et al., 2009). It would be difficult to discern whether the level of reactivity detected, using immunocytochemistry, was a product of the environment the cells were cultured in, or a response to particulate insult.

The aim for this part of the study was to determine the effect of increasing particle concentrations of cobalt chrome and stainless steel ($0.5\mu m^3$-$50\mu m^3$) wear particles on the viability, cellular reactivity and TNF-α release of primary astrocytes and microglia in co-culture and astrocytes in isolation using a 3D type I collagen gel cell culture system. The effect of cobalt chrome and stainless steel on CNS cell viability was determined using a live dead assay. The effect of these particles on cellular reactivity was assessed using immunocytochemistry to investigate up-regulation of glial fibrillary acidic protein (GFAP) an intermediate filament protein expressed in reactive astrocytes. Finally an enzyme linked immunosorbent assay was used to measure the release of TNF-α in response to stimulation with cobalt chrome and stainless steel wear particles.

5.5.1 The effect of cobalt chrome and stainless steel wear particles on the viability of primary astrocytes and microglia in co-culture and primary astrocytes in isolation in a 3D cell culture system.

When primary astrocytes and microglia in co-culture were cultured with increasing particle volumes of cobalt chrome ($0.5\mu m^3$-$50\mu m^3$) for two days in culture the highest particle dose $50\mu m^3$ triggered significant reductions in viability were observed when compared to the cell only negative control. After five days in culture both the highest cobalt chrome particle dose, $50\mu m^3$ and $5\mu m^3$ cobalt chrome debris per cell triggered significant reductions in cell viability when compared to the cell only negative control. When primary astrocytes in isolation were cultured with increasing particle volumes of cobalt chrome ($0.5\mu m^3$-$50\mu m^3$) for two and five days in culture only the highest particle

dose significantly reduced cell viability. Interestingly the removal of microglia from the culture environment appears to reduce the sensitivity of primary astrocytes to cobalt chrome wear particles (30-39nm in length). This suggested that the resident macrophage of the CNS, microglia, played an important role in determining the cellular response to particulate stimuli.

Upon culture of primary astrocytes and microglia and primary astrocytes in isolation with increasing particle volumes of stainless steel ($0.5\mu m^3$-$50\mu m^3$) for two and five days in culture no adverse effects on cell viability were observed at any particle dose, at any time point tested.

Upon comparison of these findings in 3D culture to the results reported in Chapter 4, section 4.4.1.5 and 4.4.1.6 where in a preliminary investigation primary astrocytes and microglia were cultured with increasing particle volumes of cobalt chrome and stainless steel particles ($0.05\mu m^3$-$50\mu m^3$) in 2D monolayer culture. In 2D, after three and five days in culture all doses significantly reduced the viability of primary astrocytes and microglia, whereas in 3D culture only $50\mu m^3$ and $5\mu m^3$ debris per cell of this material caused significant reductions in viability. When primary astrocytes and microglia in co-culture were cultured with increasing volumes of stainless steel wear particles no adverse effects on cell viability were observed in 3D culture, however in 2D culture after 24 hours in culture the $0.5\mu m^3$, $5\mu m^3$ and $50\mu m^3$ stainless steel debris per cell doses significantly reduced cell viability and the highest $50\mu m^3$ adversely affected cell viability after 5 days in culture. These results indicate that when primary astrocytes and microglia were cultured with metallic wear particles in a simplistic 2D cell culture model the effect on cell viability was perhaps overestimated, when compared to the findings reported when primary astrocytes and microglia were cultured in a more physiologically relevant 3D cell culture system.

It is essential to note that a direct comparison between the 2D and 3D findings presented in this investigation cannot be achieved. Two different methodologies were utilised to determine the effects of metal particles on cell viability between the two different cell culture environments; the ATP Lite™ assay and the live dead assay. The ATP Lite™ assay used ATP as a marker of cellular metabolic activity and the assumption that increases in metabolic activity corresponded to a greater number of living cells. Considering primary astrocytes, when activated and stressed, rapidly increase in number, the use of a single metabolic activity assay in isolation could not precisely explain the full mechanism behind

the biological response observed. Similarly in 3D the use of a single live dead assay raises some limitations. The live dead assay relies on the principle that non-fluorescent calcein; upon entry into a living cells and interaction with intercellular esterases (and the removal of the acetomethoxy group) results in the emission of strong green fluorescence (Berney et al., 2007). Ethidium homodimer is capable of entering membrane-compromised cells and staining cells red. Though it seems fair to assume that a membrane-compromised cell can be classified, as dead the reverse may not necessarily be true (Joux & Lebaron, 2000). Thus the utilisation of an additional cell viability assay would have been preferential in this investigation.

Attempts were made to utilise the ATP Lite™ assay in the 3D cell culture system, however problems with penetration of the lysis solution and ATP substrate within the collagen gel caused high variance between replicates. The possibility that some of the cells towards the bottom of the gel were not lysed could not be discounted.

These findings were dissimilar to the results reported by Papageorgoiu et al. (2014) where a dura mater organ culture model was exposed to cobalt chrome wear particles of 50μm^3 and 5μm^3 debris per cell for 7 days in culture. Here the cobalt chrome particles did not adversely affect the viability of the dura tissue at any dose or any time point tested (Papageorgiou et al., 2014).

Similarly to the results presented in Chapter four there are clear differences in the cytotoxicity of nano-scale cobalt chrome and stainless steel wear particles. Suggesting once again that the differences in elemental composition between these two biomaterials could be responsible for the differing effects on cell viability.

5.5.2 The effect of metal ions from cobalt chrome and stainless steel wear particles on the viability of primary astrocytes and microglia in co-culture and primary astrocytes in isolation in a 3D culture system.

Interestingly when primary astrocytes and microglia were cultured with ions released from cobalt chrome wear particles (after a 24 hour incubation period in supplemented medium Chapter 2, section 2.3.20 at 37°C at 5% CO_2 (v/v) in air) after two days in culture no significant adverse effect on viability was observed, however after five days in culture with ions released from the 5μm^3 cobalt chrome per cell particle dose a significant reduction in primary astrocyte and microglia cell viability was observed when compared to the cell only negative control.

Intriguingly when primary astrocytes in isolation were cultured with ions released from cobalt chrome wear particles (after a 24 hour incubation period in supplemented media Chapter 2, section 2.3.20 at 37°C at 5% CO_2 (v/v) in air) after two days in culture significant adverse effects on viability were observed with all doses of ions when compared to the cell only negative control, however after five days in culture with ions released from cobalt chrome particles the effect was not as pronounced, with only ions from the highest, 50μm^3 and 5μm^3 particle doses significantly decreasing the viability of primary astrocytes in isolation.

No significant adverse effects on primary astrocyte and microglia cell viability were observed when cultured with ions from stainless steel particles after two days in culture. However after five days in culture a significant reduction in astrocyte and microglia cell viability was reported when cultured with ions from the highest stainless steel particle dose, 50μm^3 stainless steel debris per cell.

When astrocytes in isolation were cultured with increasing concentrations of stainless steel ions from increasing particle volumes (0.5μm^3 to 50μm^3 debris per cell), after two days in culture a significant reduction in astrocyte viability was observed with ions from the 5μm^3 particle dose, after five days in culture a more pronounced adverse effect was reported with ions from all particle doses, 0.5μm^3, 5μm^3 and 50μm^3 causing significant astrocyte cell death at this time point.

Upon comparison of the results from astrocytes and microglia in co-culture and astrocytes in isolation with metallic particles and ions there are clear differences in the response to the two different test conditions. Cobalt chrome particles had a more severe cytotoxic effect on primary astrocytes and microglia than the ions from cobalt chrome particles. Conversely the ions from cobalt chrome particles had a more pronounced adverse effect on astrocytes in isolation than the cobalt chrome particles. These findings suggest that the microglia, the resident macrophage of the CNS, may phagocytose the metallic particles and trigger cell death within the primary astrocytes, in the absence of these cells the cobalt chrome particles do not have as severe effects on astrocyte viability.

On the contrary the stainless steel particles do not adversely affect the viability of primary astrocytes and microglia in co-culture or primary astrocytes in isolation at any time point tested. Upon comparison of the size of the cobalt chrome and stainless steel wear particles, the cobalt chrome particles have a mode size of 30-39nm, interestingly the

stainless steel particles have a tri-modal distribution with peaks at 30-39nm, 160-169nm and >1μm. Closer inspection of the size distribution of these two biomaterials revealed that just 18.77% of cobalt chrome particles were >100nm in size whereas 47.3% of stainless steel particles were >100nm in size. This may indicate that a larger proportion of the stainless steel particles are too large for uptake by microglia and thus not have a cytotoxic effect.

Interestingly after five days in culture the ions released from the highest dose of stainless steel particles, 50μm^3 stainless steel debris per cell, caused a significant reduction in primary astrocyte and microglia viability. In the absence of microglia the effect of ions from stainless steel particles was more pronounced with ions from all particle doses adversely affecting astrocyte cell viability. Suggesting astrocytes and microglia and astrocytes in isolation are more sensitive to ions from stainless steel particles than the actual particles themselves.

Upon closer inspection of the results presented in this part of the study it is essential to question whether or not the results reported following the Two-way ANOVA and posthoc analysis were truly meaningful. For instance, when primary astrocytes and microglia in co-culture were cultured with 5μm^3 cobalt chrome debris per cell for five days a "significant reduction" in viability was observed upon comparison with the cell only negative control. The percentage of living cells in the cell only control at this time point was 90.5% compared to 86.5% with primary astrocytes cultured with 5μm^3 cobalt chrome debris per cell. Thus raising the question is this effect pronounced enough to be regarded as scientifically significant. This observation occurs repeatedly in this part of the study, when slight decreases in viability are regarded as significantly different but may not constitute being classed as scientifically significant. The question of true significance was not apparent when cells were cultured with metallic particles as greater reductions in viability were observed.

The adverse effect of ions from stainless steel particles on primary astrocytes in isolation are comparable to the findings of Ortiz et al in 2011. Here the 142BR Human Fibroblast cell line was used to determine the cytotoxic effect of ions from orthodontic implants on cell viability. Ortiz found that ions released from stainless steel tubes and brackets significantly reduced the viability of Human Fibroblasts by 95.4% after seven days in culture (Ortiz et al., 2011).

David and Lobner in 2004 utilised murine cortical cell culture; including both neuronal and glial cell types, to investigate the neurotoxicity of metallic ions released from orthodontic metallic archwire alloys. The metals investigated included; nickel titanium, copper-nickel titanium, titanium molybdenum, Elgiloy and stainless steel. Ions released from stainless steel and Elgiloy were found to be significantly toxic to murine cortical cell cultures. David found that the use of Trolox, a water soluble analogue of vitamin E, an oxide radical scavenger, significantly reduced cell death as a result of culture with ions from stainless steel in cortical cell cultures. Indicating the cell death was free radical mediated. The use of Z-VAI.ALa-Asp fluromethylketone, a caspase inhibitor also blocked the toxic effect of ions from stainless steel biomaterial suggesting these ions induced apoptosis.

No adverse effects on cell viability were reported when U937 cells were cultured with cobalt ions, however cobalt chrome wear particles (150nm-6.05μm) did trigger a significant reduction in cell viability when cultured with 5mg/1 x 10^6 cells when compared to the cell only negative control (Posada et al., 2014). This was supported by the work presented in this part of the study.

Behl et al in 2013 cultured dural epithelial and dural fibroblasts with ions from increasing particle volumes of cobalt chrome particles (0.062 $mg.ml^{-1}$, 0.62 $mg.ml^{-1}$, 6.2 $mg.ml^{-1}$, 62$mg.ml^{-1}$ and 121 $mg.ml^{-1,}$). Each particle dose was cultured at 37°C in 5% CO_2 in air, in supplemented media for 24 hours. Following this incubation period the particles were removed by centrifugation at 3000g for 20 minutes and. The highest cobalt chrome particle dose yielded the following concentrations of metallic ions; Co- 368 $ng.ml^{-1}$, Cr-433 $ng.ml^{-1}$ and Mo-291$ng.ml^{-1}$. The ions released from cobalt chrome particles did not significantly affect the viability of dural fibroblasts. Only ions released from the highest particle dose 121 $mg.ml^{-1}$ significantly reduced the viability of dural epithelial cells after three and four days in culture. These findings compared with the results presented in this part of the study suggest that primary astrocytes in isolation are more sensitive to ions released from cobalt chrome particles compared to dural epithelial cells.

5.5.3 The effect of cobalt chrome and stainless steel wear particles on the expression of GFAP by primary astrocytes and microglia in co-culture and primary astrocytes in isolation.

Immunocytochemistry was used to determine the effect of increasing particle volumes of cobalt chrome and stainless steel wear particles on the activation of primary astrocytes in the presence and absence of microglia. Up-regulation of glial fibrillary acidic protein, a

know marker of primary astrocyte activation was reported in this part of the study. This marker of cellular reactivity has been reported widely in the literature (Phillips et al., 2004; Pekny & Nilsson, 2005; DeGuzman & VandeVord, 2007; East et al., 2009; Grissa et al., 2016; Tasneem et al., 2016).

The positive control utilised in this part of the study was. TGF-β1. *In vivo* and *in vitro* this cytokine is known to up-regulate the expression of GFAP and has been reported to be involved in the formation of the glial scar (Gomes et al., 1999). East et al in 2009 had also previously used TGF- β1 as an inducer of reactive astrocytes.

When primary astrocytes and microglia were cultured with the highest cobalt chrome particle dose of 50μm^3 per cell an up-regulation of GFAP expression was observed (+) at both time points tested. No GFAP was expressed in the cell only negative control. Glial fibrillary acidic protein was not expressed after 48 hours when primary astrocytes and microglia were cultured with 5μm^3 and 0.5μm^3 cobalt chrome particle concentrations. However after five days in culture GFAP (+) was expressed when primary astrocytes and microglia were exposed to both 5μm^3 and 0.5μm^3 cobalt chrome particle doses.

After 48 hours in culture an up-regulation in GFAP expression was not observed when primary astrocytes in isolation were cultured with increasing cobalt chrome particle volumes. However after five days in culture GFAP (+) was expressed when primary astrocytes in isolation were exposed to both 5μm^3 and 0.5μm^3 cobalt chrome particle doses. This effect may be due to cell death in primary astrocytes when culture with the highest cobalt chrome particle dose. Upon comparison with the earlier findings of this study where primary astrocytes in isolation were cultured with 50μm^3 cobalt chrome debris per cell it can be seen that a significant reduction in viability was reported, thus with significant cell death cellular reactivity may have been missed, the addition of an earlier time point may have been beneficial in this investigation.

Glial fibrillary acidic protein was not expressed when primary astrocytes and microglia in co-culture and primary astrocytes in isolation were exposed to stainless steel particles at any particle dose at any time point tested.

Due to large levels of variance of GFAP expression within test conditions, a simplistic positive/negative method of analysis was selected. However a more quantitative approach may have provided a more thorough evaluation. The use of advanced software

packages such as Volocity or Imaris and the use of 3D confocal imaging techniques, the volume of red staining (corresponding to glial fibrillary acidic protein expression) to blue staining (DNA) could have been compared. This could have been used to approximate the amount of GFAP expression per cell. Attempts were made in this study to utilise confocal microscopy to evaluate the level of reactivity induced. However the time taken to obtain a single Z stack was too great, with six replicates per test condition, seven conditions per experiment and eight experiments in total this level of analysis was not possible in the time frame of the study.

The effect of cobalt chrome and stainless steel wear particles on the activation of primary astrocytes has not been investigated previously, Grissa et al. 2016 investigated the effect of titanium dioxide TiO_2 on neuro-inflammation in the rat brain. TiO_2 nano-particles (5-10nm) in length at increasing concentrations; 0 $mg.kg^{-1}$, 50 $mg.kg^{-1}$, 100 $mg.kg^{-1}$ and 200 $mg.kg^{-1}$ body weight were administered daily for 60 days. The effects of these particles on GFAP expression were examined to quantify brain damage. Grissa observed an increase in GFAP expression in the rat cerebral cortex when the animals were exposed to 100 $mg.kg^{-1}$ and 200 $mg.kg^{-1}$ TiO_2 nano-particle doses. By converting the doses utilised in Grissas' study and to the weight of a single cell these particle doses are similar to the lowest particle dose utilised in this part of the study. Thus the findings of Grissa's study demonstrate that rat cortical cell cultures are slightly more sensitive to TiO_2 particles, than primary astrocytes and microglia and primary astrocytes are to cobalt chrome and stainless steel wear particles presented here.

5.5.4 The effect of cobalt chrome and stainless steel wear particles on the release of TNFα by primary astrocytes and microglia in co-culture and primary astrocytes in isolation.

An enzyme linked immunosorbent assay (ELISA) was used to determine the effect of cobalt chrome and stainless steel wear particles on the release of TNF-α by primary astrocytes and microglia in co-culture and primary astrocytes in isolation. Enzyme linked immunosorbent assays have been used widely in the literature to determine the expression of cytokines by cells in response to wear particle stimuli (Green et al., 1998; Ingram et al., 2004; Bailey et al., 2005; East et al., 2009; Xue et al., 2012; Papageorgiou et al., 2014; Liu et al., 2015).

For this part of the study lipopolysaccharide, LPS, was used as a positive control for the stimulation of TNF-α production. It has been reported in the literature that lipopolysaccharide activates signal transduction pathways including the activation of

nuclear factor Kappa B and mitogen activated protein kinases, which are involved in the control of cellular responses to a wide array of stimuli and induce the production of TNF-α. Lipopolysaccharide has been used previously in the literature as a positive control for the induction of TNF-α release (Van der Bruggen et al., 1999; Dumitru et al., 2000).

Interestingly when primary astrocytes and microglia in co-culture and primary astrocytes in isolation were cultured with increasing particle volumes of cobalt chrome and stainless steel wear particles (0.5μm^3 -50μm^3 wear debris per cell) for two and five days in culture cobalt chrome did not stimulate TNF-α production with either cell condition at any particle dose at time point tested. However, after two days in culture primary astrocytes and microglia cultured with the highest stainless steel particle dose triggered a slight production of TNF-α, 29.9pg.ml^{-1}.

So as to implement the 3R's principle implicit to the Animal Welfare Act, for ethical use of animals in scientific research (replacement, reduction and refinement) and considering the cellular expense that would be incurred by the addition of another time point in the 3D cellular viability assays, supernatants from the 48 hour and five day time points were used in this study. Though there have been reports of TNF-α being produced at an optimum after five days (Posada et al., 2014) in culture, predominantly in macrophages this particular cytokine is produced within the first 24 hours of stimulation, this may be a limitation of this part of the study and the effect of cobalt chrome and stainless steel on TNF-α release investigated at shorter time points in future work.

Similar to the effect of metallic wear particles on cell viability, to date much of the work conducted to determine the effect of wear from metal-on-metal prostheses has been conducted in 2D monolayer culture and so cannot be directly compared to the work performed in this part of the study. The potential for cell-particle interactions is greatly elevated in 2D culture and may not be representative of mechanism of *in vivo* exposure. Fini et al. In 2003 investigated the effect of nickel-reduced stainless steel (P558) on cytokine production by primary osteoblasts in 2D culture. An increase in TNF-α production was not observed in response to this biomaterial. This work correlated well with the findings presented in this part of the study.

Posada et al in 2014 investigated the effect of cobalt chrome wear particles at a dose of 5mg/1 x 10^6 cells and subsequent metallic ions on the cytokine release of U937 cells using an enzyme linked Immunosorbent assay. Significant increases in IFN-γ expression were

reported after 120 hours in culture when U937 cells were exposed to both cobalt chrome and ions. Interestingly TNF-α expression was significantly lower than cell only controls when U937 cells were exposed to particles only and ions only.

Similar to the findings reported in this part of the study, upon culture of primary human fibroblasts with increasing particle volumes of cobalt chrome wear debris, Papageorgiou et al in 2007 did not observe a significant increase in the production of TNF-α at any time point tested with any particle dose. Dissimilarly when the dura mater was exposed to increasing concentrations of cobalt chrome particles as part of an organ culture study significant increases in TNF-α production were reported after just 24 hours of culture with 50μm^3 and 5μm^3 cobalt chrome debris per cell.

Bailey et al in 2005 investigated the response of bulk and particulate 316L stainless steel on the cytokine expression of RAW murine macrophage cells. Bailey et al. (2005) used RT-PCR to determine the effect of bulk stainless steel and 316L stainless steel particles on murine macrophage cytokine release. Bailey found a three-fold increase in TNF-α production by RAW cells in response to stainless steel particles compared to the level of TNF-α produced by the cell only negative control Though increased levels of TNF-α were observed when primary astrocytes and microglia were cultured with the highest stainless steel particle dose for two days in culture, this was not as high as pronounced as the effects reported by Bailey et al. (2005).

5.5.5 Conclusion

This part of the study highlighted the importance of the spatial arrangement of primary astrocytes and microglia in determining the biological response of CNS cells to cobalt chrome and stainless steel wear particle stimuli. Within 2D culture primary astrocytes exhibit a reactive phenotype, which is not representative of primary astrocytes in their physiological environment. It can be seen by the results presented here that, in this application, with these cell types, that the adverse effect on cell viability in conjunction with increasing concentrations of cobalt chrome and stainless steel wear particles may be overestimated in a 2D monolayer system. Thus the use of a type I collagen hydrogel provided an appropriate environment in which to more precisely determine the biological response to particle insult.

5.5.6 Key findings

- In 3D culture cobalt chrome and stainless steel wear particles (30-39nm in size) had very different effects on the viability of primary astrocytes and microglia in co-culture and primary astrocytes in isolation.
- When primary astrocytes and microglia were cultured with increasing concentrations of cobalt chrome wear particles ($0.5\mu m^3$ -$50\mu m^3$ cobalt chrome debris per cell) after 48 hours in culture the highest particle dose adversely affected the viability of primary astrocytes and microglia, after five days in culture both the $5\mu m^3$ and the $50\mu m^3$ particle doses had an adverse effect on cell viability. The viability of primary astrocytes and microglia was not affected by any stainless steel particle dose at any time point tested.
- When primary astrocytes in isolation were cultured with the highest cobalt chrome particle dose, $50\mu m^3$ debris per cell, an adverse effect on viability was observed after both 48 hours and five days in culture. The viability of primary astrocytes in isolation was not affected by any stainless steel particle dose at any time point tested.
- When primary astrocytes and microglia in co-culture were challenged with ions from cobalt chrome wear particles an adverse effect on cell viability was observed after five days in culture with the mid $5\mu m^3$ particle dose. When primary astrocytes in isolation were cultured with cobalt chrome ions adverse effects on viability were observed with all ion concentrations after 48 hours in culture, the effect was less pronounced after five days in culture with only ions from the $50\mu m^3$ and $5\mu m^3$ causing a significant reduction in cell viability. When primary astrocytes and microglia were cultured with stainless steel ions an adverse effect on viability was only observed after five days in culture with the largest stainless steel ion concentration. This effect was more pronounced when primary astrocytes in isolation were challenged with stainless steel ions. After 48 hours in culture ions from the mid $5\mu m^3$ particle dose caused a significant reduction in cell viability. After five days in culture all ion concentrations caused significant reductions in viability.
- When primary astrocytes and microglia were cultured with the highest dose of cobalt chrome particles GFAP production was observed after 48 hours. After five days in culture all particle doses triggered elevated GFAP expression. The effect on GFAP expression was less pronounced when primary astrocytes in isolation were cultured with increasing concentrations of cobalt chrome particles, no GFAP expression was observed with any particle dose after 48 hours in culture and after

five days in culture GFAP expression was reported when primary astrocytes in isolation were cultured with 0.5μm^3 and 5μm^3 cobalt chrome debris per cell. Stainless steel did not induce GFAP production in primary astrocytes and microglia in co-culture or primary astrocytes in isolation at any particle dose and time point tested.

- No changes in TNF-α production were observed when primary astrocytes and microglia or primary astrocytes in isolation were cultured with increasing cobalt chrome wear particle doses. However the highest stainless steel particle dose (50μm^3 stainless steel debris per cell) triggered an increase in TNF-α production (29.9pg.ml^{-1}) in primary astrocytes and microglia after two days in culture.

Chapter 6
Discussion

6.1 General discussion

The underpinning hypothesis of this study was that, utilising a 3D type-I collagen gel, whereby primary astrocytes and microglia could behave in a physiologically relevant manner, the biological response to increasing cobalt chrome and stainless steel particle volumes could be more precisely determined. This study was the first to culture rat primary astrocytes and microglia with clinically relevant cobalt chrome and stainless steel wear particles at physiologically representative particle doses in a 3D cell culture system. A more thorough understanding of the response of cells of the CNS to metallic wear products could be used to improve the design of metal-on-metal total disc replacements used to treat back pain associated with degenerative disc disease. Such modifications to implant design have the potential to improve the quality of care provided to patients.

Back pain is a major public health concern in the UK, which affects 84% of the population at any given point in their lifetime and can be triggered by a wide array of pathologies, in association with any part of the complex interconnected network of spinal muscles, vertebrae, ligaments or intervertebral disc (Taylor & Twomey, 1986; Wheeler et al., 2016). Degeneration of the intervertebral disc can cause a reduction in disc height, which may impact upon localised structures, for instance the facet joints and spinal ligaments, which may cause pain (Hughes et al., 2012). If conservative treatment options such as non-steroidal anti-inflammatory drugs, epidural steroidal injections, physical therapy or rest fail to alleviate adverse symptoms caused by a degenerated disc, the two main surgical treatment options considered by spinal surgeons include spinal fusion and total disc replacement. As spinal fusion limits the motion of the spine it has been associated with ALE, the incidence of which has been reported at a rate of 2.9-8% per year of follow up (Hillibrand et al., 1999; Goffin et al., 2004). As a result there has been renewed interest in the use of cervical total disc replacements (TDR), to restore normal motion and kinematics of the functional spinal unit and relieve pain associated with degenerative disc disease.

The longevity of these devices is compromised by wear. Metal biomaterials form two types of wear product *in vivo*; metal wear debris (from frictional articulation) and metal ions (from corrosion) (Doorn et al., 1996; Tipper et al., 2005). Previously within the literature, metallic wear debris and metallic ions from implants have been associated with hypersensitivity (Sun et al., 2009; Shang et al., 2014), genotoxicity (Faccioni et al., 2003;

Papageorgiou et al., 2007; Landsiedel et al., 2009; Parry et al., 2010; Brown et al., 2013; Raghunathan et al., 2013) cytotoxicity (Allen et al., 1997; Germain et al., 2003; Williams et al., 2003; Bailey et al., 2005; Papageorgiou et al., 2007; Tsaousi et al., 2010; Behl et al., 2013; Posada et al., 2014; Li et al., 2014;) the development of pseudotumours (Cavanaugh et al., 2009; Berry et al., 2010; Guyer et al., 2011), and in very rare instances osteolysis (Park et al., 2005). These reports have raised questions about the long-term clinical implications of wear products from metal-on-metal total disc replacements in particularly in relation to periprosthetic tissues including the spinal cord.

Presently, there is a limited amount of literature regarding retrieval analysis of metal-on-metal TDR. Since UHMWPE particles produced by metal-on-polyethylene total disc replacements are similar in size and morphology to those produced by metal on polyethylene total hip replacements it is reasonable to assume that particles produced by metal-on-metal total disc replacements will be similar to those produced by metal-on-metal total hip replacements, thus the particles would be in the nanometre size range. This was supported by a spine simulation study conducted by Pasko et al. (2016). Here wear particles (154nm diameter) were generated using a spine simulator (50-150N axial loading, ±7.5° flexion/extension, ±4° axial rotation and ±6° lateral bending) using custom made cervical total disc replacements.

In previous years, numerous *in vitro* studies have been conducted to further understand the biological response of fibroblasts, epithelial cells, histiocytes, osteoblasts and macrophage cells to metallic wear particles from orthopaedic biomaterials. Cobalt chrome and stainless steel wear particles have been found to have adverse effects on cell viability, DNA integrity and have been associated with the release of pro-inflammatory cytokines at varying particle concentrations (Germain et al., 2003; Williams et al., 2003; Bailey et al., 2005; Papageorgiou et al., 2007; Tsaousi et al., 2010; Brown et al; 2013 Behl et al., 2013; Posada et al., 2014; Li et al., 2014;). With increasing evidence in the literature that nanoparticles (silver and cobalt chrome) are capable of crossing *in vitro* models of the blood brain barrier (Tang et al., 2010, Cramer et al., 2014; Shilo et al., 2015) combined with a recent organ culture study which reported that nanoscale cobalt chrome particles altered the structural integrity of the outermost layer of the meninges by loosening of the epithelial layer and the underlying collagen matrix of the dura mater (Papageorgiou et al., 2014), it is imperative to study the effects of cobalt chrome and stainless steel wear products on cells of the central nervous system.

The first objective of this study was to generate clinically relevant cobalt chrome and stainless steel wear particles using a six-station pin-on-plate wear simulator. Wear simulation was performed using smooth Ra ≤0.01μm high carbon (0.27% w/w) wrought cobalt chromium molybdenum and 316L stainless steel pins and plates. The materials utilised in this study were comparable in terms of elemental composition to materials used in TDR. High carbon wrought cobalt chrome molybdenum alloy has been utilised due to its superior wear properties compared to low carbon and cast materials and is the material of choice for medical devices (Tipper et al., 1999). Utilising a stroke length of 28mm, with 30° rotation at a velocity of 1Hz, with multidirectional motion, metallic wear particles were produced under a load of 80N using water as a lubricant. These parameters have been used previously to replicate the loading and kinematics of the hip joint (Tipper et al., 1999; Galvin et al., 2006, Behl et al., 2013 Papageorgiou et al., 2014). In addition, a load of 80N has been used previously in the literature to simulate cervical spine loading characteristics and is representative of two times head weight (Rapoff et al., 1999; Reidy et al., 2004).

Scanning electron microscopy (SEM) was used to image the cobalt chrome and stainless steel wear particles and energy-dispersive x-ray spectroscopy (EDX) used to determine the elemental composition of the wear products. Within the literature there are two commonly used image acquisition techniques to determine the size and morphology of wear particles from orthopaedic implants; scanning electron microscopy (SEM) and transmission electron microscopy (TEM). Samples prepared for TEM are embedded in resin and cut into 80nm thin sections, this causes significant problems for precise imaging. Depending on the orientation of the particle in the section, the size of the particle may be underestimated. TEM passes an electron bean through the sample and the image generated represents the projection of the particles in the path of the electron beam. Due to the fact that nanoscale particles have a high surface-area to volume ratio they have a tendency to aggregate, individual particles within aggregates are not easy to visualise with this method of microscopy, and therefore it was not the most appropriate imaging technique for this application. A key limitation in determining the size distribution of the cobalt chrome and stainless steel wear particles in this study was in the processing of the SEM images, it was extremely difficult to ascertain the size of each particle within large aggregates. Particles were only included in the size distribution if the whole perimeter of the particle could be measured. This was necessary so as not to over-estimate or under estimate the length of the particle. However, this did result in a proportion of the particles being excluded from the size analysis. Attempts were made to reduce particle aggregation,

with sonication in between each filtering step. Increasing the number of images captured per filter and sizing more particles may have reduced the effect of this problem.

Both the cobalt chrome and stainless steel wear particles generated in the six-station pin-on-plate wear simulator had a mode length of 30-39nm. Interestingly the lengths of the stainless steel wear particles were more widely distributed than the cobalt chrome particles. The percentage of the total number of particles >1μm for cobalt chrome debris was 2.6% and for stainless steel debris was 5%, the percentage of the total number of particles <100nm for cobalt chrome debris was 81.3% and for stainless steel debris was 52.7%, suggesting a greater number of larger particles were produced by stainless steel pin on plate articulation. The cobalt chrome and stainless steel particles generated in this part of the study were comparable to the size of metallic nanoparticles (~50nm) observed around failed metal-on-metal total hip replacements reported in the literature. (Doorn et al., 1998).

The wider size distribution of the stainless steel wear particles compared to the cobalt chrome wear debris, may be a consequence of the differing mechanical properties of the two metals. The Young's modulus (elastic modulus) of a material is a measure of the materials elasticity, equal to the ratio of the stress acting on a substance to the strain produced. Stainless steel has a Young's modulus of approximately 190 GPa, whereas medical grade cobalt chrome has a higher Young's modulus of approximately 230 GPa. The elastic modulus of a material, from statistical trends, is usually considered to be an increasing function of hardness (Bao et al., 2004). The hardness of a biomaterial is an important parameter in determining the materials resistance to abrasion. A harder material has a reduced depth of penetration by abrasion resulting in a lower wear rates and smaller sized wear particles (Murray et al., 1982), therefore the lower Young's modulus of stainless steel may explain why the size range was more widely distributed.

Furthermore, Tipper et al. (1999) used etching to detect differences in the microstructure of wrought; high and low carbon cobalt chrome (CoCr) alloys. This study revealed that the high carbon wrought CoCr alloy possessed a bi-phasic structure. The wrought high carbon CoCr was made up of small CoCr grains, which were encircled by embedded hard, scratch resistant carbides. Carbides are compounds of carbon and are a less electromagnetic element than carbon. Tipper et al. (1999) found that the low carbon specimens produced significantly larger particles than the other material combinations, additionally the high carbon on high carbon articulations generated lower wear rates than low carbon on low carbon articulations. The positive effect on wear resistance of an elevated level of carbon

in the alloy was accounted for by the greater number of carbides within the matrix of the material. Due to a reduced carbon content in 316L stainless steel (0.03%) compared to medical grade cobalt chromium (<0.35%) this may also explain why there was a greater proportion of <100nm cobalt chrome wear particles than stainless steel particles.

The second aim of this study was to establish whether or not increasing volumes of cobalt chrome and stainless steel particles, (with mode lengths of 30-39nm) had a toxic effect on C6 glial, PC12 neuronal cell lines, primary rat astrocytes and microglia in co-culture for 24 hours, three days and five days in 2D culture. The effect of metallic wear particles on cell viability was assessed using an ATP-Lite cell viability assay. Though previous *in vitro* investigations have been performed to ascertain the biological response of cells to cobalt chrome and stainless steel wear particles, this is the first time C6 glial, PC12 neuronal cell lines and primary astrocytes with microglia in co-culture had been cultured with clinically relevant cobalt chrome and stainless steel wear particles at physiologically relevant particle doses in 2D culture.

This study found that cobalt chrome wear particles adversely affected the viability of C6 glial cells at all time points tested with all particle doses tested. Similarly cobalt chrome adversely affected the viability of PC12 neuronal cells after three and five days in culture. The cobalt chrome particles did not adversely affect the viability of primary astrocytes and microglia in co-culture after 24 hours in culture. Significant reductions in cell viability were observed after three and five days in culture with all cobalt chrome particle doses in these primary cells. In 2D culture limited cytotoxicity was observed with stainless steel wear particles. When increasing particle volumes of stainless steel were cultured with primary astrocytes and microglia a cytotoxic effect was observed but this did not last for the duration of the investigation.

A key limitation of this part of the study is the use of a single assay to determine the effect of metal particle stimuli on cell viability. It can be seen from the results reported that over the time course of the investigation (five days), that although significant reductions and elevations in counts per seconds readings were observed, upon comparison with the cell only negative control, these findings may not be indicative of cell death. In some instances within this investigation (such as the culture of C6 glial cells with 5μm^3 cobalt chrome wear particles per cell) the average counts per second reading was significantly lower than that of the cell only control, however over the five day time period the level of ATP produced continuously increased. The cells exposed to the particle stimuli may simply be dividing at a lower rate than those of the cell only negative control. The use of a cell

proliferation assay or live dead assay would have enabled a more complete understanding of this biological response.

Furthermore, the use of the ATP-Lite™ assay in this study may have certain limitations especially when used in conjunction with primary astrocytes and microglia. It has been well established in the literature that astrogliosis involves a rapid proliferation of cells, an adverse process triggered by neurological damage, infection and inflammation. By using a cell viability assay that measures cellular metabolism, an increase in cell proliferation prior to death may falsely be seen as a beneficial effect on cell viability. A live dead assay or the use of propidium iodide may be a more appropriate method of cell viability assessment as this stain can differentiate between apoptotic, necrotic and normal living cells.

Though there is limited information in the literature regarding the effect of stainless steel wear products on cell viability, a small number of studies have been performed to determine the effect of bulk and particulate stainless steel on RAW macrophage and MC3T3 mouse osteoblast cells. Bailey at al. (2005) observed a reduction in the viability of RAW macrophages when cultured with 316L stainless steel particles, 1-100μm in size, after 24 hours in culture. However, the dose of stainless steel particles administered to the cells was not reported for this particular investigation and so cannot be directly compared to the findings presented in this study. Moreover, the effect on cell viability was only qualitatively measured using a live dead stain, a quantitative measure of assessment would have been more appropriate. Conversely, Li et al. (2014) did not report any adverse effects on viability when MC3T3 mouse osteoblast cells were cultured with bulk 316L stainless steel. Though the results reported by Li et al. (2014) are similar to the results reported in this study, where C6 glial cells were not adversely affected by stainless steel wear particles, and PC12 neuronal cells and primary astrocytes and microglia were only adversely affected by the highest particle dose, 50μm^3 stainless steel debris per cell. A direct comparison between the two investigations cannot be performed as in this study the cells were cultured with particulate stimuli not the bulk material.

The results presented in this study revealed that similar levels of DNA damage were observed when primary astrocytes and microglia in co-culture and astrocytes in isolation were cultured with cobalt chrome and stainless steel wear particles. Interestingly the level of DNA damage observed with cells of the CNS to stainless steel particles did not correlate with a cytotoxic response. It is important to note that to assess the effect of cobalt chrome and stainless steel wear particles on the DNA integrity of primary astrocytes and microglia

in co-culture and astrocytes in isolation, the cells were cultured with the debris in a 2D environment, and then suspended in an agarose gel to perform the comet assay. As stated previously the use of 2D culture is not representative of the spatial arrangement of these cells *in vivo,* consequently the use of the more physiologically relevant 3D culture environment may have been necessary, however problems were encountered with the retrieval of these primary cells from the collagen matrix without causing additional cellular damage.

The results presented here are similar to previous reports in the literature regarding the effect of nanoscale cobalt chrome particles on DNA integrity. Papageorgiou et al. (2007), Parry et al. (2010) and Tsaousi et al. (2010) reported that nanoscale cobalt chrome particles caused significant DNA damage to human fibroblast cells after just 24 hours in culture. In contrast to these findings, Gajski et al. (2014) reported no significant DNA damage upon culture of human lymphocytes with micron size cobalt chrome particles using the alkaline comet assay, this may be due to the micron size of the particles reducing metal ion production and limiting entry into the cell via phagocytosis. Similar to the results presented in this study, Ortiz et al. (2011) reported significant levels of DNA damage when human fibroblasts were cultured with ions from stainless steel buccal tubes and brackets used in orthodontic treatments.

Recently there have been growing concerns regarding the high levels of cobalt and chromium ions released by metal-on-metal biomedical implants (Scharf et al., 2014). The associated toxicity of cobalt and chromium is dependent on their oxidation state (Beyersmann & Hartwig, 2008). Chromium and cobalt can be found in a range of different oxidation states; Cr(I), Cr(III), Cr(IV), Cr(V), Cr(VI), Co(II) and Co(III). Trivalent and hexavalent chromium are the most energetically stable and so are most commonly observed, however Cr (III) has a limited capacity to enter cells. Cr (VI) has been categorised as carcinogenic to humans by the International Agency for Research and Cancer (Keegan et al., 2008). Reports within the literature suggest that cobalt is highly toxic asserting cytotoxic effects by means of oxidative stress and chromosomal damage (Sansone et al., 2013). Whereas chromium appears to have a genotoxic effect on cells (Singh et al., 1998; Catelas et al., 2003; Papageorgiou et al., 2007). The genotoxic effects caused by cobalt and chromium ions are thought to be triggered either by direct action, causing DNA breaks involving free radicals, or by an indirect method, whereby the repair of DNA is prevented (Daley et al., 2004). Stainless steel and cobalt chrome used in the manufacture of orthopaedic implants have very different elemental compositions. More precisely, the high carbon wrought cobalt chrome utilised in this study was made up of 27-

30%, chromium, 5-7% molybdenum and ~60% cobalt. Medical grade 316L is made up of 62-72% iron, 16-18% chromium and 10-14% nickel. Such large differences in elemental composition may explain the differences in toxicity to primary astrocytes and microglia. Stainless steel (316L) does not contain any cobalt and has a reduced chromium content compared to high carbon wrought cobalt chrome. As cobalt is regarded to be more cytotoxic, this may explain why the cobalt chrome wear particles were more toxic to the CNS cells than stainless steel but why similar levels of DNA damage were seen in response to the two biomaterials.

To date many of the investigations into the biological response of cells to nanoscale metallic wear particles has been performed using 2D monolayer cell culture systems. The use of a 2D model in isolation may not accurately represent the natural behaviour of cells, in particular CNS cells which exhibit a different phenotype in 2D and 3D culture (East et al., 2009; Haycock et al., 2011; Baker et al., 2012). This study utilised an advanced 3D culture system to provide a more physiologically relevant cell culture environment. The final aim of this study was to determine the biological response of primary astrocytes and microglia in co-culture and primary astrocytes in isolation to cobalt chrome and stainless steel wear particles in a physiologically relevant 3D cell culture system. More specifically the effects of metallic wear products on cell viability, cellular reactivity and TNF-α production were investigated.

When primary astrocytes and microglia were cultured with increasing particle volumes of cobalt chrome, the highest particle dose adversely affected cell viability at all time points tested. After five days in culture 5μm^3 per cell cobalt chrome debris triggered significant reductions in cell viability when compared to the cell only negative control. When primary astrocytes in isolation were cultured with increasing particle volumes of cobalt chrome only the highest particle dose adversely affected cell viability. The removal of microglia from the culture environment appeared to reduce the sensitivity of primary astrocytes to cobalt chrome wear particles. Thus it is postulated that the microglia may take up the particles by phagocytosis and cause cell death in primary astrocytes possibly by the release of pro-inflammatory cytokines and other mediators of inflammation. No adverse effects on cell viability were observed at any particle dose, at any time point upon culture of primary astrocytes and microglia and primary astrocytes in isolation, with increasing particle volumes of stainless steel. Similarly to the results reported using 2D culture, cobalt chrome particles were more toxic to primary astrocytes and microglia than stainless steel particles. In this 3D investigation, stainless steel particles did not appear to

induce a toxic response at all. As mentioned previously this may be due to differing elemental compositions between the two biomaterials.

These results of this study demonstrate the importance of the use of an appropriate cell culture environment in *in vitro* biocompatibility investigations. Upon comparison of the effects of primary astrocytes and microglia to metallic particle stimuli between the two culture environments, it was observed that the cells were more sensitive to both biomaterials in 2D culture. Cells cultured in 2D are often cultured at a solid-liquid interface between the surface of the matrix and the culture medium, these surroundings are unlikely to occur *in vivo.* In this static monolayer environment the particles were applied directly on top of the cells thus increasing the incidence of cell-particle interaction. This method of particle administration did not replicate the intricacies of the gradual production of wear, the transport of metallic particles and ions or the cell-cell interactions in the native tissue and may provide an explanation for the heightened sensitivity of primary astrocytes and microglia cultured on tissue culture plastic to particle stimuli. In 3D culture the primary astrocytes and microglia were less likely to be in contact with the debris and thus less likely to elicit a cellular response. Thus by use of a simplistic 2D culture model, the effects of wear particles on cell viability may be overestimated and not representative of the effect that would be seen *in vivo*.

Clinically relevant 3D culture environments have been developed to more accurately mimic the properties of tissue and ECM *in vivo*. Using murine macrophages RAW cells in a novel 3D culture environment, Hashimoto et al. (2014) investigated the biological response to polyvinylpyrrolidone-coated silver nano particles. The toxicity of these particles differed between 2D and 3D culture environments. The cells in the 3D culture system were less sensitive to the NP cytotoxic effects. This observation was similar to the findings reported in the present study where the cells cultured in 3D tolerated the presence of the particles better than in 2D. In an additional investigation, a 3D *in vitro* model was used to assess the potential of carbon nanotubes to develop epithelioid granulomas in non-adherent primary murine bone marrow-derived macrophages in 3D culture (Sanchez et al., 2011). Differing morphological and phenotypic responses were observed with 3D culture, suggesting the use of a more advanced spatial environment may be a crucial alternative to both traditional 2D monolayer cultures and *in vivo* animal models.

The findings presented in this part of the study were in contrast to the results reported by Papageorgoiu et al. (2014). In the latter study cobalt chrome particles of similar size to the

ones utilised in this study did not adversely affect the viability of the dura mater tissue at any dose or any time point tested (Papageorgiou et al., 2014). However, the results presented here did correspond to levels of toxicity observed in previous *in vitro* studies using 2D culture (Germain et al., 2003; Williams et al., 2003; Bailey et al., 2005; Papageorgiou et al., 2007; Tsaousi et al., 2010; Brown et al., 2013; Behl et al., 2013; Posada et al., 2014; Li et al., 2014). Using clinically relevant (29.5nm in length) cobalt chrome particles, Germain et al. (2003) found particle concentrations of 50μm^3 and 5μm^3 debris per cell caused a significant reduction in the viability of U937 macrophage cells and L929 fibroblasts. The findings reported by Germain et al. (2003) were supported by the work of Williams et al. (2003) here cobalt chrome wear particles (<20nm in length) at particle doses of 50μm^3, 5μm^3 and 0.5μm^3 were reported to significantly reduced the viability of U937 cells. The authors found that the L929 cells were less sensitive than U937 cells upon exposure to cobalt chrome wear particles, as only the highest dose of 50μm^3 caused a significant reduction in L929 viability after five days in culture. Papageorgiou et al. (2007) and Tsaousi et al. (2010) both cultured human fibroblast cells with cobalt chrome wear particles, particle doses ranging from 0.5μm^3 to 500μm^3 cobalt chrome debris per cell and 1mg, 2mg and 5mg per flask of human fibroblasts significantly reduced cell viability after five days in culture. Similarly to the results reported in this study, Behl et al (2013) reported that cobalt chrome particles (50-59nm in length) significantly reduced the viability of dural epithelial cells at doses of 6.05 μm^3 to 121μm^3 of debris per cell. Conversely, no significant reduction in the viability of the dural fibroblasts at all the particle doses and time points studied was reported.

A key limitation of the present study was that the biological response of primary microglia in isolation to cobalt chrome and stainless steel wear particles was not investigated. Numerous attempts were made to culture primary microglia in isolation, however significant adaptations to the cell isolation procedure would have been necessary to yield a large enough number of cells for subculture. This was not possible in the time frame of this study. As postulated earlier the "macrophage like" microglia may have been responsible for uptake of the metallic wear particles and stimulation of an adverse effect on cell viability in primary astrocytes. Culture of these cells in isolation with the cobalt chrome and stainless steel wear debris, and use of TEM analysis may have provided more evidence to refute or confirm this supposition.

An additional limitation to this work was that different assays were utilised to assess viability between the 2D and 3D culture system and thus direct comparisons between the two investigations cannot be made as the two assays were measuring different markers of

viability (metabolic activity and esterase activity). Attempts were made to utilise the ATP Lite™ assay in the 3D culture system, however the reagents failed to fully permeate the gels and thus resulted in incomplete cell lysis. Additional work using the live dead assay in 2D would have been beneficial to enable a direct comparison between the cytotoxic effects of cobalt chrome and stainless steel wear particles on primary astrocyte and microglia cell viability between the two culture systems.

Interestingly, when primary astrocytes and microglia were cultured with ions released from cobalt chrome wear particles, limited levels of cytotoxicity were observed. Conversely when primary astrocytes in isolation were cultured with ions released from cobalt chrome wear particles significant adverse effects on viability were observed with all doses of ions when compared to the cell only negative control after two days in culture. This effect was not as pronounced after five days in culture. No significant adverse effects on primary astrocyte and microglia cell viability were observed when cultured with ions from stainless steel particles after two days in culture. Although after five days in culture, a significant reduction in viability was reported when astrocytes and microglia were cultured with ions from the highest stainless steel particle dose, 50μm^3 stainless steel debris per cell. In the absence of microglia, after two days in culture a significant decline in astrocyte viability was observed with ions from the 5μm^3 stainless steel particle dose, the adverse effect was more pronounced after five days in culture as ions from all particle doses caused significant astrocyte cell death. These results would suggest that astrocytes and microglia and astrocytes in isolation are more sensitive to ions from stainless steel particles than the actual particles themselves.

A closer examination of the results presented in this part of the study raises the question of true significance between means. Although, upon comparison with the cell only control, test conditions induced significant decreases/increases in viability only minor alterations in the percentage of living cells were reported. This observation occurs repeatedly in this part of the study, when slight decreases in viability are regarded as significantly different but may not constitute being classed as “scientifically significant”. The uncertainty regarding true significance was not apparent when cells were cultured with metallic particles as greater reductions in viability were observed. This may be the result of an underestimation in the number of dead cells as a limitation of the live dead cell viability assay selected.

The use of the live dead assay in isolation represents a limitation for this part of the study. The live dead assay works on the principle that upon cell death the integrity of the cell

membrane is lost, thus enabling the entry of the ethidium homodimer into the cell (providing a red stained cell) however this assay is not capable of detecting cells that have been lost in culture after cell death and detached from the extracellular matrix. Therefore there may be an underestimation in the number of dead cells within the gel. The use of an additional cell viability assay would have been beneficial for this investigation.

The increasing ion concentrations were produced by incubating supplemented medium containing increasing particle volumes of cobalt chrome and stainless steel particles at 37°C in 5% CO_2 (v/v) in air for 24 hours. After this time point the particles were removed and primary astrocytes and microglia in 3D culture were exposed to the conditioned medium. It is important to consider, when the cells are exposed to increasing volumes of metallic wear particles, after 24 hours ions will also be released, meaning the cells will be exposed to both ions and particles. Therefore the addition of a 24-hour time point may have been useful in order to compare the effect of ions in isolation and particles and ions on CNS cell viability in 3D.

A major limitation in this part of the study was that the concentration of ions released from each particle dose was not quantified. Previous research has utilised inductively coupled plasma mass spectroscopy to quantify ion release from metallic particles in medium (Kumazawa et al., 2002; Ortiz et al., 2011; Behl et al., 2013; Shilo et al., 2015). This information would have been useful to determine which concentrations of ions were lethal and which were not

Similar *in vitro* studies have reported adverse effects on cell viability in association with ions released from stainless steel particles. Ortiz et al. (2011) reported that ions released from stainless steel tubes and brackets significantly reduced the viability of human fibroblasts. Behl et al. (2013) reported that upon culture of dural epithelial and fibroblasts with ions from increasing volumes of cobalt chrome particles (0.062μm^3, 0.62μm^3, 6.2μm^3, 62μm^3 and 121μm^3), the ions released from cobalt chrome particles did not have an adverse effect on dural fibroblast viability. However, ions released from the highest particle dose significantly reduced the viability of dural epithelial cells. It is important to note that the highest particle dose used by Behl et al. 2013 was more than double the particle dose utilised in this investigation, thus suggesting that primary astrocytes in isolation may be more sensitive to ions released from cobalt chrome particles compared to dural epithelial cells. In the present study, cobalt chrome particles had a more pronounced effect on the viability of primary astrocyte and microglia than the ions from cobalt chrome particles. Conversely, the ions from cobalt chrome particles had a more pronounced

adverse effect on astrocytes in isolation than the cobalt chrome particles. These findings support the previous hypothesis that the microglia may take up the metallic particles and trigger cell death within the primary astrocytes.

The culture of primary astrocytes and microglia in co-culture and primary astrocytes in isolation with cobalt chrome wear particles did not stimulate TNF-α production from either cell type at any particle dose. Conversely, after two days in culture primary astrocytes and microglia cultured with the highest stainless steel particle dose triggered a slight increase in production of TNF-α, (29.9pg.ml^{-1}).

Similar to the findings reported in this part of the study, upon culture of primary human fibroblasts with increasing particle volumes of nanoscale cobalt chrome wear debris, Papageorgiou et al. (2007) did not observe a significant increase in the production of TNF-α at any time point tested with any particle dose. However, when the dura mater was exposed to increasing concentrations of cobalt chrome particles as part of an organ culture, significant increases in TNF-α production were reported after just 24 hours of culture with 50μm^3 and 5μm^3 cobalt chrome debris per cell (Papageorgiou et al., 2014). The findings presented in this study were different from previous reports within the literature, where nanoscale cobalt chrome, stainless steel, cadmium and lead (Bailey et al., 2005; Posada et al., 2014; Papageorgiou et al.,2014; Tasneem et al., 2016) wear particles caused a significant increase in TNF-α production.

The main limitation with this part of the study was that the assessment of cytokine release was performed after 48 hours. In macrophages TNF-α is predominantly produced within the first 24 hours, thus it would have been useful to assess the effect of debris on cytokine release at this time point. Tasneem et al. (2016), cultured neural stem cells in 3D hydrogels with increasing doses of heavy metals and pooled together supernatants from over the entire 14- day experiment to assess TNF-α release. The levels of cytokine release reported were extremely low (1-3pg.ml^{-1}). Perhaps the ELISA using in this part of the study was not sensitive enough and that only low levels of TNF-α are produced with primary astrocytes and microglia. Alternative cytokines such as IL-6 and IL-8 may have been more appropriate. In future TNF- α release would be investigated at earlier time points (12 and 24 hours, respectively).

The effect of cobalt chrome and stainless steel wear particles on the activation of primary astrocytes has not been previously investigated. When primary astrocytes and microglia were cultured with the highest cobalt chrome particle dose of 50μm^3 per cell, an up-

regulation of GFAP expression was observed at both time points tested (two and five days in culture). Glial fibrillary acidic protein was only expressed when primary astrocytes in isolation were exposed to both 5μm^3 and 0.5μm^3 cobalt chrome particle doses after five days in culture. Stainless steel particles did not trigger glial fibrillary acidic protein expression at any particle dose at any time point tested with either cellular condition.

The use of GFAP as a marker of astrocyte reactivity has been extensively researched and reported in the literature (Phillips et al., 2004; Pekny & Nilsson, 2005; De Guzman & VandeVord, 2007; East et al., 2009; Grissa et al., 2016; Tasneem et al., 2016). Though there are a limited number of studies within the literature investigating the effect of nanoparticles on the expression of GFAP, Tasneem et al. (2016) investigated the effect of gold nanoparticles on GFAP expression in the rat cerebral cortex. It can be seen from the results of this study that once again the different biomaterials have significantly different effects on astrocyte reactivity. Stainless steel wear particles did not induce GFAP expression in primary astrocytes and microglia and astrocytes in isolation at any dose or time point tested. Cobalt chrome induced significant GFAP expression in primary astrocytes and microglia with all particle doses after five days in culture and induced significant GFAP expression in primary astrocytes in isolation with the 0.5μm^3 and 5μm^3 per cell particle volume after five days in culture. Further analysis regarding the underlying mechanism behind these differences is necessary. The investigation of additional markers of astrocyte reactivity such as Nestin, Vimentin and IL-6 (Wang et al., 2004; Sergent-Tanguy et al., 2006; Pekny & Pekna, 2014) would have been useful in conjunction with GFAP up-regulation to further investigate the potential for cobalt chrome and stainless steel wear particles to cause astrocyte reactivity.

It can be observed from the results presented in this study that stainless steel wear products have fewer adverse effects on primary astrocyte and microglia viability and cellular reactivity. Though similar levels of DNA damage were observed when primary astrocytes and microglia in co-culture and primary astrocytes in isolation were cultured with increasing concentrations of cobalt chrome and stainless steel wear particles, the level of DNA damage caused by stainless steel wear particles did not equate to cell death. In the context of the neurosurgical community these findings would suggest that the use of 316L stainless steel in the manufacture of metal-on-metal total disc replacements would be less toxic to the host and would be a biologically safer option for patients.

The use of a 3D type-I collagen gel, where glial cells behave in a more physiologically relevant manner, with a low baseline of reactivity, and which is more representative of the

in vivo cellular spatial arrangement, was found to be a more appropriate cell culture environment for determining the biological responses of CNS cells to metal wear particles.

6.2 Future work

Though this study has provided numerous insights into the biological responses of primary astrocytes and microglia to metallic wear particles there is much more work to be conducted in this area. Further work would allow better understanding of the host response to metal-on-metal total disc replacements and provide surgeons and clinicians with essential information regarding the appropriate use of metal-on-metal total disc replacements, leading to better long term clinical outcomes in patients. The main priority for future work would be to isolate metallic wear particles from periprosthetic tissue from around failed metal-on-metal total disc replacements and spinal fusion instrumentation and confirm the size and elemental composition of these wear particles generated *in vivo*. Wear particles could then be generated using a fretting simulator (to simulate the fretting wear of spinal fusion instrumentation) and spine simulator (to simulate the articulating wear from metal-on-metal total disc replacements) to generate clinically relevant wear products.

Titanium is a commonly used biomaterial in spinal fusion instrumentation and is often used in the design of total disc replacements as a material for coating metallic end plates to promote osseointegration (Powell et al., 2005; Chen & Thouas, 2015), There are also concerns within the neurosurgical community regarding the wear and corrosion of this material *in vivo.* Though previous studies have shown titanium to have limited toxic effect when compared to cobalt chrome and stainless steel (Davies, 2003; Kwon et al., 2009) and reduced wear resistance (Chen & Thouas, 2015). There has also been growing interest in the use of alternative biomaterials such as PEEK and ceramic coatings such as silicon nitride in the design of total disc replacements. With the increase in use of alternative biomaterials in the design of fusion instrumentation and motion preservation devices, this is a crucial area for future research, in particular in terms of the wear rate of these materials, the size, morphology and chemical composition of their wear products and the biological response of cells of the CNS to these particles. In future investigations titanium, PEEK and silicon nitride particles could also be cultured with primary astrocytes and microglia and the biological response investigated.

Within this study it was observed that primary astrocytes and microglia in co-culture and primary astrocytes in isolation responded differently to both cobalt chrome and stainless steel particles and their ions. However, the underlying mechanism behind these responses

was not established during this study, though it was hypothesised that microglia may take up the particles and subsequently trigger cell death within astrocytes. Transmission electron microscopy could be used to determine whether or not astrocytes or microglia are capable of taking up the particles, and if so, identify where within the cell the debris became localised. In order to understand this effect in more detail cells could be challenged with conditioned media. In larger 24 well plates (so as to provide an excess of supernatant), astrocytes and microglia could be cultured with increasing concentrations of cobalt chrome particles, stainless steel particles, ions from cobalt chrome particles and ions from stainless steel particles for 24 hours in culture. At the same time setting up separate 24 well plates with just astrocytes in isolation not exposed to wear particles. Following this incubation period the supernatant from the cells cultured with debris and ions could be removed, a small sample taken for ELISA, and the remaining conditioned media transferred to the astrocytes in isolation (without debris), then after three and five days in culture assess the effect of the culture swap on cell viability and compare the level of viability of the primary astrocytes in isolation which received the supernatant with astrocyte only controls. This may determine whether or not the microglia were responsible for cytokine release which triggered astrocyte cell death.

It would also be imperative in the future to investigate the effect of cobalt chrome and stainless steel wear particles on the viability, DNA integrity and cytokine release of primary neurons, both in isolation, and in co-culture with primary astrocytes and microglia in order to gain a deeper understanding of the cellular interactions and biological response to metallic wear particles and ions produced from metal-on-metal total discs. Oligodendrocytes and oligodendrocyte precursor cells would perpetuate the advanced 3D cellular system utilised in this study in an attempt to fully re-create the complexity of the spinal cord. This cellular model could then be used to assess the biological response of the cells of the spinal cord to metallic wear products.

As an extension of the work performed in this study to further understand the effects of cobalt chrome and stainless steel wear particles on primary astrocytes and microglia in co-culture and astrocytes in isolation, investigation into alternative cytokines would be invaluable. For instance investigation of IL-1, IL-6, IL-8 and IL-10 release. The effects of these particles on IL-6 and IL-8 release would be of particular importance, due to the fact that IL-6 is also associated with expression of glial fibrillary acidic protein and astrocyte reactivity. This cytokine could be used to validate the findings presented in this study regarding the effect of metallic wear products on primary astrocytes reactivity in the presence and absence of microglia.

Finally, the use of *in vitro* cell studies provides a platform for the investigation of the role of single cell types in the biological response and they have been used previously to quantitatively screen the cytotoxic and inflammatory response to wear particles. This study could be broadened to include *in vivo* models. Though animal models have been used previously to assess the effect of wear products from orthopaedics on local and systemic tissues following the epidural application of particulate wear debris (Cunningham et al., 2013), the somewhat crude method of application of the particles was a key limitation. Thus efforts should be made to simulate a more physiologically relevant mechanism of particle dosing such as numerous injections, as performed by Brown et al. (2013) or continuous perfusion.

6.3 Key Findings

In summary the main findings of this study were:

- In 2D culture CoCr wear particles adversely affected the viability of C6 glial cells at all time points and at all particle doses tested. Conversely, in 2D culture when PC12 neuronal cells were cultured with CoCr wear particles, adverse effects on viability were only observed after three and five days in culture with the 0.5μm^3, 5μm^3 and 50μm^3 particle doses. Finally, when primary astrocytes and microglia in co-culture were cultured with CoCr wear particles, adverse effects on viability were observed after three and five days with all particle doses.
- Stainless steel wear particles only adversely affected the viability of C6 glial and PC12 neuronal cells after five days in culture. Interestingly, stainless steel particles caused a significant reduction in the viability of primary astrocytes and microglia after 24 hours in 2D culture with the 0.5μm^3, 5μm^3 and 50μm^3 particle doses, but this affect did not persist for the duration of the investigation, five days.
- It was observed that there were clear differences in the responses of C6 glial, PC12 neuronal cells and primary astrocytes and microglia to stainless steel and cobalt chrome particles. The differences in responses to the two biomaterials tested may be attributed to the elevated cobalt content in cobalt chrome compared to stainless steel.
- In 3D culture, CoCr wear particles caused a dose dependent adverse effect on the viability of primary astrocytes and microglia in co-culture. In astrocyte only cultures, a reduced sensitivity to CoCr was observed compared to astrocytes and microglia in co-culture. In 3D culture, stainless steel particles did not adversely affect the viability of primary astrocytes and microglia in co-culture or astrocytes in isolation. When comparing these findings to the results obtained in 2D culture, the need for physiologically relevant cell culture environments was highlighted for

in vitro biomaterial testing with cells of the spinal cord. A simplistic 2D culture environment may overestimate the adverse effects.

- When primary astrocytes and microglia in co-culture were challenged with CoCr ions in 3D culture, an adverse effect on viability was only observed after five days in culture. Conversely, when astrocytes in isolation were cultured with CoCr ions adverse effects were reported at early time points (two days in culture) but did not persist. When primary astrocytes and microglia were cultured with stainless steel ions an adverse effect on viability was only observed after five days in culture, this effect was more pronounced when primary astrocytes in isolation were challenged with stainless steel ions, thus suggesting that both cell types were more sensitive to stainless steel ions than stainless steel particles.
- Cobalt chrome particles caused significant levels of DNA damage to astrocytes and microglia at all time points tested. Interestingly CoCr particles caused DNA damage in primary astrocytes in isolation after only 24 hours, although the effect did not persist for the duration of the investigation (five days). When primary astrocytes and microglia were cultured with stainless steel wear particles, significant DNA damage was observed with all particle doses at all time points, interestingly in the absence of microglia, stainless steel wear particles only caused significant DNA damage after five days in culture. These results indicate that both CoCr and stainless steel particles caused significant levels of DNA damage, although when glial cells were cultured with stainless steel particles this DNA damage did not relate to cytotoxicity.
- Cobalt chrome wear particles did not cause a significant increase in the production of TNF-α in primary astrocytes and microglia in co-culture or astrocytes in isolation. However the highest stainless steel particle dose 50μm^3 stainless steel per cell caused significant increase in TNF-α production in primary astrocytes and microglia in co-culture after two days in culture.
- Stainless steel particles did not cause significant GFAP production in either astrocytes and microglia in co-culture or astrocytes in isolation. However, when primary astrocytes and microglia were cultured with the highest dose of CoCr particles GFAP production was significantly elevated. In addition, when primary astrocytes in isolation were cultured with the lower 5μm^3 and 0.5μm^3 CoCr particle doses the level of GFAP was up-regulated.

Chapter 7

References

7th Annual Report 2010 National Joint Registry for England, Wales, Northern Ireland and the Isle of Man.

12th Annual Report 2015 National Joint Registry for England, Wales, Northern Ireland and the Isle of Man.

Abu-Amer, Y., Darwech, I., Clohisy, J.C., 2007. Aseptic loosening of total joint replacements: mechanisms underlying osteolysis and potential therapies. *Arthritis Research & Therapy*, 9 (Supplement 1) S6, pp. 1-7

Adams, M.A. & Dolan, P. 2005. Spine Biomechanics. *Journal of Biomechanics*, 38 (10), pp. 1972–1983.

Adcock, A.F., Trivedi, G., Edmondson, R., Spearman, C., Yang, L. 2015. Three-Dimensional (3D) Cell Cultures in Cell-based Assays for *In-Vitro* Evaluation of Anticancer Drugs. *Journal of Analytical and Bioanalytical Techniques*, 6 (3), pp.1-12

Allen, M.J., Myer, B.J., Millett, P.J., Rushton, N. 1997. Effect of particulate cobalt, chromium and cobalt-chromium alloy on human osteoblast-like cells *in vitro*. *The Journal of Bone and Joint Surgery (British Volume)*, 79-B (3), pp. 475–487.

Altinova, H., Mollers, S., Fuhrmann, T., Deumens, R., Bozkurt, A., Heschel, I., Leon, H.H., Damink, O., Schugner, F., Weis, J., Brook, G.A. 2014. Functional improvement following implantation of a microstructured, type-I collagen scaffold into experimental injuries of the adult rat spinal cord. *Brain Research,* 1585, pp. 37–50.

Andersen, T., Auk-Emblem, P., Dornish, M. 2015. 3D Cell Culture in Alginate Hydrogels. *Microarrays*, 4, pp. 133–161.

Anderson, P.A., Kurtz, S.M., Toth, J.M. 2006. Explant Analysis of Total Disc Replacement. *Seminars in Spine Surgery*, 18 (2), pp. 109–116.

Assis, L.C., Straliotto, M.R., Engel, D., Hort, M.A., Dutra, R.C., De Bem, A.F. 2014. β-Caryophyllene protects the C6 glioma cells against glutamate-induced excitotoxicity through the Nrf2 pathway. *Neuroscience*, 279, pp. 220–231.

Athanasou, N. A. 2016. The pathobiology and pathology of aseptic implant failure. *Bone and Joint Research*, 5 pp.162-168.

Auerbach, J.D., Jones, K.J., Fras, C.I, Balderston, J.R., Ruschton, S.A., Chin, K.R., 2008. The prevalence of indications and contraindications to cervical total disc replacement. *The Spine Journal*, 8, pp. 711–716.

Aulisa, L., Di Benedetto, A., Vinciguerra, A., Lorini, G., Tranquilli-Leali, P. 1982. Corrosion of the Harrington's instrumentation and biological behaviour of the rod-human spine system. *Biomaterials*, 3 (4), pp. 246–249.

Austen, S., Punt, I.M., Cleutjens, J.P., Willems, O.C., Kurtz, S.M., MacDonald, D.W., Van Rhijn, L.W., Van Ooij, A. 2012. Clinical, radiological, histological and retrieval findings of Activ-L and Mobidisc total disc replacements: a study of two patients. *European Spine Journal*, 21 (Supplement 4), pp. 13–20.

Ayotte, D.C., Ito, K., Tepic, S. 2001. Direction-dependent resistance to flow in the endplate of the intervertebral disc : an *ex vivo* study. *Journal of Orthopaedic Research*, 19, pp. 1073–1077.

Bago, J., Ramirez, M., Pellise, F., Villanueva, C. 2003. Survivorship analysis of Cotrel-Dubousset instrumentation in idiopathic scoliosis. *European Spine Journal*, 12 (4), pp. 435–439.

Bailey, L.O., Lippiatt, S., Biancanello, F.S., Ridder, S.D., Washburn, N.E. 2005. The quantification of cellular viability and inflammatory response to stainless steel alloys. *Biomaterials*, 26 (26), pp. 5296–5302.

Baker, B.M. & Chen, C.S. 2012. Deconstructing the third dimension – how 3D culture microenvironments alter cellular cues. *Journal of Cell Science*, 125 (13), pp. 3015–3024.

Baldwin, E.L., Byl, J.A., Osheroff, N. 2004. Cobalt enhances DNA cleavage mediated by human topoisomerase II alpha *in vitro* and in cultured cells. *Biochemistry,* 43 (3), pp. 728-735

Banerjee, S., Cherian, J.J., Bono, J.V., Kurtz, S.M., Geesink, R., Meneghini, R.M., Delanois, R.E., Mont, M.A. 2015. Gross Trunnion Failure After Primary Hip Arthroplasty. *The Journal of Arthroplasty*, 30, pp. 641–648.

Bankston, A.B., Faris, P.M., Keating, E.M., Ritter, M. 1993. Polyethylene wear in total hip arthroplasty in patient-matched groups. A comparison of stainless steel, cobalt chrome, and titanium-bearing surfaces. *Journal of Arthroplasty*, 8 (3), pp. 15–22.

Bao, Y.W., Wang, W., Zhou, Y.C. 2004. Investigation of the relationship between elastic modulus and hardness based on depth-sensing indentation measurements. *Acta Materialia,* 52 (18) pp.5397-5404.

Bartels, R., Donk, R., Verbeek, A. 2010. No Justification for Cervical Disc Prostheses in Clinical Practice: A MetaAnalysis of Randomised Control Trials. *Neurosurgery,* 66(6), pp.1153-1160.

Baykal, D., Siskey, R.S., Haider, H., Saikko, V., Ahlroos, T., Kurtz, S.M. 2014. Advances in tribological testing of artificial joint biomaterials using multidirectional pin-on-disk testers. *Journal of the Mechanical Behaviour of Biomedical Materials*, 31, pp. 117–134.

Behl, B., Papageorgiou, I., Brown, C., Hall, R., Tipper, J.L., Fisher, J., Ingham, E. 2013. Biological effects of cobalt-chromium nanoparticles and ions on dural fibroblasts and dural epithelial cells. *Biomaterials*, 34, (14) pp. 3547–3558.

Benzel, E.C. 2001 Biomechanics of Spine Stabilization. (Thieme Medical Publishers).

Berney, M., Hammes, F., Bosshard, F., Weilenmann, H-U., Egli, T. 2007. Assessment and Interpretation of Bacterial Viability by using the LIVE/DEAD BacLight Kit in Combination with Flow Cytometry. *Applied and Environmental Microbiology,* 73 (10), pp. 3283-3290.

Berry, M., Peterson, B., Alander, D., 2010. A granulomatous mass surrounding a maverick total disc replacement causing iliac vein occlusion and spinal stenosis a case report. *Journal of Bone and Joint Surgery*, 92, pp. 1242–1245.

Beyersmann, D. & Hartwig, 2008. A. Carcinogenic metal compounds: recent insight into molecular and cellular mechanisms. *Archives of Toxicology*, 82, pp.493–512.

Billi, F., Benya, P., Kavanaugh, A., Adams, J., McKellop, H. 2012. The John Charnley Award: An Accurate and Extremely Sensitive Method to Separate, Display, and Characterize Wear Debris Part 2: Metal and Ceramic Particles. *Clinical Orthopaedics and Related Research,* 470 (2), pp.339-350.

Billi, F., Benya, P., Ebramzadeh, E., Campbell, P., Chan, F., McKellop, H.A. 2009. Metal wear particles : What we know, what we do not know, and why. *ESAS Journal*, 3 (4), pp. 133–142.

Billi, F., & Campbell, P. 2010. Nanotoxicology of metal wear particles in total joint arthroplasty: a review of current concepts. *Journal of Applied Biomaterials and Biomechanics,* 8 (1), pp.1–6.

Boden, S.D., Balderston, R.A., Heller, J.G., Hanley, E.N., Edward. N., Zigler, J.E., 2004. An AOA Critical issue: Disc replacements: This time will we really cure low-back and neck pain? *Journal of Bone and Joint Surgery*, 86-A (2), pp. 411–422.

Bohlman, H.H., Emery, S.E., Goodfellow, D.B. 1993. Anterior cervical discectomy and arthrodesis for cervical radiculopathy. Long-term follow-up of one hundred and twenty-two patients. *Journal of Bone and Joint Surgery (American Volume)*, 75, pp. 1298–1307.

Bonnier, F., Keating, M.E., Wróbel, T. P., Majzner, K., Baranska, M., Garcia-Munoz, A., Blanco, A., Byrne, H.J. 2015. Cell viability assessment using the Alamar blue assay : A comparison of 2D and 3D cell culture models. *Toxicology In Vitro*, 29 (1), pp. 124–131.

Boos, N., Marchesi, D., Aebi, M., 1992. Survivorship analysis of pedicular fixation systems in the treatment of degenerative disorders of the lumbar spine: a comparison of Cotrel-Dubousset instrumentation and the AO internal fixator. *Journal of Spinal Disorders*, 5 (4), pp. 403–409.

Botti, T.P., Gent, J., Martell, J.M., Manning, D.W. 2005. Trunion fracture of a fully porous-coated femoral stem. Case report. *The Journal of Arthroplasty.* 20 (7), pp. 943-945.

Bozic, K.J. & Ries, M.D., 2005. Wear and osteolysis in total hip arthroplasty. *Seminars in Arthroplasty*, 16 (2), pp. 142–152.

Brahmachari, S., Fung, Y.K., Pahan, K. 2006. Induction of Glial Fibrillary Acidic Protein Expression in Astrocytes by Nitric Oxide. *Journal of Neuroscience*, 26 (18), pp. 4930–4939.

Brown, C., Williams, S., Tipper, J.L., Fisher, J., Ingham, E. 2007. Characterisation of wear particles produced by metal on metal and ceramic on metal hip prostheses under

standard and microseparation simulation. *Journal of Materials Science. Materials in Medicine,* 18 (5), pp. 819–827.

Brown, C., Lacharme-Lora, L., Mukonoweshuro, B., Sood, A., Newson, R.B., Fisher, J., Case, P.C., Ingham, E. 2013. Biomaterials Consequences of exposure to peri-articular injections of micro- and nano-particulate cobalt chromium alloy. *Biomaterials*, 34, pp. 8564–8580.

Bryant, M.G. 2013. Fretting-Crevice Corrosion of Cemented Metal on Metal Total Hip Replacements. University of Leeds

Burnett, R.S.J. 2010 Total hip arthroplasty: Techniques and results. *British Columbia Medical Journal,* 52 (9), pp.455-464.

Büttner-Janz, K., Hochschuler, S.H., McAfee, P.C., 2003. The Artificial Disc. (Springer).

Cabraja, M., Schmeding, M., Koch, A., Podrabsky, P., Kroppenstedt, S. 2012. Delayed formation of a devastating granulomatous process after metal-on-metal lumbar disc arthroplasty. *Spine*, 37, pp. E809–E813.

Calvo, J.L., Carbonell, A.L., Boya, J. 1991 Co-expression of glial fibrillary acidic protein and vimentin in reactive astrocytes following brain injury in rats. *Brain Research,* 566 (1-2), pp. 333-336.

Campbell, P., Urban, R., Catelas, I., Skipor, A.K., Schmalzried, T.P. 2003. Autopsy analysis thirty years after metal-on-metal total hip replacement. A case report. *Journal of Bone and Joint Surgery (American Volume)*, 85(11), pp. 2218–2222.

Campbell, P., Ebramzadeh, E., Nelson, S., Takamura, K., De Smet, K., Amstutz, H.C. 2010. Histological features of pseudotumor-like tissues from metal-on-metal hips. *Clinical Orthopaedics and Related Research*, 468 (9), pp. 2321–2327.

Cancilla, P.A., Bready, J., Berliner, J., Sharifi –Nia, H., Toga, A.W., Santori, E.M., Scully, S., deVellis, J. 1992. Expression of mRNA for glial fibrillary acidic protein after experimental cerebral injury. *Journal of Neuropathology and Experimental Neurology*, 51 (5) pp. 560–565.

Carletti, E., Motta, A., Migliaresi, C. 2010. Scaffolds for Tissue Engineering and 3D Culture. *Methods in Molecular Biology*, 685, pp. 17–39.

Case, C.P., Langkamer, V.G., James, C., Palmer, M.R., Kemp, A.J., Heap, P.F., Solomon, L. 1994. Widespread dissemination of metal debris from implants. *Journal of Bone and Joint Surgery (British Volume)*, 76 (5), pp. 701–712.

Catelas, I., Bobyn, J.D., Medley, J.B., Krygier, J.J., Zukor, D.J., Petit, A., Huk, O.L. 2001. Effects of digestion protocols on the isolation and characterisation of metal-metal wear particles. I. Analysis or particle size and shape. *Journal of Biomedical Materials Research*, 5 (55), pp. 320–329.

Catelas, I., Bobyn, J.D., Medley, J.B., Krygier, J.J., Zukor, D.J., Huk, O.L. 2003. Size, shape, and composition of wear particles from metal-metal hip simulator testing: effects of alloy and number of loading cycles. *Journal of Biomedical Materials Research. Part A*, 67 (1), pp. 312–327.

Catelas, I., Petit, A., Zukor, D.J, Antoniou, J., Huk, O.L. 2003. TNF-alpha secretion and macrophage mortality induced by cobalt and chromium ions in vitro-qualitative analysis of apoptosis. *Biomaterials.* 24, pp.383–391.

Cavanaugh, D.A., Nunley, P.D., Kerr, E.J., Werner, D.J., Jawahar, A. 2009. Delayed hyper-reactivity to metal ions after cervical disc arthroplasty: a case report and literature review. *Spine*, 34 (7), pp. E262–265.

Chang, B-S., Brown, P.R., Sieber, A., Kostuik, J.P. 2004. Evaluation of the biological response of wear debris. *The Spine Journal*, 4(6 Supplement), pp. S239–S244.

Chapman, J. & Riew, D., 2012. Cervical artificial disc replacement: still experimental? Introduction and perspectives on cervical artificial disc replacement. *Evidence-Based Spine-Care Journal*, 3 (1), pp. 5–8.

Chen, Q. & Thouas, G.A. 2015. Metallic implant biomaterials. *Materials Science and Engineering R: Reports*, 87, pp. 1–57.

Chiba, A., Kumagai, K., Nomura, N., Miyakawa, S. 2007. Pin-on-disk wear behaviour in a like-on-like configuration in a biological environment of high carbon cast and low carbon forged Co-29Cr-6Mo alloys. *Acta Materialia*, 55 (4), pp. 1309–1318.

Chithrani, B.D., Ghazani, A.A., Chan, W.C.W. 2006. Determining the Size and Shape Dependence of Gold Nanoparticle Uptake into Mammalian Cells. *Nano Letters,* 6 (4), pp. 662-668.

Choma, T.J., Miranda, J., Siskey, R., Baxter, R., Steinbeck, M., Kurtz, S.M. 2009. Retrieval Analysis of a ProDisc-L Total Disc Replacement. *Journal of Spinal Disorders and Techniques*, 22 (4), pp. 290–296.

Chueh, P.J., Liang, R.Y., Lee, Y.H., Zeng, Z.M., Chuang, S.M. 2014. Differential cytotoxic effects of gold nanoparticles in different mammalian cell lines. *Journal Hazardous Materials*, 264, pp. 303–312.

Chun, S.I. & Mun, C.W. 2015. Cytotoxicity of TSP in 3D Agarose Gel Cultured Cell. *PLoS ONE*, 10 (6), pp. 1-11.

Chwalek, K., Tsurkan, M.V., Freudenberg, U., Werner, C. 2014. Glycosaminoglycan-based hydrogels to modulate heterocellular communication in *in vitro* angiogenesis models. *Scientific Reports*, 4 (4414) pp. 1-8.

Colle, K.O., Butler, J.B., Reyes, P.M., Newcomb, A.G.U.S., Theodore, N., Crawford, N.R. 2013. Biomechanical evaluation of a metal-on-metal cervical intervertebral disc prosthesis. *The Spine Journal*, 13 (11), pp. 1640–1649.

Colombier, P., Clouet, J., Hamel, O., Lescaudron, L., Guicheux, J. 2014. The lumbar intervertebral disc : From embryonic development to degeneration. *Joint Bone Spine*, 81 (2), pp. 125–129.

Cooper, J.H, Della Valle, C.J., Berger, R.A., Tetreault, M., Paprosky, W.G., Sporer, S.M., Jacobs, J.J. 2012 Corrosion at the head-neck taper as a cause for adverse local tissue reactions after total hip arthroplasty. *Journal of Bone and Joint Surgery (American Volume)* 94 (18), pp. 1655-1661.

Coric, D., Nunley, P.D., Guyer, R.D., Musante, D., Carmody, C.N., Gordon, C.R., Lauryssen, C., Ohnmeiss, D.D., Boltes, M.O. 2011. Prospective, randomized, multicenter study of cervical arthroplasty: 269 patients from the Kineflex|C artificial disc investigational device exemption study with a minimum 2-year follow-up: clinical article. *Journal of Neurosurgery. Spine*. 15 (4), pp. 348–358.

Cramer, S., Tacke, S., Bornhorst, J., Sachan, A.K., Klingauf, J., Schwerdtle, T., Galla, H-J. 2014. The Influence of Silver Nanoparticles on the Blood-Brain and the Blood-Cerebrospinal Fluid Barrier *in vitro*. *Journal of Nanomedicine & Nanotechnology*, 5 (5), pp. 2–13.

Cunningham, B.W., Hallab, N.J., Hu, N., McAfee, P.C. 2013. Epidural application of spinal instrumentation particulate wear debris: a comprehensive evaluation of neurotoxicity using an *in vivo* animal model. *Journal of Neurosurgery. Spine*. 19 (3), pp. 336–350.

Daley, B., Doherty, A.T, Fairman, B., Case, C.P. 2004. Wear debris from hip or knee replacements causes chromosomal damage in human cells in tissue culture. *Journal of Bone and Joint Surgery (British volume)* 86 (4), pp.598–606.

Daniel, J., Holland, J., Quigley, L., Sprague, S., Bhandari, M., 2012. Pseudotumors associated with total hip arthroplasty. *Journal of Bone and Joint Surgery (American Volume)*, 94 (1), pp. 86–93.

Daroui, P., Desai, S.D., Li, T-K., Liu, A.A., Liu, L.F. 2004. Hydrogen Peroxide Induces Topoisomerase I-mediated DNA Damage and Cell Death. *The Journal of Biological Chemistry*, 279 (15), pp. 14587–14594.

David, A & Lobner, D., 2004. *In vitro* cytotoxicity of orthodontic archwires in cortical cell cultures. *European Journal of Orthodontics*, 26 (4), pp. 421–426.

Davies, J.R. 2003 Metallic materials Handbook of Materials for Medical Devices, *ASM International,* pp. 21–50.

Davis, D.L. & Morrison, J.J. 2016. Hip Arthroplasty Pseudotumors: Pathogenesis, Imaging and Clinical Decision Making. *Journal of Clinical Imaging Science*, 6 (17), pp. 1-9.

De Guzman, R.C. & VandeVord, P.J., 2007. Variations in astrocyte and fibroblast response due to biomaterial particulates *in vitro*. *Journal of Biomedical Materials Research - Part A*, 85 (1), pp. 14–24.

De Kleuver, M., Oner, F.C., Jacobs, W.C.H. 2003. Total disc replacement for chronic low back pain: background and a systematic review of the literature. *European spine journal : official publication of the European Spine Society, the European Spinal Deformity Society, and the European Section of the Cervical Spine Research Society*, 12 (2), pp. 108–116.

Depault, F., Cojocaru, M., Fortin, F., Chakrabarti, S., Lemieux, N. 2006. Genotoxic effects of chromium(VI) and cadmium(II) in human blood lymphocytes using the electron

microscopy in situ end-labeling (EM-ISEL) assay. *Toxicology In Vitro: An International Journal Published in Association with BIBRA.* 20 (4), pp. 513-518.

Devin, C.J., Myers, T.G., Kang, J.D., 2008. Chronic failure of a lumbar total disc replacement with osteolysis. Report of a case with nineteen-year follow-up. *Journal of Bone and Joint Surgery (American Volume)*, 90 (10), pp. 2230–2234.

Doorn, P.F., Campbell, P.A. & Amstutz, H.C. 1996. Metal versus polyethylene wear particles in total hip replacements. A review. *Clinical Orthopaedics and Related Research*, (329 Supplement), pp. S206–S216.

Doorn, P. F., Campbell, P. A., Worrall, J., Benya, P. D., McKellop, H. A., Amstutz, H.C. 1998. Metal wear particle characterization from metal on metal total hip replacements: Transmission electron microscopy study of periprosthetic tissues and isolated particles. *Journal of Biomedical Materials Research*, 42 (1), pp. 103–111.

Driessens, N., Versteyhe, S., Ghaddhab, C., Burniat, A., De Deken, X., Van Sande, J., Dumont, J-E., Miot, F., Corvilain, B. 2009. Hydrogen peroxide induces DNA single- and double-strand breaks in thyroid cells and is therefore a potential mutagen for this organ. *Endocrine-Related Cancer*, 16 (3), pp. 845–856.

Drummond, J., Tran, P., Fray, C. 2015. Metal-on-Metal Hip Arthroplasty: A Review of Adverse Reactions and Patient Management. *Journal of Functional Biomaterials*, 6 (3) pp.485-499.

Dumitru, C.D., Ceci, J.D., Tsatsanis, C., Kontoyiannis, D., Stamatkis, K., Lin, J.H., Patriotis, C., Jenkins, N.A., Copeland, N.G., Kollias, G., Tsichlis, P.N. 2000. TNF-α induction by LPS is regulated post transcriptionally via a Tpl2/ERK-dependent pathway. *Cell*, 103 (7), pp. 1071–1083.

East, E. & Phillips, J.B. 2008 Tissue engineered cell culture models for nervous system research. *Tissue Engineering Research Trends* Nova science publishers. pp. 141-160.

East, E., Golding, J.P., Phillips, J.B. 2009. A versatile 3D culture model facilitates monitoring of astrocytes undergoing reactive gliosis. *Journal of Tissue Engineering and Regenerative Medicine*, 3 pp. 634-646.

East, E., Golding, J.P. & Phillips, J.B. 2012. Engineering an integrated cellular interface in three-dimensional hydrogel cultures permits monitoring of reciprocal astrocyte and neuronal responses. *Tissue Engineering Part C: Methods*, 18 (7), pp. 526–536.

Eddleston, M.,& Mucke, L., 1993. Molecular profile of reactive astrocytes- implications for their role in neurologic disease. *Neuroscience*, 54 (1), pp. 15–36.

Erwin, W.D., Dickson, J.H., Harrington, P.R. 1980. Clinical review of patients with broken Harrington Rods. *The Journal of Bone & Joint Surgery (American Volume)*, 62 (8), pp. 1302–1307.

Eyre, T.S. 1976. Wear characteristics of metals. *Tribology International*, 9 (5), pp. 203–212.

Faccioni, F., Franceschetti, P., Cerpelloni, M., Fracasso, M.E. 2003. *In vivo* study on metal release from fixed orthodontic appliances and DNA damage in oral mucosa cells. *American Journal of Orthodontics and Dentofacial Orthopaedics,* 124 (6), pp.687–693.

Fairbank, J., Frost, H., Wilson-MacDonald, J., Yu, L-M., Barker, K., Collins, R. 2005. Randomised controlled trial to compare surgical stabilisation of the lumbar spine with an intensive rehabilitation programme for patients with chronic low back pain: the MRC spine stabilisation trial. *The BMJ*, 330, pp.1–7.

Fini, M., Nicoli Aldinia, N., Torricellia, P., Giavaresia, G., Borsaria, V., Lengerb, H., Bernauerb, J., Giardinoa, R., Chiesad, R., Cigadad, A. 2003. A new austenitic stainless steel with negligible nickel content : an *in vitro* and *in vivo* comparative investigation. *Biomaterials,* 24, pp. 4929–4939

Firkins, P.J., Tipper, J.L., Saadatzadeh, M.R., Ingham, E., Stone, M.H., Farrar, R., Fisher, J. 2001. Quantitative analysis of wear and wear debris from metal-on-metal hip prostheses tested in a physiological hip joint simulator. *Bio-Medical Materials and Engineering*, 11 (2), pp. 143–157.

Firkins, P.J., Tipper, J.L., Ingham, E., Stone, M.H., Farrad, R., Fisher, J. 2001. A novel low wearing differential hardness, ceramic-on-metal hip joint prosthesis. *Journal of Biomechanics*, 34, pp. 1291–1298.

Fisichella, M., Dsabboue, H., Bhattacharyya, S., Saboungi, M.L., Salvetat, J.P., Hevor, T., Guerin, M., 2009. Mesoporous silica nanoparticles enhance MTT formazan exocytosis in HeLa cells and astrocytes. *Toxicology in Vitro*, 23 (4), pp. 697–703.

Fritzell, P., Hagg, O., Wessberg, P., Nordwall, A., 2001. Volvo Award Winner in Clinical Studies: Lumbar fusion versus nonsurgical treatment for chronic low back pain: a multicenter randomized controlled trial from the Swedish Lumbar Spine Study Group. *Spine*, 26 (23), pp. 2521–2532.

Fu, T.S., Wang, I.C., Lu, M-L., Hsieh, M-K., Chen, L-H., Chen, W-J. 2016. The fusion rate of demineralised bone matrix compared with autogenous iliac bone graft for long multi-segment posterolateral spinal fusion. *BMC Musculoskeletal Disorders*, 17 (3), pp. 1-6.

Galvin, A., Kang, L., Tipper, J., Stone, M., Ingham, E., Jin, Z., Fisher, J. 2006 Wear of crosslinked polyethylene under different tribological conditions. *Journal of Materials Science, Materials in Medicine.* 17 (3), pp. 235–243.

Garrido, B.J., Wilhite, J., Nakano. M., Crawford, C., Baldus, C., Riew, K.D., Sasso, R.C. 2011. Adjacent-level cervical ossification after Bryan cervical disc arthroplasty compared with anterior cervical discectomy and fusion. *Journal of Bone and Joint Surgery (American Volume),* 93 (13), pp. 1185–1189.

Gajski, G., Jelcic, Z., Orescanin, V., Geric, M., Kollar, R., Garaj-Vrhovac, V. 2014. Physico-chemical characterisation and the *in vitro* genotoxicity of medical implants metal alloy (TiAlV and CoCrMo) and polyethylene particles in human lymphocytes. *Biochimica et Biophysica Acta (BBA) - General Subjects*, 1840 (1), pp.565–576.

Gehrmann, J., Matsumoto, Y., Kreutzberg, G.W. 1995. Microglia: intrinsic immuneffector cell of the brain. *Brain Research. Brain Research Reviews*, 20 (3), pp.269–287.

Germain, M.A., Hatton, A., Williams, S., Matthews, J.B., Stone, M.H., Fisher, J., Ingham, E. 2003. Comparison of the cytotoxicity of clinically relevant cobalt-chromium and alumina ceramic wear particles *in vitro*. *Biomaterials*, 24 (3), pp.469–479.

Goffin, J., Geusens, E., Vantomme, N., Quintens, E., Waerzeggers, Y., Depreitere, B., Van Calenbergh, F., Van Loon, J. 2004 Long-term follow-up after interbody fusion of the cervical spine. *Journal of Spinal Disorders and Techniques*, 17 (2), pp. 79–85.

Golish, S.R. & Anderson, P.A. 2012. Bearing surfaces for total disc arthroplasty: metal-on-metal versus metal-on-polyethylene and other biomaterials. *The Spine Journal*, 12 (8), pp.693–701.

Gomes, F.C.A., Paulin, D., Neto, V.M. 1999. Glial fibrillary acidic protein (GFAP): Modulation by growth factors and its implication in astrocyte differentiation. *Brazilian Journal of Medical and Biological Research*, 32 (5), pp.619–631.

Good, C.R. 2010. Evolution in the Treatment of Spinal Deformity and Spinal Instrumentation. *Journal of The Spinal Research Foundation*, 5 (1), pp.19–25.

Goodman, S.B. 2007. Wear particles, periprosthetic osteolysis and the immune system. *Biomaterials*, 28 (34), pp.5044–5048.

Gowland, N.J. 2014. The Wear and Biological Activity of Antioxidant UHMWPE for use in Total Hip Replacements. University of Leeds.

Gratton, S.E., Ropp, P.A., Pohlhaus, P.D., Luft, J.C., Madden, V.J., Napier, M.E., DeSimone, J.M. 2008. The effect of particle design on cellular internalization pathways. *Proceedings of the National Academy of Sciences of the United States of America,* 105 (33), pp.11613–11618.

Gray, H. 1918. Anatomy of the Human Body. Philadelphia: Lea & Febiger.

Green, T.R., Fisher, J., Stone, M., Wroblewski, B.M., Ingham, E. 1998. Polyethylene particles of a "critical size" are necessary for the induction of cytokines by macrophages *in vitro*. *Biomaterials*, 19 (24), pp.2297–2302.

Green, T. R., Fisher, J., Matthews, J. B., Stone, M. H., Ingham, E. 2000. Effect of size and dose on bone resorption activity of macrophages by *in vitro* clinically relevant ultra high molecular weight polyethylene particles. *Journal of Biomedical Materials Research,* 53 (5), pp.490-497.

Grissa, I., Guezguez, S., Ezzi, L., Chakroun, S., Sallem, A., Kerkeni, E., Elghoul, J., El Mir, L., Mehdi, M., Ben Cheikh, H., Haouas, Z. 2016. The effect of titanium dioxide nanoparticles on neuroinflammation response in rat brain. *Environmental Science and Pollution Research International.* 23 (20), pp.20205-20213.

Grobben, B., De Deyn, P.P., Slegers, H., 2002. Rat C6 glioma as experimental model system for the study of glioblastoma growth and invasion. *Cell and Tissue Research*, 310 (3), pp.257–270.

Grupp, T.M., Yue, J.J., Garcia, R., Basson, J., Schwiesau, J., Fritz, B., Blömer, W. 2009. Biotribological evaluation of artificial disc arthroplasty devices: Influence of loading

and kinematic patterns during *in vitro* wear simulation. *European Spine Journal*, 18 (1), pp.98–108.

Guerin, H. L. & Elliot, D. M. 2006. Degeneration affects the fiber reorientation of human annulus fibrosus under tensile loading. *Journal of Biomechanics,* 39 (8), pp.1410-1418.

Guyer, R.D., McAfee, P.C., Banco, R.J., Bitan, F.D., Cappuccino, A., Geisler, F.H., Hochschuler, S.H., Holt, R.T., Jenis, L.G., Majd, M.E., Regan, J.J., Tromanhauser, S.G., Wong, D.C., Blumenthal, S.L. 2009 Prospective, randomized, multicenter Food and Drug Administration investigational device exemption study of lumbar total disc replacement with the CHARITE artificial disc versus lumbar fusion: five-year follow up. *The Spine Journal,* 9 (5), pp.374–386

Guyer, R.D., Shellock, J., MacLennan, B., Hanscom, D., Knight, R.Q., McCombe, P., Jacobs, J.J., Urban, R.M., Bradford, D., Ohnmeiss, D.D. 2011. Early Failure of Metal-on-Metal Artificial Disc Prostheses Associated with Lymphocytic Reaction. *Spine*, 36 (7), pp.E492–E497.

Ha, L., Ceryak, S., Patierno, S.R. 2004. Generation of S phase-dependent DNA double-strand breaks by Cr(VI) exposure: involvement of ATM in Cr(VI) induction of γ-H2AX. *Carcinogenesis.* 25 (11) pp. 2265-2274.

Hailey, J. L., Ingham, E., Stone, M., Wroblewski, B. M., Fisher, J. 1996. Ultra- high molecular weight polyethylene wear debris generated *in vivo* and in laboratory tests; the influence of counterface roughness. *Proceedings of the Institute of Mechanical Engineers. Part H, Journal of Engineering in Medicine* 210 (1), pp. 3-10.

Hallab, N., Merritt, K., Jacobs, J.J. 2001. Metal sensitivity in patients with orthopaedic implants. *The Journal of Bone and Joint Surgery. American Volume*, 83-A (3), pp.428–436.

Hallab, N.J. 2009. A review of the biologic effects of spine implant debris: Fact from fiction. *SAS Journal*, 3 (4), pp.143–160.

Hallab, N.J. & Singh, V. 2014. Intervertebral disc joint replacement technology. *Joint Replacement Technology*. pp. 531–570.

Han, Q., Jin, W., Xiao, Z., Ni, H., Wang, J., Kong, J., Wu, J., Liang, W., Chen, L., Zhaoa, Y., Chen, B., Dai, J. 2010. The promotion of neural regeneration in an extreme rat spinal cord

injury model using a collagen scaffold containing a collagen binding neuroprotective protein and an EGFR neutralizing antibody. *Biomaterials*, 31 (35), pp.9212–9220.

Hashimoto, M., Hirokazu, T., Yonezawa, T., Kawai, K., Iijima, M., Endo, K. 2014. Evaluation of Silver Nanoparticle toxicity to RAW264.7 cells in a three-dimensional cell culture. *Journal of Biomaterials and Tissue Engineering*, 4 (1), pp.51–58.

Haw, R.T.Y., Tong, C.K., Yew, A., Lee, H.C., Phillips, J.B., Vidyadaran, S. 2014. A three-dimensional collagen construct to model lipopolysaccharide-induced activation of BV2 microglia. *Journal of Neuroinflammation*, 11 (1), pp.1–10.

Haycock, J. 2011. 3D Cell Culture: A Review of Current Approaches and Techniques. *3D Cell culture*, (695), pp.1–16.

HCUP Nationwide Inpatient Sample (NIS). Healthcare Cost and Utilization Project (HCUP). 2007/2011. Agency for Healthcare Research and Quality, Rockville, MD.

He, J.L., Chen, W.L., Jin, L.F., Jin, H.Y. 2000. Comparative evaluation of the *in vitro* micronucleus test and the comet assay for the detection of genotoxic effects of X-ray radiation. *Mutation research*, 469 (2), pp.223–231.

Head, W.C., Bauk, D.J., Emerson, R.H. 1995. Titanium as the material of choice for cementless femoral components in total hip arthroplasty. *Clinical Orthopaedics & Related Research*, 311, pp.85–90.

Heary, R.F. & Madhavan, K. 2008. The History of Spinal Deformity. *Neurosurgery*, 63 (3) supplement, pp.A5–A15.

Heller, J.G., Sasso, R.C., Papadopoulos, S.M., Anderson, P.A., Fessler, R.G., Hacker, R.J., Coric, D., Cauthen, J.C., Riew, D.K. 2009. Comparison of BRYAN cervical disc arthroplasty with anterior cervical decompression and fusion: clinical and radiographic results of a randomized, controlled, clinical trial. *Spine,* 34 (2), pp.101–107.

Hesketh, J.E.T., 2012. *Tribocorrosion of Total Hip Replacements*. University of Leeds

Hilibrand, H., Carlson, A.S., Palumbo, M.A., Jones, P.K., Bohlman, H.H., 1999. Radiculopathy and myelopathy at segments adjacent to the site of a previous anterior cervical arthrodesis. *Journal of Bone and Joint Surgery (American Volume)*, 81 (4), pp.519–528.

Hochschuler, S.H., Ohnmeiss, D.D., Guyer, R.D., Blumenthal, S.L. 2002. Artificial disc: preliminary results of a prospective study in the United States. *European spine journal : official publication of the European Spine Society, the European Spinal Deformity Society, and the European Section of the Cervical Spine Research Society*, 11 (Supplement 2), pp.S106–S110.

Hohman, D.W., Affonso, J., Anders, M. 2011 Ceramic-on-ceramic failure secondary to head neck taper mismatch. *American Journal of Orthopedics (Belle Mead NJ),* 40 (11), pp.571-573.

Holloway, I., Walter, W.L., Zicat, B., Walter, W.K. 2009. Osteolysis with a cementless second generation metal-on-metal cup in total hip replacement. *International Othropaedics (SICOT),* 33, pp.1537–1542.

Horsting, P.P., Pavlov, P.W., Jacobs, W.C., Obradov-Rajic, M., De-Kleuver, M. 2012. Good functional outcome and adjacent segment disc quality 10 years after single-level anterior lumbar interbody fusion with posterior fixation. *Global Spine Journal*, 2 (1), pp.21–26.

Hug, K.T., Watters, T.S., Vail, T.P., Bolognesi, M.P. 2013. The withdrawn ASR™ THR and hip resurfacing systems: How have our patients fared over 1 to 6 years? *Clinical Orthopaedics and Related Research*, 471 (2), pp.430–438.

Hughes, S.P.F., Freemont, A.J., Hukins, D.W.L., McGregor, A.H., Roberts, S., 2012. The pathogenesis of degeneration of the intervertebral disc and emerging therapies in the management of back pain. *The Journal of Bone and Joint Surgery (British Volume)*, 94 (10), pp.1298–1304.

Hyde, P.J. 2012 Bio-tribology of Total Disc Replacements of the Lumbar Spine University of Leeds

Hyde, P.J., Tipper, J.L., Fisher, J., Hall, R.M. 2015. Wear and biological effects of a semi-constrained total disc replacement subject to modified ISO standard test conditions. *Journal of the Mechanical Behaviour of Biomedical Materials*, 44, pp.43–52.

Iatridis, J.C. & Gwynn, I. 2004. Mechanisms for mechanical damage in the intervertebral disc annulus fibrosus. *Journal of Biomechanics*, 37, pp.1165–1175.

Ingham, E. & Fisher, J., 2000. Biological reactions to wear debris in total joint replacement. *Proceedings of the Institution of Mechanical Engineers, Part H: Journal of Engineering in Medicine*, 214 (1), pp.21–37.

Ingram, J.H., Stone, M., Fisher, J., Ingham, E. 2004. The influence of molecular weight, crosslinking and counterface roughness on TNF-α production by macrophages in response to ultra high molecular weight polyethylene particles. *Biomaterials*, 25 (17), pp.3511–3522.

Ishihara, H., Kanamori, M., Kawaguchi, Y., Nakamura, H., Kimura, T., 2004. Adjacent segment disease after anterior cervical interbody fusion. *Spine Journal*, 4 (6), pp.624–628.

Jacobs, J. J., Skipor, A. K., Doom, P. F., Campbell, P., Schmalzried, T. P., Black, J., Amstutz, H. C. 1996 Cobalt and chromium concentrations in patients with metal on metal total hip replacements. *Clinical Orthopaedics and Related Research*. 329 Supplement: S256-S263, pp.154.

Jacobs, J.J., Gilbert, J.L., Urban, R.M., 1998. Current Concepts Review - Corrosion of Metal Orthopaedic Implants Corrosion of Metal Orthopaedic Implants. *The Journal of Bone and Joint Surgery.* 80-A (2), pp.268-282.

Jacobs, J.J., Skipor, A.K., Patterson, L.M., Hallab, N.J., Paprosky, W.G., Black, J. 1998. Metal Release in Patients Who Have Had a Primary Total Hip Arthroplasty. A Prospective, Controlled, Longitudinal Study. *The Journal of Bone & Joint Surgery*, 80 (10), pp.1447–1458.

Jacobs, J.J., Urban, R.M., Hallab, N.J., Skipor, A.K., Fischer, A., Wimmer, M.A., 2009. Metal-on-metal bearing surfaces. *The Journal of The American Academy of Orthopaedic Surgeons.* 17 (2), pp.69–76.

Jacobs, V.L., Valdes, P.A., De Leo, J.A. 2011. Current reviews of *in vivo* GBM rodent models: emphasis on the CNS-1 tumour model. *ASN Neuro*, 3 (3), pp.171-181.

Jacobs, J.J., Cooper, H.J., Urban, R.M., Wixson, R.L., Della Valle, C.J. 2014. What do we know about taper corrosion in total hip arthroplasty? *The Journal of Arthroplasty*. 29 (4), pp.668-669.

Jaumard, N.V., Welch, W.C., Winkelstein, B.A., 2011. Spinal Facet Joint Biomechanics and Mechanotransduction in Normal, Injury and Degenerative Conditions. *Journal of Biomechanical Engineering*, 133 (7), pp.1-31.

Jones, C.F. & Grainger, D.W., 2009. *In vitro* assessments of nanomaterial toxicity. *Advanced Drug Delivery Reviews*, 61 (6), pp.438–456.

Joux, F., and P. Lebaron. 2000. Use of fluorescent probes to assess physiological functions of bacteria at single-cell level. *Microbes and Infection,* 2, pp.1523-1535.

Kaja, S., Payne, A.J., Naumchuk, Y., Levy, D., Zaidi, D.H., Altman, A.M., Nawazish, S., Ghuman, J.K., Gerdes, B.C., Moore, M., Koulen, P. 2015. Plate reader-based cell viability assays for glioprotection using primary rat optic nerve head astrocytes. *Experimental Eye Research*, 138, pp.159–166.

Kanaji, A., Orhue, V., Caicedo, M.S., Virdi, A.S., Sumner, D.R., Hallab, N.J., Yoshiaki, T., Sena, K. 2014. Cytotoxic effects of cobalt and nickel ions on osteocytes in vitro. *Journal of Orthopaedic Surgery and Research.* 9 (91), pp. 1-8.

Kandahari, A.M., Yang, X., Laroche, K.A., Dighe, A.S., Pan, D., Cui, Q. 2016. A review of UHMWPE wear-induced osteolysis: the role for early detection of the immune response. *Bone Research*, 4, pp.1-13.

Karlsson, H.L., Cronholm, P., Gustafsson, J., Moller, L. 2008. Copper Oxide Nanoparticles Are Highly Toxic: A Comparison between Metal Oxide Nanoparticles and Carbon Nanotubes. *Chemical Research in Toxicology*, 21 (9), pp.1726–1732.

Karnoub, M-A., Zairi, F., Aboukais, R., Assaker, R. 2015. Delayed Hypersensitivity Reaction: An Increasingly Recognized Complication of Metal-on-Metal Total Disc Replacement. *Case Reports in Orthopaedics,* 2015, pp. 1-3.

Kaur, G. & Dufour, J., 2012. Cell lines: valuable tools or useless artefacts. *Spermatogenesis*, 2 (1), pp.1–5.

Keegan, G. M., Learmonth, I. D. & Case, C. P. 2008. A systematic comparison of the actual, potential, and theoretical health effects of cobalt and chromium exposures from industry and surgical implants. *Critical Reviews in Toxicology*, 38, pp.645–674.

Kim, H.-D., Kim, K-S., Ki, S-C., Choi, Y-S. 2007. Electron Microprobe Analysis and Tissue Reaction around Titanium Alloy Spinal Implants. *Asian spine journal*, 1 (1), pp.1–7.

Kim, D.H., Lee, N., Shin, D.A., Yi, S., Kim, K., Ha, Y. 2016. Matched Comparison of Fusion Rates between Hydroxyapatite Demineralized Bone Matrix and Autograft in Lumbar Interbody Fusion. *Journal of korean Neurosurgical Society*, 59 (4), pp.363–367.

Kinbrum, A. & Unsworth, A. 2008. The wear of high-carbon metal-on-metal bearings after different heat treatments. *Proceedings of the Institution of Mechanical Engineers, Part H: Journal of Engineering in Medicine*, 222 (6), pp.887–895.

Kirkpatrick, J.S., Venugopalan, R., Beck, P., Lemons, J., 2005. Corrosion of spinal implants. *Journal of Spinal Disorders and Techniques*, 18 (3), pp.247–251.

Kopera, E., Schwerdtle, T., Hartwig, A., Bal, W. 2004. Co(II) and Cd(II) substitute for Zn(II) in the zinc finger derived from the DNA repair protein XPA, demonstrating a variety of potential mechanisms of toxicity. *Chemical Research in Toxicology.* 17 (11), pp.1452-1458.

Korovessis, P., Petsinis, G., Repanti, M., Repantis, T. 2006. Metallosis after contemporary metal-on-metal total hip arthroplasty. Five to nine-year follow-up. *Journal of Bone and Joint Surgery (American Volume)*, 88 (6), pp.1183–1191.

Kretzer, J.P., Kleinhans, J.A., Jakubowitz, E., Thomsen, M., Heisel, C. 2009. A meta-analysis of design- and manufacturing-related parameters influencing the wear behavior of metal-on-metal hip joint replacements. *Journal of Orthopaedic Research*, 27 (11), pp.1473–1480.

Kumazawa, R., Watari, F., Takashi, N., Tanimura, Y., Uo, M., Totsuka, Y. 2002. Effects of Ti ions and particles on neutrophil function and morphology. *Biomaterials*, 23 (17), pp.3757–3764.

Kurtz, S. M., Muratoglu, O. K., Evans, M., Edidin, A. A. 1999. Advances in the processing, sterilization, and crosslinking of ultra-high molecular weight polyethylene for total joint arthroplasty. *Biomaterials*, 20 (18), pp.1659-1688.

Kurtz, S.M., McCombe, P., Ciccarelli, L., Villarraga, M., Chan, F., 2005. Retrieval analysis of short-term implanted Maverick total disc arthroplasty. *Proceedings of the NASS 20th Annual Meeting/ The Spine Journal* 5, p.1S–189S.

Kurtz, S.M. & Edidin, A.A., 2006. *Spine Technology Handbook*. (Academic Press).

Kurtz, S.M., Ianuzzi, A., MacDonald, D. 2008. Does chronic rim impingement influence dome wear in mobile bearing TDR? Transactions of the 2008 Spine Arthroplasty Society Meeting, Miami, May 6-9. 8, pp.57

Kurtz, S.M., Steinbeck, M., Ianuzzi, A., Van Ooij, A., Punt, I.M., Isaza, J., Ross, E.R.S. 2009. Retrieval analysis of motion preserving spinal devices and periprosthetic tissues. *SAS Journal*, 3 (4), pp.161–177.

Kurtz, S.M., MacDonald, D., Ianuzzi, A., Van Ooij, A., Isaza, J., Ross, E.R., Regan, J., 2009. The natural history of polyethylene oxidation in total disc replacement. *Spine*, 34 (22), pp. 2369–2377.

Kurtz, S.M., Ciccarelli, L., Harper, M.L., Siskey, R., Shorez, J., Chan, F.W. 2012. Comparison of *in vivo* and simulator-retrieved metal-on-metal cervical disc replacements. *International Journal of Spine Surgery*, 6 (1), pp.145–156.

Kurtz, S.M., Toth, J.M., Siskey, R., Ciccarelli, L., MacDonald, D., Isaza, J., Lanman, T., Punt, I., Steinbeck. M., Goffin, J., Van Ooij, A. 2012. The Latest Lessons Learned from Retrieval Analyses of Ultra-High Molecular Weight Polyethylene, Metal-on-Metal, and Alternative Bearing Total Disc Replacements. *Seminars in Spine Surgery*, 24 (1), pp.57–70.

Kwon, Y.M., Xia, Z., Glyn-Jones, S., Beard, D., Gill, H.S. Murray, D.W. 2009. Dose- dependent cytotoxicity of clinically relevant cobalt nanoparticles and ions on macrophages *in vitro*. *Biomedical Materials.* 4 (2), pp.1-9.

Lal, S., Hall, R.M., Tipper, J.L. 2016. A novel method for isolation and recovery of ceramic nanoparticles and metal wear debris from serum lubricants at ultra-low wear rates. *Acta Biomaterialia.* 42 pp.420-428.

Landsiedel, R., Diana, M., Schulz, M., Wiench, K., Oesch, F. 2009. Genotoxicity investigations on nanomaterials : Methods, preparation and characterization of test material, potential artifacts and limitations — Many questions, some answers. *Mutation Research/Reviews in Mutation Research.* 681, pp.241–258.

Langkamer, V.G., Case, C.P., Heap, P., Taylor, A., Collins, C., Pearse, M., Solomon, L., 1992. Systemic distribution of wear debris after hip replacement. A cause for concern? *The Bone and Joint Journal*, 74 (6), pp.831–839.

Langton, D.J., Jameson, S.S., Joyce, T.J., Gandhi, J.N., Sidaginamale, R., Mereddy, P., Nargol, A.V.F., Lord, J. 2011. Accelerating failure rate of the ASR total hip replacement. *Journal of Bone and Joint Surgery (British Volume)*, 93-B (8), pp.1011–1016.

Langton, D.J., Joyce, T.J., Jameson, S.S., Lord J., van Orsouw, M., Holland, J.P., Nargol, A.V.F., de Smet, K.A. 2011. Adverse reaction to metal debris following hip resurfacing: the influence of component type, orientation and volumetric wear. *Journal of Bone and Joint Surgery (British Volume),* 93 pp.164–171.

LaPlaca, M.C., Simon, C.M., Prado, G.R., and Cullen, D.K. 2007. CNS injury biomechanics and experimental models. *Progress in Brain Research*. *161*, pp. 13–26.

Lark, R.K., Caputo, A.M., Brown, C.R., Michael, K.W., Thacker, J.K., Richardson, W.J. 2013. Distant Harrington rod migration 35 years after implantation. *Journal of Clinical Neuroscience*, 20 (10), pp. 1452–1453.

Li, M., Yin, T., Wang, Y., Du, F., Zou, X., Gregersen, H., Wang, G. 2014. Study of biocompatibility of medical grade high nitrogen nickel-free austenitic stainless steel *in vitro*. *Materials Science and Engineering C*, 43, pp. 641–648.

Li, X., Katsanevakis, E., Liu, X., Zhang, N., Wen, X. 2012. Progress in Polymer Science Engineering neural stem cell fates with hydrogel design for central nervous system regeneration. *Progress in Polymer Science*, 37 (8), pp. 1105–1129.

Liu, A., Richards, L., Bladen, C., Ingham, E., Fisher, J., Tipper, J.L. 2015. The biological response to nanometre-sized polymer particles. *Acta biomaterialia*, 23, pp. 38–51.

Lotz, J.C., Fields, A.J., Liebenberg, E.C., 2013. The role of the vertebral end plate in low back pain. *Global spine journal*, 3 (3), pp. 153–164.

Macaya, D.J., Hayakawa, K., Arai, K., Spector, M. 2013. Biomaterials Astrocyte in filtration into injectable collagen-based hydrogels containing FGF-2 to treat spinal cord injury. *Biomaterials*, 34 (14), pp. 3591–3602.

Markiewicz, I., & Lukomska, B. 2006. The role of astrocytes in the physiology and pathology of the central nervous system. *Acta Neurobiologiae Experimentalis,* 66 pp. 343-358.

Maroudas, A., Stockwell, R.A., Nachemson, A., Urban, J. 1975. Factors involved in the nutrition of the human lumbar intervertebral disc: cellularity and diffusion of glucose *in vitro*. *Journal of Anatomy*, 120 (Part 1), pp. 113–130.

Martin, S.F. 2004. T Lymphocyte-Mediated Immune Responses to Chemical Haptens and Metal Ions: Implications for Allergic and Autoimmune Disease. *International Archives of Allergy and Immunology*, 134 (3), pp. 186–198.

Martini, F.H., Nath, J.L. 2008 Fundamentals of Anatomy and Physiology. Eighth Edition (Benjamin Cummings Publishing Company).

Matthews, J. B., Mitchell, W., Stone, M. H., Fisher, J., Ingham, E. 2001. A novel three-dimensional tissue equivalent model to study the combined effects of cyclic mechanical strain and wear particles on the osteolytic potential of primary human macrophages *in vitro*. *Proceedings of the Institution of Mechanical Engineers Part H-Journal of Engineering in Medicine,* 215 (5)**,** pp. 479- 486.

McAfee, P.C., Reah, C., Gilder, K., Eisermann, L., Cunningham B. 2012. A meta-analysis of comparative outcomes following cervical arthroplasty or anterior cervical fusion: results from 4 prospective multicenter randomized clinical trials and up to 1226 patients. *Spine*, 37 (11), pp.943–952.

McKellop, H., Shen, F-W., Lu, B., Campbell, P., Salovey, R. 1999. Development of an extremely wear-resistant ultra high molecular weight polyethylene for total hip replacements. *Journal of Orthopaedic Research*, 17 (2), pp. 157–167.

McTighe, T., Brazil, D., Clarke, I., Keppler, L., Keggi, J., Tkach, T., McPherson, E. 2015. Metallic Modular Taper Junctions in Total Hip Arthroplasty. *Reconstructive Review*, 5 (2) pp. 29-42.

Meachim, G. & Brooke, G., 1983. The synovial response to intra-articular Co-Cr-Mo particles in Guinea pigs. *Biomaterials*, 4 (3), pp.153–159.

Mohanty, M., Baby, S., Menon, K.V. 2003. Spinal fixation device: a 6-year postimplantation study. *Journal of Biomaterials Applications,* 18 (2) pp. 109-121.

Morris, E.J. & Geller, H.M., 1996. Induction of Neuronal Apoptosis by Camptothecin, An Inhibitor of DNA Topoisomersase-I: Evidence for cell cycle-independent toxicity. *The Journal of Cell Biology*, 134 (3), pp. 757–770.

Muratoglu, O.K., Bragdon, C.R., O'Connor, D.O., Jasty, M., Harris, W.H. 2001. A novel method of cross-linking ultra-high-molecular-weight polyethylene to improve wear, reduce oxidation, and retain mechanical properties. *The Journal of Arthroplasty*, 16 (2), pp. 149–160.

Murphy, K., Travers, P., Walport, M., 2008. Janeway's Immunobiology. (Garland Science).

Murray, M.J., Mutton, P.J., Watson, P.J., 1982. Abrasive wear mechanisms in steels. *Journal of Lubrication Technology,* 104 (1), pp.9-16.

Murrey, D., Janssen, M., Delamarter, R., Goldstein, J., Zigler, J., Tay, B., Darden, B. 2009. Results of the prospective, randomized, controlled multicenter Food and Drug Administration investigational device exemption study of the ProDisc-C total disc replacement versus anterior discectomy and fusion for the treatment of 1-level symptomatic cervical disc disease. *Spine Journal*. 9 (4), pp.275–286.

Nakamura, J., Purvis, E.R., Swenberg, J.A., 2003. Micromolar concentrations of hydrogen peroxide induce oxidative DNA lesions more efficiently than millimolar concentrations in mammalian cells. *Nucleic Acids Research*, 31 (6), pp. 1790–1795.

Nechtow, W., Long, W., Dana, C., Bushelow, M., Ochs, A., Hintner, M., Kaddick, C. 2007. Vertebral Motion Segment Dynamics Influence Prodisc-L Wear Performance 1 Synthes , West Chester , PA ; 2 Endolab Mechanical Engineering GmbH , Thansau / Rosenheim , Germany Poster No . 1928 • 54th Annual Meeting of the Orthopaedic Research Society. 31 (1928), pp. 18192.

Neuman, B.J. 2014. Cervical disc arthroplasty: A selective alternative to fusion. *Seminars in Spine Surgery*, 26 (3), pp. 160–166.

Neumann, D.A. 2010. *Kinesiology of the Musculoskeletal System, Foundations for Rehabilitation*, 2nd Edition

NIH Consensus statement: Improving medical performance through retrieval information: Challenges and opportunities. National Institutes of Health Technology Assessment Conference. 2000

Nine, J., Choudhury, D., Hee, A-C., Mootanah, R., Osman, N.A.A. 2014. Wear Debris Characterization and Corresponding Biological Response: Artificial Hip and Knee Joints. *Materials,* 7, pp. 980–1016.

Nogueira, D.R., Mitjans, M., Rolim, C.M.B., Vinardell, M.P. 2014. Mechanisms Underlying Cytotoxicity Induced by Engineered Nanomaterials : A Review of *In Vitro* Studies. *Nanomaterials,* 4, pp. 454–484.

Nunley, P.D., Jawahar, A., Cavanaugh, D.A., Gordon, C.R., Kerr, E.J., Utter, P.A. 2013. Symptomatic adjacent segment disease after cervical total disc replacement: Re-examining the clinical and radiological evidence with established criteria. *The Spine Journal*, 13 (1), pp.5–12.

Obarzanek-Fojt, M., Curdy, C., Loggia, N., Di Lena, F., Grieder, K., Bitar, M., Wick, P. 2016. Tracking immune-related cell responses to drug delivery microparticles in 3D dense collagen matrix. *European Journal of Pharmaceutics and Biopharmaceutics*, 107, pp. 180–190.

O'Boynick, C.P. & Darden, B.V. 2016. Arthroplasty-A Comprehensive Review Chapter 4, pp.83-103.

O'Brien, T.J., Ceryak, S., Patierno, S.R. 2003. Complexities of chromium carcinogenesis: role of cellular response, repair and recovery mechanisms. *Mutation Research/Fundamental and Molecular Mechanisms of Mutagenesis,* 533 (1-2) pp. 3-36.

O'Leary, P., Nicolakis, M., Lorenz, M.A., Voronov, L.I., Zindrick, M.R., Ghanayem, A., Havey, R.M., Carandang, G., Sartori, M., Gaitanis, I.N., Fronczak, S., Patwardhan, A.G. 2005. Response of Charité total disc replacement under physiologic loads: Prosthesis component motion patterns. *The Spine Journal*, 5 (6), pp. 590–599.

Oral, E., Wannomae, K.K., Hawkins, N., Harris, W.H., Muratoglu, O.K. 2004. α-Tocopherol-doped irradiated UHMWPE for high fatigue resistance and low wear. *Biomaterials*, 25 (24), pp. 5515–5522.

Oral, E., Wannomae, K.K., Rowell, S.L., Muratoglu, O.K. 2007 Diffusion of vitamin E in ultra-high molecular weight polyethylene. *Biomaterials* 28 (35) pp. 5225–5237.

Oral, E. & Muratoglu, O.K., 2011. Vitamin E diffused, highly crosslinked UHMWPE: A review. *International Orthopaedics*, 35 (2), pp.215–223.

Ortiz, A.J., Fern, E., Vicente, A., Calvo, J.L., Ortiz, C. 2011. Metallic ions released from stainless steel, nickel-free, and titanium orthodontic alloys: Toxicity and DNA

damage. *American Journal of Orthodontics and Dentofacial Orthopaedics*, 140 (3), pp. 115–122.

Palepu, V., Kodigudla, M., Goel, V.K. 2012. Biomechanics of Disc Degeneration. *Advances in Orthopedics*.

Pansard, E., Fouilleron, N., Dereudre, G., Migaud, H., Girard, J. 2012. Severe corrosion after malpositioning of a metallic head over the Morse taper of a cementless hip arthroplasty. A case report. *Orthopaedics and Traumatology Surgery and Research* 98 (2) pp. 247-250.

Papageorgiou, I., Yin, Z., Ladon, D., Baird, D., Lewis, A.C., Sood, A., Newson, R., Learnmonth, I.D., Case, C.P. 2007. Genotoxic effects of particles of surgical cobalt chrome alloy on human cells of different age in vitro. *Mutation Research*. 619 (1-2), pp. 45–58.

Papageorgiou, I., Brown, C., Schins, R., Singh, S., Newson, R., Davis, S., Fisher, J., Ingham, E., Case, C.P. 2007. The effect of nano- and micron-sized particles of cobalt – chromium alloy on human fibroblasts *in vitro*. *Biomaterials*, 28, pp. 2946–2958.

Papageorgiou, I., Shadrick, V., Davis, S., Hails, S., Schins, R., Newson, R., Fisher, J., Ingham, E., Case, C.P. 2008. Macrophages detoxify the genotoxic and cytotoxic effects of surgical cobalt chrome alloy particles but not quartz particles on human cells *in vitro*. *Mutation Research / Fundamental and Molecular Mechanisms of Mutagenesis*, 643, pp. 11–19.

Papageorgiou, I., Marsh, R., Tipper, J.L., Hall, R.M., Fisher, J., Ingham, E. 2014. Interaction of micron and nano-sized particles with cells of the dura mater. *Journal of Biomedical Materials Research Part B.* 102, pp. 1496-1505.

Papageorgiou, I., Abberton, T., Fuller, M., Tipper, J.L., Fisher, J., Ingham, E. 2014. Biological Effects of Clinically Relevant CoCr Nanoparticles in the Dura Mater: An Organ Culture Study. *Nanomaterials*, 4 (2), pp. 485–504.

Paré, P.E., Chan, F.W., Powell, M. I., Matthews, H.H. 2007. Wear characterisation of the A-MAV anterior motion replacement using a spine wear simulator. *Wear*, 263 (7-12), pp. 1055–1059.

Park, Y-S., Moon, Y-W., Lim, S-J., Yang, J.M., Ahn, G., Choi, Y.-L. 2005. Early Osteolysis Following Second-Generation Metal-on-Metal Hip Replacement. *The Journal of Bone & Joint Surgery*, 87–A(7), pp. 1515–1521.

Parry, M.C., Bhabra, G., Sooda, A., Machadoa, F., Cartwright, L., Saunders, M., Ingham,E., Newson, R., Bloma, A.W., Case, C.P. 2010. Biomaterials Thresholds for indirect DNA damage across cellular barriers for orthopaedic biomaterials. *Biomaterials*, 31 (16), pp. 4477–4483.

Pasko, K., Papageorgiou, I., Hall, R.M., Neville, A., Tipper, J.L. 2016. Biological effects of cobalt-chromium nanoparticles and silicon nitride submicron and nanoparticles on L929 murine fibroblasts and primary porcine dural fibroblasts. In *10th World Biomaterials Congress- Montreal, Canada May 17-22*. pp. 4045.

Pekny, M. & Nilsson, M. 2005. Astrocyte activation and reactive gliosis. *Glia*, 50 (4), pp. 427–434.

Pekny, M. & Pekna, M. 2014. Astrocyte reactivity and astrogliosis: costs and benefits starting with a healthy brain. *Physiological Reviews.* 94, pp.1077–1098.

Pentreath, V.W. & Mead, C. 2004. Responses of Cultured Astrocytes, C6 Glioma and 1321Ni Astrocytoma Cells To Amyloid ß-Peptide Fragments. *Nonlinearity in Biology, Toxicology, and Medicine*, 2 (1), pp. 45–63.

Perry, M.J., Mortuza, F.Y., Ponsford, F.M., Elson, C.J., Atkins, R.M. 1995. Analysis of cell types and mediator production from tissues around loosening joint implants. *British Journal of Rheumatology*, 34 pp.1127-1134.

Pham, M.H., Mehta, V.A., Tuchman, A., Hsieh, P.C. 2015. Material Science in Cervical Total Disc Replacement. *BioMed Research International*.

Phillips, F.M. & Garfin, S.R. 2005. Cervical Disc Replacement. *Spine*, 30 (17 supplement), pp. S27–S33.

Phillips, J.B., King, V.R., Ward, Z., Porter, R.A., Priestley, J.V., Brown, R.A. 2004. Fluid shear in viscous fibronectin gels allows aggregation of fibrous materials for CNS tissue engineering. *Biomaterials*, 25 (14), pp. 2769–2779.

Poitout, D.G. 2016. Biomechanics and Biomaterials in Orthopaedics.(Springer)

Posada, O.M., Gilmour, D., Tate, R.J., Grant, H. 2014. CoCr wear particles generated from CoCr alloy metal-on-metal hip replacements , and cobalt ions stimulate apoptosis and expression of general toxicology-related genes in monocyte-like U937 cells. *Toxicology and Applied Pharmacology*, 281 (1), pp. 125–135.

Pourzal, R., Catelas, I., Theissmann, R., Kaddick, C., Fischer, A. 2011. Characterization of wear particles generated from CoCrMo alloy under sliding wear conditions. *Wear*, 271 (9–10), pp. 1658–1666.

Powell, M.L., Medley, J.B., Varano, R. 2005. Metal-metal cervical disc implants: A material investigation using pin-on-plate tests. *Life cycle tribology*. 48, pp. 845-852.

Prikryl, M., Srivastava, S.C., Viviani, G.R., Ives, M.B., Purdy, G.R. 1989. Role of corrosion in Harrington and Luque rods failure. *Biomaterials*, 10 (2), pp. 109–117.

Punt, I., Baxter, R., Van Ooij, A., Willems, P., Van Rhijn, L., Kurtz, S., Steinbeck, M. 2011. Submicron sized ultra-high molecular weight polyethylene wear particle analysis from revised SB Charite III total disc replacements. *Acta Biomaterialia*, 7 (9), pp. 3404–3411.

Quincozes-Santos, A., Bobermin, L.D., Latini, A., Wajner, M., Sourza, D.O., Goncalves, C-A., Gottfried, C. 2013. Resveratrol Protects C6 Astrocyte Cell Line against Hydrogen Peroxide-Induced Oxidative Stress through Heme Oxygenase 1. *PLoS ONE*, 8 (5), pp. 1–10.

Radziun, E., Wilczyn, J.D., Ksaizek, I., Nowak, K., Anuszewska, E.L., Kunicki, A., Olszyna, A., Zabkowski, T. 2011. Toxicology *in Vitro* Assessment of the cytotoxicity of aluminium oxide nanoparticles on selected mammalian cells. *Toxicology in Vitro*, 25, pp. 1694–1700.

Raghunathan, K.V., Deveya, M., Hawkins, S., Hails, L., Davis, S.A., Mann, S., Chang, I.T., Ingham,E. Malhas, A., Vaux, D.J., Lane, J.D. Case, C.P. 2013. Influence of particle size and reactive oxygen species on cobalt chrome nanoparticle-mediated genotoxicity. *Biomaterials*, 34 (14), pp. 3559–3570.

Raj, P.P. 2008. Intervertebral disc: Anatomy-physiology-pathophysiology-treatment. *Pain Practice*, 8 (1), pp. 18–44.

Rana, S. & Vir, S. 2008. Metals and apoptosis : Recent developments. *Journal of Trace Elements in Medicine and Biology*, 22, pp. 262–284.

Rapoff, A.J., O'Brien, T.J., Ghanayem, A.J,, Heisey, D.M., Zdeblick, T.A. 1999 Anterior cervical graft and plate load sharing. *Journal of Spinal Disorders*, 12 (1) pp. 45–49.

Reeks, J. & Liang, H., 2015. Materials and Their Failure Mechanisms in Total Disc Replacement. *Lubricants*, 3 (2), pp. 346–364.

Reidy, D., Finkelstein, J., Nagpurkar, A., Mousavi, P., Whyne, C. 2004. Cervical Spine Loading Characteristics in a Cadaveric C5 Corpectomy Model Using a Static and Dynamic Plate. *Journal of Spinal Disorders and Techniques*, 17 (2), pp. 117–122.

Reno, F. & Cannas, M. 2006. UHMWPE and vitamin E bioactivity: An emerging perspective. *Biomaterials*, 27 (16) pp. 3039-3043.

Richards, L., Brown, C., Stone, M.H., Fisher, J., Ingham, E., Tipper, J.L. 2008. Identification of nanometre-sized ultra-high molecular weight polyethylene wear particles in samples retrieved *in vivo. The Bone and Joint Journal,* 90-B (8), pp.1106-1113.

Robertson, J.T., Papadopoulos, S.M., Traynelis, V.C. 2005 Assessment of adjacent-segment disease in patients treated with cervical fusion or arthroplasty: a prospective 2-year study. *Journal of Neurosurgery. Spine.* 3 (6) pp. 417–423.

Rovetta, F., Stacchiotti, A., Faggi, F., Catalani, S., Apostoli, P., Fanzani, A., Aleo, M.F. 2013. Cobalt triggers necrotic cell death and atrophy in skeletal C2C12 myotubes. *Toxicology and Applied Pharmacology*, 271 (2), pp. 196–205.

Sansone, V., Pagani, D., Melato, M. 2013. The effects on bone cells of metal ions released from orthopaedic implants. A review. *Clinical Cases in Mineral and Bone Metabolism,* 10 (1), pp. 34-40.

Saikko, V. 2015. High frequency circular translation pin-on-disk method for accelerated wear testing of ultrahigh molecular weight polyethylene as a bearing material in total hip arthroplasty. *Journal of Biomechanics*, 48 (2), pp.401–404.

Salgado, A.J., Coutinho, O.P., Reis. R.L. 2004. Novel Starch-Based Scaffold for Bone Tissue Engineering: Cytotoxicity, Cell Culture and Protein Expression. *Tissue Engineering*, 10 (3-4), pp. 465–474.

Sanchez, V.C., Weston, P., Yan, A., Hurt, R.H., Kane, A.B. 2011. A 3-dimensional *in vitro* model of epithelioidgranulomas induced by high aspect ratio nanomaterials. *Particle and Fibre Toxicology*. 8 (17) pp.1-18

Sargeant, A. & Goswami, T. 2007. Hip implants - Paper VI - Ion concentrations. *Materials and Design*, 28 (1), pp. 155–171.

Sasso, R.C., Anderson, P.A. Riew, D.K., Heller, J.G. 2011. Results of Cervical Arthroplasty Compared with Anterior Discectomy and Fusion: Four-Year Clinical Outcomes in a Prospective, Randomized Controlled Trial. *Journal of Bone and Joint Surgery (American Volume)*, 93 (18), pp. 1684–1692.

Saura, J. 2007. Microglial cells in astroglial cultures : a cautionary note. *Journal of Neuroinflammation*, 4 (26), pp. 1–11.

Schaaf, T.A. 1998. Spinal Implants: Increasing Growth, Accelerating Competition. MedPro Month VIII.

Scharf, B., Clement, C.C., Zolla, V., Perino, G., Yan, B., Elci, S.G., Purdue, E., Goldring, S., Macaluso, F., Cobelli, N., Vachet, R.W., Santambrogio, L. 2014. Molecular analysis of chromium and cobalt related toxicity. *Nature Scientific Reports*, 4 (5729), pp.1-12.

Schlachetzki, J.C.M., Saliba, S.W., De Oliveira, A.C.P., 2013. Studying neurodegenerative diseases in culture models. *Revista Brasileira de Psiquiatria*, 35 (Supplement 2), pp. 92–100.

Schmiedberg, S.K., Chang, D.H., Frondoza, C.G., Valdevit, A.D.C., Kostuik, J.P. 1994. Isolation and characterisation of metallic wear debris from dynamic intervertebral disc prosthesis. *Journal of Biomedical Materials Research*, 28 (11), pp. 1277–1288.

Senaran, H., Atilla, P., Kaymaz, F., Acaroglu, E., Surat, A. 2004. Ultrastructural analysis of metallic debris and tissue reaction around spinal implants in patients with late operative site pain. *Spine*, 29 (15), pp. 1618–1623.

Sergent-Tanguy, S., Michel, D.C., Neveu, I., Navelihan, P. 2006. Long-lasting co-expression of nestin and glial fibrillary acidic protein in primary cultures of astroglial cells with a major participation of nestin+/GFAP− cells in cell proliferation. *Journal of Neuroscience Research*, 83 (8), pp. 1515–1524.

Serhan, H., Mhatre, D., Defossez, H., Bono, C.M. 2011. Motion-preserving technologies for degenerative lumbar spine: The past, present, and future horizons. *SAS Journal* , 5 (3), pp. 75–89.

Setton, L.A. & Chen, J. 2004. Cell Mechanics and Mechanobiology in the Intervertebral Disc. *Spine*, 29 (23), pp. 2710–2723.

Shahgaldi, B.F., Heatley, F.W., Dewar, A., Corrin, B., 1995. *In Vivo* corrosion of cobalt-chromium and titanium wear particles. *The Journal of Bone & Joint Surgery (British Volume)*, 77 (6), pp. 962–966.

Shang, X., Wang, L., Kou, D., Jia, X., Yang, X., Zhang, M., Tang, Y., Wang, P., Wang, S., Xu, Y., Wang, H. 2014. Metal hypersensitivity in patient with posterior lumbar spine fusion: a case report and its literature review. *BMC musculoskeletal disorders*, 15 (314), pp. 1-6

Shea, K.G., Lundeen, G.A., Bloebaum, R.D., Bachus, K.N., Zou, L. 1997. Lymphoreticular dissemination of metal particles in patients with primary joint replacements. *Clinical Orthopaedics and Related Research.* 338 pp. 219-226.

Shichang, L., Yueming, S., Limin, L., Lei, W., Zhongjie, Z., Chunguang, Z., Xi, Y. 2016. Clinical and radiologic comparison of dynamic cervical implant arthroplasty and cervical total disc replacement for single-level cervical degenerative disc disease. *Journal of Clinical Neuroscience*, 27 pp. 102–109.

Shilo, M., Sharon, A., Baranes, K., Motiei, M., Lellouche, J-P.M., Popovtzer, R. 2015. The effect of nanoparticle size on the probability to cross the blood-brain barrier: an *in-vitro* endothelial cell model. *Journal of Nanobiotechnology*, 13 (19), pp.1-7.

Siepe, C.J., Wiechert, K., Khattab, M.F., Korge, A., Mayer, H.M. 2007. Total lumbar disc replacement in athletes: clinical results, return to sport and athletic performance. *European Spine Journal,* 16 (7), pp.1001-1013

Silver, J., & Miller, J.H. 2004. Regeneration beyond the glial scar. *Nature Reviews Neuroscience,* 5 pp.146–156.

Singh, J. Carlisle, D.L., Pritchard, D.E., Patierno. S.R. 1998. Chromium-induced genotoxicity and apoptosis: relationship to chromium carcinogenesis (review). *Oncology reports*, 5 (6), pp. 1307-1325.

Singh, N., Manshian, B., Jenkins, G.J.S., Griffiths, S. M., Williams, P.M., Maffeis, T.G.G., Wright, C.J., Doak, S.H. 2009. NanoGenotoxicology: The DNA damaging potential of engineered nanomaterials. *Biomaterials*, 30 (23-24), pp. 3891–3914.

Slotkin, T.A., Card, J., Stadler, A., Levin, E.D., Seidler, F.J. 2014. Effects of tobacco smoke on PC12 cell neurodifferentiation are distinct from those of nicotine or benzo[a]pyrene. *Neurotoxicology and Teratology*, 43, pp. 19–24.

Smith, T.J. & Fernie, G.R. 1991. Functional Biomechanics of the Spine. *Spine*, 16(10) pp. 1197-1203

Sruthi, S. & Mohanan, P. V. 2015. Investigation on cellular interactions of astrocytes with zinc oxide nanoparticles using rat C6 cell lines. *Colloids and Surfaces B: Biointerfaces*, 133, pp. 1–11.

Sun, D., Wharton, J.A., Wood, R.J.K. 2009. Micro-abrasion-corrosion of cast CoCrMo-Effects of micron and sub-micron sized abrasives. *Wear*, 267(1-4), pp. 52–60.

Suñer, S., Bladen, C.L., Gowland, N., Tipper, J.L., Emamia, N. 2014. Investigation of wear and wear particles from a UHMWPE / multi-walled carbon nanotube nanocomposite for total joint replacements. *Wear*, 317(1-2), pp. 163–169.

Taksali, S., Grauer, J.N., Vaccaro, A.R. 2004. Material considerations for intervertebral disc replacement implants. *The Spine Journal*, 4 (6 supplement), pp. S231–S238.

Tang, B., Fang, G., Gao, Y., Liu, Y., Liu, J., Zou, M., Wang, L., Cheng, G. 2015. Lipid-albumin nanoassemblies co-loaded with borneol and paclitaxel for intracellular drug delivery to C6 glioma cells with P-gp inhibition and its tumor targeting. *Asian Journal of Pharmaceutical Sciences*, 10 (5), pp. 363–371.

Tang, J., Xiong, L., Zhou, G., Wang, S., Wang, J., Liu, L., Li, J., Yuan, F., Lu, S., Wan. Z., Chou, L., Xi, T., 2010. Silver nanoparticles crossing through and distribution in the blood-brain barrier *in vitro*. *Journal of Nanoscience and Nanotechnology*, 10 (10), pp. 6313–6317.

Tasneem, S., Farrell, K., Lee, M-Y., Kothapalli, C.R. 2016. Sensitivity of neural stem cell survival, differentiation and neurite outgrowth within 3D hydrogels to environmental heavy metals. *Toxicology Letters*, 242, pp. 9–22.

Taylor, J. R. & Twomey, L. T. 1986. Ages changes in lumbar zygapophyseal joints. Observations on structure and function. *Spine* 11, pp. 739-745.

Teo, W.Z.W & Schalock, P.C. 2016. Metal Hypersensitivity Reactions to Implanted Devices – Facts and Fictions. *Journal of Investigational Allergology and Clinical Immunology*, 26 (5) pp.279-294

Thyssen, J.P., Johansen, J.D., Menne, T., Lidén, C., Bruze, M., White, I.R. 2010 Hypersensitivity reactions from metallic implants: a future challenge that needs to be addressed. *British Journal of Dermatology* 162, pp.235-236.

Tipper, J.L., Firkins, P.J., Ingham, E., Fisher, J., Stone, M.H., Farrar, R. 1999. Quantitative analysis of the wear and wear debris from low and high carbon content cobalt chrome alloys used in metal on metal total hip replacements. *Journal of Materials Science: Materials in Medicine*, 10 (6), pp. 353–362.

Tipper, J.L., Ingham, E., Hailey, J.L., Besong, A.A., Fisher,J., Wroblewski, B.M., Stone, M.H. 2000. Quantitative analysis of polyethylene wear debris, wear rate and head damage in retrieved Charnley hip prostheses. *Journal of Materials Science. Materials in Medicine,* 11 (2), pp. 117-124.

Tipper, J.L., Firkins, P.J., Besong, A.A., Barbour, P.S.M., Nevelos, J., Stone, M.H., Ingham, E., Fisher, J. 2001. Characterisation of wear debris from UHMWPE on zirconia ceramic, metal-on-metal and alumina ceramic-on-ceramic hip prostheses generated in a physiological anatomical hip joint simulator. *Wear*, 250-251(Part 1), pp. 120–128.

Tipper, J.L., Ingham, E., Jin, Z.M., Fisher, J. 2005. (iv) The science of metal-on-metal articulation. *Orthopaedics and Trauma*, 19 (4), pp. 280–287.

Tipper, J.L., Galvin, A.L., Williams, S., McEwen, H.M.J., Stone, M.H., Ingham. E., Fisher, J. 2006 Isolation and characterization of UHMWPE wear particles down to ten nanometers in size from in vitro hip and knee joint simulators *Journal of Biomedical Materials Research. Part A*, 78-A (3), pp.473-480

Tipper, J.L., Vicars, R., Prokopovich, P., Brown, T.D., Ingham, E., Fisher, J., Hall, R.M. 2012. Quantitative Comparison of UHMWPE Wear Particles Generated from SB Charité III Total Disc Replacements Tested Under Different Input Kinematics. ORS 2012 Annual meeting. Paper number 0306.

Tipper, J.L. Hyde, P.J., Brown, T.D., Ingham, E., Fisher, J., Hall, R.M.2013. Quantitative Comparison of UHMWPE Wear Particles Generated from ProDisc-L Total Disc

Replacements Tested Under Altered Simulation Inputs. ORS 2013 Annual Meeting. Paper Number 0382.

Torgersen, S., Moe, G., Jonsson, R. 1995 Immunocompetent cells adjacent to stainless steel and titanium miniplates and screws. *European Journal of Oral Sciences*, 103, pp.46-54.

Tsaousi, A., Jones, E., Case. C.P. 2010 The *in vitro* genotoxicity of orthopaedic ceramic (Al_2O_3) and metal (CoCr alloy) particles. *Mutation research*, 697 (1-2), pp.1-9.

Urban, R.M., Jacobs, J.J., Tomlinson, M.J., Gavrilovic, J., Black, J., Peoc'h, M., 2000. Dissemination of Wear Particles to the Liver, Spleen, and Abdominal Lymph Nodes of Patients with Hip or Knee Replacement. *The Journal of Bone and Joint Surgery (American Volume)*, 82 (4), pp. 457–477.

Urban, J.P.G. & Roberts, S., 2003. Degeneration of the intervertebral disc. *Arthritis Research & Therapy*, 5 (3), pp. 120–130.

Urban, R.M., Tomlinson, M.J., Hall, D.J., Jacobs, J.J. 2004. Accumulation in liver and spleen of metal particles generated at nonbearing surfaces in hip arthroplasty. *The Journal of Arthroplasty*, 19 (8 Supplement 3), pp. 94–101.

Vaccaro, A., Beutler, W., Peppelman, W., Marzluff, J.M., Highsmith, J., Mugglin, A., DeMuth, G., Gudipally, M., Baker, K.J. 2013. Clinical Outcomes With Selectively Constrained SECURE-C Cervical Disc Arthroplasty. *Spine*, 38 (26), pp. 2227–2239.

Van Der Bruggen, T., Nijenhuis, S., Van Raaij, E., Verhoef, J., Van Asbeck, S.B. 1999. Lipopolysaccharide-Induced Tumor Necrosis Factor Alpha Production by Human Monocytes Involves the Lipopolysaccharide-Induced Tumor Necrosis Factor Alpha Production by Human Monocytes Involves the Raf-1/MEK1-MEK2/ERK1-ERK2 Pathway. *Infection and Immunity*, 67 (8), pp. 3824–3829.

Van Ooij, A., Kurtz, S.M., Stessels, F., Noten, H., Van Rhijn, L. 2007. Polyethylene wear debris and long-term clinical failure of the Charite disc prosthesis: a study of 4 patients. *Spine*, 32 (2), pp. 223–229.

Veruva, S.Y., Steinbeck, M.J., Toth, J., Alexander, D.D., Kurtz, S.M. 2014. Which design and biomaterial factors affect clinical wear performance of total disc replacements? A

systematic review. *Clinical Orthopaedics and Related Research*, 472 (12), pp. 3759–3769.

Vetten, M.S., Tlotleng., N., Rascher, D.T., Skepu, A., Keter, F.K., Boodhia, K., Koekemoer, L.A., Andraos, L., Tshikhudi, R., Gulumian, M. 2013. Label-free *In Vitro* toxicity and uptake assessment of citrate stabilised gold nanoparticles in three cell lines. *Particle and Fibre Toxicology*, 10 (50), pp.1-15.

Vicars, R., Hyde, P.J., Brown, T.D., Tipper, J.L., Ingham, E., Fisher, J., Hall, R.M. 2010. The effect of anterior-posterior shear load on the wear of ProDisc-L TDR. *European Spine Journal*, 19 (8), pp. 1356–1362.

Vital, J.M. & Boissiere, L. 2014. Total Disc Replacement. *Orthopaedics and traumatology: Surgery and Related Research*, 100(1 Supplement), pp. S1–S14.

Von der Mark, K.V.G.H, Von der Mark., Muller. P. 1977. Relationship between cell shape and type of collagen synthesised as chondrocytes lose their cartilage phenotype in culture. *Nature,* 267, pp. 531-532.

Vundelinckx, B.J., Verhelst, L.A., De Schepper, J. 2013. Taper corrosion in modular hip prostheses: analysis of serum metal ions in 19 patients. *The Journal of Arthroplasty* 28 (7) pp. 1218-1223.

Wang, K., Bekar, L.K., Furber, K., Walz, W. 2004. Vimentin-expressing proximal reactive astrocytes correlate with migration rather than proliferation following focal brain injury. *Brain Research*, 1024 (1–2), pp. 193–202.

Waterhouse, R.B. 1972 Fretting Corrosion: International series of monographs on materials science and technology, Pergamon press.

Watson, C., Paxinos, G., Kayalioglu, G. 2008 The Spinal Cord, 1st Edition. Academic Press.

Watters, T.S., Cardona, D.M., Menon, K.S., Vinson, E.N., Bolognesi, M.P., Dodd, L.G. 2010. Aseptic lymphocyte-dominated vasculitis-associated lesion: A clinicopathologic review of an underrecognized cause of prosthetic failure. *American Journal of Clinical Pathology,* 134, pp.886–893.

Weaver, V.M., Peterson, O.W., Wang, F., Larabell, C.A., Briand, P., Damsky, C., Bissell, M.J. 1997. Reversion of the malignant phenotype of human breast cells in three-

dimensional culture and *in vivo* by integrin blocking antibodies. *Journal of Cell Biology,* 137 (1) pp. 231-245.

Williams, S., Tipper, J.L., Ingham, E., Stone, M.H., Fisher, J. 2003. *In vitro* analysis of the wear, wear debris and biological activity of surface-engineered coatings for use in metal-on-metal total hip replacements. *Proceedings of the Institution of Mechanical Engineers. Part H, Journal of engineering in medicine*, 217 (3), pp. 155–163.

Williams, S., Isaac, G., Hatto, P., Stone, M.H., Ingham, E., Fisher, J. 2004. Comparative Wear Under Different Conditions of Surface-Engineered Metal-on-Metal Bearings for Total Hip Arthroplasty. *The Journal of Arthroplasty*, 19 (8), pp. 112–117.

Winkelstein, B.A. 2012. Orthopaedic Biomechanics. (CRC Press)

Xue, Y., Wu, J., Sun, J. 2012. Four types of inorganic nanoparticles stimulate the inflammatory reaction in brain microglia and damage neurons *in vitro*. *Toxicology Letters*, 214 (2), pp. 91–98.

Yoshihara, H. 2013. Rods in spinal surgery: a review of the literature. *The Spine Journal*, 13 (10), pp. 1350–1358.

Yu, J., Tirlapur, U., Fairbank, J., Handford, P., Roberts, S., Winlove, P., Zhanfeng, C., Urban, J. 2007. Microfibrils, elastin fibres and collagen fibres in the human intervertebral disc and bovine tail disc. *Journal of Anatomy*, 210 (4), pp. 460–471.

Yu, J., Winlove, P.C., Roberts, S., Urban, J.P. 2002. Elastic fibre organization in the intervertebral discs of the bovine tail. *Journal of Anatomy*. 201 (6) pp. 465–475.

Zigler, J., Delamarter, R., Spivak, J.M., Linovitz, R.J., Danielson, G.O., Haider, T.T., Cammisa, F., Zuchermann, J., Balderston, R., Kitchel, S., Foley, K., Watkins, R., Bradford, D., Yue, J., Yuan, H., Herkowitz, H., Geiger, D., Bendo, J., Peppers, T., Sachs, B., Girardi, F., Kropf, M.G.J., 2007. Results of the prospective, randomized, multicenter Food and Drug Administration investigational device exemption study of the ProDisc-L total disc replacement versus circumferential fusion for the treatment of 1-level degenerative disc disease. *Spine*, 32 (11), pp. 1155–1162.

Appendices

General chemicals and reagents used in this study are shown in Appendix I

Appendix I General chemicals and reagents

Chemicals/reagents	Storage conditions	Supplier
ATP Lite™ Assay. Luminescent ATP detection assay kit	Substrate buffer solution, Mammalian cell lysis and lyophilised substrate stored at 4°C	PerkinElmer, Windsor UK
Bovine Serum Albumin (BSA)	4°C	Sigma-Aldrich Ltd., Dorset UK
Calcein	-20°C	ThermoFisher Scientific, Northumberland UK
Carbon paste	Room Temperature	Agar Scientific, Stanstead UK
Collage (type I rat tail >2mg/ml in 0.6% (v/v) Acetic acid)	4°C	First Link Ltd, Wolverhampton UK
CometAssay lysis solution	4°C	Bio-Techne , Abingdon UK
Dimethyl Sulphoxide (DMSO)	Solvents cupboard Room Temperature	Fisher Scientific, Loughborough UK
DNase type II from bovine pancreas	-20°C	Sigma-Aldrich Ltd., Dorset UK
DPBS	Room Temperature	Bio-Whittaker, Lonza, Verviers, Belgium
Dulbecco's modified Eagle's medium (DMEM) with and without phenol red	4°C	Lonza Biological, Cambridge UK
Earle's balanced salt solution (EBSS)	Room Temperature	Sigma-Aldrich Ltd., Dorset UK
Ethidium Homodimer	-20°C	ThermoFisher Scientific, Northumberland UK
Ethylenediaminetetraacetic acid (EDTA)	Room Temperature	Sigma-Aldrich Ltd., Dorset UK
Ethanol	Room temperature, Flammables cupboard	VWR international, Poole UK
ELISA kit (TNF-α)	4°C	2B Scientific, Oxfordshire UK.
Fairy liquid	Room Temperature	Local Store
Foetal Bovine Serum (FBS)	-20°C	Bio-Whittaker, Lonza, Verviers, Belgium
Goat Serum Blocking Solution (5%)	4°C	Sigma-Aldrich Ltd., Dorset UK
Glucose Powder	Room Temperature	Sigma-Aldrich Ltd., Dorset UK

Ham's F12 (Without phenol red)	4°C	ThermoFisher Scientific, Northumberland UK
Horse Serum	-20°C	Sigma-Aldrich Ltd., Dorset UK
Hydrochloric Acid (HCl)	Room Temperture	Fisher Scientific, Loughborough UK
Hydrogen peroxide	4°C	Sigma-Aldrich Ltd., Dorset UK
Isopropanol	Flammables cupboard, Room Temperature	Fisher Scientific, Loughborough UK
L-glutamine	-20°C	Sigma-Aldrich Ltd., Dorset UK
Lipopolysaccharide (LPS)	4°C	Sigma-Aldrich Ltd., Dorset UK
LM Agarose	4°C	Bio-Techne , Abingdon UK
Magnesium Sulphate ($MgSO_4$)	Room Temperature	Sigma-Aldrich Ltd., Dorset UK
10X Minimum Essential Media	4°C	Sigma-Aldrich Ltd., Dorset UK
MTT powder	4°C	Sigma-Aldrich Ltd., Dorset UK
Neutralising solution (predominantly sodium hydroxide)	4°C	Tap Biosystems now part of Sartorium Stedim Biotech, Hertfordshire UK
Paraformaldehyde (PFA) powder	Room Temperature	Sigma-Aldrich Ltd., Dorset UK
Penicillin/Streptomycin	-20°C	Bio-Whittaker, Lonza, Verviers, Belgium
PBS tablets	Room Temperature	Oxoid Thermo Scientific,Northumberland UK
pH Standards	-20°C	Scientific Laboratory Supplies Ltd, Nottingham UK
Poly-D-lysine powder	Room Temperature	Sigma-Aldrich Ltd., Dorset UK
Rosslyn Park Memorial Institute (RPMI) 1640 Media (with and without phenol red)	4°C	Bio-Whittaker, Lonza, Verviers, Belgium
Sterile Water	Room Temperature	Baxter Healthcare, UK
Sodium Hydroxide (NaOH)	Room Temperature	Fisher Scientific, Loughborough UK
Soy-bean Trypsin Inhibitor (SBTI)	4°C	Sigma-Aldrich Ltd., Dorset UK
SYBR gold	-20°C	ThermoFisher Scientific, Life technologiesNorthumberland UK
Transforming growth factor beta (TGF-)β	-20°C	Sigma-Aldrich Ltd., Dorset UK
Trigene	Room Temperature	Scientific Laboratory Supplies Ltd, Nottingham UK
Tris	Room temperature	Sigma-Aldrich Ltd., Dorset UK
Trypan Blue	Room Temperature	Sigma-Aldrich Ltd., Dorset UK
Trypsin from bovine pancreas	-20°C	Sigma-Aldrich Ltd., Dorset UK
Trypsin (passaging cells)	-20°C	Sigma-Aldrich Ltd., Dorset UK

Triton X-100	Room Temperature	BDH laboratory supplies, Poole UK
Virkon	Room Temperature	Scientific Laboratory Supplies Ltd, Nottingham UK

The general equipment used in this study is shown in Appendix II

Appendix II General Equipment used in this investigation

Equipment	Supplier
Absorbance microplate reader Chameleon plate, multi-label detection platform.	HIDEX , Finland.
Accublock Digital dry bath	Labnet International Inc Global, Edison USA.
Aluminium stub holder	Agar Scientific Ltd. Essex UK
Autoclave	Priorclave, London UK
Automatic Pipette (Pipetteboy®)	Scientific Laboratory Supplies Ltd, Nottingham UK
Balance AT21 Comparator	A&D Instruments Ltd, Oxford UK
Balance GR200 (Accuracy 0;01g)	A&D Instruments Ltd, Oxford UK
Balance GX-2000 EC	Sartorius, Goettingen, Germany
Bunsen Burner	-
Carbon Coater	
Centrifuge (Tissue Culture) Harrier 15/80	Sanyo, Japan.
Centrifuge (L6) MIKRO 22R	Hettich, Tuttlingen Germany
Class I Laminar Flow Cabinet	Howorth Airtech Ltd, UK
Class II Laminar Flow Cabinet	Heraeus, Hanau Germany
Confocal Microscope laser scanning upright LSM510	Carl Zeiss Ltd, UK.
Cryopreservation Freezer	-
Eppendorf Centrifuge 5415R	Hyland Scientific, Stanwood, Washington USA.
Field Emission Gun Scanning Electron Microscope (FEGSEM)	Hitachi, Schaumburg USA
-20°C Freezer	Jencons Plc, East Grinstead UK
-80°C Freezer	Sanyo Biomedical Europe, BV
Fluorescent Microscope	Zeiss
Fume Cupboard	Whiteley fume extraction solutions Ltd, Bradford UK
Gilson Pipettes P2, P20, P200 and P1000	Fisher Brand, Fisher Scientific Loughborough UK
25mm Glass filtration system	Sartorius, Goettingen, Germany
Glass Universals	Scientific Laboratory Supplies Ltd, Nottingham UK
High Speed Harrier Centrifuge 15/80	Sanyo, Watford UK
Ice blocks	Medicool MC28 Laminar Medica UK
Image Pro Plus image analysis software version 6.0	Media Cybernetics, Maryland USA.
Incubator	Sanyo Biomedical Europe, BV Amsterdam, Holland
Infra Red Lamp (100 W bulb)	Infraphil Phillips®, Surrey UK
Inverted Microscope (IX71)	Olympus Optical Co. Ltd, London UK
Light Microscope	Olympus Optical Co. Ltd, London UK
Liquid Nitrogen Dewar BIO65	Jencons Plc, East Grinstead UK
Magnetic Stirrer	Scientific Laboratory Supplies Ltd,

	Nottingham UK
Magnetic Stirrer Bar	Scientific Laboratory Supplies Ltd, Nottingham UK
Microcentaur microfuge	MSE, London UK
Microwave	ProLine, France
Oven	Genlab Ltd, Cheshire UK
pH meter (Jenway 3510)	VWR International Poole UK
Plastic Tray for CometSlides	-
Plate Shaker	Bibby Sterilin Stone, Staffordshire UK.
Plate Spinner	
4°C Refrigerator	Jencons Plc, East Grinstead UK
Sonicator	Fisher Scientific, Leicestershire UK.
Sorvall Evolution RC High Speed Centrifuge and SLA 1500 Rotors	-
Spirit Level	Camlab UK.
Sputter Coater (B7341) and Film Thickness Monitor (B7348)	Agar Scientific Ltd, Stanstead Essex UK
Uktrasonic Waterbath	Grant Instruments Ltd, Harts UK
Vortex-MS2 Minishaker	Fisher Scientific, Leicestershire UK.
Water Bath	Fisher Scientific, Leicestershire UK.
Water Purifier	Triple Red Laboratory Technology UK.

The general consumables used in this study are shown in Appendix III

Appendix III General consumables used throughout this study

Item	Size	Supplier
Bijou	5ml	Scientific Laboratory Supplies Ltd, Nottingham UK
Blue Roll	-	-
Cell scraper	18mm blade length 260mm handle	Fisher Scientific, Leicestershire UK.
Closed Flask Caps	For 75cm^3 tissue culture flasks	Scientific Laboratory Supplies Ltd, Nottingham UK
Comet Assay Slides	2 well x 100	Trevigen, USA
Coplin jar	25ml	-
Cryovial	1.5ml	Nange Nunc International Corporation. New York USA
Disposable Plastic syringe	1ml,2ml,5ml,10ml, 20ml 50ml	Scientific Laboratory Supplies Ltd, Nottingham UK
Electrophoresis power pack	-	Pharmacia, New Jersey USA.
Electrophoresis Tank Bio-rad DNA SUB CELL	30cmx10cm	Bio-Rad Hertfordshire UK.
Eppendorf Tubes	1.5ml	Sarstedt, Germany
Falcon Tubes	15ml, 50ml	Fisher Scientific, Leicestershire UK.
Glass Beaker	100ml 250ml 600ml	-
Glass Duran Bottle	1L 5L	Fisher Scientific, Leicestershire UK.
Glass cover slips	22mmx47mm	Scientific Laboratory Supplies Ltd, Nottingham UK
Haemocytometer neubauer	22mmx47mm	VWR International Poole UK
Microplate Adhesive Sealing Film	96 well plate	PerkinElmer, Windsor UK
Optiplate™	96 well plate	PerkinElmer, Windsor UK
Parafilm	To seal edges of 96 well plate	Bemis, Oshkosh, Wisconsin USA
Pipette tips	20µl, 200µl, 1000µl	Starlab, Ahrensburg Germany
Polycarbonate Filter Membranes	5µm, 1µm, 0.1µm, 0.015µm	Whatman, Kent UK
Scalpel Blade flat edge		Swann-Morton UK
Scalpel Holder	130mm	Swann-Morton UK
Scissors (curved blade for dissoction)	-	Karl Hammacher, Germany
Spatula	-	-

Sterile Pot	60ml, 150ml, 250ml	Scientific Laboratory Supplies Ltd, Nottingham
Syringe Filter (single use)	0.22μm pore size	Millex Merck Millipore, Germanys
Test Tube Holder	-	-
Tissue Culture Dishes	60mmx10mm	Corning BV
Tissue Culture Flasks	25cm^2, 75cm^2, 125cm^2,	ThermoFisher Scientific, Northumberland UK
Tweezers	Extra fine point	TAAB
Universal	30ml	Scientific Laboratory Supplies Ltd, Nottingham
Weighing Boat	-	-
Well Plates nunclon delta surface	96well (flat and U bottom), 24well, 12 well	ThermoScientific, Northumberland UK
Wide Bore optifit pipette tips pre-sterilised	1000μl	Biohit UK.

Antibodies and stains used in this study are shown in Appendix IV

Appendix IV Antibodies used in this study

Antibody/ Stain	Isotype	Concentration	Dilution	Supplier/Product code	Incubation Time
GFAP primary antibody	IgG	2.9g/L	1:300 In PBS	Dako	Overnight
GFAP secondary antobody DyLight® 549 Anti-rabbit IgG	IgG (H+L)	N/A	1:300 in PBS	Vector Laboratories, Peterborough UK	90 Minutes
Hoescht 33258	N/A	1µg/ml	1:1000 in PBS	Sigma-Aldrich Ltd., Dorset UK	90 Minutes

Appendix V. The effects of increasing particle volumes of cobalt chrome and stainless steel wear particles on the expression of GFAP by primary astrocytes and microglia in co-culture and primary astrocytes in isolation after two and five days In culture.

The effect of increasing cobalt chrome particle volumes on the level of GFAP expression by primary astrocytes in the presence of microglia after two days in culture. Each gel was imaged a total of six times. A + is indicative of the expression of GFAP, a – indicates GFAP was not expressed.

	Gel 1						Gel 2						Gel 3						Gel 4						Gel 5						Gel 6					
Gel type	**1**	**2**	**3**	**4**	**5**	**6**	**1**	**2**	**3**	**4**	**5**	**6**	**1**	**2**	**3**	**4**	**5**	**6**	**1**	**2**	**3**	**4**	**5**	**6**	**1**	**2**	**3**	**4**	**5**	**6**	**1**	**2**	**3**	**4**	**5**	**6**
0.5µm³	+	+	+	-	+	+	-	-	-	+	+	+	-	-	-	-	-	-	-	-	-	-	-	-	-	-	-	+	+	+	+	+	+	+	-	-
5µm³	-	-	-	-	-	-	-	-	+	+	+	+	-	-	+	+	-	-	-	+	+	+	+	-	-	-	-	-	+	-	+	+	+	+	-	-
50µm³	+	+	-	+	+	-	+	+	+	+	+	+	+	-	+	+	+	+	-	-	-	+	-	-	-	-	-	+	+	-	-	+	-	-	-	+
Cell only	-	-	-	+	+	+	-	-	-	-	-	-	-	-	+	-	-	+	-	-	-	-	-	-	-	-	-	-	-	-	+	-	+	+	+	+
Particle only	-	-	-	-	-	-	-	-	-	-	-	-	-	-	-	-	-	-	-	-	-	-	-	-	-	-	-	-	-	-	-	-	-	-	-	-
Blank	-	-	-	-	-	-	-	-	-	-	-	-	-	-	-	-	-	-	-	-	-	-	-	-	-	-	-	-	-	-	-	-	-	-	-	-
TGF-1β	+	+	+	+	+	+	+	+	+	-	+	+	-	+	+	-	+	-	-	-	-	-	-	-	+	+	+	+	+	+	+	+	-	+	-	-

The effect of increasing cobalt chrome particle volumes on the level of GFAP expression by primary astrocytes in the presence of microglia after five days in culture. Each gel was imaged a total of six times. A + is indicative of the expression of GFAP, a – indicates GFAP was not expressed.

	Gel 1						Gel 2						Gel 3						Gel 4						Gel 5						Gel 6					
Gel type	**1**	**2**	**3**	**4**	**5**	**6**	**1**	**2**	**3**	**4**	**5**	**6**	**1**	**2**	**3**	**4**	**5**	**6**	**1**	**2**	**3**	**4**	**5**	**6**	**1**	**2**	**3**	**4**	**5**	**6**	**1**	**2**	**3**	**4**	**5**	**6**
0.5μm³	-	+	-	+	-	-	-	-	-	+	-	+	+	-	+	+	+	-	-	+	+	+	+	+	+	+	+	+	+	+	-	+	+	+	+	+
5μm³	+	+	-	+	+	+	-	-	+	+	-	+	+	-	+	+	+	+	+	-	+	+	+	-	-	+	+	+	+	-	+	-	-	+	+	+
50μm³	-	+	-	+	+	+	-	+	+	+	+	-	-	+	-	+	-	-	-	-	-	-	+	+	+	+	+	-	+	+	-	+	+	-	-	+
Cell only	-	-	-	+	+	-	-	-	+	+	-	-	-	+	-	-	-	+	+	-	-	+	-	-	-	-	+	-	+	+	+	-	-	-	-	-
Particle only	-	-	-	-	-	-	-	-	-	-	-	-	-	-	-	-	-	-	-	-	-	-	-	-	-	-	-	-	-	-	-	-	-	-	-	-
Blank	-	-	-	-	-	-	-	-	-	-	-	-	-	-	-	-	-	-	-	-	-	-	-	-	-	-	-	-	-	-	-	-	-	-	-	-
TGF-1β	+	-	+	+	-	-	+	+	+	-	-	-	+	+	+	+	+	-	+	+	+	+	-	+	+	+	+	+	+	-	+	+	-	+	-	-

The effect of increasing cobalt chrome particle volumes on the level of GFAP expression by primary astrocytes in the absence of microglia after two days in culture. Each gel was imaged a total of six times. A + is indicative of the expression of GFAP, a – indicates GFAP was not expressed.

	Gel 1						Gel 2						Gel 3						Gel 4						Gel 5						Gel 6					
Gel type	**1**	**2**	**3**	**4**	**5**	**6**	**1**	**2**	**3**	**4**	**5**	**6**	**1**	**2**	**3**	**4**	**5**	**6**	**1**	**2**	**3**	**4**	**5**	**6**	**1**	**2**	**3**	**4**	**5**	**6**	**1**	**2**	**3**	**4**	**5**	**6**
0.5µm³	-	-	-	-	-	-	-	-	-	-	-	-	-	-	-	-	-	-	-	-	-	-	+	+	-	-	-	-	+	-	-	+	+	+	+	+
5µm³	-	-	+	+	-	-	+	-	-	-	-	-	-	-	-	-	-	-	-	-	-	-	+	-	-	-	+	-	-	-	-	-	-	-	-	-
50µm³	-	-	-	-	+	-	+	+	-	-	-	-	-	-	-	-	-	-	-	-	-	-	-	-	-	-	+	+	+	-	+	+	-	-	-	-
Cell only	-	-	-	-	-	-	-	-	-	-	-	-	-	-	+	-	-	-	-	-	-	-	-	+	-	-	-	-	-	-	-	-	-	-	-	-
Particle only	-	-	-	-	-	-	-	-	-	-	-	-	-	-	-	-	-	-	-	-	-	-	-	-	-	-	-	-	-	-	-	-	-	-	-	-
Blank	-	-	-	-	-	-	-	-	-	-	-	-	-	-	-	-	-	-	-	-	-	-	-	-	-	-	-	-	-	-	-	-	-	-	-	-
TGF-1β	+	-	+	+	+	+	-	-	+	-	-	+	+	+	+	+	+	-	+	+	+	+	-	-	+	+	+	+	+	-	+	+	+	+	-	-

The effect of increasing cobalt chrome particle volumes on the level of GFAP expression by primary astrocytes in the absence of microglia after five days in culture. Each gel was imaged a total of six times. A + is indicative of the expression of GFAP, a – indicates GFAP was not expressed.

	Gel 1						Gel 2						Gel 3						Gel 4						Gel 5						Gel 6					
Gel type	**1**	**2**	**3**	**4**	**5**	**6**	**1**	**2**	**3**	**4**	**5**	**6**	**1**	**2**	**3**	**4**	**5**	**6**	**1**	**2**	**3**	**4**	**5**	**6**	**1**	**2**	**3**	**4**	**5**	**6**	**1**	**2**	**3**	**4**	**5**	**6**
0.5μm³	+	+	+	+	-	-	+	+	+	+	+	+	+	+	+	+	-	-	+	+	+	+	+	+	+	-	+	+	+	+	+	+	+	+	+	+
5μm³	+	+	+	+	+	+	+	+	+	+	+	+	+	+	+	+	+	-	+	+	+	-	+	+	+	+	+	+	+	+	+	+	+	+	+	+
50μm³	+	-	-	-	-	-	-	-	-	-	-	-	-	-	-	-	-	-	-	-	-	-	-	-	-	-	-	-	-	+	-	+	-	-	+	+
Cell only	-	-	-	-	-	-	-	-	-	-	-	-	-	-	-	-	-	-	-	-	-	-	-	-	-	-	-	-	-	-	-	-	-	-	-	-
Particle only	-	-	-	-	-	-	-	-	-	-	-	-	-	-	-	-	-	-	-	-	-	-	-	-	-	-	-	-	-	-	-	-	-	-	-	-
Blank	-	-	-	-	-	-	-	-	-	-	-	-	-	-	-	-	-	-	-	-	-	-	-	-	-	-	-	-	-	-	-	-	-	-	-	-
TGF-1β	+	+	-	+	+	-	-	+	+	+	+	-	-	+	+	+	-	-	-	+	+	+	+	-	-	+	+	+	+	+	+	+	+	-	-	+

The effect of increasing stainless steel particle volumes on the level of GFAP expression by primary astrocytes in the presence of microglia after two days in culture. Each gel was imaged a total of six times. A + is indicative of the expression of GFAP, a – indicates GFAP was not expressed.

	Gel 1						Gel 2						Gel 3						Gel 4						Gel 5						Gel 6					
Gel type	**1**	**2**	**3**	**4**	**5**	**6**	**1**	**2**	**3**	**4**	**5**	**6**	**1**	**2**	**3**	**4**	**5**	**6**	**1**	**2**	**3**	**4**	**5**	**6**	**1**	**2**	**3**	**4**	**5**	**6**	**1**	**2**	**3**	**4**	**5**	**6**
0.5µm³	+	-	+	+	+	+	-	-	+	+	+	-	-	+	-	-	-	-	-	-	-	+	+	-	-	+	-	-	-	-	-	-	-	-	-	+
5µm³	-	-	-	-	+	-	-	-	+	+	-	-	-	-	-	-	-	-	-	-	+	+	-	-	-	-	-	-	-	-	-	-	+	+	-	-
50µm³	-	-	-	+	+	-	-	-	-	-	-	+	-	-	-	+	+	-	+	-	-	+	-	-	-	-	+	+	-	-	-	-	+	+	+	+
Cell only	+	+	-	+	+	-	-	-	-	-	-	-	-	-	-	-	-	-	-	-	+	-	-	-	-	-	-	+	-	-	+	-	+	-	-	-
Particle only	-	-	-	-	-	-	-	-	-	-	-	-	-	-	-	-	-	-	-	-	-	-	-	-	-	-	-	-	-	-	-	-	-	-	-	-
Blank	-	-	-	-	-	-	-	-	-	-	-	-	-	-	-	-	-	-	-	-	-	-	-	-	-	-	-	-	-	-	-	-	-	-	-	-
TGF-1β	+	+	+	+	+	+	+	+	+	+	+	+	+	+	-	-	-	-	-	+	-	+	-	-	+	+	+	+	-	+	+	-	+	+	+	+

The effect of increasing stainless steel particle volumes on the level of GFAP expression by primary astrocytes in the presence of microglia after five days in culture. Each gel was imaged a total of six times. A + is indicative of the expression of GFAP, a – indicates GFAP was not expressed.

	Gel 1						Gel 2						Gel 3						Gel 4						Gel 5						Gel 6					
Gel type	**1**	**2**	**3**	**4**	**5**	**6**	**1**	**2**	**3**	**4**	**5**	**6**	**1**	**2**	**3**	**4**	**5**	**6**	**1**	**2**	**3**	**4**	**5**	**6**	**1**	**2**	**3**	**4**	**5**	**6**	**1**	**2**	**3**	**4**	**5**	**6**
0.5µm³	-	-	-	-	+	+	-	-	-	+	+	+	+	-	+	-	+	-	-	-	-	+	+	-	+	+	-	-	+	+	+	-	-	+	+	+
5µm³	-	-	-	-	-	-	-	+	-	+	+	-	-	-	-	-	-	-	-	-	+	-	-	-	-	-	-	+	+	+	+	+	-	-	-	-
50µm³	-	-	-	-	+	+	+	+	-	+	+	+	-	+	+	+	+	-	-	+	-	+	+	+	-	-	+	-	-	-	-	-	-	-	-	-
Cell only	+	-	-	-	-	-	-	-	-	+	+	-	-	-	-	-	-	-	-	-	-	-	-	-	-	-	-	+	-	-	-	-	-	+	-	-
Particle only	-	-	-	-	-	-	-	-	-	-	-	-	-	-	-	-	-	-	-	-	-	-	-	-	-	-	-	-	-	-	-	-	-	-	-	-
Blank	-	-	-	-	-	-	-	-	-	-	-	-	-	-	-	-	-	-	-	-	-	-	-	-	-	-	-	-	-	-	-	-	-	-	-	-
TGF-1β	+	+	+	+	+	+	+	+	+	-	-	+	+	-	+	+	+	-	+	-	+	+	+	-	+	+	-	-	+	-	+	-	+	+	-	+

The effect of increasing stainless steel particle volumes on the level of GFAP expression by primary astrocytes in the absence of microglia after two days in culture. Each gel was imaged a total of six times. A + is indicative of the expression of GFAP, a – indicates GFAP was not expressed.

	Gel 1						Gel 2						Gel 3						Gel 4						Gel 5						Gel 6					
Gel type	**1**	**2**	**3**	**4**	**5**	**6**	**1**	**2**	**3**	**4**	**5**	**6**	**1**	**2**	**3**	**4**	**5**	**6**	**1**	**2**	**3**	**4**	**5**	**6**	**1**	**2**	**3**	**4**	**5**	**6**	**1**	**2**	**3**	**4**	**5**	**6**
0.5µm³	-	-	-	-	-	-	-	-	-	-	-	-	-	-	-	-	-	-	-	-	-	-	-	-	-	-	-	-	-	-	-	-	-	-	-	-
5µm³	-	-	-	-	-	-	-	-	-	-	-	-	-	-	-	-	-	-	-	-	-	-	-	-	-	-	-	-	-	-	-	-	-	-	-	-
50µm³	-	-	-	-	-	-	-	-	-	-	-	-	-	-	-	-	-	-	-	-	-	-	-	-	-	-	-	-	-	-	-	-	-	-	-	-
Cell only	-	-	-	-	-	-	-	-	-	-	-	-	-	-	-	-	-	-	-	-	-	-	-	-	-	-	-	-	-	-	-	-	-	-	-	-
Particle only	-	-	-	-	-	-	-	-	-	-	-	-	-	-	-	-	-	-	-	-	-	-	-	-	-	-	-	-	-	-	-	-	-	-	-	-
Blank	-	-	-	-	-	-	-	-	-	-	-	-	-	-	-	-	-	-	-	-	-	-	-	-	-	-	-	-	-	-	-	-	-	-	-	-
TGF-1β	-	+	+	-	+	+	+	+	-	-	+	+	+	+	+	+	+	+	+	+	+	+	+	-	-	+	-	-	-	-	-	+	+	-	-	-

The effect of increasing stainless steel particle volumes on the level of GFAP expression by primary astrocytes in the absence of microglia after five days in culture. Each gel was imaged a total of six times. A + is indicative of the expression of GFAP, a – indicates GFAP was not expressed.

	Gel 1						Gel 2						Gel 3						Gel 4						Gel 5						Gel 6					
Gel type	**1**	**2**	**3**	**4**	**5**	**6**	**1**	**2**	**3**	**4**	**5**	**6**	**1**	**2**	**3**	**4**	**5**	**6**	**1**	**2**	**3**	**4**	**5**	**6**	**1**	**2**	**3**	**4**	**5**	**6**	**1**	**2**	**3**	**4**	**5**	**6**
0.5µm³	-	-	-	-	-	-	-	-	-	-	-	-	-	-	-	-	-	-	-	-	-	-	-	-	-	-	-	-	-	-	-	-	-	-	-	-
5µm³	-	-	-	-	-	-	-	-	-	-	-	-	-	-	-	-	-	-	-	-	-	-	-	-	-	-	-	-	-	-	-	-	-	-	-	-
50µm³	-	-	-	-	-	-	-	-	-	-	-	-	-	-	-	-	-	-	-	-	-	-	-	-	-	-	-	-	-	-	-	-	-	-	-	-
Cell only	-	-	-	-	-	-	-	-	-	-	-	-	-	-	-	-	-	-	-	-	-	-	-	-	-	-	-	-	-	-	-	-	-	-	-	-
Particle only	-	-	-	-	-	-	-	-	-	-	-	-	-	-	-	-	-	-	-	-	-	-	-	-	-	-	-	-	-	-	-	-	-	-	-	-
Blank	-	-	-	-	-	-	-	-	-	-	-	-	-	-	-	-	-	-	-	-	-	-	-	-	-	-	-	-	-	-	-	-	-	-	-	-
TGF-1β	+	+	+	+	-	+	+	+	+	+	+	-	+	+	+	-	+	+	+	+	+	+	-	-	+	+	+	+	-	-	-	+	+	+	+	+